Control of lymphoid organ CD169+ macrophage differentiation by stromal cells through the RANK-RANKL axis

Abdouramane Camara

Université
de Strasbourg

UNIVERSITÉ DE STRASBOURG

École Doctorale
des Sciences de la Vie
et de la Santé
S T R A S B O U R G

ÉCOLE DOCTORALE DES SCIENCES DE LA VIE ET DE LA SANTÉ

I²CT - Immunologie, Immunopathologie & Chimie Thérapeutique

THÈSE présentée par :

Abdouramane CAMARA

Soutenue le : **18 décembre 2019**

pour obtenir le grade de : **Docteur de l'université de Strasbourg**

Discipline/Spécialité : Aspects moléculaires et cellulaires de la biologie/Immunologie

---

Control of lymphoid organ CD169⁺ macrophage differentiation by stromal cells through the RANK-RANKL axis

---

THÈSE dirigée par :

    Dr MUELLER Christopher   DR2, CNRS, IBMC, UPR3572, Université de Strasbourg

---

RAPPORTEURS EXTERNES

    Prof. Jens Volker STEIN   Faculté de Science et Médecine, OMI

    Université de Fribourg, Suisse

    Dr. Pierre GUERMONPREZ   Centre de Rechercher sur l'Inflammation

    UMR 1149 Inserm – Université Paris Diderot

EXAMINATRICE INTERNE :

    Dr. Susan CHAN   IGBMC, Génomique fonctionnelle et cancer

    CNRS UMR 7104 - Inserm U 1258

Table of content

List of abbreviations

A:

ACK	Ammonium-chloride-potassium
Aire	Autoimmune regulatory element
AP-1	Activator protein 1
APC	Antigen presenting cell
APRIL	A proliferation-inducing ligand

B:

BAFF	B-cell activating factor
BEC	Blood endothelial cell
BLC	B lymphocyte chemoattractant

C:

CALCR	Calcitonin receptor
CCL	Chemokine (C-C motif) ligand
CCR	Chemokine (C-C motif) receptor
CD	Cluster of differentiation
CpG	Cytosine–phosphate–Guanine
CLCA1	Calcium-activated chloride channel regulator 1
CLLs	Clodronate liposomes
CRD	Cystein-rich domain
CXCL	Chemokine (C-X-C motif) ligand
CXCR	Chemokine (C-X-C motif) receptor

D:

DAMP	Damage-associated molecular pattern
DC	Dendritic cell
DC-SIGN	Dendritic Cell-Specific Intercellular adhesion molecule-3-Grabbing Non-integrin
DD	Death domain
DDH	Death domain homologous
DNA	Deoxyribonucleic acid
DR6	Death receptor 6
DSS	Dextran sulfate sodium
DTR	Diphtheria toxin receptor

E:

EDAR	Ectodysplasin A receptor
EGF	Epidermal growth factor
EMP	Erythro-myeloid progenitor
ELISA	Enzyme-linked immunosorbent assay
ER-TR7	Reticular fibroblast and reticular fibre

F:

Fc	Fragment crystallizable region
FcR	Fc receptor
FCS	Fetal calf serum
FDC	Follicular dendritic cell
FRC	Fibroblastic reticular cell

G:
Gp38 Glycoprotein 38

H:
HEV High endothelial venule
HLA-DR Human Leukocyte Antigen – DR isotype
HSC Hematopoietic stem cell

I:
IBD Inflammatory bowel disease
ICAM Interacellular Adhesion Molecule
IFN Interferon
IKK IκB kinase
IL Interleukin
iNOS inducible nitric oxide synthase
ITGA2b Integrin alpha-II beta
ITIM Immunoreceptor tyrosine-based inhibitory motif

K:
KLH Keyhole limpet hemocyanin

L:
LEC Lymphatic endothelial cell
LN Lymph node
LN-LEC Lymph node lymphatic endothelial cell
LT Lymphotoxin
LTi Lymphoid tissue inducer
LTO Lymphoid tissue organizer
LYVE1 Lymphatic vessel endothelial hyaluronan receptor 1

M:
MAdCAM-1 Mucosal vascular addressin cell adhesion molecule 1
Mac-1 Macrophage antigen 1
MALT Mucosal associated lymphoid tissue
MAPKs Mitogen activated protein kinases
MARCO Macrophage receptor with collagenous structure
M-CSF-1 Macrophage-colony stimulating factor 1
M-CSFR Macrophage-colony stimulating factor receptor 1
MERTK Myeloid-epithelial-reproductive tyrosine kinase
MHC Major histocompatibility complex
MIP Macrophage Inflammatory Protein
MMM Marginal metallophilic macrophage
MSM Medullary sinus macrophage
MRC Marginal reticular cell
mRNA messenger RNA
mTEC medullary thymic epithelial cell
MZ Marginal zone
MZM Marginal zone macrophage

N:
NFATc1/2 Nuclear factor of activated T-cells, cytoplasmic 1 or 2

NF-κB	Nuclear factor of kappa B
NIK	NF-kB-inducing kinase
NGFR	Nerve growth factor receptor
Null	Nullizygous

O:

OB	Osteoblast
OC	Osteoclast
OPG	Osteoprotegerin

P:

PAMP	Pathogen-associated molecular pattern
PDB	Paget's disease of bone
PBS	Phosphate buffer saline
PCR	Polymerase chain reaction
PD-1	Programmed death protein 1
PD-L1	Programmed death protein – ligand 1
PDGF	Platelet-derived growth factor
PECAM	Platelet endothelial cell adhesion molecule
PF4	Platelet factor 4
PLVAP	Plasmalemma vesicle-associated protein
PRR	Pathogen-recognition receptor
Prox1	Prospero homeobox 1
PTA	Peripheral tissue restricted antigen

Q:

| **qRT-PCR** | quantitative Real time – polymerase chain reaction |

R:

RALDH2	Retinoic acid synthesizing enzyme, retinol dehydrogenase 2
RBC	Red blood cell
RANK	Receptor activator of NF-κB
RANKL	Receptor activator of NF-κB ligand
RNA	Ribonucleic acid
RP	Red pulp
RPM	Red pulp macrophage
RT	Reverse transcription

S:

SCS	Subcapsular sinus
SDF	Stromal cell derived factor-1
Siglec	Sialic-acid-binding immunoglobulin-like lectin
SIGN-R1	Specific ICAM-3 grabbing nonintegrin-related 1
SLC	Secondary lymphoid organ chemokine
SLO	Secondary lymphoid organs
SMA	Alpha smooth muscle actin
SMP	Splanchnic mesodermal plate
Src	Sarcoma virus kinase
SR	Scavenger receptor
SSM	Subcapsular sinus macrophage
S1P	Sphingosine-1-phosphate

T:

TACE	Tumor necrosis factor-α-converting enzyme
TBM	Tingible-body macrophage
TGF-β	Transforming growth factor β
THD	TNF homology domain
TLR	Toll-like receptor
TNF	Tumor necrosis factor
TNFRSF	Tumor necrosis factor receptor superfamily
TNFSF	Tumor necrosis factor superfamily
TRAF	TNF receptor associated factor
TRAP	Tartrate-resistant acid phosphatase
TRAIL	Tumor-necrosis-factor related apoptosis inducing ligand
TRAMP	Tumor-necrosis-factor related apoptosis-mediating protein
TRANCE	TNF-related activation-induced cytokine
TRANCER	TNF-related activation-induced cytokine receptor
Treg	regulatory T cells
TrMφ	Tissue-resident macrophage
TZM	T cell zone macrophage

V:

VCAM-1	Vascular cell adhesion protein 1
VE-cadherin	Vascular endothelial cadherin
VEGF	Vascular endothelial growth factor
VEGFR	Vascular endothelial growth factor receptor
VEGI	Vascular endothelial growth inhibitor

General introduction

Tumor necrosis factor superfamily (TNFSF) and tumor necrosis factor receptor superfamily (TNFRSF) members are biological molecules that can induce survival, proliferation or death transduction signalings in cells. They have some redundant and pleiotropic effects and are involved in many biological processes such as bone formation and homeostasis, lymphoid organogenesis, morphogenesis of epithelial appendages, hematopoiesis as well as immune cell regulation. Many TNFSFs and TNFRSFs are constitutively expressed or inducible in T and B lymphocytes and in antigen presenting cells (APCs) such as dendritic cells (DCs) and macrophages. However, they are also expressed by non-immune cells including fibroblasts, endothelial cells and epithelial cells.

TNFα (TNFSF1A), TNFβ also known as lymphotoxin alpha (TNFSF1B) and their receptors TNFR1 and TNFR2 (TNFRSF1A and TNFRSF1B), Receptor activator of nuclear factor kappa B ligand (RANKL, or TNFSF11) and its receptor RANK (TNFSF11A) are examples of TNFSF and TNFRSF superfamilies. They are expressed by different cells and tissues and function in different biological processes. However, their biological functions may overlap. For instance, the cooperation between RANKL and TNFα drives the osteoclastogenesis. Both RANKL and TNFβ (LTα) are required for secondary lymphoid organogenesis. Moreover, the cooperation between RANKL and TNFSF member CD40 ligand controls DC activation and function.

The stroma of tissues is built of diverse cell types depending on the resident tissues where they construct the extracellular matrix and support the parenchyma. Because they support tissue functional cells (parenchyma), the fate of the latter may be shaped by residing stromal cells. Critical roles of the non-immune compartment (stroma) of lymphoid organs have emerged over years.

In my Ph.D. work, the roles of lymph node (LN) stromal mesenchymal cells (lymphoid tissue organizers, LTOs and marginal reticular cells, MRCs) and lymphatic endothelial cells (LECs) on the fate of sinusoidal macrophages were studied. The outcomes of stroma-targeted genetic deletion of RANKL and RANK as well as macrophage-targeted genetic deletion of RANK and lymphotoxin α1β2 receptor (LTβR) on the differentiation of CD169$^+$ macrophages of lymphoid organs were analyzed.

Chapter 1. Tumor necrosis factor superfamily (TNFSF) and TNF receptor superfamily (TNFRSF)

The TNFSF and TNFRSF superfamilies comprise 19 ligands and 29 receptors in human and mouse. TNFα and TNFβ (LTα), were the first members of ligands to be identified and named as tumor necrosis factors for their necrotic action on tumor cells[1,2]. The ligands are type II homo or heterotrimeric transmembrane proteins that share a common structural motif called TNF homology domain (THD) in their extracellular C-terminus. The THD domains bind specifically to variable cysteine-rich domains (CRDs) of their receptors. Otherwise, the extracellular domains of some ligands can be specifically cleaved by metalloproteases to form soluble cytokines.

The receptors are type I or III transmembrane proteins that contain extracellular heterogeneous modules of CRDs which determine the specificity binding of their related ligands. Many of them including TRAIL-R1/2, TRAMP, DR6, NGFR, TNFR1, Fas and EDAR contain death domains (DDs) in their intracellular region, which can recruit caspase-interacting proteins to induce cell death. The intracellular domains of the other receptors lack DDs and deliver activating or survival signals to the cell.

Human TNFSFs and TNFRSFs with the documented interactions between ligands and receptors in shown in figure 1.
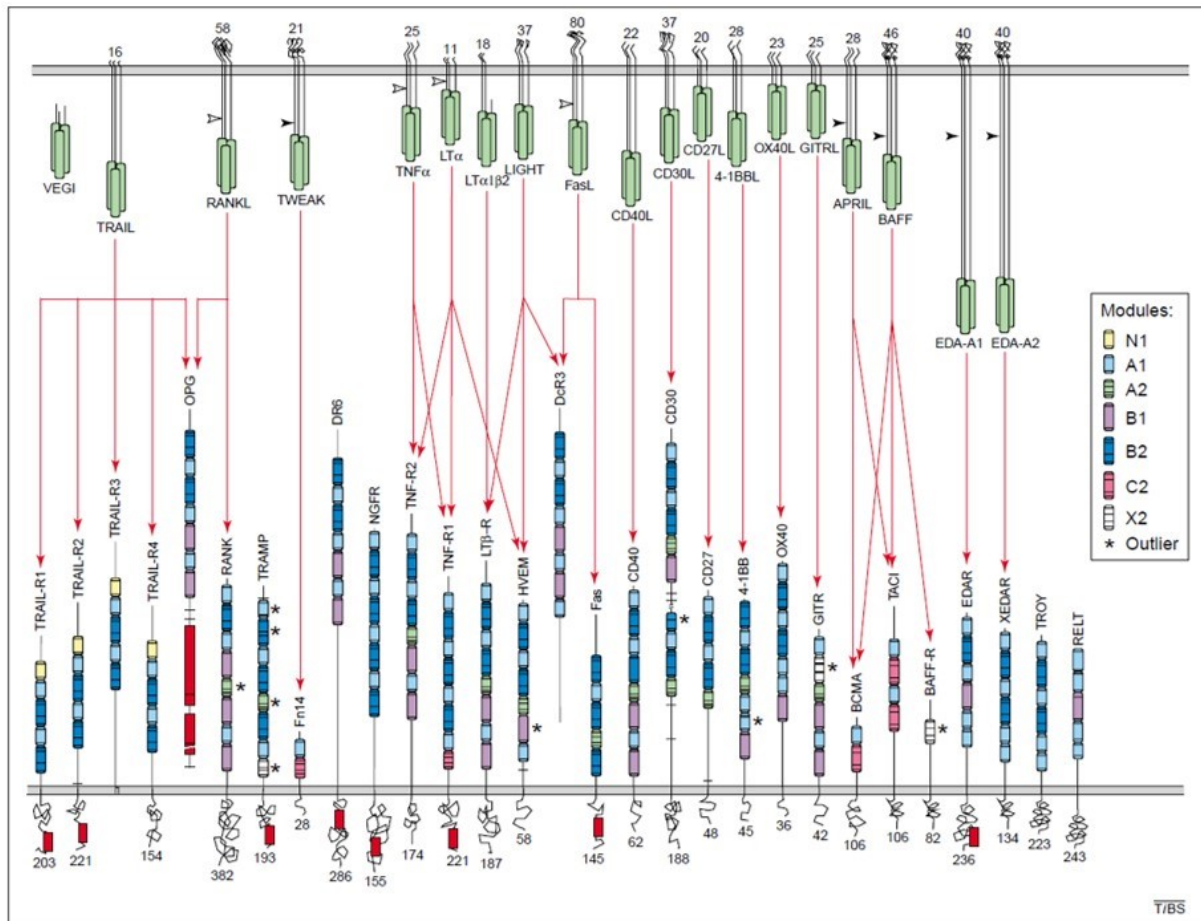
Figure 1. TNF superfamily (TNFSF) and TNF receptor superfamiy (TNFRSF) in humans. The documented interactions (red arrows) between ligands (top) and receptors (bottom) are shown. With the exception for VEGI which is expressed as soluble protein, ligands are trimeric type II transmembrane proteins containing THDs (TNF homology domains, green boxes) in their extracellular regions. Some ligands can be cleaved by proteases (white and black arrowheads indicate cleavage sites) to form soluble cytokines. The receptors are type I or type III transmembrane proteins but can also exist as soluble or anchored proteins. Their extracellular ligand binding regions are cysteine-rich domains (CRDs) comprising variable tandems of modules (N1, A1, A2, B1, B2, C2 and X2 as shown color-coded in the box). The intracellular death domains (DDs) of some receptors are shown as red boxes. Some ligands interact with more than one receptor whereas other show a unique receptor interaction. The numbers indicate the lengths of extracellular domains of ligands and receptors. Modified after[3].

1 Examples of TNF superfamily members: TNFα, LTα/β and RANKL

1.1 TNFα and TNFβ (LTα)

Human TNFα and TNFβ were the first members of TNF superfamily to be cloned and expressed in 1984[4-6]. They are secreted glycosylated proteins of 157 and 171 amino acid residues respectively, share 33% of sequence homology and have high structure similarity. They compete for binding to their receptors TNFR1 and TFNR2. LTα can associate with membrane-bound LTβ to form $LT\alpha_1\beta_2$ heterodimer, the predominant form found at the surface of lymphocytes[7] that binds to LTβR, its primary receptor. The murine lymphotoxin cDNA was cloned and expressed in 1987 and its gene structure shows 74% of homology with human LTα[5]. The extracellular domains of TNF receptors are composed of CRDs. Each CRD is typically characterized by six cysteine residues that form three disulfide bonds. TNFR1 and TNFR2 contain four CRDs that have different functions. CRD1 is important for the anchorage of the receptor at the cell surface, CRD2 and CRD3 mainly contain the ligand binding regions while the function of CRD4 is still known[10]. The structure of LTβR is similar to those of TNFR1. However, the orientation of the ligand binding domain in their CRD2 and CRD3 differs, consistent with the different cognate ligands[11]. In contrast to both TNFR2 and LTβR, the intracellular domain of TNFR1 contains a death domain (see figure 1). Examples of TNFSF-TFNRSF interactions are shown in figure 2.
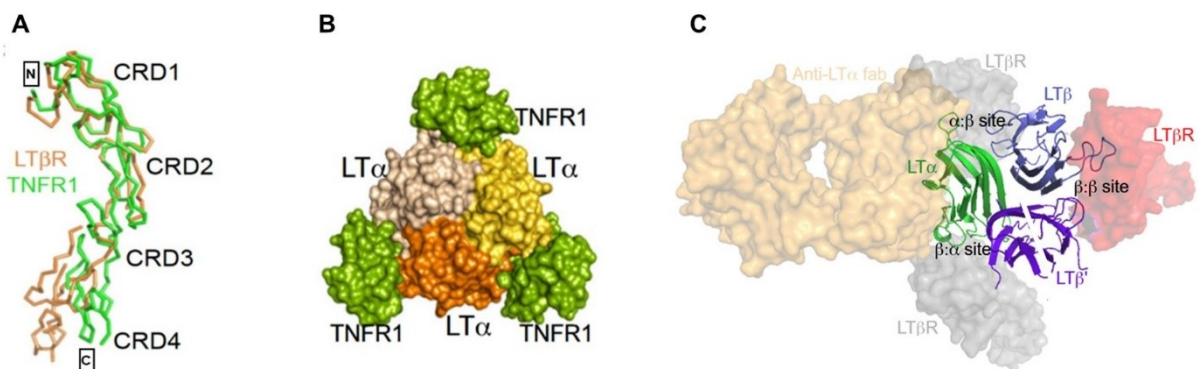
Figure 2. Crystal structures of LTα₃-TNFR1 and LTα₁β₂-LTβR complexes. (A) Alignment of the secondary structures of TNFR1 (Green) and LTβR (Orange) revealing structure similarity. Modified after[11]. (B) Structure of lymphotoxin-α homotrimer (LTα₃, shown in beige, yellow and orange) bound to TFNR1 trimer (green). (C) Models of LTβR binding to the β:β site (Red) and to either the α:β site or β:α site (gray) at the surface of complex LTα₁β₂. The yellow highlights an antibody that recognizes and binds to LTα outside the LTβR binding domains. Modified after[11].

1.2 RANKL and its receptors RANK and Osteoprotegerin

RANKL, also known as TRANCE, osteoprotegerin ligand (OPGL) or tumor necrosis factor superfamily member 11 (TNFSF11) was identified as a dendritic cell survival factor and regulator of bone homeostasis[12,13]. It is a type II transmembrane glycoprotein of around 45 kilo Daltons (kDa) but can be cleaved from its extracellular domain by the metalloprotease tumor necrosis factor-α-converting enzyme (TACE), to form a soluble cytokine of around 31 kDa[14]. Human RANKL shares 87% of sequence homology with murine RANKL. Its expression is restricted to few tissues in mouse and human with higher expression in LNs and bone marrow, compared to the spleen and the thymus. In mouse embryo, RANKL is expressed in the spleen, LN, thymus and Payer's patches and in the same tissues in adult[13]. Beyond these lymphoid organs, RANKL is also expressed in neonatal and adult brain, intestine, heart, kidney, liver, lung, skeletal muscle and testes[15]. Its forms a homotrimer and binds to its RANK through its ectodomain, which can also bind its decoy receptor (osteoprotegerin, OPG).

Receptor activator of nuclear factor κ B (RANK), also known as TRANCER (TNF-related activation-induced cytokine receptor) or tumor necrosis factor receptor superfamily member 11a (TNFRSF11A), was discovered by Anderson et al (1997) while sequencing cDNAs from a human bone-marrow-derived myeloid dendritic-cell (DC) DNA library and identified as an enhancer of DC functions[12]. RANK is a type I transmembrane protein of a full-length of 616 amino acids and represents the longest member of TNF receptor superfamily. Human RANK shares 70% of sequence homology with mouse RANK[12]. It is ubiquitously expressed in human tissues and various cell types. Like TNFR1, TNFR2 and LTβR, RANK lacks intrinsic enzymatic activity. Thus, the ligand binding triggers its trimerization and the downstream signaling cascades in the cell requires the recruitment of intracellular adaptors for signal transduction.

OPG is the highly conserved decoy receptor of RANKL, initially identified in rat as a secreted glycoprotein that can exist as a monomer of 60 kDa or a disulfide-linked homodimer. It lacks cell membrane-interacting domain and acts as soluble factor involved in the regulation of bone mass[16,17]. Rat OPG shares 85% and 94% of sequence homology with mouse and human OPG respectively[16]. It harbors two non-functional death domain homologous (DDHs) and a C-terminal heparin binding domain of dimerization. However, the DDHs of OPG can interact with the transmembrane region of Fas to form OPG-Fas fusion protein, that can trigger apoptosis[17]. Beyond RANKL blocking, OPG also functions as decoy receptor with low affinity for tumor

necrosis factor-related apoptosis-inducing ligand (TRAIL) that may conversely block its anti-osteoclastogenic activity[18]. A schematic representation of the architecture of RANKL, RANK and OPG is shown in figure 3.
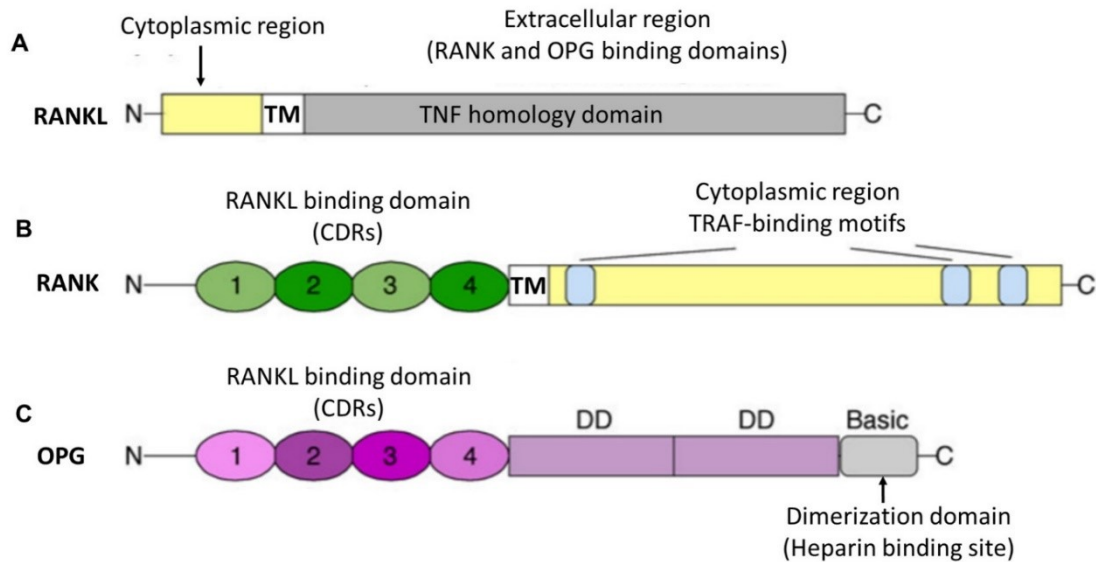
Figure 3. Schematic representation of the architecture of RANKL, RANK and OPG. The different regions with the corresponding ligand or receptor binding domains as well as recruitment motifs and dimerization domain are indicated. N: amino terminal, TM: transmembrane region, CRD: cystein-rich domain, DD: death domain homologous, C: carboxy-terminal. Modified after[19].

RANK binds RANKL with a strong affinity with a dissociation constant of the complex going up to 10^{-11} molar[20]. Key surface amino acid residues of RANK, including mainly Asparate, Arginine, Lysine are involved in this interaction by salt bridges formation with RANKL[21]. The biological RANK-RANKL complex is formed by the interaction between the extracellular region of one molecule of RANK with the ectodomain of one RANKL monomer to form a heterodimer. Then three heterodimers assembly to form the biological hetero-hexameric complex[20].

OPG binds RANKL with higher affinity than RANK. It engages a different set of amino acid residues at the interface of interaction with RANKL. The nature of OPG-RANKL interactions is primarily hydrophobic whereas RANK-RANKL interactions are mainly charge driven (ionic) and imply hydrogen bonds. The aromatic ring of the amino acid Phenylalanine 96 of OPG may significantly account for the better affinity with RANKL[19]. The crystal structures of RANK-RANKL and OPG-RANKL complexes are shown in figure 4.
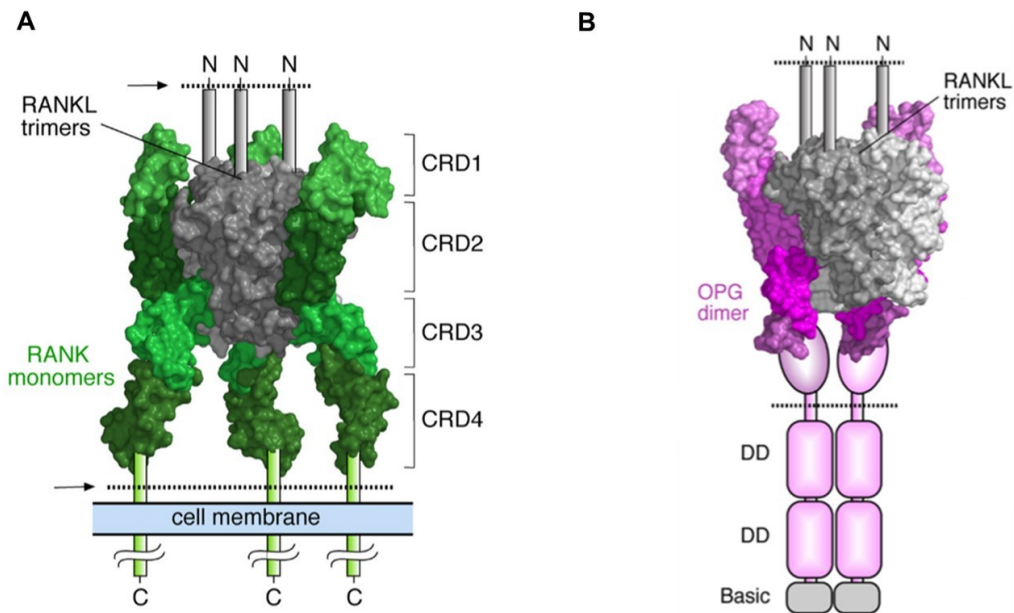
Figure 4. Crystal structures of RANK-RANKL and OPG-RANKL complexes. (A) The biological RANK-RANKL complex in the context of cell membrane insertion. By moving through the hinge linking CRD2 and CRD3, RANK closely contact with the ectodomain of RANKL. RANKL monomers self-associate to form a homotrimer. Three monomers of RANK bind the ectodomains of RANKL trimer, leading to the assembly of the biological hetero-hexameric complex. (B) The biological complex of OPG dimer and RANKL trimer in the context of cell membrane insertion. Two monomers of OPG covalently dimerizes to form a disulfide-linked homodimer which bind the ectodomains of RANKL trimer. Doted lines indicate the extracellular and the intracellular amino terminal (N) regions of RANK and RANKL, respectively or relative to OPG death domain homologous (DD). The gray boxes of OPG indicate the basic heparin binding domain of dimerization. Modified after[19].

1.3 Nuclear factor of kappa B (NF-kB) signaling pathways

In mammals, the NF-kB consists of five related transcription factors including p50, p52, RelA (p56), c-Rel and RelB. These transcription factors are characterized by a N-terminal DNA binding (dimerization) domains called Rel homology domains, that relates them. These domains allow them to form homo or heterodimers that bind to a range of related target sequences on the DNA called kappa B sites. In contrast to p50 and p52, the other members contain a C-terminal transcription activation domain, which enables them to bind and modulate target genes. There are two different pathways of NF-kB signaling that can be activated by different sets of stimuli: the canonical (classical) pathway that relays the activation of p50:RelA (p65) and p50:c-Rel complexes and the non-canonical (alternative) pathway that relays the activation of p52:RelB complexes. The activation of both pathways can overlap but each pathway regulates the expression of different target genes.

1.4 Canonical NF-kB pathway

RANKL, TNFα and LTα$_1$β$_2$ heterodimer can activate the canonical pathway of NF-kB. Since their cognate receptors lack intrinsic enzymatic activities, the downstream signaling cascades after their ligation require the recruitment of adaptor proteins such as TRAF6 (TNF receptor-associated factor 6) and TRAF2/5. This is followed by the activation of the trimeric IkB Kinase (IKK) complex, that consists of the catalytically active kinases (IKKα and IKKβ) and the regulatory subunit NF-kB essential modulator (NEMO, also called IKKγ). This complex phosphorylates IkBα, leading to its polyubiquitination and proteasomal degradation. IkBα degradation leads to the release of the heterodimer p50:RelA triggering its translocation to nucleus where it induces target gene expression such as transcription factors c-Fos, nuclear factor of activated T-cells, cytoplasmic 1 (NFATc1/2), osteoclast precursor differentiation factors, the protein inhibitor of the non-canonical pathway (p100), and inflammatory genes such as VCAM-1, MIP-1β, MIP-2[22]. The canonical pathway is implicated in cell differentiation, proliferation and survival as well as production of cytokines and antimicrobial mediators. A basal processing of p100 generated through this pathway may activate the non-canonical pathway that relies essentially on the activity of IKKα kinase.

1.5 Non-canonical NF-kB pathway

The non-canonical NF-kB pathway is also activated by RANKL. The downstream signaling cascades following RANKL ligation requires the recruitment of TRAF3 and TRAF2. The interaction of TRAF2 with TRAF3 may facilitate the ubiquitination and degradation of the latter, leading to the release of NF-kB-inducing kinase (NIK). The latter phosphorylates and activates the alpha subunit of IkB kinase (IKKα). This leads to the proteasomal processing of p100 to generate p52. The latter associates with its partner (RelB) to form the heterodimer RelB:p52 that translocates to the nucleus. The heterodimer induces the expression of genes mainly involved in secondary lymphoid organogenesis and homeostasis such as the stromal cell derived factor-1 (SDF-1 or CXCL12), the secondary lymphoid tissue chemokine (SLC or CCL21), the B cell activation factor (BAFF), CCL19 as well as the B lymphocyte chemoattractant (BLC or CXCL 13)[23]. The mechanisms of NF-kB pathway activation are shown in figure 5.
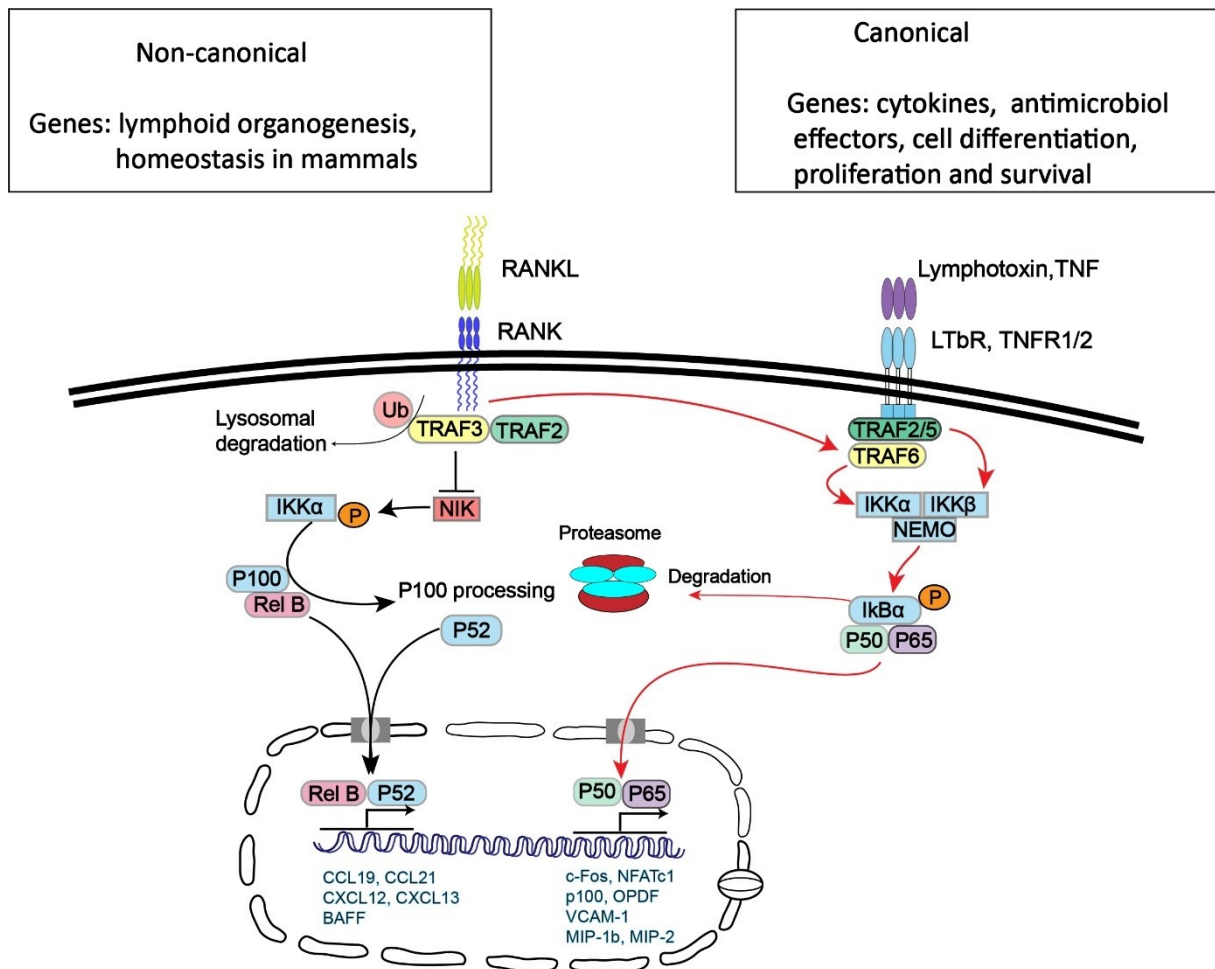
Figure 5. Nuclear factor of kB transcription factor signaling pathways. The Nuclear factor of kB family consists of p50, p52, RelA, RelB and c-Rel (not shown here) transcription factors. They form heterodimers that are blocked in the cytoplasm of unstimulated cells by IkB type inhibitory proteins such as IkBα and p100 and can be activated in two pathways. The canonical pathway is activated when RANKL, TNF or Lymphotoxin bind to their cognate receptors. The downstream signaling relay on the recruitment of TRAF family adaptors (TRAF6 and TRAF2 or 5), resulting to the activation of IkB Kinases (IKKα and IKKβ and NEMO) that phosphorylate IkBα, leading to its degradation and the release of p50:p65 (p50:RelA) heterodimer. The latter translocates to the nucleus and activates target gene expression. The non-canonical pathway is efficiently activated in response to RANKL but not to TNFs. A series of signaling cascades involving TRAF3 and 2, as well as NIK and IKKα kinases leads to the processing of p100 and the generation of p52. The latter associates with RelB to form RelB:p52 heterodimer that translocates to the nucleus and activates target genes.

2   Biological functions of TNFSF molecules

TNFα and LTα are cytotoxic cytokines with very similar biological activities, initially discovered for their antiproliferative activities and killing effects on tumor cells. TNFα is produced by Toll-like receptor-stimulated monocytes and macrophages and by activated CD4^{+} and CD8^{+} T cells whereas LTα is produced mainly by T and B lymphocytes and lymphoid tissue inducer (LTi) cells, which also showed surface expression of LTβ during LN development[24].

2.1   Lymphotoxin LTα$_1$β$_2$ in secondary and tertiary lymphoid organogenesis

The LTα$_1$β$_2$-LTβR axis is crucial for secondary lymphoid organ (SLO) development. Mice deficient for either LTα$_1$β$_2$ or LTβR lack LNs, Payer's patches, follicular dendritic cell (FDC) network and exhibit severe defects in spleen B and T cell architecture and impaired cellularity[25,26]. Mice transgenic for LTα (RIPLTα mouse) exhibited infiltrates in kidney and pancreas, that resemble tertiary lymphoid organs, a non-lymphoid tissue characterized by the ordered accumulation of lymphocytes during chronic infection or inflammation and autoimmunity. These infiltrates form at sites of transgene derived LTα expression, revealing the ectopic lymphoid tissues formation upon LTα overproduction during chronic inflammation[27]. The LTα$_1$β$_2$-LTβR axis controls the maturation of high endothelial venules (HEVs) during LN development and homeostatic maintenance in adults[28] and is thought to foster cell infiltration through HEVs during inflammation. Different inhibitors of this axis have been developed to be used in several mouse models of autoimmunity[29] and inflammation such as Sjögren's syndrome[30].

2.2   TNFα in sepsis and other inflammatory disorders

Sepsis is a syndrome that occurs when microbial pathogens invade the bloodstream of patients and is characterized by a systemic inflammation that can lead to septic shock and death. This systemic inflammation is due to an excessive production of natural pro-inflammatory cytokines leading to lethal tissue injury. A series of studies in human and animals have highlighted the role of TNFα (produced by activated macrophages) as a significant mediator for septic shock[31,32] leading to a worldwide hope for the development of anti-TNF therapies for patients with sepsis[33]. However, the clinical trials using inhibitors or anti-TNF antibodies unfortunately and surprisingly failed to improve the overall mortality in the highly heterogeneous group of patients[33,34]. Yet, TNFα blocking and inhibitory agents are widely

administered to patients with rheumatoid arthritis, psoriasis as well as inflammatory bowel disease (IBD) in which TNFα is involved in the pathogenesis[35-37].

2.3 The RANK-RANKL axis in osteoclastogenesis

The homeostatic control of bone mass is accomplished through bone formation by osteoblasts (OBs) and resorption by osteoclasts (OCs). This process constantly maintains bone remodeling and repair. OBs are bone forming cells that arise from bone marrow mesenchymal stem cells and OCs are hematopoietic lineage-derived macrophages specialized in bone destruction[38,39]. They secrete acids that digest and remove bone material to form lacunae, a process important for the formation of marrow cavity, the reservoir for hematopoiesis. RANKL is expressed by OBs whereas RANK is expressed by OCs; RANK is upregulated by the macrophage colony stimulating factor-1 (M-CSF-1)[40,41]. TNFα also stimulates RANK expression by OC precursors as well as RANKL expression by bone stromal cells, promoting osteoclastogenesis[42,43]. The direct RANK-RANKL interaction between OBs and OC precursors in bone stroma drive osteoclast differentiation, a process known as osteoclastogenesis. Various factors such as vitamin D3, prostaglandin E2, IL-1, IL-11, TNFα and glucocorticoids known as calciotropic factors promote osteoclastogenesis by inducing RANKL expression in OBs. On the other hand, factors such as estrogen and TGFβ negatively regulate osteoclast formation by upregulating OPG expression by OBs[53].

In addition to p50:RelA and p52:RelB transcription factors, RANK activation in OCs can trigger other signaling cascades involving NFATc1/2, mitogen activated protein kinases (MAPKs) as well as c-Src proto-oncogene kinase (Src kinase), that control the lineage commitment and OC differentiation[44]. The activation of MAPKs induces AP-1 family members of transcription factors that control the expression of genes and mRNA stability for osteoclastogenesis[44]. Stimulation of pre-OCs with RANKL increases the level of NFATc1/2, leading to terminal differentiation of OCs by promoting the expression specific genes such as tartrate-resistant acid phosphatase (TRAP) and calcitonin receptor (CALCR)[44,45]. The interaction of Src kinase with TRAF6 after RANK activation enhances its kinase activity and the phosphorylation and activation of the anti-apoptotic serine/threonine kinase Akt, that may support OC survival and functions. Indeed, mice deficient in c-src proto-oncogene show osteopetrosis, due to impaired OC activity[46]. Mice deficient in RANKL or RANK show severe osteopetrosis characterized by a complete absence of TRAP$^+$ OCs, growth retardation and lack of tooth eruption[47,61]. A

schematic diagram of the RANK-RANKL axis-induced signaling cascades that control the oscletoclastogenesis and OC activation is shown in figure 6.
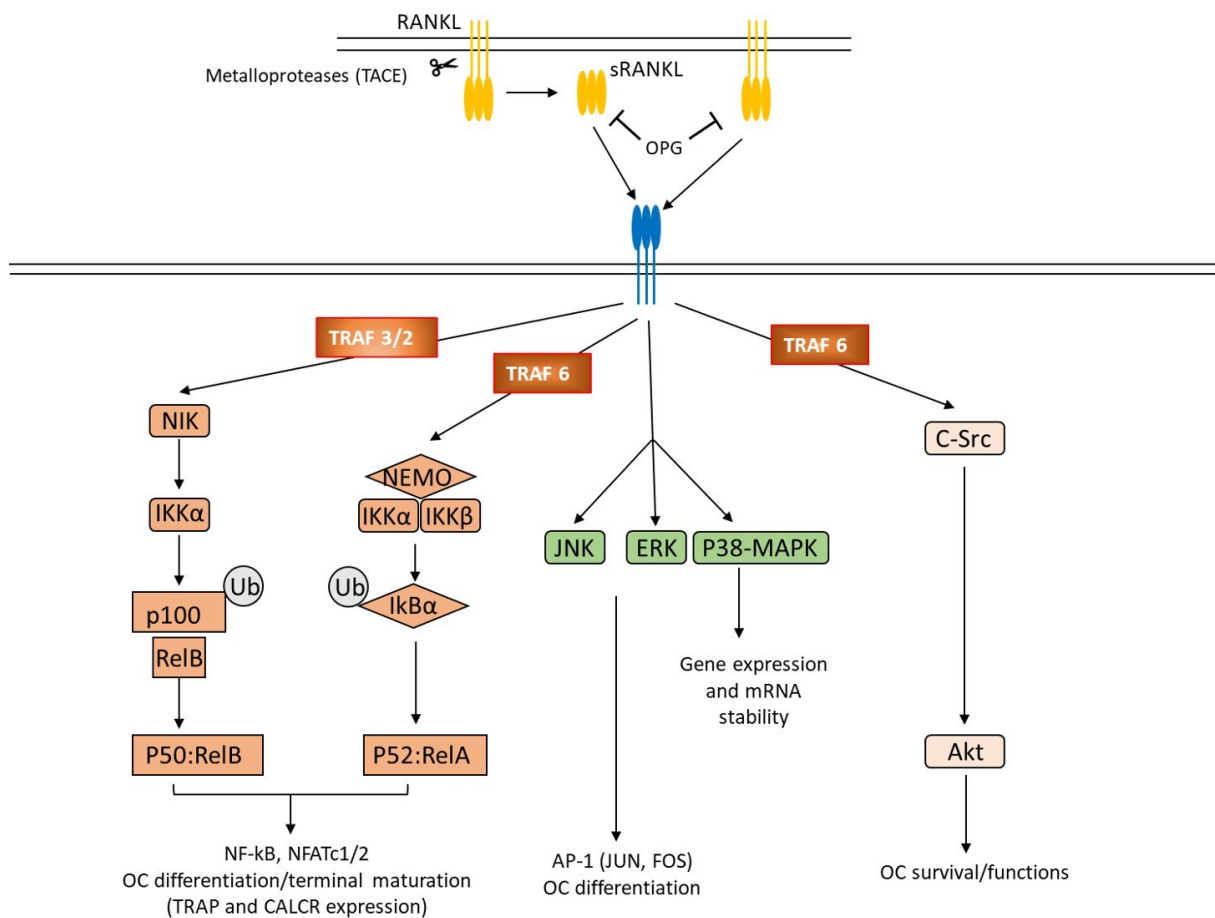
Figure 5. **Schematic diagram of the RANK-RANKL axis-induced signaling cascades that control the osteoclastogenesis and OC activation**. Membrane-bound RANKL or soluble RANKL (sRANKL) released from the cleavage by the metalloproteases such as TACE, binds and activates RANK. RANK stimulation induces the both canonical and non-canonical NF-kB, MAPK as well as the phosphatidylinositol pathways to control osteoclastogenesis through adaptor molecules such as TRAF proteins. MAPK family members (JNK1 and JNK2) control AP-1 family members, such as JUN, FOS which regulate expression of important genes required for osteoclast differentiation and mRNA stability. Src kinase interacts with TRAF6 after RANKL ligation and triggers the phosphatidylinositol pathway, consisting of coordinated actions of a variety of lipid kinases and phosphatases, resulting in activation of kinases such as the anti-apoptotic serine/threonine kinase Akt that supports OC survival and activation. RelA/B, rel avian reticuloendotheliosis viral oncogene homolog A/B. JNK, c-Jun N-terminal kinases. Adapted after[44] .

OPG is a negative regulator of osteoclastogenesis and is capable to inhibit mature OC function *in vitro*[48]. Transgenic mice overexpressing OPG exhibit severe osteopetrosis (increased bone mass) due to defects in OC differentiation[49]. On the contrary, mice deficient for OPG are osteoporotic (decreased bone mass) due to an excessive number of OCs[50]. The cytokine M-CSF-1, produced by mature OBs but also by OC precursors is crucial for the proliferation and differentiation of OCs. Mice deficient for M-CSF-1 are osteopetrotic, with an almost complete absence of osteoclasts, increased bone matrix and absence of marrow cavities[51].

Chronologically, bone development starts by the formation of cartilage rudiment during fetal life and is coupled to the differentiation of OBs and OCs. For instance, in mouse, the cartilage rudiment of the metatarsal bone is formed by embryonic day 15 (E15) and starts to mineralize at E16, concomitantly with the apparition of early OBs, which progressively form bone around the center of the cartilage. This is correlated with the apparition and the proliferation of the premitotic progenitors of OCs during the same period. From E16 to E17, the mineralization and bone deposition significantly progresses along the cartilage, and the progenitors acquire OC specific markers (TRAP and CALCR). At E18, mature OCs become active, invade and digest the mineralized cartilage, forming bone marrow cavities for hematopoiesis niche[52]. The chronology and the control of osteoclastogensis by the RANK-RANKL axis are shown in figure 7 and 8, respectively.
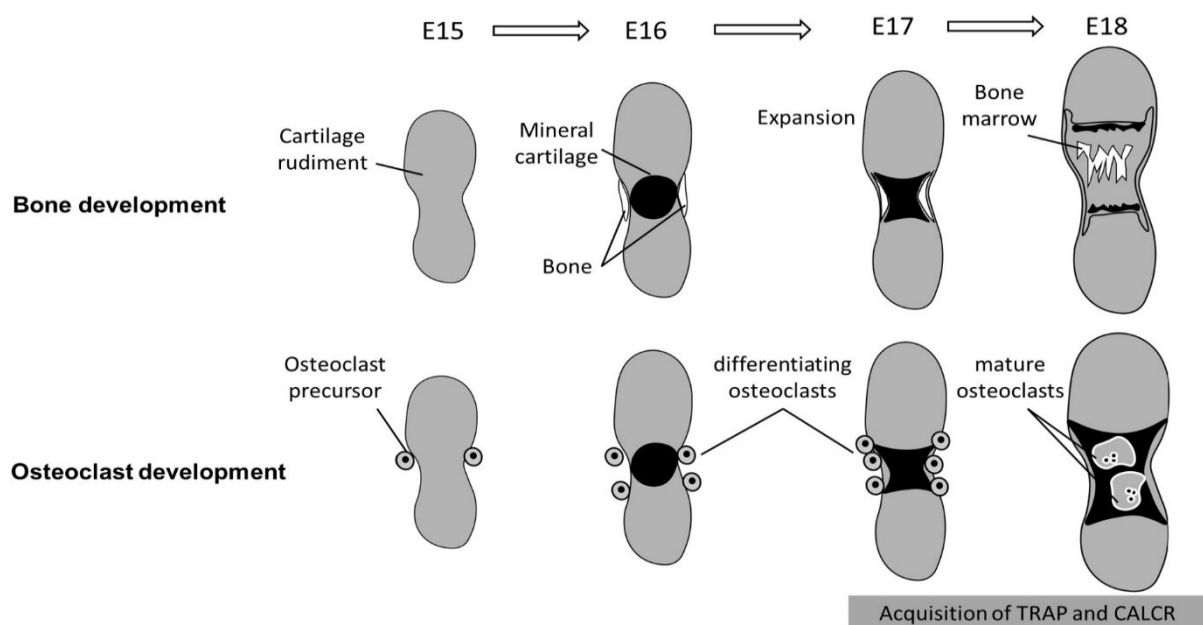
Figure 7. Concomitant and chronological development of bone and oscteoclast. Schema is an example for mouse metatarsal bone. TRAP: tartrate-resistant acid phosphatase. CALCR: calcitonin receptor. Modified after[52].
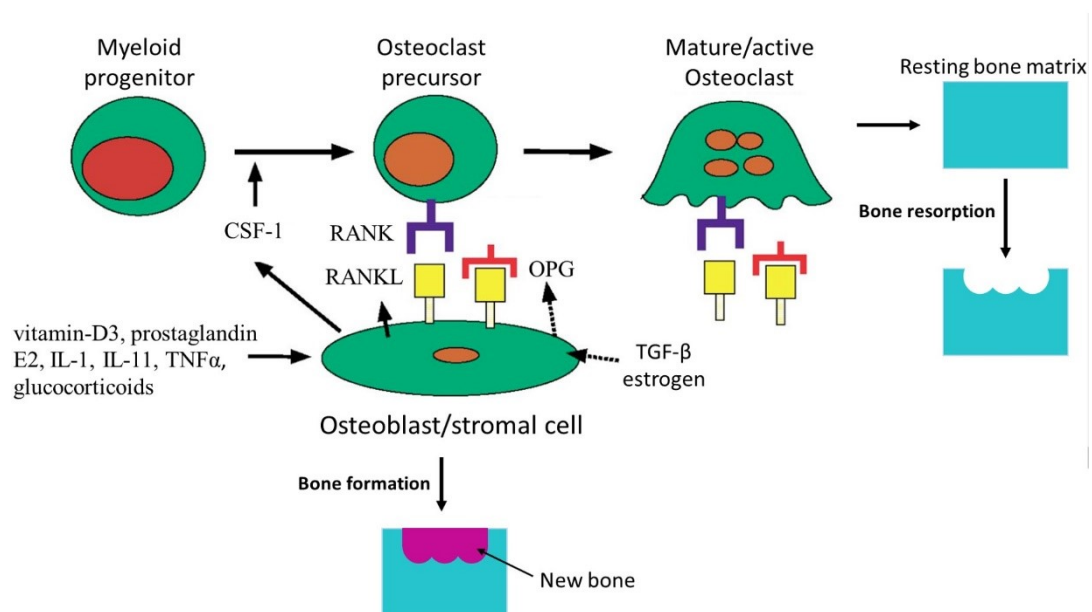
Figure 8. Mechanisms of osteoclastogenesis. Various calciotropic factors including vitamin D3, prostaglandin E2, IL-1, IL-11, TNFα and glucocorticoids induce RANKL expression on osteoblast. The latter activates RANK expressing osteoclast precursor derived from myeloid progenitor upon the survival factor M-CSF-1, leading to osteoclast formation. Mature osteoclast also expresses RANK and requires RANKL stimulation for its bone resorbing activity. Factors such as estrogen and TGFβ negatively regulate osteoclast formation by upregulating OPG expression on osteoblast. Modified after[53].

Increased osteoclast activity leading to excessive bone resorption or damage (lesions) is responsible for many disorders such as the Paget's disease of bone (PDB), rheumatoid arthritis, lytic bone metastases, etc[40]. Mutations that disrupt RANK-RANKL signaling also underlie diseases. For instance, an increased RANK-mediated NF-kB activation due to heterozygous mutation in the exon 1 of *Rank* has been linked to PDB and familial expansile osteolysis, an autosomal dominant bone disease characterized by deafness, loss of teeth, skeletal change or deformation, etc. This mutation disrupts the function of RANK signaling leading to a constitutive activity of the receptor[54]. Another inherited bone disease known as expansile skeletal hyper-phosphatasia is due to the duplication of a 15 base pair tandem repeat in the signaling moiety of RANK. It is also characterized by accelerated bone remodeling, premature loss of teeth, early onset of deafness, episodic hypercalcemia, etc[55]. An inactivating mutation in the gene encoding OPG that results in loss of function is responsible for juvenile Paget's disease in which children gradually develop loss of bone density (osteopenia), progressive skeletal deformity and strong susceptibility to fractures[56]. Otherwise, many factors including environmental changes, homeostatic dysregulation,

hormonal changes, etc, cause bone disorders. For instance in post-menopausal women, the natural decrease of estrogen resulting in an imbalance in OC activity versus new bone formation by OBs causes postmenopausal osteoporosis[57,58,60]. The levels of RANKL is increased on bone marrow pre-OBs of post-menopausal osteoporotic women[59]. Moreover, women and men suffering from breast and prostate cancers that undergo estrogen or testosterone suppression may also suffer from osteoporosis due to increased RANKL expression[58,60].

2.4 The RANK-RANKL axis in secondary lymphoid organogenesis

In addition to severe osteopetrosis, mice deficient for RANKL fail to develop LNs and show marked deficiency of spleen B cells but display normal Payer's patches[47]. Mice deficient for RANK exhibit similar phenotypes[61]. Other intracellular signaling molecules have been reported to be crucial for LN organogenesis and other lymphoid organs in genetically deficient mice. A summary of these mutant mice with defective lymphoid organogenesis has been reported in 2003 by Mebius et al., and summarized in table 1.

Gene mutation (in mice)	LN formation	Payer's patches	NALTs
Ltα⁻ᐟ⁻, Ltβr ⁻ᐟ⁻, Nik ⁻ᐟ⁻, *aly/aly, Rela × Tnfr⁻ᐟ⁻*	-	-	+
Nfκb2⁻ᐟ⁻, Relb⁻ᐟ⁻	+*	-	N.D
Ltβ ⁻ᐟ⁻	CLN, MLN	-	+
Light⁻ᐟ⁻ × Ltβ⁻ᐟ⁻	Less MLN than *Ltβ⁻ᐟ⁻*	-	N.D
Tnfr p55⁻ᐟ⁻	+	- or reduced in number	+
Tnf⁻ᐟ⁻	+	reduced in number	+
Ltα⁺ᐟ⁻ × Ltβ ⁺ᐟ⁻	+	-	N.D
Ikkα⁻ᐟ⁻	N.D	-	N.D
Rankl⁻ᐟ⁻, Rank⁻ᐟ⁻, Traf6⁻ᐟ⁻	Some CLN	+	+
Ikaros⁻ᐟ⁻	-	-	N.D
Rorγ⁻ᐟ⁻	-	-	+
Il7r ⁻ᐟ⁻, Jak3⁻ᐟ⁻, γ c⁻ᐟ⁻	BLN, ALN, MLN	-	+
Id2⁻ᐟ⁻	-	-	-
Il7⁻ᐟ⁻	MLN?	- ‡	N.D
Cxcl13⁻ᐟ⁻, Cxcr5⁻ᐟ⁻	CLN, FLN, MLN	0-2 formed	N.D

Table 1. Summary of mutant mice with defective secondary lymphoid organogenesis. NALT stands for nasal-associated lymphoid tissue. ⁻ᐟ⁻ and ⁺ᐟ⁻: homozygous and heterozygous null mutants respectively. *aly*: alymphoplasia. *Lt:* Lymphotoxin. *Nik*: nuclear factor κB-inducing kinase. *Tnf*: tumor-necrosis factor. *Nf-κb2*: nuclear factor-κB2. *Light:* lymphotoxin inducible glycoprotein D on T lymphocytes. *Ikk*: inhibitor of κB kinase. *Rank* (l): Receptor activator of NF-kB (ligand). *Traf6*: TNF-receptor-associated factor 6. *Ikaros* is important primarily for the development of the lymphoid lineage[62]. *Rory*: retinoid-related orphan receptor γ. *Il-7*:

interleukin-7. *Jak3*: Janus kinase 3. γc: common cytokine receptor γ-chain. *Id2*: Helix-loop-helix inhibitor Id2[63]. CXCL13 stands for chemokine (C-X-C motif) ligand 13 and CXCR5 is its receptor. Minus (–) indicates the absence of lymphoid organs and plus (+) indicates that the mentioned lymphoid organ can develop. The star (*) means lymphoid decline of LNs at 10 day after birth whereas LN development was reported to be normal at birth. N.D: not determined. A, B, C, F and M stands for Axillary, Brachial, Cervical, Facial and Mesenteric LNs. ‡ means some controversial observations about the loss and normal numbers of Paper's patches in IL-7-deficient mice. Modified after[76].

2.5 The RANK-RANKL axis in thymic development

The thymus is the primary lymphoid organ where T cells develop. T cell development proceeds by positive and negative selection of thymocytes successively from the cortex to the medulla of the thymus. In the medulla, specialized stromal cells called medullary thymic epithelial cells (mTECs) express self-tissue–restricted antigens under the control of the transcription factor Aire (Auto-Immune Regulator) and interact with migrating C-C chemokine receptor type 7 (CCR7)-expressing-thymocytes, leading to the elimination of self-reactive T cells. In 2007, Rossi et al., have shown that Aire+ mTECs derive from Aire- progenitors as result of RANK activation. RANK activation in mTEC progenitors is mediated by an intrathymic RANKL-expressing CD4+ LTi population[64]. RANK deficient mice support normal T cell development[61] but lack Aire+ mTECs in their thymic microenvironment[64]. Yet, the authors have also shown that RANK deficiency in thymic epithelial cells promotes the onset of autoimmunity, revealing the crucial role of this signaling in self-tolerance[64].

2.6 The RANK-RANKL axis in mammary gland and hair follicles formation

Mammary gland morphogenesis proceeds in different steps from fetal life to pregnancy. The RANK-RANKL axis is essential for the development of lactating mammary glands. Mice lacking RANKL or its receptor display impaired morphogenesis of mammary gland during pregnancy and defect in the production of breast milk, leading to the death of newborns due to the absence of milk[65]. RANKL regulates mammary gland formation by inducing the proliferation of RANK-expressing mammary epithelial cells, a process that requires the nuclear translocation of the helix-loop-helix protein (Id2) in these cells[66].

RANK signaling also regulates both hair renewal and epidermal homeostasis by stimulating the proliferation of epithelial cells of the epidermo-pilosebaceous unit, comprising the

interfollicular epidermis (IFE), the hair follicle (HF) and the sebaceous gland. *Rank* and *Rankl-null* mice fail to initiate a new growth phase of the hair cycle and display a reduction in epidermal growth. Moreover, mice administrated with recombinant RANKL as well as mice that overexpress RANK in the epidermis show premature hair cycle entry[67].

2.7 The RANK-RANKL axis in intestine microfold cell differentiation

Gut is associated with lymphoid tissues including Payer's patches where most of the IgA production occurs. Similar to other lymphoid organs, the Payer's patches are functionally structured into B cell follicles and the interfollicular areas of T cells below the subepithelial dome. The Payer's patches are colonized by a population of subepithelial RANKL^{+} MAdCAM-1^{-} Podoplanin^{+} CD31^{-} CD45^{-} mesenchymal cell type and by the follicle-associated Microfold (M) cells, the epithelial cells specialized in antigen sampling for IgA induction[71,72]. In 2017, Nagashima et al., have shown that these subepithelial RANKL^{+} mesenchymal cells directly induce M cell differentiation[73]. Specific ablation of RANKL in mesenchymal cells or RANK in epithelial cells severely reduces M cell differentiation and results in a strong reduction of IgA production and loss of CCL20, the cytokine produced by gut epithelium important for B cell migration into the subepithelial dome[73].

2.8 The RANK-RANKL axis in dendritic cell activation and functions

DCs are APCs that reside or migrate into tissues where they capture, process and present antigens to T cells for the induction of adaptive immunity. In 1997, Anderson et al., have identified a subset of human DCs (CD1a^{+} DCs) that express surface RANK and interact with T cells to enhance their growth[74]. Unlike CD40L (the closest counterpart of RANKL) that increases the expression of HLA-DR, RANK as well as co-stimulatory molecules (CD80/86) on DCs, human RANKL only stimulates surface RANK expression on these cells. Moreover, the authors have shown that cytokines such as IL-4 and TGF-β upregulate RANKL expression on T cells. DC interaction with T cells through RANK-RANKL may upregulate CD40L on activated T cells, leading to HLA-DR and CD80/86 expression on DCs to functionally induce T cell proliferation[74]. In 2006, Loser et al., have shown that RANKL expression is upregulated on keratinocytes in inflammatory disease such psoriasis in human and following exposure to inflammatory stimuli in mice[75]. Yet, the authors also have shown that RANKL expressed by keratinocytes modulates the function of RANK^{+} Langerhans cells, the DCs residing in the epidermis, to induce the peripheral expansion of CD4^{+}CD25^{+} T regulatory cells and immune

suppression in mice overexpressing RANKL in the skin[75]. Thus, the RANK-RANKL axis may promote DC-induced immune tolerance.

3   References

1. Granger, G. A., S. J. Shacks, T. W. Williams, and W. P. Kolb. 1969. "Lymphocyte *in vitro* Cytotoxicity: Specific Release of Lymphotoxin-like Materials from Tuberculin-Sensitive Lymphoid Cells." Nature 221 (5186): 1155–57. https://doi.org/10.1038/2211155a0.

2. Carswell, E. A., L. J. Old, R. L. Kassel, S. Green, N. Fiore, and B. Williamson. 1975. "An Endotoxin-Induced Serum Factor That Causes Necrosis of tumors." *Proceedings of the National Academy of Sciences* 72 (9): 3666–70. https://doi.org/10.1073/pnas.72.9.3666.

3. Bodmer, Jean-Luc, Pascal Schneider, and Jürg Tschopp. 2002. "The Molecular Architecture of the TNF Superfamily." *Trends in Biochemical Sciences* 27 (1): 19–26. https://doi.org/10.1016/S0968-0004(01)01995-8.

4. Gray, P. W., B. B. Aggarwal, C. V. Benton, T. S. Bringman, W. J. Henzel, J. A. Jarrett, D. W. Leung, B. Moffat, P. Ng, and L. P. Svedersky. 1984. "Cloning and Expression of CDNA for Human Lymphotoxin, a Lymphokine with tumor Necrosis Activity." Nature 312 (5996): 721–24. https://doi.org/10.1038/312721a0.Kratz, A. 1996. "Chronic Inflammation Caused by Lymphotoxin Is Lymphoid Neogenesis." *Journal of Experimental Medicine* 183 (4): 1461–72. https://doi.org/10.1084/jem.183.4.1461.

5. Pennica, D., G. E. Nedwin, J. S. Hayflick, P. H. Seeburg, R. Derynck, M. A. Palladino, W. J. Kohr, B. B. Aggarwal, and D. V. Goeddel. 1984. "Human tumor Necrosis Factor: Precursor Structure, Expression and Homology to Lymphotoxin." Nature 312 (5996): 724–29. https://doi.org/10.1038/312724a0.

6. Li, C B, P W Gray, P F Lin, K M McGrath, F H Ruddle, and H Ruddle. 1987."Cloning and Expression of Murine Lymphotoxin CDNA."7. J Immunol. 1987; 138:4496-4501. http://www.jimmunol.org/content/138/12/4496

7. Browning, J L, I Dougas, A Ngam-ek, P R Bourdon, K Miatkowski, M Zafari, A M Yampaglia, and W Meier. 1995. "Characterization of Surface Lymphotoxin Forms. Use of Specific Monoclonal Antibodies and Soluble Receptors." J Immunol January 1, 1995, 154 (1) 33-46. http://www.jimmunol.org/content/154/1/33

8. Banner, David W, Allan D'Arcy, Wolfgang Janes, Reiner Gentz, Hans-Joachim Schoenfeld, Clemens Broger, Hansruedi Loetscher, Werner Lesslauer. 1993. "Crystal Structure of the Soluble Human 55 kd TNF Receptor-Human TNFP Complex: Implications for TNF Receptor Activation." Cell, Vol. 73, 431-445. https://doi.org/10.1016/0092-8674(93)90132-A

9. Eck, M. J., and S. R. Sprang. 1989. "The Structure of tumor Necrosis Factor-Alpha at 2.6 A Resolution. Implications for Receptor Binding." The Journal of Biological Chemistry 264 (29): 17595–605. https://doi.org/10.2210/pdb1tnf/pdb.

10. Mukai, Y., T. Nakamura, M. Yoshikawa, Y. Yoshioka, S.-i. Tsunoda, S. Nakagawa, Y. Yamagata, and Y. Tsutsumi. 2010. "Solution of the Structure of the TNF-TNFR2 Complex." *Science Signaling* 3 (148): ra83–ra83. https://doi.org/10.1126/scisignal.2000954.

11. Sudhamsu, J., J. Yin, E. Y. Chiang, M. A. Starovasnik, J. L. Grogan, and S. G. Hymowitz. 2013. "Dimerization of LT R by LT 1 2 Is Necessary and Sufficient for Signal Transduction." *Proceedings of the National Academy of Sciences* 110 (49): 19896–901. https://doi.org/10.1073/pnas.1310838110.

12. Anderson, Dirk M., Eugene Maraskovsky, William L. Billingsley, William C. Dougall, Mark E. Tometsko, Eileen R. Roux, Mark C. Teepe, Robert F. DuBose, David Cosman, and Laurent Galibert. 1997. "A Homologue of the TNF

Receptor and Its Ligand Enhance T-Cell Growth and Dendritic-Cell Function." Nature 390 (6656): 175–79. https://doi.org/10.1038/36593.

13. Lacey, D.L, E Timms, H.-L Tan, M.J Kelley, C.R Dunstan, T Burgess, R Elliott, et al. 1998. "Osteoprotegerin Ligand Is a Cytokine That Regulates Osteoclast Differentiation and Activation." Cell 93 (2): 165–76. https://doi.org/10.1016/S0092-8674(00)81569-X.

14. Lum, L., B. R. Wong, R. Josien, J. D. Becherer, H. Erdjument-Bromage, J. Schlöndorff, P. Tempst, Y. Choi, and C. P. Blobel. 1999. "Evidence for a Role of a tumor Necrosis Factor-Alpha (TNF-Alpha)-Converting Enzyme-like Protease in Shedding of TRANCE, a TNF Family Member Involved in Osteoclastogenesis and Dendritic Cell Survival." The Journal of Biological Chemistry 274 (19): 13613–18. https://doi.org/10.1074/jbc.274.19.13613.

15. Kartsogiannis, V., H. Zhou, N. J. Horwood, R. J. Thomas, D. K. Hards, J. M. Quinn, P. Niforas, K. W. Ng, T. J. Martin, and M. T. Gillespie. 1999. "Localization of RANKL (Receptor Activator of NF Kappa B Ligand) MRNA and Protein in Skeletal and Extraskeletal Tissues." Bone 25 (5): 525–34. https://doi.org/10.1016/s8756-3282(99)00214-8.

16. Simonet, W.S, D.L Lacey, C.R Dunstan, M Kelley, M.-S Chang, R Lüthy, H.Q Nguyen, et al. 1997. "Osteoprotegerin: A Novel Secreted Protein Involved in the Regulation of Bone Density." Cell 89 (2): 309–19. https://doi.org/10.1016/S0092-8674(00)80209-3.

17. Yamaguchi, Kyoji, Masahiko Kinosaki, Masaaki Goto, Fumie Kobayashi, Eisuke Tsuda, Tomonori Morinaga, and Kanji Higashio. 1998. "Characterization of Structural Domains of Human Osteoclastogenesis Inhibitory Factor." Journal of Biological Chemistry 273 (9): 5117–23. https://doi.org/10.1074/jbc.273.9.5117.

18. Emery, John G., Peter McDonnell, Michael Brigham Burke, Keith C. Deen, Sally Lyn, Carol Silverman, Edward Dul, et al. 1998. "Osteoprotegerin Is a Receptor for the Cytotoxic Ligand TRAIL." Journal of Biological Chemistry 273 (23): 14363–67. https://doi.org/10.1074/jbc.273.23.14363.

19. Nelson, Christopher A., Julia T. Warren, Michael W.-H. Wang, Steven L. Teitelbaum, and Daved H. Fremont. 2012. "RANKL Employs Distinct Binding Modes to Engage RANK and the Osteoprotegerin Decoy Receptor." Structure 20 (11): 1971–82. https://doi.org/10.1016/j.str.2012.08.030.

20. Liu, Changzhen, Thomas S. Walter, Peng Huang, Shiqian Zhang, Xuekai Zhu, Ying Wu, Lucy R. Wedderburn, et al. 2010. "Structural and Functional Insights of RANKL–RANK Interaction and Signaling." The Journal of Immunology 184 (12): 6910–19. https://doi.org/10.4049/jimmunol.0904033.

21. Lam, Jonathan, Christopher A. Nelson, F. Patrick Ross, Steven L. Teitelbaum, and Daved H. Fremont. 2001. "Crystal Structure of the TRANCE/RANKL Cytokine Reveals Determinants of Receptor-Ligand Specificity." Journal of Clinical Investigation 108 (7): 971–79. https://doi.org/10.1172/JCI200113890.

22. Boyce, Brendan F., Yan Xiu, Jinbo Li, Lianping Xing, and Zhenqiang Yao. 2015. "NF-KB-Mediated Regulation of Osteoclastogenesis." Endocrinology and Metabolism 30(1):35–44. https://doi.org/10.3803/EnM.2015.30.1.35.

23. Dejardin, Emmanuel, Nathalie M. Droin, Mireille Delhase, Elvira Haas, Yixue Cao, Constantin Makris, Zhi-Wei Li, Michael Karin, Carl F. Ware, and Douglas R. Green. 2002. "The Lymphotoxin-Beta Receptor Induces Different Patterns of Gene Expression via Two NF-KappaB Pathways." Immunity 17 (4): 525–35. https://doi.org/10.1016/s1074-7613(02)00423-5.

24. Ruddle, Nancy H. 2014. "Lymphotoxin and TNF: How It All Began—A Tribute to the Travelers." *Cytokine & Growth Factor Reviews* 25 (2): 83–89. https://doi.org/10.1016/j.cytogfr.2014.02.001.

25. Koni, Pandelakis A., Rosalba Sacca, Pornsri Lawton, Jeffrey L. Browning, Nancy H. Ruddle, and Richard A. Flavell. 1997. "Distinct Roles in Lymphoid Organogenesis for Lymphotoxins α and β Revealed in Lymphotoxin β–Deficient Mice." Immunity 6 (4): 491–500. https://doi.org/10.1016/S1074-7613(00)80292-7.

26. Alimzhanov, Marat B., Dmitry V. Kuprash, Marie H. Kosco-Vilbois, Arne Luz, Regina L. Turetskaya, Alexander Tarakhovsky, Klaus Rajewsky, Sergei A. Nedospasov, and Klaus Pfeffer. 1997. "Abnormal Development of Secondary Lymphoid Tissues in Lymphotoxin β-Deficient Mice." Proceedings of the National Academy of Sciences 94 (17): 9302–7. https://doi.org/10.1073/pnas.94.17.9302.

27. Kratz, A. 1996. "Chronic Inflammation Caused by Lymphotoxin Is Lymphoid Neogenesis." Journal of Experimental Medicine 183 (4): 1461–72. https://doi.org/10.1084/jem.183.4.1461.

28. Browning, Jeffrey L., Norm Allaire, Apinya Ngam-ek, Evangelia Notidis, Jane Hunt, Steven Perrin, and Roy A. Fava. 2005. "Lymphotoxin-β Receptor Signaling Is Required for the Homeostatic Control of HEV Differentiation and Function." Immunity 23 (5): 539–50. https://doi.org/10.1016/j.immuni.2005.10.002.

29. Fava, Roy A., Evangelia Notidis, Jane Hunt, Veronika Szanya, Nora Ratcliffe, Apinya Ngam-ek, Antonin R. de Fougerolles, Andrew Sprague, and Jeffrey L. Browning. 2003. "A Role for the Lymphotoxin/LIGHT Axis in the Pathogenesis of Murine Collagen-Induced Arthritis." *The Journal of Immunology* 171 (1): 115–26. https://doi.org/10.4049/jimmunol.171.1.115.

30. Fava, Roy A, Susan M Kennedy, Sheryl G Wood, Anne I Bolstad, Jadwiga Bienkowska, Adrian Papandile, John A Kelly, et al. 2011. "Lymphotoxin-Beta Receptor Blockade Reduces CXCL13 in Lacrimal Glands and Improves Corneal Integrity in the NOD Model of Sjögren's Syndrome." Arthritis Research & Therapy 13 (6): R182. https://doi.org/10.1186/ar3507.

31. Spooner, Christopher E., Norman P. Markowitz, and Louis D. Saravolatz. 1992. "The Role of tumor Necrosis Factor in Sepsis." *Clinical Immunology and Immunopathology* 62 (1): S11–17. https://doi.org/10.1016/0090-1229(92)90036-N.

32. Tracey, K., B Beutler, S. Lowry, J Merryweather, S Wolpe, I. Milsark, R. Hariri, et al. 1986. "Shock and Tissue Injury Induced by Recombinant Human Cachectin." Science 234 (4775): 470–74. https://doi.org/10.1126/science.3764421.

33. Deutschman, Clifford S., and Kevin J. Tracey. 2014. "Sepsis: Current Dogma and New Perspectives." *Immunity* 40 (4): 463–75. https://doi.org/10.1016/j.immuni.2014.04.001.

34. Marshall, John C. 2008. "Sepsis: Rethinking the Approach to Clinical Research." *Journal of Leukocyte Biology* 83 (3): 471–82. https://doi.org/10.1189/jlb.0607380.

35. Brennan, F. M., D. Chantry, A. M. Jackson, R. N. Maini, and M. Feldmann. 1989. "Cytokine Production in Culture by Cells Isolated from the Synovial Membrane." Journal of Autoimmunity, T-cell Activation in Health and Disease Disorders of Immune Regulation Infection and Autoimmunity, 2 (June): 177–86. https://doi.org/10.1016/0896-8411(89)90129-7

36. Papamichael, Konstantinos, Niels Vande Casteele, Marc Ferrante, Ann Gils, and Adam S. Cheifetz. 2017. "Therapeutic Drug Monitoring During Induction of Anti–tumor Necrosis Factor Therapy in Inflammatory Bowel Disease: Defining a Therapeutic Drug Window." Inflammatory Bowel Diseases 23 (9): 1510–15. https://doi.org/10.1097/MIB.0000000000001231.

37. Kerdel, Francisco A., and Bruce E. Strober. 2014. "Tumor Necrosis Factor Inhibitors in Psoriasis: An Update." Seminars in Cutaneous Medicine and Surgery 33 (2 Suppl 2): S31-36. https://doi.org/10.12788/j.sder.0066.

38. Boyce, B.F. 2013. "Advances in the Regulation of Osteoclasts and Osteoclast Functions." *Journal of Dental Research* 92 (10): 860–67. https://doi.org/10.1177/0022034513500306.

39. Boyle, William J., W. Scott Simonet, and David L. Lacey. 2003. "Osteoclast Differentiation and Activation." *Nature* 423 (6937): 337–42. https://doi.org/10.1038/nature01658.

40. Roodman, G. D. 1999. "Cell Biology of the Osteoclast." *Experimental Hematology* 27 (8): 1229–41.

41. Yoshida, H., S. Hayashi, T. Kunisada, M. Ogawa, S. Nishikawa, H. Okamura, T. Sudo, L. D. Shultz, and S. Nishikawa. 1990. "The Murine Mutation Osteopetrosis Is in the Coding Region of the Macrophage Colony Stimulating Factor Gene." *Nature* 345 (6274): 442–44. https://doi.org/10.1038/345442a0.

42. Kobayashi, K., N. Takahashi, E. Jimi, N. Udagawa, M. Takami, S. Kotake, N. Nakagawa, et al. 2000. "Tumor Necrosis Factor Alpha Stimulates Osteoclast Differentiation by a Mechanism Independent of the ODF/RANKL-RANK Interaction." *The Journal of Experimental Medicine* 191 (2): 275–86. https://doi.org/10.1084/jem.191.2.275.

43. Kitaura, Hideki, Keisuke Kimura, Masahiko Ishida, Haruka Kohara, Masako Yoshimatsu, and Teruko Takano-Yamamoto. 2013. "Immunological Reaction in TNF-α-Mediated Osteoclast Formation and Bone Resorption *in vitro* and in Vivo." *Clinical & Developmental Immunology* 2013: 181849. https://doi.org/10.1155/2013/181849.

44. Wada, Teiji, Tomoki Nakashima, Nishina Hiroshi, and Josef M. Penninger. 2006. "RANKL-RANK Signaling in Osteoclastogenesis and Bone Disease." *Trends in Molecular Medicine* 12 (1): 17–25. https://doi.org/10.1016/j.molmed.2005.11.007.

45. Takayanagi, Hiroshi, Sunhwa Kim, Takako Koga, Hiroshi Nishina, Masashi Isshiki, Hiroki Yoshida, Akio Saiura, et al. 2002. "Induction and Activation of the Transcription Factor NFATc1 (NFAT2) Integrate RANKL Signaling in Terminal Differentiation of Osteoclasts." *Developmental Cell* 3 (6): 889–901.

46. Soriano, P., C. Montgomery, R. Geske, and A. Bradley. 1991. "Targeted Disruption of the C-Src Proto-Oncogene Leads to Osteopetrosis in Mice." *Cell* 64 (4): 693–702. https://doi.org/10.1016/0092-8674(91)90499-o.

47. Kong, Y. Y., H. Yoshida, I. Sarosi, H. L. Tan, E. Timms, C. Capparelli, S. Morony, et al. 1999. "OPGL Is a Key Regulator of Osteoclastogenesis, Lymphocyte Development and Lymph-Node Organogenesis." Nature 397 (6717): 315–23. https://doi.org/10.1038/16852.

48. Hakeda, Y., Y. Kobayashi, K. Yamaguchi, H. Yasuda, E. Tsuda, K. Higashio, T. Miyata, and M. Kumegawa. 1998. "Osteoclastogenesis Inhibitory Factor (OCIF) Directly Inhibits Bone-Resorbing Activity of Isolated Mature Osteoclasts." *Biochemical and Biophysical Research Communications* 251 (3): 796–801. https://doi.org/10.1006/bbrc.1998.9523.

49. Simonet, W. S., D. L. Lacey, C. R. Dunstan, M. Kelley, M. S. Chang, R. Lüthy, H. Q. Nguyen, et al. 1997. "Osteoprotegerin: A Novel Secreted Protein Involved in the Regulation of Bone Density." *Cell* 89 (2): 309–19. https://doi.org/10.1016/s0092-8674(00)80209-3.

50. Bucay, N., I. Sarosi, C. R. Dunstan, S. Morony, J. Tarpley, C. Capparelli, S. Scully, et al. 1998. "Osteoprotegerin-Deficient Mice Develop Early Onset Osteoporosis and Arterial Calcification." *Genes & Development* 12 (9): 1260–68. https://doi.org/10.1101/gad.12.9.1260.

51. Marks, S. C., and P. W. Lane. 1976. "Osteopetrosis, a New Recessive Skeletal Mutation on Chromosome 12 of the Mouse." The Journal of Heredity 67 (1): 11–18. https://doi.org/10.1093/oxfordjournals.jhered.a108657.

52. Cecchini, M. G., W. Hofstetter, J. Halasy, A. Wetterwald, and R. Felix. 1997. "Role of CSF-1 in Bone and Bone Marrow Development." *Molecular Reproduction and Development* 46 (1): 75–84. https://doi.org/10.1002/(SICI)1098-2795(199701)46:1<75::AID-MRD12>3.0.CO;2-2.

53. Theill, Lars E., William J. Boyle, and Josef M. Penninger. 2002. "RANK-L AND RANK: T Cells, Bone Loss, and Mammalian Evolution." *Annual Review of Immunology* 20 (1): 795–823. https://doi.org/10.1146/annurev.immunol.20.100301.064753.

54. Hughes, Anne E., Stuart H. Ralston, John Marken, Christine Bell, Heather MacPherson, Richard G. H. Wallace, Wim van Hul, et al. 2000. "Mutations in TNFRSF11A, Affecting the Signal Peptide of RANK, Cause Familial Expansile Osteolysis." *Nature Genetics* 24 (1): 45–48. https://doi.org/10.1038/71667.

55. Whyte, Michael P., and Anne E. Hughes. 2002. "Expansile Skeletal Hyperphosphatasia Is Caused by a 15-Base Pair Tandem Duplication in TNFRSF11A Encoding RANK and Is Allelic to Familial Expansile Osteolysis." Journal of Bone and Mineral Research: The Official Journal of the American Society for Bone and Mineral Research 17 (1): 26–29. https://doi.org/10.1359/jbmr.2002.17.1.26.

56. Whyte, Michael P., Sara E. Obrecht, Patrick M. Finnegan, Jonathan L. Jones, Michelle N. Podgornik, William H. McAlister, and Steven Mumm. 2002. "Osteoprotegerin Deficiency and Juvenile Paget's Disease." The New England Journal of Medicine 347 (3): 175–84. https://doi.org/10.1056/NEJMoa013096.

57. Ebeling, P. R., L. M. Atley, J. R. Guthrie, H. G. Burger, L. Dennerstein, J. L. Hopper, and J. D. Wark. 1996. "Bone Turnover Markers and Bone Density across the Menopausal Transition." *The Journal of Clinical Endocrinology and Metabolism* 81 (9): 3366–71. https://doi.org/10.1210/jcem.81.9.8784098.

58. Mundy, Gregory R. 2007. "Osteoporosis and Inflammation." *Nutrition Reviews* 65 (12 Pt 2): S147-151. https://doi.org/10.1111/j.1753-4887.2007.tb00353.x.

59. Eghbali-Fatourechi, Guitty, Sundeep Khosla, Arunik Sanyal, William J. Boyle, David L. Lacey, and B. Lawrence Riggs. 2003. "Role of RANK Ligand in Mediating Increased Bone Resorption in Early Postmenopausal Women." *The Journal of Clinical Investigation* 111 (8): 1221–30. https://doi.org/10.1172/JCI17215.

60. Raisz, L. G., and G. A. Rodan. 2003. "Pathogenesis of Osteoporosis." *Endocrinology and Metabolism Clinics of North America* 32 (1): 15–24. https://doi.org/10.1016/S0889-8529(02)00055-5.

61. Dougall, W. C., M. Glaccum, K. Charrier, K. Rohrbach, K. Brasel, T. De Smedt, E. Daro, et al. 1999. "RANK Is Essential for Osteoclast and LN Development." Genes & Development 13 (18): 2412–24. https://doi.org/10.1101/gad.13.18.2412.

62. Georgopoulos, Katia, Susan Winandy, and Nicole Avitahl. 1997. "The Role of the Ikaros Gene in Lymphocyte Development and Homeostasis." Annual Review of Immunology 15 (1): 155–76. https://doi.org/10.1146/annurev.immunol.15.1.155.

63. Yokota, Yoshifumi, Ahmed Mansouri, Seiichi Mori, Seiichi Sugawara, Satoko Adachi, Shin-Ichi Nishikawa, and Peter Gruss. 1999. "Development of Peripheral Lymphoid Organs and Natural Killer Cells Depends on the Helix–Loop–Helix Inhibitor Id2." Nature 397 (6721): 702–6. https://doi.org/10.1038/17812.

64. Rossi, Simona W., Mi-Yeon Kim, Andreas Leibbrandt, Sonia M. Parnell, William E. Jenkinson, Stephanie H. Glanville, Fiona M. McConnell, et al. 2007. "RANK Signals from CD4 $^+$ 3 $^-$ Inducer Cells Regulate Development of Aire-Expressing Epithelial Cells in the Thymic Medulla." *The Journal of Experimental Medicine* 204 (6): 1267–72. https://doi.org/10.1084/jem.20062497.

65. Fata, Jimmie E, Young-Yun Kong, Ji Li, Takehiko Sasaki, Junko Irie-Sasaki, Roger A Moorehead, Robin Elliott, et al. 2000. "The Osteoclast Differentiation Factor Osteoprotegerin-Ligand Is Essential for Mammary Gland Development." *Cell* 103 (1): 41–50. https://doi.org/10.1016/S0092-8674(00)00103-3.

66. Kim, N.-S., H.-J. Kim, B.-K. Koo, M.-C. Kwon, Y.-W. Kim, Y. Cho, Y. Yokota, J. M. Penninger, and Y.-Y. Kong. 2006. "Receptor Activator of NF- B Ligand Regulates the Proliferation of Mammary Epithelial Cells via Id2." *Molecular and Cellular Biology* 26 (3): 1002–13. https://doi.org/10.1128/MCB.26.3.1002-1013.2006.

67. Duheron, V., E. Hess, M. Duval, M. Decossas, B. Castaneda, J. E. Klopper, L. Amoasii, et al. 2011. "Receptor Activator of NF- B (RANK) Stimulates the Proliferation of Epithelial Cells of the Epidermo-Pilosebaceous Unit." *Proceedings of the National Academy of Sciences* 108 (13): 5342–47. https://doi.org/10.1073/pnas.1013054108.

68. Kartsogiannis, V., H. Zhou, N. J. Horwood, R. J. Thomas, D. K. Hards, J. M. Quinn, P. Niforas, K. W. Ng, T. J. Martin, and M. T. Gillespie. 1999. "Localization of RANKL (Receptor Activator of NF Kappa B Ligand) MRNA and Protein in Skeletal and Extraskeletal Tissues." Bone 25 (5): 525–34. https://doi.org/10.1016/s8756-3282(99)00214-8.

69. Hanada, Reiko, Andreas Leibbrandt, Toshikatsu Hanada, Shiho Kitaoka, Tomoyuki Furuyashiki, Hiroaki Fujihara, Jean Trichereau, et al. 2009. "Central Control of Fever and Female Body Temperature by RANKL/RANK." *Nature* 462 (7272): 505–9. https://doi.org/10.1038/nature08596.

70. Guerrini, Matteo M., Cristina Sobacchi, Barbara Cassani, Mario Abinun, Sara S. Kilic, Alessandra Pangrazio, Daniele Moratto, et al. 2008. "Human Osteoclast-Poor Osteopetrosis with Hypogammaglobulinemia Due to TNFRSF11A (RANK) Mutations." *The American Journal of Human Genetics* 83 (1): 64–76. https://doi.org/10.1016/j.ajhg.2008.06.015.

71. Owen, Robert L., and Albert L. Jones. 1974. "Epithelial Cell Specialization within Human Payer's patches: An Ultrastructural Study of Intestinal Lymphoid Follicles." *Gastroenterology* 66 (2): 189–203. https://doi.org/10.1016/S0016-5085(74)80102-2.

72. Hase, Koji, Kazuya Kawano, Tomonori Nochi, Gemilson Soares Pontes, Shinji Fukuda, Masashi Ebisawa, Kazunori Kadokura, et al. 2009. "Uptake through Glycoprotein 2 of FimH (+) Bacteria by M Cells Initiates Mucosal Immune Response." *Nature* 462 (7270): 226–30. https://doi.org/10.1038/nature08529.

73. Nagashima, Kazuki, Shinichiro Sawa, Takeshi Nitta, Masanori Tsutsumi, Tadashi Okamura, Josef M. Penninger, Tomoki Nakashima, and Hiroshi Takayanagi. 2017. "Identification of Subepithelial Mesenchymal Cells That

Induce IgA and Diversify Gut Microbiota." Nature Immunology 18 (6): 675–82. https://doi.org/10.1038/ni.3732.

74. Anderson, Dirk M., Eugene Maraskovsky, William L. Billingsley, William C. Dougall, Mark E. Tometsko, Eileen R. Roux, Mark C. Teepe, Robert F. DuBose, David Cosman, and Laurent Galibert. 1997. "A Homologue of the TNF Receptor and Its Ligand Enhance T-Cell Growth and Dendritic-Cell Function." *Nature* 390 (6656): 175–79. https://doi.org/10.1038/36593.

75. Loser, Karin, Annette Mehling, Stefanie Loeser, Jenny Apelt, Annegret Kuhn, Stephan Grabbe, Thomas Schwarz, Josef M Penninger, and Stefan Beissert. 2006. "Epidermal RANKL Controls Regulatory T-Cell Numbers via Activation of Dendritic Cells." *Nature Medicine* 12 (12): 1372–79. https://doi.org/10.1038/nm1518.

76. Mebius, Reina E. 2003. "Organogenesis of Lymphoid Tissues." Nature Reviews Immunology 3 (4): 292–303. https://doi.org/10.1038/nri1054.

Chapter 2. Organogenesis of lymph node and spleen in mammals

1 Lymph node ontogeny

LN is a secondary lymphoid organ, center of immune surveillance where antigens contained in the lymph and the mucous are examined with great efficiency for the implementation of the adaptive immune response. LN formation starts during embryogenesis. The initial steps consist in the formation of lymphatic sacs by the budding of endothelial cells from the large veins near E12.5. This is followed by the protrusion of the connective tissue in the lymphatic sacs, establishing the first LN anlagen. The lymphatic sacs give rise to the lymphatic vasculature through the growth of the lymphatic vessels that are completely formed at E15.5. Lymphatic vessel formation required the expression of the transcription Prospero homeobox 1 (Prox1) as *Prox1 nullizygous (null)* embryos failed to form lymphatic vasculature at E11.5[2]. The LNs do not develop simultaneously. Different LNs at different anatomical sites develop sequentially following the embryogenesis with an order of appearance from the anterior to the posterior side of the body[1]. LNs develop along the large veins and the sites of blood vessels branching where some signals are likely to be delivered for the instruction of development.

1.1 Two-cell paradigm of lymph node development

The current paradigm of LN formation is based on the interactions that involve two-cell types: the fetal liver derived hematopoietic LTi cells and the mesenchymal LTOs. The first steps consist of the clustering (accumulation) of CXCR5-expressiong LTi cells at the site of LN initiation through attraction by the chemokine CXCL13 produced by LTβR-expressing LTOs. In addition to CXCL13, LTi cell attraction is also stimulated by CCL21 produced by the lymphatic endothelium, to guide these cells to the developing LN. LTi cells produce the lymphotoxin $LT\alpha_1\beta_2$ and interact with LTOs cells by ligation of LTβR. This interaction upregulates expression of genes encoding adhesion molecules such as VCAM-1, MAdCAM-1, ICAM-1 and genes involved in lymphoid organogenesis in mammals such as CCL19, CCL21, CXCL13 that attract and retain the hematopoietic cells within the LN anlagen. Mice deficient for $LT\alpha_1\beta_2$ in LTi cells or its receptor LTβR in LTOs show normal clustering of LTi cells at LN anlagen, indicating that other molecular pathways are involved in LN formation[3,4]. Indeed, in mice lacking the retinoic acid synthetizing enzyme (RALDH2), LTi cells clusters fail to form, indicating a role for the retinoic acid in LN initiation. The retinoic acid produced by nerve fibers near LN anlagen may

stimulate LTOs cells to express CXCL13 to guide and retain LTi cells to the site of LN formation[5,6]. The mechanism of the two-cell paradigm of LN formation is shown in figure 1.
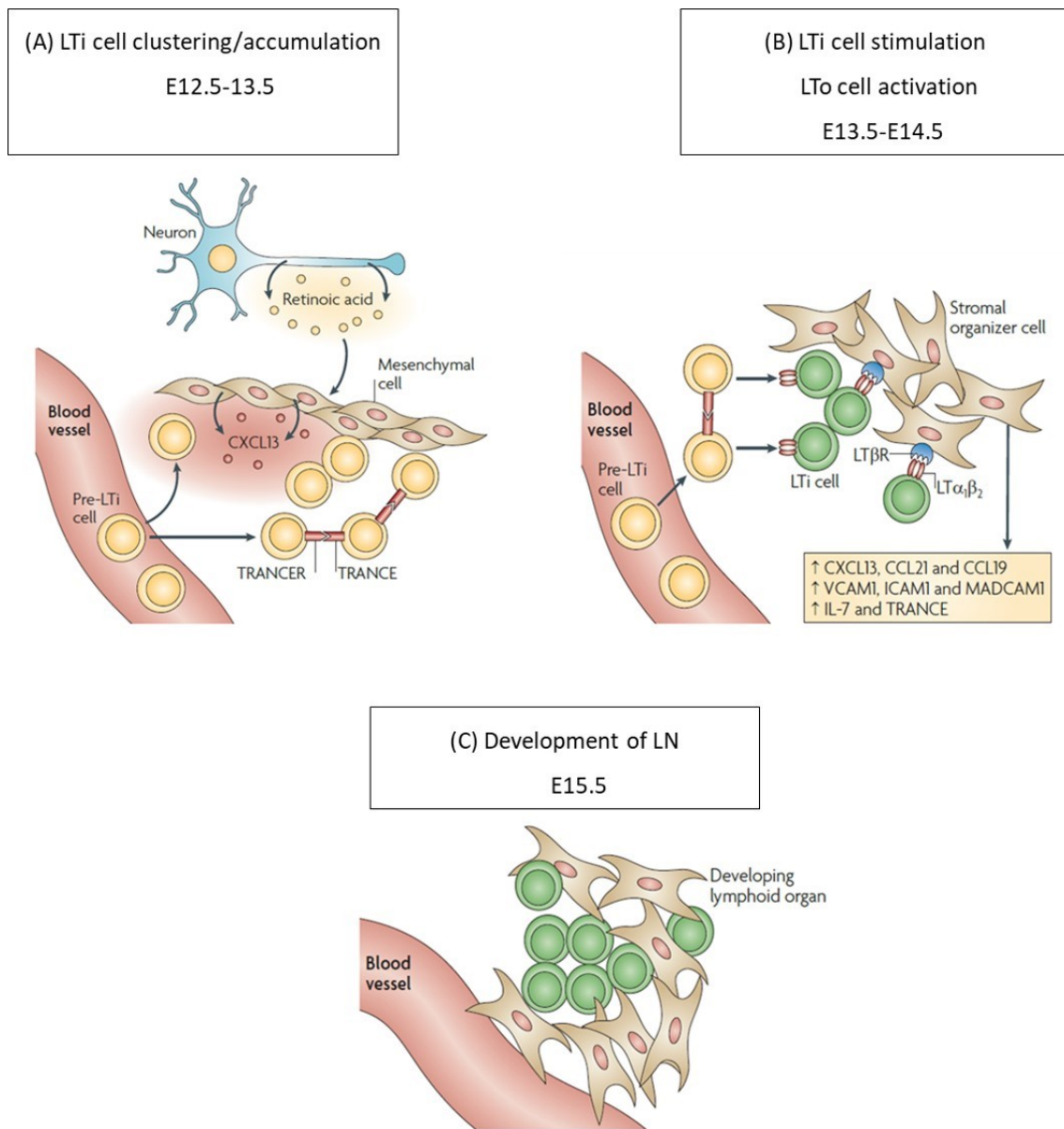
Figure 1. Two-cell paradigm of LN formation. (A) From the embryonic days E12.5 to E13.5, the LTi cell precursors are attracted at LN initiation site through the CXCL13 chemokines produced by the connective tissue-derived mesenchymal cells that are activated by the retinoic acid delivered by nerve fibers. LTi cell precursors accumulate and interact each other through RANK-RANKL signaling which stimulates them to mature as $LT\alpha_1\beta_2$ expressing LTi cells. (B) From the embryonic days E13.5 to E14.5, mature LTi cells interact with the mesenchymal cells through $LT\alpha_1\beta_2$-$LT\beta R$, leading to the differentiation of stromal organizer LTOs and the upregulation of chemokines and adhesion molecules. (C) These factors support the recruitment and the retention of hematopoietic cells for LN growth from E15.5 to the early life. TRANCE (RANKL): TNF-related activation-induced cytokine. IL-7: interleukin 7. Modified after[6].

1.2 The new view of lymph node development

In 2013, Onder et al., have shown that the LTβR signaling in LECs and in the blood endothelial cells (BECs) is critical for peripheral LN development and HEV maturation[7]. This was demonstrated by targeting of LTβR in these cells using *VE-cadherin-cre recombinase transgenic mice*. A recent study of the authors unveils an important role for LECs and defined them as additional organizer cell type in the initiation of LN development. By generating mice deficient for RANK signaling in LECs, they have observed that RANK-mediated signaling in LECs drives LN organogenesis by retaining LTi cells (cluster formation)[8]. These studies suggest that the integration of NF-kB signaling pathways through RANK and LTβR in the LECs govern their interaction with LTi cells and the activation of LTOs, upregulating adhesion molecules and organogenic chemokines. As consequences, LTi cells accumulate to initiate LN development followed by high endothelial venule maturation to enable the entry of other lymphocytes for LN growth. The mechanism of the new view of LN formation is shown in figure 2.
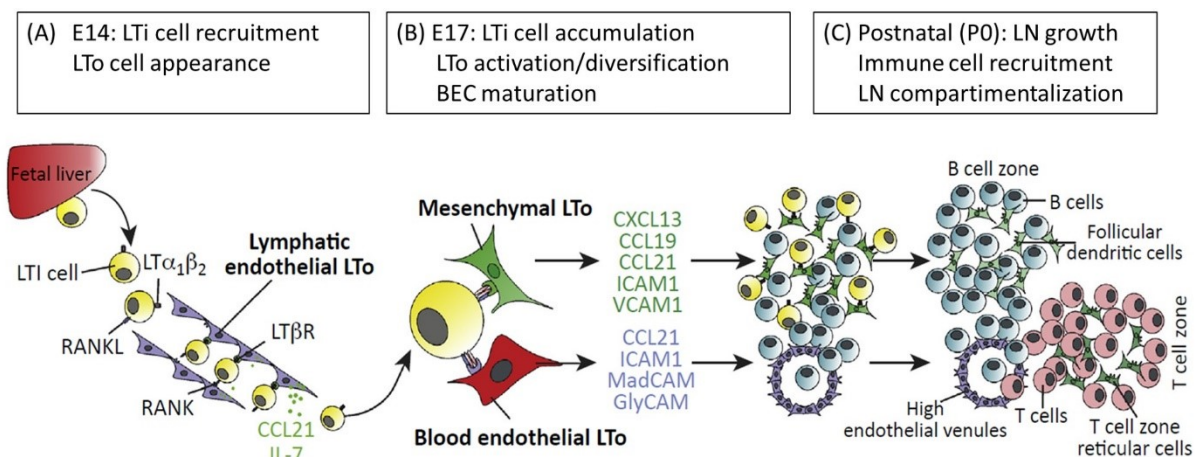
Figure 2. New views on LN formation. (A) at E14, the fetal liver-derived LTi cells are recruited and retained at the perivascular niches by CCL21-expressing LECs, that interact with the LTi cells through RANK and LTβR. (B) LTi-cell-LEC interaction leads to LTi cell clustering/accumulation by E17. This cluster interact with the CXCL13-expressing LTOs and BECs, leading to LTO activation and diversification as well as LTβR-dependent BEC maturation and HEV network formation. The activated LTOs upregulate chemokines and adhesion molecules. (C) At the postnatal days, LTO subets at different sites support the recruitment of naive lymphocytes and other immune cells to establish distinct immune compartments in the growing LN. Modified after[9].

1.3 Adult lymph node structure and cell organization

Adult LN is surrounded by a fibrous capsule that is connected to the afferent lymphatics through which the lymph drains into the LN and the efferent lymphatic where the lymph

egresses. The capsule is composed of an outer layer, the *ceiling* and an inner layer, the *floor*. Both layers are lined by LECs that constitute the vascular endothelium along which the lymph flows. This process governs the trafficking of microorganisms and immune cells such as T cells and DCs into the LN. LECs are spread all over the LN, from the cortical zone to the medulla. The substance of LN is structured into the cortical zone of B cell follicles, the para-cortical zone of T cells, T cell zone macrophages and DCs and a basal medullary zone that is connected to blood vessels through which immune cells enter and egress the LN. The layer of the floor LECs is strategically lined by subcapsular sinus macrophages (SSMs), overlying B cell follicles areas and the interfollicular zones. Some irregularly shaped, fluid-containing spaces called medullary sinuses are colonized by the medullary sinus macrophages (MSMs). The medulla also contain numerous immune cells such as lymphocytes that egress the LN, a small numbers of plasma cells and the medullary Cord Macrophages (MCMs)[10]. The marginal reticular cells (MRCs) construct a reticulum of fibroblasts between the subcapsular sinus and the underlying FDCs network in the B cell follicles. LN structure and cell organization is illustrated in figure 3.
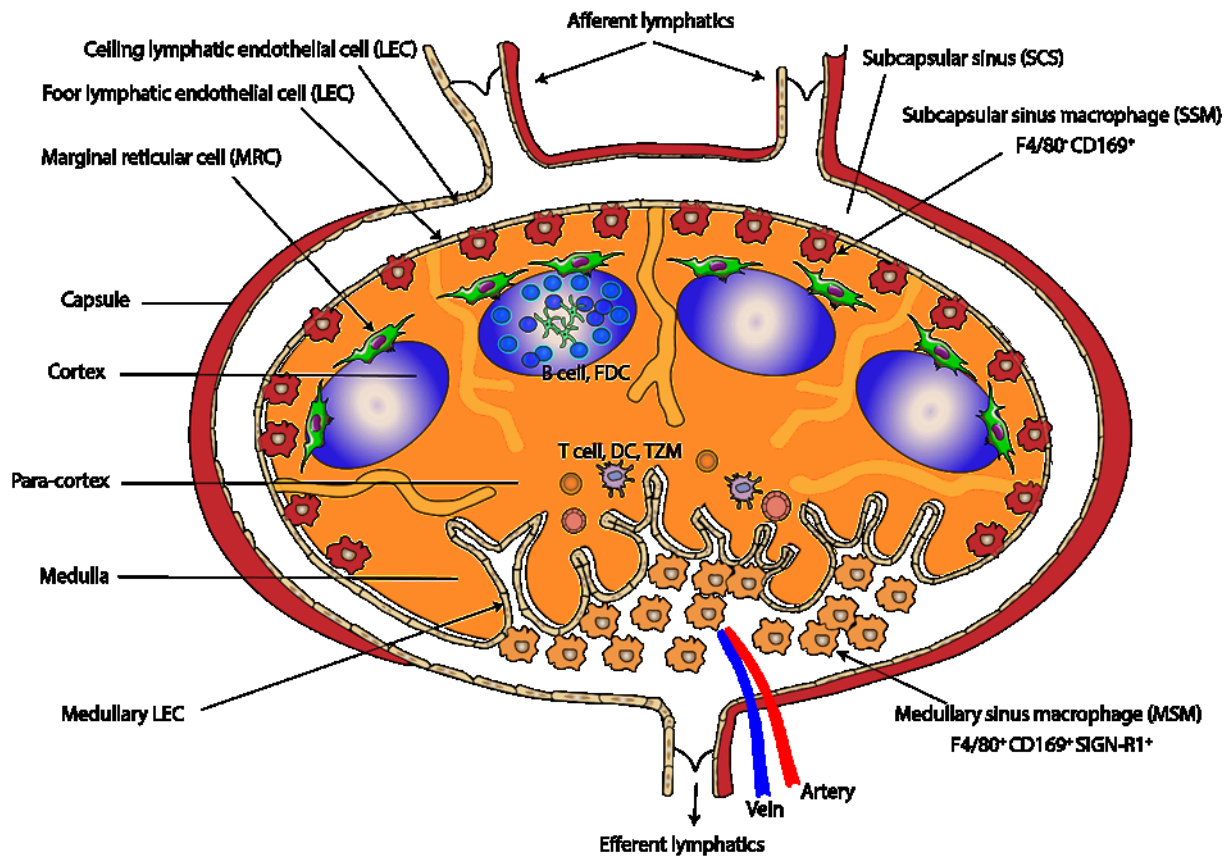
Figure 3. Compartimentalized adult LN structure with some stromal cells and immune cells of interest. Diagram of LN surrounded by the capsule composed of the outer and the inner layers lined by LECs. LECs line the vascular endothelium from the periphery to afferent lymphatics and spread all over the LN and play a role in lymph draining and the trafficking of antigens and immune cell. SSMs reside between the subcapsular sinus floor LECs and B cell follicles where they are involved in the clearance of lymph-borne microorganisms and the transfer of antigens to cognate B cells. Their counterparts MSMs reside in the sinuses of the medulla. Both subsets express CD169 marker but F4/80 and SIGN-R1 markers are restricted to MSMs. The cortical zone contains B cells and FDCs, important for antibody production and affinity maturation. The para-cortical zone is populated by T cells, DCs and T cell zone macrophages (TZMs). MRCs construct a network of fibroblasts at the marge of B cell follicles. The medulla branches to blood circulation (artery in red and vein in blue) through which, immune cells entry and egress. LN is connected to many afferent lymphatics but to a single efferent lymphatic through which the lymph exits. Bars indicate the anatomical areas and the arrows point to cells. Valves indicate the directions of lymph flow.

2   Spleen ontogeny

Spleen is the largest secondary lymphoid organ that combines innate and adaptive immunity. It is the body's largest filter that remove senescent erythrocytes from the blood and efficiently removes blood-borne microorganisms[11]. The first steps of spleen organogenesis consist of the formation of and organized center (anlagen) by the formation of a mesoderm-derived cell layer called splanchnic mesodermal plate (SMP) by embryonic day 12. Mice deficient for the transcription factor Bagpipe Homeobox homologue 1 or carrying the Dominant hemimelia mutation lack or have defective SMP and fail to form the spleen[12,13]. Other transcription factors such as Homeobox-leucine zipper protein 11 and Helix-loop-helix capsulin are crucial for the initiation of spleen formation. Mice homozygous for null mutations in these genes are asplenic[14,15]. The next steps of spleen formation are characterized by the appearance of the lymphotoxin-expressing $CD4^+ CD3^-$ LTi cells from E13.5 in the fetal spleen anlagen and its colonization by the erythroid and myeloid progenitors[16]. The LTi cells are essential for the development of splenic white pulp. Spleen development has many overlaps with LN development but show differences in the molecular processes and cellular events.

Adult spleen structure and cell organization

Spleen is surrounded by a fibrous capsule connected to the blood circulation. Its substance is structured into the red pulp (RP) and the white pulp (WP) separated by the marginal zone (MZ). The WP consists of $B220^+CD23^+CD21^+IgM^+IgD^+$ follicular B cell[17] and the T cell areas. It is sheathed by the central arteriole through which lymphocytes entry. The central arteriole is branched to the splenic artery through which cells and blood borne antigens are drained into the spleen. The marginal zone is made of an outer and inner sides, lined by $MAdCAM-1^+$ sinus-lining fibroblasts. The outer side is associated with $MARCO^+ SIGN-R1^+$ marginal zone macrophages (MZMs) and $B220^+CD21^{hi}IgM^{hi}CD23^-$ marginal zone B cells[17]. Some populations of migratory cells including DCs, T cells as well as granulocytes are also found in this side of the MZ[11]. Finally, the inner side of the marginal zone is populated by the sialic-acid-binding immunoglobulin-like lectin 1 (Siglec-1 or CD169) expressing metallophilic macrophages (MMMs), residing beneath the layer of $MAdCAM-1^+$ sinus-lining fibroblasts (Figure 4B).

The RP is sheathed by the collecting veins which connect into the splenic artery and ends in venous sinuses. These sinuses contain the red blood cells (RBCs) and connect into cords

populated by F4/80$^+$CD11b^{low} CD68$^+$CD163$^+$ RP macrophages (RPMs)[18]. The central arteriole in the WP emits extensions that end as cords in the RP. This enables the trafficking and the exchanges between both compartments. Spleen structure and cell organization is illustrated in figure 4.
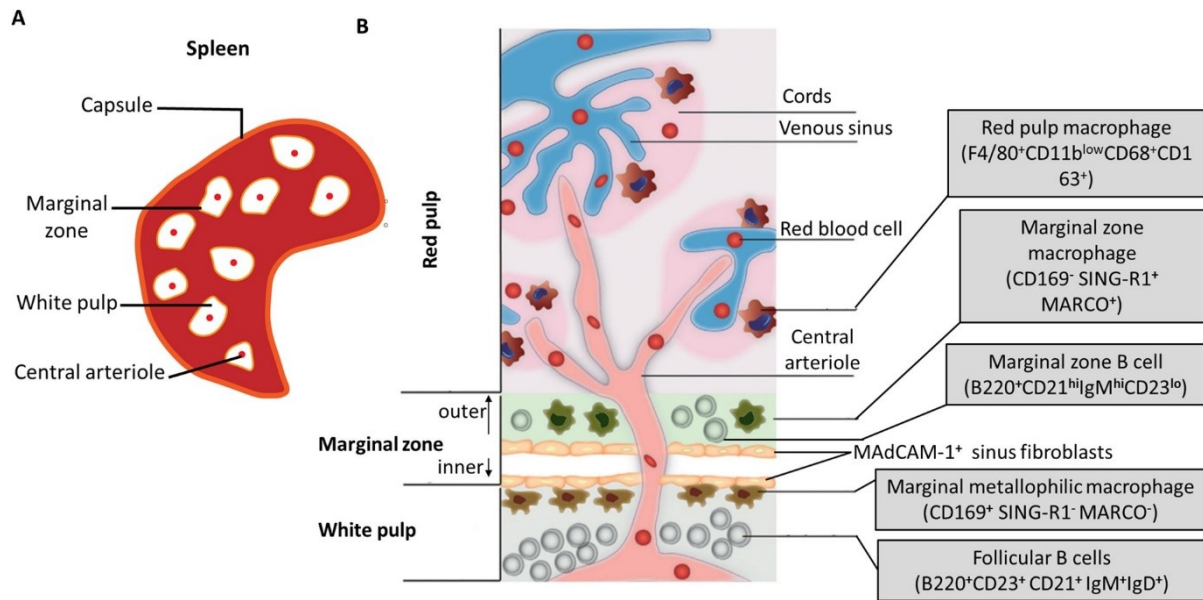
Figure 4. **Structure of the spleen with cell localization and markers**. (A) Diagram of the spleen with the surrounding capsule and the red pulp separated to the white pulp by the marginal zone. (B) A broad scheme of the positioning of lymphocytes, fibroblasts and macrophages inside spleen and their phenotypic markers. The rep pulp connects to the WP through extensions emanating from the central arteriole. It is populated by F4/80$^+$CD11b^{low} CD68$^+$CD163$^+$ RP macrophages residing in the cords where they remove infected or senescent red blood cells. The marginal zone separates RP and WP and is lined by MAdCAM-1$^+$ fibroblasts. Its outer side is populated by MARCO$^+$ SIGN-R1$^+$ marginal zone macrophages (MZMs) and B220$^+$CD21^{hi}IgM^{hi}CD23$^-$ marginal zone B cells. The inner side of the MZ beneath the layer of fibroblasts is populated by the sialic-acid-binding immunoglobulin-like lectin 1 (Siglec-1 or CD169) $^+$ marginal metallophilic macrophages (MMMs). They are involved in the uptake and the transfer of blood-borne antigens to B220$^+$CD23$^+$CD21$^+$IgM$^+$ IgD$^+$ follicular B cells residing in the white pulp. The WP also contains the T cell zone (not shown here) underlying follicular B cells. Panel B is modified after[18].

3 References

1. Mebius, Reina E. 2003. "Organogenesis of Lymphoid Tissues." *Nature Reviews Immunology* 3 (4): 292–303. https://doi.org/10.1038/nri1054.

2. Wigle, J. T. 2002. "An Essential Role for Prox1 in the Induction of the Lymphatic Endothelial Cell Phenotype." *The EMBO Journal* 21 (7): 1505–13. https://doi.org/10.1093/emboj/21.7.1505.

3. Yoshida, Hisahiro, Asuka Naito, Jun-Ichiro Inoue, Mizuho Satoh, Sybil M. Santee-Cooper, Carl F. Ware, Atsushi Togawa, Satomi Nishikawa, and Shin-Ichi Nishikawa. 2002. "Different Cytokines Induce Surface Lymphotoxin-Alphabeta on IL-7 Receptor-Alpha Cells That Differentially Engender LNs and Payer's patches." *Immunity* 17 (6): 823–33. https://doi.org/10.1016/s1074-7613(02)00479-x.

4. Coles, Mark C., Henrique Veiga-Fernandes, Katie E. Foster, Trisha Norton, Stamatis N. Pagakis, Ben Seddon, and Dimitris Kioussis. 2006. "Role of T and NK Cells and IL7/IL7r Interactions during Neonatal Maturation of LNs." *Proceedings of the National Academy of Sciences of the United States of America* 103 (36): 13457–62. https://doi.org/10.1073/pnas.0604183103.

5. Pavert, Serge A van de, Brenda J Olivier, Gera Goverse, Mark F Vondenhoff, Mascha Greuter, Patrick Beke, Kim Kusser, et al. 2009. "Chemokine CXCL13 Is Essential for LN Initiation and Is Induced by Retinoic Acid and Neuronal Stimulation." *Nature Immunology* 10 (11): 1193–99. https://doi.org/10.1038/ni.1789.

6. Pavert, Serge A. van de, and Reina E. Mebius. 2010. "New Insights into the Development of Lymphoid Tissues." *Nature Reviews Immunology* 10 (9): 664–74. https://doi.org/10.1038/nri2832.

7. Onder, Lucas, Renzo Danuser, Elke Scandella, Sonja Firner, Qian Chai, Thomas Hehlgans, Jens V. Stein, and Burkhard Ludewig. 2013. "Endothelial Cell–Specific Lymphotoxin-β Receptor Signaling Is Critical for LN and High Endothelial Venule Formation." *The Journal of Experimental Medicine* 210 (3): 465–73. https://doi.org/10.1084/jem.20121462.

8. Onder, Lucas, Urs Mörbe, Natalia Pikor, Mario Novkovic, Hung-Wei Cheng, Thomas Hehlgans, Klaus Pfeffer, et al. 2017. "Lymphatic Endothelial Cells Control Initiation of LN Organogenesis." *Immunity* 47 (1): 80-92. e4. https://doi.org/10.1016/j.immuni.2017.05.008.

9. Onder, Lucas, and Burkhard Ludewig. 2018. "A Fresh View on LN Organogenesis." *Trends in Immunology* 39 (10): 775–87. https://doi.org/10.1016/j.it.2018.08.003.

10. Gray, Elizabeth E., and Jason G. Cyster. 2012. "LN Macrophages." *Journal of Innate Immunity* 4 (5–6): 424–36. https://doi.org/10.1159/000337007.

11. Mebius, Reina E., and Georg Kraal. 2005. "Structure and Function of the Spleen." *Nature Reviews Immunology* 5 (8): 606–16. https://doi.org/10.1038/nri1669.

12. Green, Margaret C. 1967. "A Defect of the Splanchnic Mesoderm Caused by the Mutant Gene Dominant Hemimelia in the Mouse." *Developmental Biology* 15 (1): 62–89. https://doi.org/10.1016/0012-1606(67)90006-1.

13. Hecksher-Sorensen, J. 2004. "The Splanchnic Mesodermal Plate Directs Spleen and Pancreatic Laterality and Is Regulated by Bapx1/Nkx3.2." *Development* 131 (19): 4665–75. https://doi.org/10.1242/dev.01364.

14. Roberts, C. W., A. M. Sonder, A. Lumsden, and S. J. Korsmeyer. 1995. "Development Expression of Hox11 and Specification of Splenic Cell Fate." *The American Journal of Pathology* 146 (5): 1089–1101.

15. Lu, J., P. Chang, J. A. Richardson, L. Gan, H. Weiler, and E. N. Olson. 2000. "The Basic Helix-Loop-Helix Transcription Factor Capsulin Controls Spleen Organogenesis." *Proceedings of the National Academy of Sciences* 97 (17): 9525–30. https://doi.org/10.1073/pnas.97.17.9525.

16. Mebius, R. E., P. Rennert, and I. L. Weissman. 1997. "Developing LNs Collect CD4+CD3- LTbeta+ Cells That Can Differentiate to APC, NK Cells, and Follicular Cells but Not T or B Cells." *Immunity* 7 (4): 493–504. https://doi.org/10.1016/s1074-7613(00)80371-4.

17. Schneider, Pascal, Hisakazu Takatsuka, Anne Wilson, Fabienne Mackay, Aubry Tardivel, Susanne Lens, Teresa G. Cachero, Daniela Finke, Friedrich Beermann, and Jürg Tschopp. 2001. "Maturation of Marginal Zone and Follicular B Cells Requires B Cell Activating Factor of the Tumor Necrosis Factor Family and Is Independent of B Cell Maturation Antigen." *The Journal of Experimental Medicine* 194 (11): 1691–98. https://doi.org/10.1084/jem.194.11.1691.

18. Borges da Silva, Henrique, Raíssa Fonseca, Rosana Moreira Pereira, Alexandra dos Anjos Cassado, José Maria Álvarez, and Maria Regina D'Império Lima. 2015. "Splenic Macrophage Subsets and Their Function during Blood-Borne Infections." *Frontiers in Immunology* 6 (September). https://doi.org/10.3389/fimmu.2015.00480.

Chapter 3. Lymph node stroma and the lymphatic system

1 Stromal compartments in secondary lymphoid organs

Tissues and organs are formed by two parts: the parenchyma consisting of cells that carry out their functions and the stroma that structurally supports and secures them. The stroma is made of the extracellular matrix, a substance essentially consists in proteoglycan aggregates and stromal cells (endothelial cells, fibroblasts, epithelial cells, nerve cells, etc) that supports the parenchyma. Different subsets of stromal cells including fibroblastic reticular cells (FRCs), FDCs, MRCs, medullary fibroblastic reticular cells of LN, marginal zone fibroblasts of spleen, BECs and LECs can be found in the lymphoid tissues as summarized in figure 1.
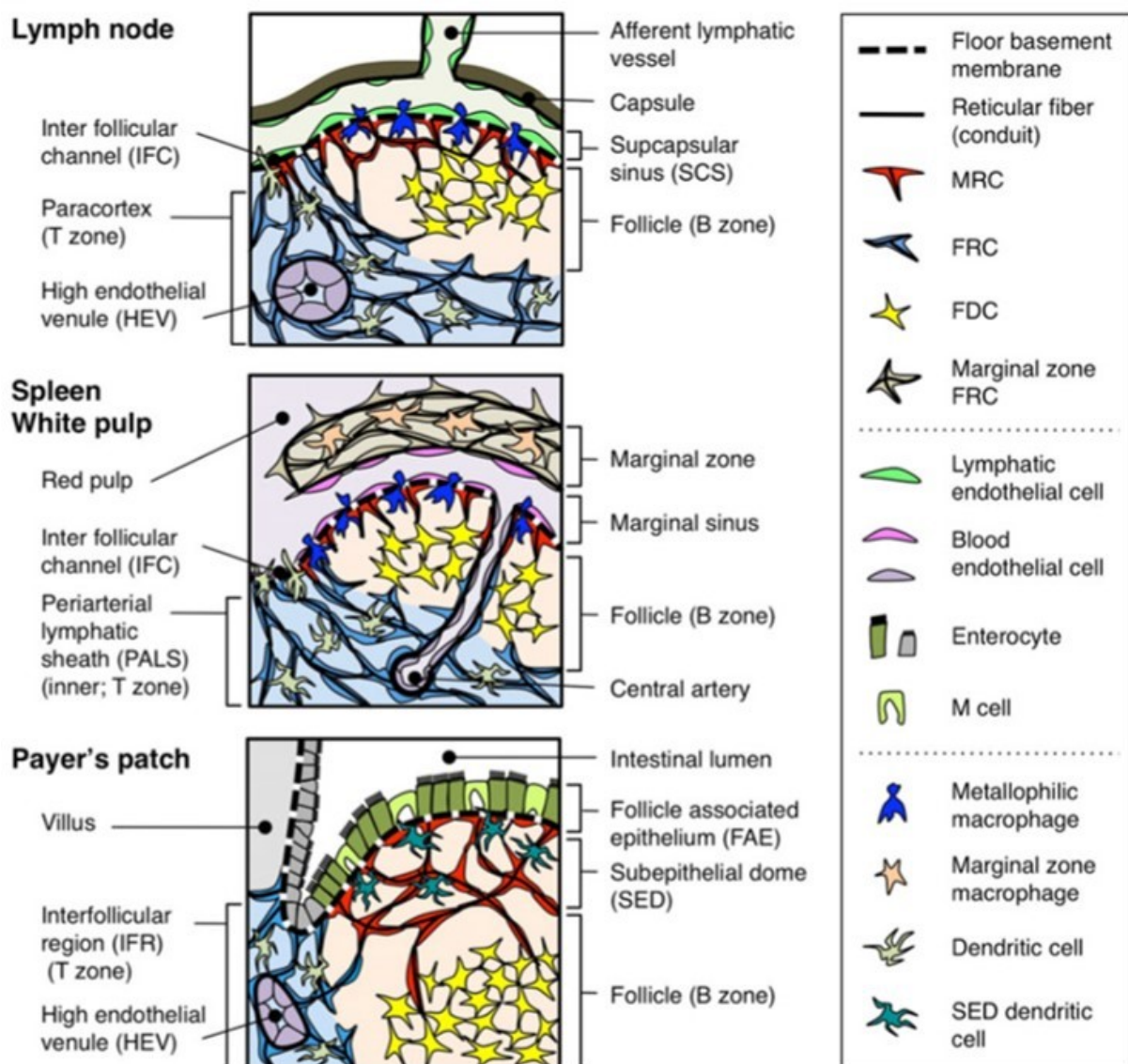

Figure 1. Stromal cell subsets in lymphoid organs. The diagrams represent the structural organization of mouse LN, spleen and Payer's patches with the resident stromal cells and non-stromal cells drawn at different location. FRC, fibroblastic reticular cell; FDC, follicular dendritic cell; MRC, marginal reticular cell. Modified after[25].

Based on their location, phenotype and biological functions, a summary of stroma cells in the SLOs and the mucosa associated lymphoid tissues (MALT) is shown in table 1.

Stromal cell subsets	Tissue of location	Markers	Biological functions
Fibroblastic Reticular cell (FRC)	SLOs (LN, spleen), Payer's patches, MALT, T cell zones.	ER-TR7[7] Gp38[8], CCL21 and CCL19[9] laminin, desmin, fibrillin, fibronectin, VCAM-1, ICAM1, collagen I, II, IV[1]	Conduit formation and transport (cytokines, chemokines, antigens)[4,5] Support and lymphocyte migration[6] Directing T cell-DC interactions[9]
Follicular Dendritic cell (FDC)	SLOs (LN, spleen), Payer's patches, MALT, B cell zones	CD35, CD21, CD16, CD23, CD32, FDC-M2, VCAM-1, ICAM1, MAdCAM-1, laminin, desmin, CXCL13, CXCL12, BAFF[1]	Antigen capture and presentation (immune complexes)[44] CXCL13 production for B cell homing[11] GC formation, antibody development[12,13]
Marginal Reticular cell (MRC)	Layer underneath SCS (LN) and MZ (spleen), Payer's patches, MALT.	ER-TR7, Gp38, RANKL, CXCL13, VCAM-1, ICAM1, MAdCAM-1[2,3]	SLO formation[2,3] Conduit formation/ small antigen delivery[13] FDC formation[45]
Spleen marginal zone fibroblast	Spleen	ER-TR7, desmin, laminin, integrins[16] ICAM1, CXCL12 and IL-6[15,17]	Assist macrophages in removal of dying red blood cells[1] Plasma cell guiding and function [15,17] Barrier formation upon stress and infection[18,19] and regulating blood flow[18]
LN medullary fibroblast	LN	ER-TR7, desmin, laminin, collagen I and IV, fibronectin[46] CXCL12[17] IL-6, BAFF, APRIL[46]	Directing plasma cell localization[15] Plasma cell survival and homeostasis[46]
Lymphatic endothelial cell (LEC)	LNs, Payer's patches, MALT.	CD31, LYVE1[26-27] Gp38[29] CCL21[24], VCAM-1[30], Calcium-activated chloride channel regulator-1 (CLCA1)[35] VGFR-3[50], Sphingosine-1-phosphate (S1P)[31] β-Chemokine Receptor D6[32], Prox1[20,28] MAdCAM1, CD41[47,48] CCL20, RANK, ACKR4 [48] MHC class I[33]	Lymphatic development[20] Transport (lymph, antigens)[21] Entry of APCs and T cells into LN [22,23] Chemokine production[24,25] Peripheral antigen presentation [33-35] Deletional tolerance[34,35] VCAM-1-mediated Treg migration to LN[30]
Blood endothelial cell (BEC)	Brain, SLOs (LN, spleen), Payer's patches, MALT.	CD31, VE-Cadherin, claudin 5[36], GlyCAM1[41], CD34, MECA-79[42] LTβR (LN)[43]	Transport of blood[38] Lining HEVs (LN) Physical barrier [36,37] Controlling exchange between the blood and the tissues[38,39]

Table 1. Stromal cell subsets in LN, spleen and Payer's patches. SLO, secondary lymphoid organ; MALT, mucosa-associated lymphoid tissue; SCS, subcapsular sinus; MZ, marginal zone; LTβR, lymphotoxin-beta receptor; ICAM-1, intercellular adhesion molecule 1; VCAM-1, vascular cell adhesion molecule 1; MAdCAM-1, mucosal vascular addressin cell adhesion molecule 1; BAFF, B cell activating factor; IL-6, interleukin 6; LYVE1, lymphatic vessel endothelial hyaluronan receptor 1; GC, germinal center; APC, antigen presenting cell; Treg, T regulatory cell; VE, vascular endothelium; APRIL, a proliferation-inducing ligand. Adapted after[1].

LN stroma is very heterogenous. Recently, by using single-Cell RNA Sequencing and flow cytometry, studies have highlighted distinct subsets of non-endothelial LN stromal cells based on their differential gene expression profiles and localization[46,49]. In the sections below, I will describe the lymphatic system and focus on LEC heterogeneity and functions.

2   Lymphatic vascular system

Extensive characterization of anatomic features of the lymphatic vasculature development started during the 20th century, mostly by using pig and mouse embryos[51,52]. Pioneering researchers suggested that the lymphatic vessels arise from preexisting blood vessels[51] and recent live imaging in mammals and zebrafish demonstrate that the progenitors of LECs that form the lymphatic vessels are of venous origin during embryogenesis[53,54]. The lymphatic vascular system is a network of vessels that carry lymph, the aqueous component of blood composed of water and plasma proteins, released through tissue blood capillary leaking. With exception of the central nervous system (brain and spinal cord), the lymphatic vessels are extended throughout the body, such as the skin, the intestine, the SLOs, etc. They drain the lymph, a process essential for the maintaining interstitial fluid homeostasis and immune cell trafficking. Another system of fluid drainage, called glymphatic system, takes up the cerebrospinal fluid from the brain and transports antigens and immune cell to the cervical LNs. However, the glymphatic system displays no structural similarities with the lymphatic vascular system[55,56]. A schematic illustration of the lymphatic vascular network within the intestine, the LN, the heart and peripheral tissues is shown in figure 2.
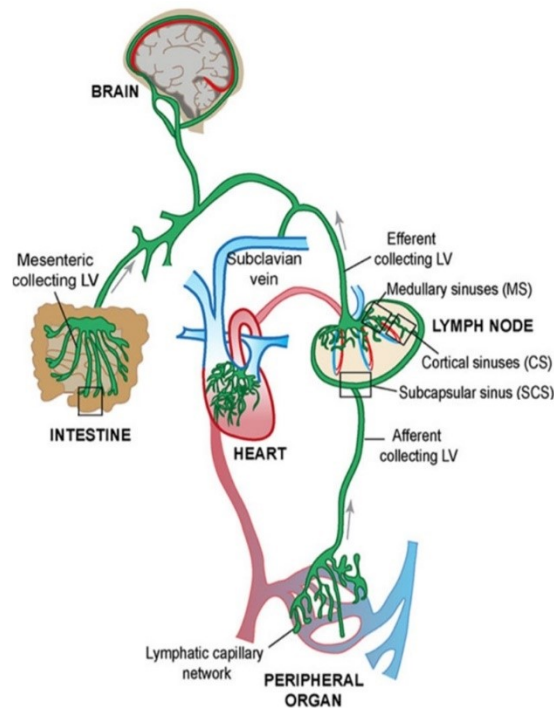
Figure 2. Organization of the lymphatic vasculature and the specialized lymphatic vessels within the intestine, the LN, the heart and peripheral tissue/organ. In green is shown the network of collecting lymphatics that drain lymph to LNs and lymphatic capillaries that absorb the lymph continuously leaked out from blood capillaries inside tissues. Red show blood circulation where lymph returns. The brain is avoided of lymphatic capillaries unlike other tissues. LV, lymphatic vessel. The arrows indicate the direction of fluid flow. Modified after[57].

The lymphatic vessel wall, also called vascular endothelium is made of a monolayer of LECs that form tight junctions but are still porous, enabling the uptake of interstitial fluids and the entry of foreign materials (harmful or not) and cells. The interstitial fluids are pumped through initial lymphatics (lymphatic capillaries) containing valves made by LECs, that function as flap to allow fluid entry into vessels and prevent retrograde flow into the tissues[58-61]. The initial lymphatics are connected to the collecting vessels that transport lymph to the LN (via afferent lymphatics) where it is filtered for immune surveillance. These collecting vessels also contain valves that allow the unidirectional flow of the lymph and are lined with vascular smooth muscle that contracts to transport and maintain the flow[62,63]. Lymph leaves the LN through efferent lymphatic and finally back to blood circulation through the inferior vena cava of the thoracic duct[64,65]. A schematic illustration of lymph collection from the peripheral tissue and the unidirectional flow through the lymphatic and blood vascular is shown in figure 3.
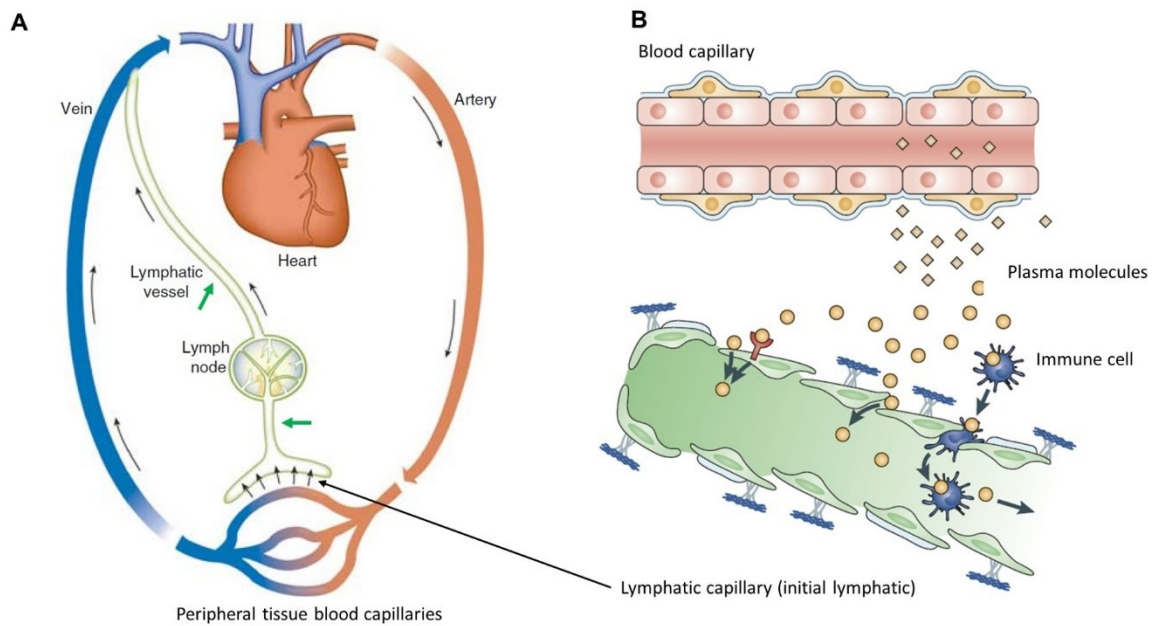
Figure 3. Schematic illustration of lymphatic and blood vascular circulation. (A) Lymph (interstitial fluid) is leaked from peripheral tissue via blood capillaries and pumped by lymphatic capillaries/initial lymphatics (lower black arrows) that convey it to the collecting lymphatic (lower green arrow). The latter drains it to the LN where it flows and egresses via the efferent collecting lymphatic (middle green arrow) and returns to blood circulation through the inferior vena cava of thoracic duct. The direction of lymph flow is indicated by the arrows. Modified after[65]. (B) The plasma-derived macromolecules and cells extravasated from blood capillaries enter the lymphatic capillaries through spaces (pores) formed by LECs lining these initial lymphatics (Green). Modified after[66].

The lymphatic capillaries and the collecting lymphatic vessels share many molecules such as Prox1, Gp38, the tyrosine kinase receptor vascular endothelial growth factor3 (VGFR3)[57] expressed by LECs as specific markers and regulators of the lymphatic vasculature development[67,68]. Inside LNs, the lymphatic vessels form a scattered network from the subcapsular area to the medulla. LN-LECs can be identified by flow cytometry as PECAM/CD31+ podoplanin/Gp38+ cells among the hematopoietic marker (CD45) negative stromal cells[69]. However, the LN-LEC population is highly heterogeneous. Based on their locations and the markers they differentially express, at least three subpopulations of LN-LECs have been identified. The PD-L1^{hi} ICAM-1^{hi} MAdCAM-1$^+$ LTβR^{lo} LECs locate in the collagenous capsule that surrounds the LN, the PD-L1^{hi} ICAM-1^{hi} MAdCAM-1$^-$ LTβR$^+$ LECs in locate in the medulla and the PD-L1^{int} ICAM-1^{int} MAdCAM-1$^-$ LTβR$^+$ LECs locate in the cortical area[70].

2.1 Subcapsular sinus lymphatic endothelial cells

The inner and the outer layers of the fibrous capsule are lined by the *ceiling* LECs (cLECs) and *floor* LECs (fLECs), respectively. The fLECs communicates with the HEVs through the reticular fibers and FRC network, to allow the access of LN parenchyma by trafficking cells. In addition to immune cells, the fLECs also allows the entry of small antigens and soluble molecules into the LN parenchyma[71]. They express the plasmalemma vesicle-associated protein (PLVAP), an endothelial glycoprotein that forms physical sieve, conferring a barrier function to these cells for selective exclusion of large molecules entering LN-SCS[72]. However, the expression of PLVAP seems to be specific to LN-LECs but not restricted to fLECs[72]. Moreover, the fLECs are lined by a laminin+ ER-TR7+ basement membrane-like extracellular matrix that allow them to interact with the MRCs and CD169+ SSMs[74]. The cLECs express CCRL1[73], also called ACKR4, a scavenger receptor that induces the internalization or the degradation of CCL19 and CCL21, the ligands for DC homing chemokine (CCR7) into lymphatic vessels and LN[75-77]. Recent studies have suggested that CCRL1 expression may scavenge target chemokines from the cLECs, to shape CCL21 gradients across the fLECs, facilitating the emigration of CCR7+ DCs from the SCS into the parenchyma, where both CCL19 and CCL21 are expressed in the paracortical T cell zone[73,78].

2.2 Medullary sinus and cortical lymphatic endothelial cells

Sphingosine-1-phosphate (S1P) is a sphingolipid which down-modulates its receptor S1P1 on the surface of lymphocytes, to enable their egress from the lymphoid organs[79,80]. Mice lacking the sphingosine kinases, the enzymes required for S1P synthesis displayed a loss of extracellular S1P production in the lymph, resulting to impaired lymphocyte egress from the LNs but also from the Payer's patches. Concomitantly, the levels of S1P1 were largely increased on the surface of naive T lymphocytes recovered from the LNs and Payer's patches of these mice compared to the controls. The medullary LECs (mLECs) and the cortical LECs (CS-LECs) are the highest cellular sources of S1P and S1P produced locally by LYVE1+ CS-LECs drives lymphocyte exit from the LNs. Mice lacking the sphingosine kinases also showed an altered lymphatic vasculature, suggesting a role of S1P in lymphatic maturation[79,80]. A schematic organization of LN structure with the different subpopulations of LECs and their location and markers is shown figure 4.
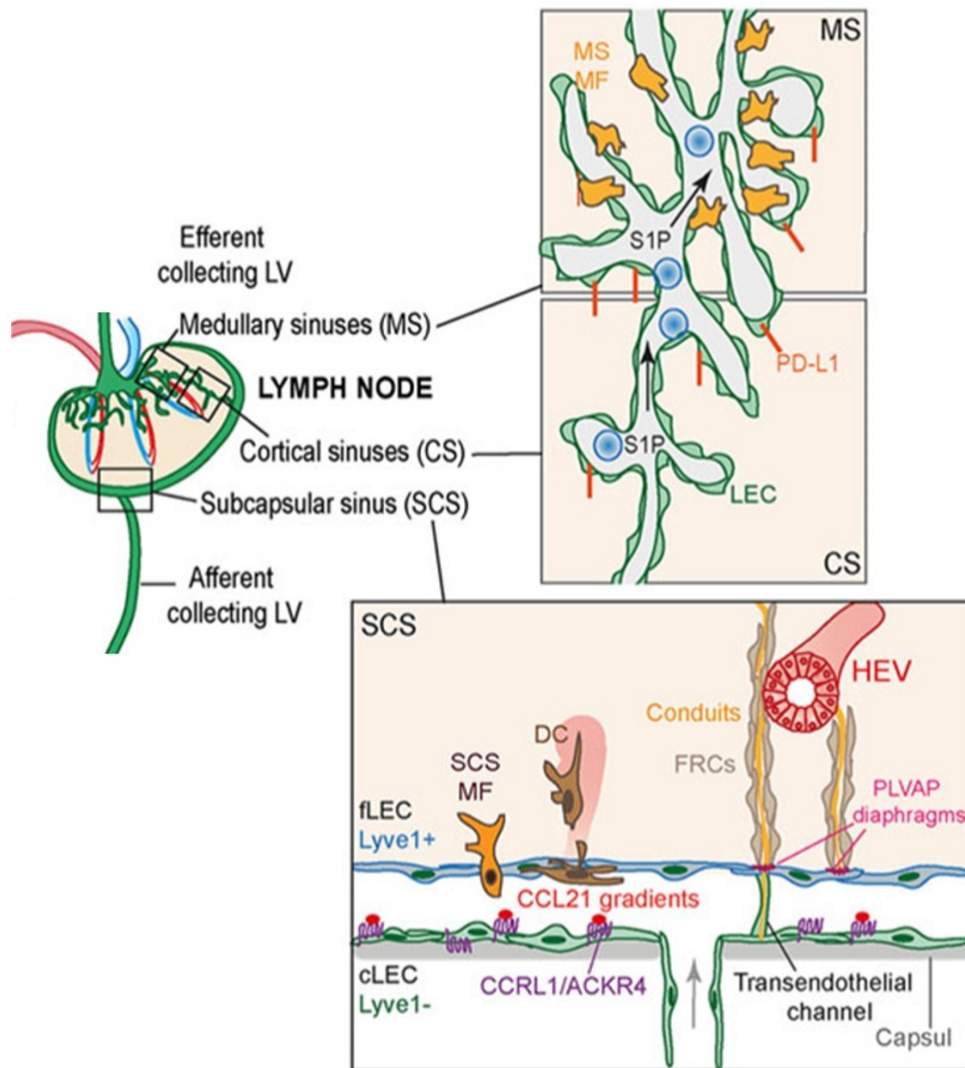
Figure 4. Organization of the LECs within LN. LECs in LN subcapsular sinus (SCS), medullary sinus (MS) and cortical sinus (CS) and their markers are shown. The SCS is lined by LYVE1⁻ceiling LECs (cLECs) and LYVE1⁺ floor LECs (fLECs). cLECs express ACKR4/CCRL1, which scavenges the chemokine CCL21, creating a gradient of CCL21 to allow CCR7⁺ DC emigration from the fLECs to LN parenchyma. The SCS and MS harbor different population of macrophages (yellow cells, indicated as MF). fLECs are linked to HEVs through the reticular fibers and the conduits formed by FRC network, allowing the transport of small antigens, cytokines as well as immune cells into the parenchyma. fLECs express also PLVAP that forms sieve-like diaphragms to restrict conduit access to low molecular weight molecules. LECs in MS and CS locally produced S1P to enable lymphocytes exit from LN and PD-L1 involved in the tolerogenic properties of LECs. Modified after[57].

3 Biological functions of lymphatic endothelial cells

3.1 Lymphatic endothelial cells in antigen presentation and immune tolerance

Self-reactive T cells that escape the thymic negative selection see tissue-derived peptides presented by quiescent tissue-resident dendritic cells to induce anergy or deletion, preventing autoimmunity. However, the peripheral tolerance is not restricted to DCs. In 2010, Cohen et al., have shown that LN-resident lymphatic endothelial cells (LN-LECs) express multiple peripheral tissue antigens (PTAs) such as the melanocyte-specific tyrosinase, the pancreatic polypeptide and the preproinsulin 2 independent of the auto-immune regulator (Aire)[81]. By using a transgenic mouse model that expresses a T cell receptor specific to tyrosinase-derived epitope (Tyr369), the authors have shown that the Gp38^{+}CD31^{+} LN-LECs can directly present antigen to tyrosinase-specific CD8^{+} T cells leading to their deletion[81]. In 2012, Tewalt et al., have discovered that LN-LECs mediate the deletion of tyrosinase-specific CD8^{+} T cells through the PD-L1-PD-1 axis and lack of costimulation[82]. They have shown that LN-LECs express high level of PD-L1 but lack the expression of CD80/86. To induce the tyrosinase-specific CD8^{+} T cell deletion, LECs present antigen without costimulation, inducing a rapid high-level expression of PD-1 on CD8^{+} T cells. PD-1 in turn inhibits the expression of IL-2 receptor, necessary for T cells survival[82]. Deficiency of either PD-1 or PD-L1 and blockade of PD-L1 rescued LEC-mediated deletion of CD8^{+} T cells, resulting to autoimmunity, as shown by depigmentation[82]. In 2014, the lab further showed that LECs in LN medulla are the main actors of LEC-induced peripheral tolerance[70]. LTβR signaling is required for the upregulation of PD-L1 on mLECs since Prox1-cre recombinase-mediated ablation of LTβR from LECs resulted in the loss of PD-L1 by mLECs[70]. B cells control PD-L1 expression in mLECs since mice deficient for B cells (μMT$^{2/2}$ and Rag1$^{2/2}$) showed reduced PD-L1 expression by mLECs[70]. These studies demonstrated that LN-LECs act as antigen presenting cells potentially involved in the peripheral tolerance. A schematic illustration of antigen presentation by LECs in the context of tolerance is shown in figure 5.
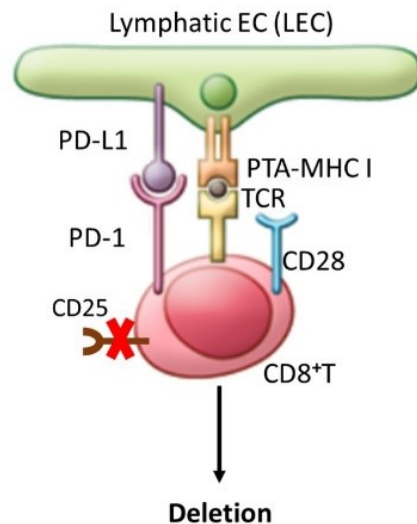
Figure 5. Schematic illustration of the peripheral tolerance induction by LN-LECs. LECs can express peripheral tissue antigen (PTA) and directly present it (in absence of costimulation) to naive CD8^{+} T cells to induce dysfunctional T cell activation and deletion through PD-L1-PD-1 axis-mediated loss of CD25 (IL-2 receptor). Modified after[83].

3.2   Lymphatic endothelial cells in inflammation

Inflammation is the response of the body to invading pathogens or endogenous signals to prevent further tissue damage by promoting tissue repair and healing. However, in some pathological conditions, prolonged inflammation can lead to tissue damage rather than repair. Immune cells including macrophages, neutrophils as well as lymphocytes are known as inflammatory cells because of their release of pro-inflammatory molecules such as cytokines, vasoactive substances, etc, that promote vasodilation, lymphangiogenesis and cell infiltration into the inflamed tissue. Lymphangiogenesis is the formation of new lymphatic vessels by the sprouting of pre-existing lymphatic vessels through the proliferation of LECs[85]. This process is a hallmark of the inflammation and can be induced by lymphangiogenic factors such as the vascular endothelial growth factor-C or D (VEGF-C/D) produced by immune cells such as the macrophages[85]. In 2010, Mounzer et al., have shown that LTα mainly produced by macrophages and lymphocytes at the inflammatory sites also promote LEC proliferation and lymphangiogensis[84]. During inflammation, lymphangiogenesis increases the trafficking of immune cells and antigens to the draining LN, maximizing their interactions. Studies have reported that inflammatory factors such as IL-1 and TNF- α induce VEGF-C/D expression in macrophages, DCs, mast cells and fibroblasts at the site of inflammation and NF-kB signaling

in LECs, leading to Prox1 activation and the upregulation of VEGFR3, the ligand for VEFG-C/D. These processes lead to neolymphangiogenesis[86-89].

Gamma interferon (IFN-γ) produced by T cells is an efficient anti-lymphangiogenic factor[109]. Chronic inflammation results from the lack of inflammation resolution, associated with lymphatic vessel dysfunction and lymphangiogenesis, as known in the pathogenesis of various diseases including psoriasis, rheumatoid arthritis, Crohn's disease, cancer, chronic infections, etc[90]. An emerging concept is to target prolymphangiogenic factors such as VEGF-C/D to help resolve chronic inflammatory diseases[90]. LN-LECs and peripheral LECs express the Toll-like receptors (TLRs)[83] and proliferate in response to inflammatory stimuli to modulate lymph drainage and the trafficking and function of leukocytes[91]. It has been shown that during inflammatory stimulation, inflamed LECs can directly interact with immature human monocyte-derived DCs to suppress their maturation and functions in a Mac–1/ICAM-1-dependent manner[92]. This impairs the ability of DCs to activate T-cells[92].

3.3   Lymphatic endothelial cells in cancer

Like in inflammation, lymphangiogenesis is activated in cancers where it promotes metastatic spread and tumor progression. In many human cancers such as the breast cancer, the lymphatic vessels in the tumor microenvironment are known as the route for tumor spreading by metastasis[93,94]. Lymphangiogenesis in tumor draining LNs precedes the metastasis and may support the survival of primary and secondary tumor cells[95]. The tumor microenvironment-derived factors (VEGF-C/D) induce lymphangiogenesis[95]. Some factors such as the prostaglandins produced by the tumor microenvironment can promote lymphangiogenesis in lung cancer by upregulating VEGF-C expression[96]. The xenografts of human cancer (breast, melanoma and lung) cells transfected with VEGF-C have been shown to induce the lymphangiogenesis and increased metastasis in LNs and lung[97]. The characterization of LECs isolated from human cancers showed that they express surface molecules that may support their interaction with tumor cells in lymphatic vessels to active the metastasis[98]. LECs lining the tumor lymphatic vessels express many factors called lymphangiocrine factors that recruit tumor cells to promote the growth[93]. In 2014, Lee et al., have shown that the treatment of mice with tumor-conditioned media activates lymphangiogenesis in LNs and lungs, accelerating metastasis to these organs[99]. By co-injecting human dermal LECs treated by tumor-conditioned media with human breast cancer cells into animals they discovered that

tumor-educated LECs secrete high amounts of the epidermal growth factor (EGF) and the platelet-derived growth factor B (PDGF-B) that promote tumor cell proliferation and angiongenesis, respectively[108]. Both EGF and PDFG-B have been shown to facilitate the intratumoral and LN metastasis by influencing the lymphangiogenesis[100,101]. Other factors, such as the transforming growth factor-β (TGFβ) has been reported to suppress the lymphangiogenesis in cancer. Inhibition of the endogenous TGFβ signaling in a mouse model of pancreatic cancer fosters lymphangiogenesis[102]. In experimental tumor models, deficiency or inhibition of the integrin $\alpha_4\beta_1$ that helps the LECs to adhere to the extracellular matrix during lymphatic vessel growth has been shown to block tumor-induced lymphangiogenesis and metastasis to the LNs[103].

The chemokine axis that facilitate the movement of cells into the LNs through the lymphatic vessels are also implicated in the metastasis. For example, CCR7 that drives DC homing to the LN through its ligand (CCL21) produced by LECs, can be expressed also by tumor cells, enabling their entry into the lymphatic vessels and the ensuing metastasis[104,105]. In many human cancers, the expression of CXC-chemokine receptor 4 (CXCR4) by the tumor cells have been significantly correlated with lymphatic and LN metastasis[105,107].

The role of LN-LECs in immune tolerance appears to be detrimental in cancer. For example, it has been shown that LECs in tumor draining LNs can present tumor antigen peptides to CD8+ T cells, leading to their dysfunction and apoptosis[110].

4 References

1. Mueller, Scott N., and Ronald N. Germain. 2009. "Stromal Cell Contributions to the Homeostasis and Functionality of the Immune System." Nature Reviews Immunology 9 (9): 618–29. https://doi.org/10.1038/nri2588.

2. Katakai, Tomoya, Hidenori Suto, Manabu Sugai, Hiroyuki Gonda, Atsushi Togawa, Sachiko Suematsu, Yukihiko Ebisuno, Koko Katagiri, Tatsuo Kinashi, and Akira Shimizu. 2008. "Organizer-Like Reticular Stromal Cell Layer Common to Adult Secondary Lymphoid Organs." The Journal of Immunology 181 (9): 6189–6200. https://doi.org/10.4049/jimmunol.181.9.6189.

3. Katakai, Tomoya. 2012. "Marginal Reticular Cells: A Stromal Subset Directly Descended from the LTO." Frontiers in Immunology 3. https://doi.org/10.3389/fimmu.2012.00200.

4. Gretz, J. Elizabeth, Christopher C. Norbury, Arthur O. Anderson, Amanda E.I. Proudfoot, and Stephen Shaw. 2000. "Lymph-Borne Chemokines and Other Low Molecular Weight Molecules Reach High Endothelial Venules via Specialized Conduits While a Functional Barrier Limits Access to the Lymphocyte Microenvironments in LN Cortex." The Journal of Experimental Medicine 192 (10): 1425–40. https://doi.org/10.1084/jem.192.10.1425.

5. Nolte, Martijn A., Jeroen A.M. Beliën, Inge Schadee-Eestermans, Wendy Jansen, Wendy W.J. Unger, Nico van Rooijen, Georg Kraal, and Reina E. Mebius. 2003. "A Conduit System Distributes Chemokines and Small Blood-Borne Molecules through the Splenic White Pulp." The Journal of Experimental Medicine 198 (3): 505–12. https://doi.org/10.1084/jem.20021801.

6. Bajénoff, Marc, Jackson G. Egen, Lily Y. Koo, Jean Pierre Laugier, Frédéric Brau, Nicolas Glaichenhaus, and Ronald N. Germain. 2006. "Stromal Cell Networks Regulate Lymphocyte Entry, Migration, and Territoriality in LNs." Immunity 25 (6): 989–1001. https://doi.org/10.1016/j.immuni.2006.10.011.

7. Van Vliet, E, M Melis, J M Foidart, and W Van Ewijk. 1986. "Reticular Fibroblasts in Peripheral Lymphoid Organs Identified by a Monoclonal Antibody." Journal of Histochemistry & Cytochemistry 34 (7): 883–90. https://doi.org/10.1177/34.7.3519751.

8. Farr, A. G. 1992. "Characterization and Cloning of a Novel Glycoprotein Expressed by Stromal Cells in T-Dependent Areas of Peripheral Lymphoid Tissues." Journal of Experimental Medicine 176 (5): 1477–82. https://doi.org/10.1084/jem.176.5.1477.

9. Luther, S. A., H. L. Tang, P. L. Hyman, A. G. Farr, and J. G. Cyster. 2000. "Coexpression of the Chemokines ELC and SLC by T Zone Stromal Cells and Deletion of the ELC Gene in the Plt/Plt Mouse." Proceedings of the National Academy of Sciences 97 (23): 12694–99. https://doi.org/10.1073/pnas.97.23.12694.

10. Gunn, M. D., K. Tangemann, C. Tam, J. G. Cyster, S. D. Rosen, and L. T. Williams. 1998. "A Chemokine Expressed in Lymphoid High Endothelial Venules Promotes the Adhesion and Chemotaxis of Naive T Lymphocytes." Proceedings of the National Academy of Sciences 95 (1): 258–63. https://doi.org/10.1073/pnas.95.1.258.

11. Gunn, Michael D., Vu N. Ngo, K. Mark Ansel, Eric H. Ekland, Jason G. Cyster, and Lewis T. Williams. 1998. "A B-Cell-Homing Chemokine Made in Lymphoid Follicles Activates Burkitt's Lymphoma Receptor-1." Nature 391 (6669): 799–803. https://doi.org/10.1038/35876.

12. Allen, C. D. C., T. Okada, H. L. Tang, and J. G. Cyster. 2007. "Imaging of Germinal Center Selection Events During Affinity Maturation." Science 315 (5811): 528–31. https://doi.org/10.1126/science.1136736.

13. Schwickert, Tanja A., Randall L. Lindquist, Guy Shakhar, Geulah Livshits, Dimitris Skokos, Marie H. Kosco-Vilbois, Michael L. Dustin, and Michel C. Nussenzweig. 2007. "In Vivo Imaging of Germinal Centres Reveals a Dynamic Open Structure." Nature 446 (7131): 83–87. https://doi.org/10.1038/nature05573.

14. Roozendaal, Ramon, Thorsten R. Mempel, Lisa A. Pitcher, Santiago F. Gonzalez, Admar Verschoor, Reina E. Mebius, Ulrich H. von Andrian, and Michael C. Carroll. 2009a. "Conduits Mediate Transport of Low-Molecular-Weight Antigen to LN Follicles." Immunity 30 (2): 264–76. https://doi.org/10.1016/j.immuni.2008.12.014.

15. Ellyard, Julia I., Danielle T. Avery, Charles R. Mackay, and Stuart G. Tangye. 2005. "Contribution of Stromal Cells to the Migration, Function and Retention of Plasma Cells in Human Spleen: Potential Roles of CXCL12, IL-6 and CD54." European Journal of Immunology 35 (3): 699–708. https://doi.org/10.1002/eji.200425442.

16. Timo K. van den Berg, Marja van der Ende, Ed A. D6pp, Georg Kraal, and Christine D. Dijkstra. 1993. Localization of (31 Integrins and Their Extracellular Ligands in Human Lymphoid Tissues. American Journtal ofPathology, Vol. 143, No. 4, October 1993.

17. Hargreaves, Diana C., Paul L. Hyman, Theresa T. Lu, Vu N. Ngo, Afshin Bidgol, Gen Suzuki, Yong-Rui Zou, Dan R. Littman, and Jason G. Cyster. 2001. "A Coordinated Change in Chemokine Responsiveness Guides Plasma Cell Movements." The Journal of Experimental Medicine 194 (1): 45–56. https://doi.org/10.1084/jem.194.1.45.

18. Weiss, Leon. 1990. "The Spleen in Malaria: The Role of Barrier Cells." Immunology Letters 25 (1–3): 165–72. https://doi.org/10.1016/0165-2478(90)90109-4.

19. Weiss, Leon. 1991. "Barrier Cells in the Spleen." *Immunology Today* 12 (1): 24–29. https://doi.org/10.1016/0167-5699(91)90108-6.

20. Wigle, Jeffrey T, and Guillermo Oliver. 1999. "Prox1 Function Is Required for the Development of the Murine Lymphatic System." Cell 98 (6): 769–78. https://doi.org/10.1016/S0092-8674(00)81511-1.

21. Grigorova, I. L., M. Panteleev, and J. G. Cyster. 2010. "LN Cortical Sinus Organization and Relationship to Lymphocyte Egress Dynamics and Antigen Exposure." Proceedings of the National Academy of Sciences 107 (47): 20447–52. https://doi.org/10.1073/pnas.1009968107.

22. Braun, Asolina, Tim Worbs, G Leandros Moschovakis, Stephan Halle, Katharina Hoffmann, Jasmin Bölter, Anika Münk, and Reinhold Förster. 2011. "Afferent Lymph–Derived T Cells and DCs Use Different Chemokine Receptor CCR7–Dependent Routes for Entry into the LN and Intranodal Migration." Nature Immunology 12 (9): 879–87. https://doi.org/10.1038/ni.2085.

23. Förster, Reinhold, Asolina Braun, and Tim Worbs. 2012. "LN Homing of T Cells and Dendritic Cells via Afferent Lymphatics." Trends in Immunology 33 (6): 271–80. https://doi.org/10.1016/j.it.2012.02.007.

24. Russo, Erica, Alvaro Teijeira, Kari Vaahtomeri, Ann-Helen Willrodt, Joël S. Bloch, Maximilian Nitschké, Laura Santambrogio, Dontscho Kerjaschki, Michael Sixt, and Cornelia Halin. 2016. "Intralymphatic CCL21 Promotes Tissue Egress of Dendritic Cells through Afferent Lymphatic Vessels." Cell Reports 14 (7): 1723–34. https://doi.org/10.1016/j.celrep.2016.01.048.

25. Randolph, Gwendalyn J., Stoyan Ivanov, Bernd H. Zinselmeyer, and Joshua P. Scallan. 2017. "The Lymphatic System: Integral Roles in Immunity." Annual Review of Immunology 35 (1): 31–52. https://doi.org/10.1146/annurev-immunol-041015-055354.

26. Lawrance, William, Suneale Banerji, Anthony J. Day, Shaumick Bhattacharjee, and David G. Jackson. 2016. "Binding of Hyaluronan to the Native Lymphatic Vessel Endothelial Receptor LYVE-1 Is Critically Dependent on Receptor Clustering and Hyaluronan Organization." Journal of Biological Chemistry 291 (15): 8014–30. https://doi.org/10.1074/jbc.M115.708305.

27. Jackson, D. 2003. "The Lymphatics Revisited New Perspectives from the Hyaluronan Receptor LYVE-1." Trends in Cardiovascular Medicine 13 (1): 1–7. https://doi.org/10.1016/S1050-1738(02)00189-5.

28. Yang, Ying, and Guillermo Oliver. 2014. "Transcriptional Control of Lymphatic Endothelial Cell Type Specification." In Developmental Aspects of the Lymphatic Vascular System, edited by Friedemann Kiefer and Stefan Schulte-Merker, 214:5–22. Vienna: Springer Vienna. https://doi.org/10.1007/978-3-7091-1646-3_2.

29. Bertozzi, Cara C., Paul R. Hess, and Mark L. Kahn. 2010. "Platelets: Covert Regulators of Lymphatic Development." Arteriosclerosis, Thrombosis, and Vascular Biology 30 (12): 2368–71. https://doi.org/10.1161/ATVBAHA.110.217281.

30. Brinkman, C. Colin, Daiki Iwami, Molly K. Hritzo, Yanbao Xiong, Sarwat Ahmad, Thomas Simon, Keli L. Hippen, Bruce R. Blazar, and Jonathan S. Bromberg. 2016. "Treg Engage Lymphotoxin Beta Receptor for Afferent Lymphatic Transendothelial Migration." Nature Communications 7 (1). https://doi.org/10.1038/ncomms12021.

31. Pham, Trung H.M., Peter Baluk, Ying Xu, Irina Grigorova, Alex J. Bankovich, Rajita Pappu, Shaun R. Coughlin, Donald M. McDonald, Susan R. Schwab, and Jason G. Cyster. 2010. "Lymphatic Endothelial Cell Sphingosine Kinase Activity Is Required for Lymphocyte Egress and Lymphatic Patterning." The Journal of Experimental Medicine 207 (1): 17–27. https://doi.org/10.1084/jem.20091619.

32. Nibbs, Robert J B, Ernst Kriehuber, Paul D Ponath, David Parent, Shixin Qin, John D M Campbell, Alison Henderson, et al. 2001a. "The Chemokine Receptor D6 Is Expressed by Lymphatic Endothelium and a Subset of Vascular tumors" 158 (3): 11.

33. Cohen, Jarish N., Cynthia J. Guidi, Eric F. Tewalt, Hui Qiao, Sherin J. Rouhani, Alanna Ruddell, Andrew G. Farr, Kenneth S. Tung, and Victor H. Engelhard. 2010. "LN–Resident Lymphatic Endothelial Cells Mediate Peripheral Tolerance via Aire-Independent Direct Antigen Presentation." The Journal of Experimental Medicine 207 (4): 681–88. https://doi.org/10.1084/jem.20092465.

34. Tewalt, E. F., J. N. Cohen, S. J. Rouhani, C. J. Guidi, H. Qiao, S. P. Fahl, M. R. Conaway, et al. 2012. "Lymphatic Endothelial Cells Induce Tolerance via PD-L1 and Lack of Costimulation Leading to High-Level PD-1 Expression on CD8 T Cells." Blood 120 (24): 4772–82. https://doi.org/10.1182/blood-2012-04-427013.

35. Cohen, Jarish N., Eric F. Tewalt, Sherin J. Rouhani, Erica L. Buonomo, Amber N. Bruce, Xiaojiang Xu, Stefan Bekiranov, Yang-Xin Fu, and Victor H. Engelhard. 2014a. "Tolerogenic Properties of Lymphatic Endothelial Cells Are Controlled by the LN Microenvironment." Edited by Derya Unutmaz. PLoS ONE 9 (2): e87740. https://doi.org/10.1371/journal.pone.0087740.

36. Delsing, Louise, Pierre Dönnes, José Sánchez, Maryam Clausen, Dimitrios Voulgaris, Anna Falk, Anna Herland, et al. 2018a. "Barrier Properties and Transcriptome Expression in Human IPSC-Derived Models of the Blood-Brain

Barrier: Barrier Properties and Transcriptome Expression in Human IPSC-Derived Models." STEM CELLS 36 (12): 1816–27. https://doi.org/10.1002/stem.2908.

37. Obermeier, Birgit, Richard Daneman, and Richard M Ransohoff. 2013. "Development, Maintenance and Disruption of the Blood-Brain Barrier." Nature Medicine 19 (12): 1584–96. https://doi.org/10.1038/nm.3407.

38. Pober, Jordan S., Wang Min, and John R. Bradley. 2009a. "Mechanisms of Endothelial Dysfunction, Injury, and Death." Annual Review of Pathology: Mechanisms of Disease 4 (1): 71–95. https://doi.org/10.1146/annurev.pathol.4.110807.092155.

39. Komarova, Yulia, and Asrar B. Malik. 2010. "Regulation of Endothelial Permeability via Paracellular and Transcellular Transport Pathways." Annual Review of Physiology 72 (1): 463–93. https://doi.org/10.1146/annurev-physiol-021909-135833.

40. Girard, Jean-Philippe, Christine Moussion, and Reinhold Förster. 2012. "HEVs, Lymphatics and Homeostatic Immune Cell Trafficking in LNs." Nature Reviews Immunology 12 (11): 762–73. https://doi.org/10.1038/nri3298.

41. lmai, Yasuyuki, Laurence A. Lasky, and Steven D. Rosen. 1993. "Sulphation Requirement for GlyCAM-1, an Endothelial Ligand for L-Selectin." Nature 361 (6412): 555–57. https://doi.org/10.1038/361555a0.

42. Hemmerich, S. 1994. "Sulfation-Dependent Recognition of High Endothelial Venules (HEV)- Ligands by L-Selectin and MECA 79, and Adhesion-Blocking Monoclonal Antibody." Journal of Experimental Medicine 180 (6): 2219–26. https://doi.org/10.1084/jem.180.6.2219.

43. Browning, Jeffrey L., Norm Allaire, Apinya Ngam-ek, Evangelia Notidis, Jane Hunt, Steven Perrin, and Roy A. Fava. 2005. "Lymphotoxin-β Receptor Signaling Is Required for the Homeostatic Control of HEV Differentiation and Function." Immunity 23 (5): 539–50. https://doi.org/10.1016/j.immuni.2005.10.002.

44. McCloskey, Megan L., Maria A. Curotto de Lafaille, Michael C. Carroll, and Adrian Erlebacher. 2011. "Acquisition and Presentation of Follicular Dendritic Cell–Bound Antigen by LN–Resident Dendritic Cells." The Journal of Experimental Medicine 208 (1): 135–48. https://doi.org/10.1084/jem.20100354.

45. Jarjour, Meryem, Audrey Jorquera, Isabelle Mondor, Stephan Wienert, Priyanka Narang, Mark C. Coles, Frederick Klauschen, and Marc Bajénoff. 2014. "Fate Mapping Reveals Origin and Dynamics of LN Follicular Dendritic Cells." The Journal of Experimental Medicine 211 (6): 1109–22. https://doi.org/10.1084/jem.20132409.

46. Huang, Hsin-Ying, Ana Rivas-Caicedo, François Renevey, Hélène Cannelle, Elisa Peranzoni, Leonardo Scarpellino, Debbie L. Hardie, et al. 2018. "Identification of a New Subset of LN Stromal Cells Involved in Regulating Plasma Cell Homeostasis." Proceedings of the National Academy of Sciences 115 (29): E6826–35. https://doi.org/10.1073/pnas.1712628115.

47. Cordeiro, Olga G., Mélanie Chypre, Nathalie Brouard, Simon Rauber, Farouk Alloush, Monica Romera-Hernandez, Cécile Bénézech, et al. 2016. "Integrin-Alpha IIb Identifies Murine LN Lymphatic Endothelial Cells Responsive to RANKL." Edited by Jörg Hermann Fritz. PLOS ONE 11 (3): e0151848. https://doi.org/10.1371/journal.pone.0151848.

48. Camara, Abdouramane, Olga G. Cordeiro, Farouk Alloush, Janina Sponsel, Mélanie Chypre, Lucas Onder, Kenichi Asano, et al. 2019. "LN Mesenchymal and Endothelial Stromal Cells Cooperate via the RANK-RANKL

Cytokine Axis to Shape the Sinusoidal Macrophage Niche." Immunity 50 (6): 1467-1481.e6. https://doi.org/10.1016/j.immuni.2019.05.008.

49. Rodda, Lauren B., Erick Lu, Mariko L. Bennett, Caroline L. Sokol, Xiaoming Wang, Sanjiv A. Luther, Ben A. Barres, Andrew D. Luster, Chun Jimmie Ye, and Jason G. Cyster. 2018. "Single-Cell RNA Sequencing of LN Stromal Cells Reveals Niche-Associated Heterogeneity." Immunity 48 (5): 1014-1028.e6. https://doi.org/10.1016/j.immuni.2018.04.006.

50. Kubo, Hajime, Takashi Fujiwara, Lotta Jussila, Hiroyuki Hashi, Minetaro Ogawa, Kenji Shimizu, Masaaki Awane, et al. 2000. "Involvement of Vascular Endothelial Growth Factor Receptor-3 in Maintenance of Integrity of Endothelial Cell Lining during tumor Angiogenesis" 96 (2): 8.

51. Sabin, Florence R. 1902. "On the Origin of the Lymphatic System from the Veins and the Development of the Lymph Hearts and Thoracic Duct in the Pig." American Journal of Anatomy 1 (3): 367–89. https://doi.org/10.1002/aja.1000010310

52. Van der Putte SC. 1975. "The early development of the lymphatic system in mouse embryos." Acta Morphol Neerl Scand. 1975 Dec;13(4):245-86.

53. Srinivasan, R. S., M. E. Dillard, O. V. Lagutin, F.-J. Lin, S. Tsai, M.-J. Tsai, I. M. Samokhvalov, and G. Oliver. 2007. "Lineage Tracing Demonstrates the Venous Origin of the Mammalian Lymphatic Vasculature." *Genes & Development* 21 (19): 2422–32. https://doi.org/10.1101/gad.1588407.

54. Yaniv, Karina, Sumio Isogai, Daniel Castranova, Louis Dye, Jiro Hitomi, and Brant M Weinstein. 2006. "Live Imaging of Lymphatic Development in the Zebrafish." *Nature Medicine* 12 (6): 711–16. https://doi.org/10.1038/nm1427.

55. Louveau, Antoine, Igor Smirnov, Timothy J. Keyes, Jacob D. Eccles, Sherin J. Rouhani, J. David Peske, Noel C. Derecki, et al. 2015. "Structural and Functional Features of Central Nervous System Lymphatic Vessels." Nature 523 (7560): 337–41. https://doi.org/10.1038/nature14432.

56. Aspelund, Aleksanteri, Salli Antila, Steven T. Proulx, Tine Veronica Karlsen, Sinem Karaman, Michael Detmar, Helge Wiig, and Kari Alitalo. 2015. "A Dural Lymphatic Vascular System That Drains Brain Interstitial Fluid and Macromolecules." The Journal of Experimental Medicine 212 (7): 991–99. https://doi.org/10.1084/jem.20142290.

57. Ulvmar, Maria H., and Taija Mäkinen. 2016. "Heterogeneity in the Lymphatic Vascular System and Its Origin." *Cardiovascular Research* 111 (4): 310–21. https://doi.org/10.1093/cvr/cvw175.

58. Moore, James E., and Christopher D. Bertram. 2018. "Lymphatic System Flows." *Annual Review of Fluid Mechanics* 50 (1): 459–82. https://doi.org/10.1146/annurev-fluid-122316-045259.

59. Baluk, Peter, Jonas Fuxe, Hiroya Hashizume, Talia Romano, Erin Lashnits, Stefan Butz, Dietmar Vestweber, et al. 2007. "Functionally Specialized Junctions between Endothelial Cells of Lymphatic Vessels." *The Journal of Experimental Medicine* 204 (10): 2349–62. https://doi.org/10.1084/jem.20062596.

60. Trzewik, Jürgen, S. K. Mallipattu, Gerhard M. Artmann, F. A. Delano, and Geert W. Schmid-Schönbein. 2001. "Evidence for a Second Valve System in Lymphatics: Endothelial Microvalves." *The FASEB Journal* 15 (10): 1711–17. https://doi.org/10.1096/fj.01-0067com.

61. Ikomi, Fumitaka, James Hunt, Gayda Hanna, and Geert W. Schmid-Schönbein. 1996. "Interstitial Fluid, Plasma Protein, Colloid, and Leukocyte Uptake into Initial Lymphatics." *Journal of Applied Physiology* 81 (5): 2060–67. https://doi.org/10.1152/jappl.1996.81.5.2060.

62. Kampmeier, Otto F. 1928. "The Genetic History of the Valves in the Lymphatic System of Man." *American Journal of Anatomy* 40 (3): 413–57. https://doi.org/10.1002/aja.1000400302.

63. Smith R.O. 1949. "A possible intrincsic mechanism of lymphatic vessels for the transport of lymph." J Exp Med. 1949 Nov;90(5):497-509.

64. Jurisic, Giorgia, and Michael Detmar. 2009. "Lymphatic Endothelium in Health and Disease." *Cell and Tissue Research* 335 (1): 97–108. https://doi.org/10.1007/s00441-008-0644-2.

65. Cueni, Leah N., and Michael Detmar. 2006. "New Insights into the Molecular Control of the Lymphatic Vascular System and Its Role in Disease." *Journal of Investigative Dermatology* 126 (10): 2167–77. https://doi.org/10.1038/sj.jid.5700464.

66. Trevaskis, Natalie L., Lisa M. Kaminskas, and Christopher J. H. Porter. 2015. "From Sewer to Saviour — Targeting the Lymphatic System to Promote Drug Exposure and Activity." *Nature Reviews Drug Discovery* 14 (11): 781–803. https://doi.org/10.1038/nrd4608.

67. Yang, Ying, and Guillermo Oliver. 2014. "Development of the Mammalian Lymphatic Vasculature." *Journal of Clinical Investigation* 124 (3): 888–97. https://doi.org/10.1172/JCI71609.

68. Koltowska, K., K. L. Betterman, N. L. Harvey, and B. M. Hogan. 2013. "Getting out and about: The Emergence and Morphogenesis of the Vertebrate Lymphatic Vasculature." *Development* 140 (9): 1857–70. https://doi.org/10.1242/dev.089565.

69. Link, Alexander, Tobias K Vogt, Stéphanie Favre, Mirjam R Britschgi, Hans Acha-Orbea, Boris Hinz, Jason G Cyster, and Sanjiv A Luther. 2007. "Fibroblastic Reticular Cells in LNs Regulate the Homeostasis of Naive T Cells." *Nature Immunology* 8 (11): 1255–65. https://doi.org/10.1038/ni1513.

70. Cohen, Jarish N., Eric F. Tewalt, Sherin J. Rouhani, Erica L. Buonomo, Amber N. Bruce, Xiaojiang Xu, Stefan Bekiranov, Yang-Xin Fu, and Victor H. Engelhard. 2014. "Tolerogenic Properties of Lymphatic Endothelial Cells Are Controlled by the LN Microenvironment." Edited by Derya Unutmaz. *PLoS ONE* 9 (2): e87740. https://doi.org/10.1371/journal.pone.0087740.

71. Gretz, J. Elizabeth, Christopher C. Norbury, Arthur O. Anderson, Amanda E.I. Proudfoot, and Stephen Shaw. 2000. "Lymph-Borne Chemokines and Other Low Molecular Weight Molecules Reach High Endothelial Venules via Specialized Conduits While a Functional Barrier Limits Access to the Lymphocyte Microenvironments in LN Cortex." *The Journal of Experimental Medicine* 192 (10): 1425–40. https://doi.org/10.1084/jem.192.10.1425.

72. Rantakari, Pia, Kaisa Auvinen, Norma Jäppinen, Maria Kapraali, Joona Valtonen, Marika Karikoski, Heidi Gerke, et al. 2015. "The Endothelial Protein PLVAP in Lymphatics Controls the Entry of Lymphocytes and Antigens into LNs." *Nature Immunology* 16 (4): 386–96. https://doi.org/10.1038/ni.3101.

73. Ulvmar, Maria H, Kathrin Werth, Asolina Braun, Poonam Kelay, Elin Hub, Kathrin Eller, Li Chan, et al. 2014. "The Atypical Chemokine Receptor CCRL1 Shapes Functional CCL21 Gradients in LNs." *Nature Immunology* 15 (7): 623–30. https://doi.org/10.1038/ni.2889.

74. Katakai, Tomoya, Hidenori Suto, Manabu Sugai, Hiroyuki Gonda, Atsushi Togawa, Sachiko Suematsu, Yukihiko Ebisuno, Koko Katagiri, Tatsuo Kinashi, and Akira Shimizu. 2008. "Organizer-Like Reticular Stromal Cell Layer Common to Adult Secondary Lymphoid Organs." *The Journal of Immunology* 181 (9): 6189–6200. https://doi.org/10.4049/jimmunol.181.9.6189.

75. Weber, M., R. Hauschild, J. Schwarz, C. Moussion, I. de Vries, D. F. Legler, S. A. Luther, T. Bollenbach, and M. Sixt. 2013. "Interstitial Dendritic Cell Guidance by Haptotactic Chemokine Gradients." *Science* 339 (6117): 328–32. https://doi.org/10.1126/science.1228456.

76. Russo, Erica, Alvaro Teijeira, Kari Vaahtomeri, Ann-Helen Willrodt, Joël S. Bloch, Maximilian Nitschké, Laura Santambrogio, Dontscho Kerjaschki, Michael Sixt, and Cornelia Halin. 2016. "Intralymphatic CCL21 Promotes Tissue Egress of Dendritic Cells through Afferent Lymphatic Vessels." *Cell Reports* 14 (7): 1723–34. https://doi.org/10.1016/j.celrep.2016.01.048.

77. Braun, Asolina, Tim Worbs, G Leandros Moschovakis, Stephan Halle, Katharina Hoffmann, Jasmin Bölter, Anika Münk, and Reinhold Förster. 2011. "Afferent Lymph–Derived T Cells and DCs Use Different Chemokine Receptor CCR7–Dependent Routes for Entry into the LN and Intranodal Migration." *Nature Immunology* 12 (9): 879–87. https://doi.org/10.1038/ni.2085.

78. Förster, Reinhold, Ana Clara Davalos-Misslitz, and Antal Rot. 2008. "CCR7 and Its Ligands: Balancing Immunity and Tolerance." *Nature Reviews Immunology* 8 (5): 362–71. https://doi.org/10.1038/nri2297.

79. Pham, Trung H.M., Peter Baluk, Ying Xu, Irina Grigorova, Alex J. Bankovich, Rajita Pappu, Shaun R. Coughlin, Donald M. McDonald, Susan R. Schwab, and Jason G. Cyster. 2010. "Lymphatic Endothelial Cell Sphingosine Kinase Activity Is Required for Lymphocyte Egress and Lymphatic Patterning." *The Journal of Experimental Medicine* 207 (1): 17–27. https://doi.org/10.1084/jem.20091619.

80. Matloubian, Mehrdad, Charles G. Lo, Guy Cinamon, Matthew J. Lesneski, Ying Xu, Volker Brinkmann, Maria L. Allende, Richard L. Proia, and Jason G. Cyster. 2004. "Lymphocyte Egress from Thymus and Peripheral Lymphoid Organs Is Dependent on S1P Receptor 1." *Nature* 427 (6972): 355– 60. https://doi.org/10.1038/nature02284.

81. Cohen, Jarish N., Cynthia J. Guidi, Eric F. Tewalt, Hui Qiao, Sherin J. Rouhani, Alanna Ruddell, Andrew G. Farr, Kenneth S. Tung, and Victor H. Engelhard. 2010. "LN–Resident Lymphatic Endothelial Cells Mediate Peripheral Tolerance via Aire-Independent Direct Antigen Presentation." *The Journal of Experimental Medicine* 207 (4): 681– 88. https://doi.org/10.1084/jem.20092465.

82. Tewalt, E. F., J. N. Cohen, S. J. Rouhani, C. J. Guidi, H. Qiao, S. P. Fahl, M. R. Conaway, et al. 2012. "Lymphatic Endothelial Cells Induce Tolerance via PD-L1 and Lack of Costimulation Leading to High-Level PD-1 Expression on CD8 T Cells." *Blood* 120 (24): 4772–82. https://doi.org/10.1182/blood-2012-04-427013.

83. Card, Catherine M., Shann S. Yu, and Melody A. Swartz. 2014. "Emerging Roles of Lymphatic Endothelium in Regulating Adaptive Immunity." *Journal of Clinical Investigation* 124 (3): 943–52. https://doi.org/10.1172/JCI73316.

84. Mounzer, R. H., O. S. Svendsen, P. Baluk, C. M. Bergman, T. P. Padera, H. Wiig, R. K. Jain, D. M. McDonald, and N. H. Ruddle. 2010. "Lymphotoxin-Alpha Contributes to Lymphangiogenesis." Blood 116 (12): 2173–82. https://doi.org/10.1182/blood-2009-12-256065.

85. Kim, Kyung Eun, Young-Jun Koh, Bong-Hyun Jeon, Cholsoon Jang, Jinah Han, Raghu P. Kataru, Reto A. Schwendener, Jin-Man Kim, and Gou Young Koh. 2009. "Role of CD11b+ Macrophages in Intrapefritoneal Lipopolysaccharide-Induced Aberrant Lymphangiogenesis and Lymphatic Function in the Diaphragm." *The American Journal of Pathology* 175 (4): 1733–45. https://doi.org/10.2353/ajpath.2009.090133.

86. Buckley, Christopher D., Francesca Barone, Saba Nayar, Cecile Bénézech, and Jorge Caamaño. 2015. "Stromal Cells in Chronic Inflammation and Tertiary Lymphoid Organ Formation." *Annual Review of Immunology* 33 (1): 715–45. https://doi.org/10.1146/annurev-immunol-032713-120252.

87. Alitalo, Kari, Tuomas Tammela, and Tatiana V. Petrova. 2005. "Lymphangiogenesis in Development and Human Disease." *Nature* 438 (7070): 946–53. https://doi.org/10.1038/nature04480.

88. Kunder, C. A., A. L. St John, and S. N. Abraham. 2011. "Mast Cell Modulation of the Vascular and Lymphatic Endothelium." *Blood* 118(20):5383–93. https://doi.org/10.1182/blood-2011-07-358432.
99. Lee, Esak, Niranjan B. Pandey, and Aleksander S. Popel. 2014. "Pre-Treatment of Mice with tumor-Conditioned Media Accelerates Metastasis to LNs and Lungs: A New Spontaneous Breast Cancer Metastasis Model." *Clinical & Experimental Metastasis* 31 (1): 67–79. https://doi.org/10.1007/s10585-013-9610-9.

89. Cursiefen, Claus, Lu Chen, Leonardo P. Borges, David Jackson, Jingtai Cao, Czeslaw Radziejewski, Patricia A. D'Amore, M. Reza Dana, Stanley J. Wiegand, and J. Wayne Streilein. 2004. "VEGF-A Stimulates Lymphangiogenesis and Hemangiogenesis in Inflammatory Neovascularization via Macrophage Recruitment." *Journal of Clinical Investigation* 113 (7): 1040–50. https://doi.org/10.1172/JCI200420465.

90. Alitalo, Kari. 2011. "The Lymphatic Vasculature in Disease." *Nature Medicine* 17 (11): 1371–80. https://doi.org/10.1038/nm.2545.

91. Aebischer, David, Maria Iolyeva, and Cornelia Halin. 2014. "The Inflammatory Response of Lymphatic Endothelium." Angiogenesis 17 (2): 383–93. https://doi.org/10.1007/s10456-013-9404-3.

92. Podgrabinska, Simona, Okebugwu Kamalu, Lloyd Mayer, Motomu Shimaoka, Hans Snoeck, Gwendalyn J. Randolph, and Mihaela Skobe. 2009. "Inflamed Lymphatic Endothelium Suppresses Dendritic Cell Maturation and Function via Mac-1/ICAM-1-Dependent Mechanism." *The Journal of Immunology* 183 (3): 1767–79. https://doi.org/10.4049/jimmunol.0802167.

93. Alitalo, A, and M Detmar. 2012. "Interaction of tumor Cells and Lymphatic Vessels in Cancer Progression." *Oncogene* 31 (42): 4499–4508. https://doi.org/10.1038/onc.2011.602.

94. Ran, Sophia, Lisa Volk, Kelly Hall, and Michael J. Flister. 2010. "Lymphangiogenesis and Lymphatic Metastasis in Breast Cancer." *Pathophysiology* 17 (4): 229–51. https://doi.org/10.1016/j.pathophys.2009.11.003.

95. Stacker, Steven A., Steven P. Williams, Tara Karnezis, Ramin Shayan, Stephen B. Fox, and Marc G. Achen. 2014. "Lymphangiogenesis and Lymphatic Vessel Remodelling in Cancer." *Nature Reviews Cancer* 14 (3): 159–72. https://doi.org/10.1038/nrc3677.

96. Su, Jen-Liang, Jin-Yuan Shih, Men-Luh Yen, Yung-Ming Jeng, Cheng-Chi Chang, Chang-Yao Hsieh, Lin-Hung Wei, Pan-Chyr Yang, and Min-Liang Kuo. n.d. "Cyclooxygenase-2 Induces EP1- and HER-2/Neu-Dependent Vascular Endothelial Growth Factor-C Up-Regulation: A Novel Mechanism of Lymphangiogenesis in Lung Adenocarcinoma." *Cancer Research*., 12.

97. Mandriota, S. J. 2001. "Vascular Endothelial Growth Factor-C-Mediated Lymphangiogenesis Promotes tumor Metastasis." *The EMBO Journal* 20 (4): 672–82. https://doi.org/10.1093/emboj/20.4.672.

98. Farnsworth, Rae H., Marc G. Achen, and Steven A. Stacker. 2006. "Lymphatic Endothelium: An Important Interactive Surface for Malignant Cells." *Pulmonary Pharmacology & Therapeutics* 19 (1): 51–60. https://doi.org/10.1016/j.pupt.2005.02.003.

99. Lee, Esak, Niranjan B. Pandey, and Aleksander S. Popel. 2014. "Pre-Treatment of Mice with tumor-Conditioned Media Accelerates Metastasis to LNs and Lungs: A New Spontaneous Breast Cancer Metastasis Model." Clinical & Experimental Metastasis 31 (1): 67–79. https://doi.org/10.1007/s10585-013-9610-9.

100. Bracher, Andreas, Ana Soler Cardona, Stefanie Tauber, Astrid M. Fink, Andreas Steiner, Hubert Pehamberger, Heide Niederleithner, Peter Petzelbauer, Marion Gröger, and Robert Loewe. 2013. "Epidermal Growth Factor Facilitates Melanoma LN Metastasis by Influencing tumor Lymphangiogenesis." *Journal of Investigative Dermatology* 133 (1): 230–38. https://doi.org/10.1038/jid.2012.272.

101. Cao, Renhai. 2004. "PDGF-BB Induces Intratumoral Lymphangiogenesis and Promotes Lymphatic Metastasis." *CANCER CELL*, 13.

102. Oka, M., C. Iwata, H. I. Suzuki, K. Kiyono, Y. Morishita, T. Watabe, A. Komuro, M. R. Kano, and K. Miyazono. 2008. "Inhibition of Endogenous TGF- Signaling Enhances Lymphangiogenesis." *Blood* 111 (9): 4571–79. https://doi.org/10.1182/blood-2007-10-120337.

103. Garmy-Susini, B., C. J. Avraamides, M. C. Schmid, P. Foubert, L. G. Ellies, L. Barnes, C. Feral, et al. 2010. "Integrin 4 1 Signaling Is Required for Lymphangiogenesis and tumor Metastasis." *Cancer Research* 70 (8): 3042–51. https://doi.org/10.1158/0008-5472.CAN-09-3761.

104. Günther, Klaus, Julia Leier, Golo Henning, Arno Dimmler, Rafael Weißbach, Werner Hohenberger, and Reinhold Förster. 2005. "Prediction of LN Metastasis in Colorectal Carcinoma by Expressionof Chemokine Receptor CCR7." *International Journal of Cancer* 116 (5): 726–33. https://doi.org/10.1002/ijc.21123.

105. Mashino, Kohjiro, Noriaki Sadanaga, Hiroshi Yamaguchi, Fumiaki Tanaka, Mitsuhiko Ohta, Kenji Shibuta, Hiroshi Inoue, and Masaki Mori. 2002. "Expression of Chemokine Receptor CCR7 Is Associated with LN Metastasis of Gastric Carcinoma." CANCER RESEARCH 62, 2937–2941, May 15, 2002.

106. Schimanski, C C, R Bahre, I Gockel, A Müller, K Frerichs, V Hörner, A Teufel, et al. 2006. "Dissemination of Hepatocellular Carcinoma Is Mediated via Chemokine Receptor CXCR4." *British Journal of Cancer* 95 (2): 210–17. https://doi.org/10.1038/sj.bjc.6603251.

107. Ishikawa, Tohru, Koh-Ichi Nakashiro, Shingo Hara, Sebastian Klosek, Chunnan Li, Satoru Shintani, and Hiroyuki Hamakawa. 2006. "CXCR4 Expression Is Associated with Lymph-Node Metastasis of Oral Squamous Cell Carcinoma." *International Journal of Oncology*, January. https://doi.org/10.3892/ijo.28.1.61.

108. Lee, Esak, Niranjan B. Pandey, and Aleksander S. Popel. 2014. "Lymphatic Endothelial Cells Support tumor Growth in Breast Cancer." *Scientific Reports* 4 (1). https://doi.org/10.1038/srep05853.

109. Kim, Honsoul, Raghu P. Kataru, and Gou Young Koh. 2014. "Inflammation-Associated Lymphangiogenesis: A Double-Edged Sword?" *Journal of Clinical Investigation* 124 (3): 936–42. https://doi.org/10.1172/JCI71607.

110. Lund, Amanda W., Fernanda V. Duraes, Sachiko Hirosue, Vidya R. Raghavan, Chiara Nembrini, Susan N.

Thomas, Amine Issa, Stéphanie Hugues, and Melody A. Swartz. 2012. "VEGF-C Promotes Immune Tolerance in B16 Melanomas and Cross-Presentation of tumor Antigen by LN Lymphatics." *Cell Reports* 1 (3): 191–99. https://doi.org/10.1016/j.celrep.2012.01.005.

Chapter 4. The mononuclear phagocyte system

1   Phagocytosis and phagocyte system

Phagocytosis is an evolutionarily conserved mechanism that was discovered by the Russian biologist Elie Metchnikoff (1845-1916)[4]. It is an active engulfment of particles, microbes or apoptotic cells within cell vacuole, leading to their destruction and limiting the dissemination throughout the body[3]. The mechanism of the phagocytosis can be divided into different steps. The first steps consist of the chemotaxis and the recognition of pathogen (or damage)-associated molecular patterns (PAMP/DAMP) through the phagocytic receptors. The recognition of the danger signal leads to the activation of the cell membrane, triggering the engulfment. The engulfed target is internalized in a vacuole called phagosome, which is adorned by reactive oxygen species (ROS) where the target degradation starts. The phagosome fuses with intracellular granules containing digestive enzymes such as peroxydases, defensines, lysosomes, accompanied by its acidification and the formation of the phagolysosome. This leads to the complete lysis and digestion of the target[6,7]. A schematic illustration of the mechanism of phagocytosis in shown in figure 1.
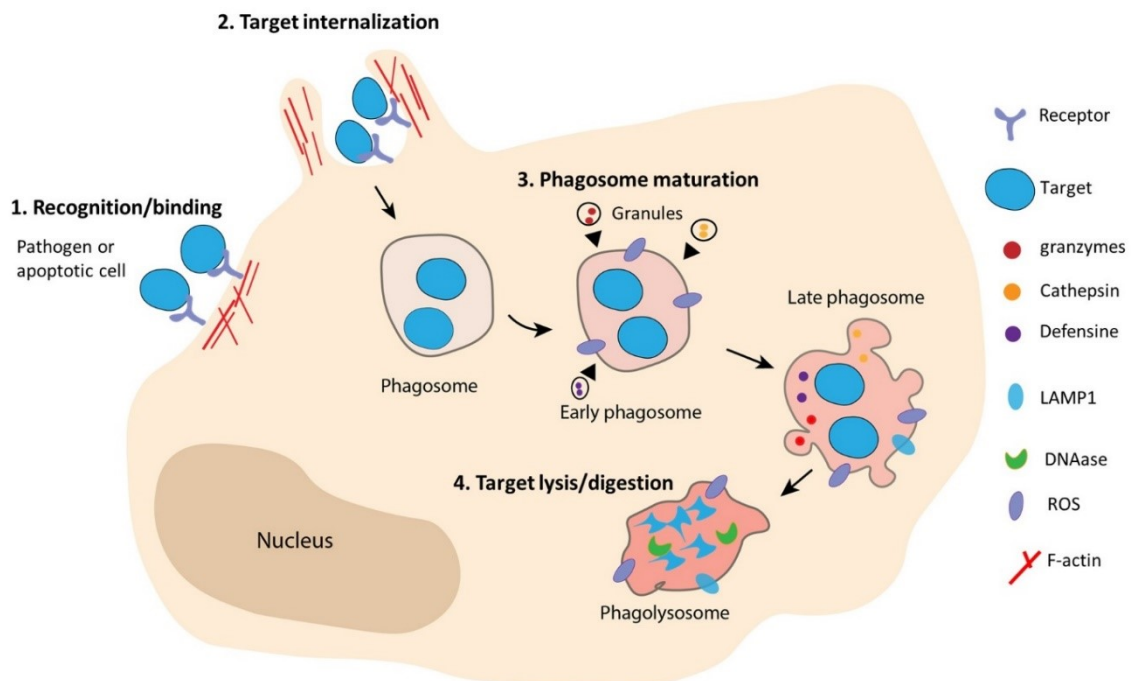
Figure 1. Mechanism of the phagocytosis. (1) The recognition of the target-associated molecular pattern by the surface receptor on phagocyte triggers membrane activation and F-actin polymerization and branching, leading to the extension and the protrusion of phagocyte plasma membrane around the target. (2) The protrusion progress until the edges of the target, resulting to its internalization and phagosome formation. (3) The newly formed phagosome undergoes a series of maturation by its fusion with cellular granules containing enzymes

(defensines, endosomes, lysosomes, etc) as well with reactive oxygen species (ROS), leading to the formation of the phagolysosome. (4) In the latter, the target is completely digested and destroyed by proteases and DNases. LAMP1, Lysosomal-associated membrane protein 1. Reproduced and modified after[8].

The phagocytes express a wide range of phagocytic receptors comprising the scavenger receptors, the complement receptors, the opsonic receptors, the apoptotic receptors and the pattern-recognition receptors such as Toll-like receptors (TLRs) and mannose receptor[6]. They can directly recognize their cognate ligands on the surface of the infectious agent or the apoptotic cell. They can also recognize opsonized targets. However, not all these receptors are found at the cell surface or mediate the phagocytosis. TLR3, 7, 8, 9 are intracellular and reside within endosomes and lysosomes where they recognize the nucleic acids released from engulfed microbe degradation[9]. In general, the activation of the TLRs causes inflammatory responses.

Based on some criteria such as ontogeny, phenotype, function and location that have been investigated in animal models, the term Mononuclear Phagocyte System had emerged to classify and define the myeloid cells comprising bone marrow progenitors, blood monocytes as well as tissue macrophages. The precursors of monocytes were originally identified by Ralph V. Furth and Zanvil A. Cohn, as bone marrow promonocytes that rapidly divide and peak in the peripheral blood 24h after labeling with the thymidine-3[1]. Two subsets of monocytes consisting of Ly6C^{hi} classical monocytes and Ly6C^{low} non-classical monocytes can be identified in mice. The classical monocytes are found as circulating in the blood but can also enter into the spleen and the LNs as well as tissues such as the skin, the liver, the kidney, the lung, etc, at the steady-state and more frequently during an inflammation. The non-classical monocytes remain mainly within the blood vessel walls where they patrol[2]. In human, the classical and the non-classical monocytes are defined as CD14^{hi} and CD14^{lo} monocytes respectively. By using staining dyes on tissues including the spleen, the LN, the lung, the liver as well as the intestine, Metchnikoff had revealed a high heterogeneity in the phagocyte populations and distinguished the polymorphic nuclear leukocytes also called microphages from the macrophages[5].

Macrophages are long-lived innate immune cells that have the ability to recognize, engulf and clear a large range of microbes and particulate antigens. They play also an important role in the homeostasis of their resident tissues. Most of our current knowledge on the ontogeny of

macrophages are from animal models, primarily the mouse. Tissue-resident macrophages (TrMφ) are known to originate from hematopoietic precursors of the embryonic yolk sac (YS), from the fetal liver precursors and from the bone marrow-derived precursors early after birth and in adult life[10]. Most of adult TrMφs develop during the embryogenesis, they self-renew locally by proliferation and can be renewed by circulating monocytes. During embryogenesis, $F4/80^+$ $CD11b^+$ Erythro-myeloid progenitors (EMPs) give rise to $CD45^+$ $CD11b^{lo}F4/80^{hi}Ly6C^-$ macrophages in the YS between E9.5 and E10.5. The apparition of the EMPs requires the transcription factor PU.1 since the cells are absent in *Pu1$^{-/-}$* mouse[11]. The YS-derived macrophages colonize the embryonic tissues including the skin, the spleen, the pancreas, the kidney, the brain as well as the lung from E14.5. The EMPs colonize also the fetal liver, giving rise to C-Myb$^+$ EMP-derived fetal monocytes. In 2015, Hoeffel et al., showed that these fetal liver monocytes can generate adult TrMφs[12]. With exception of brain microglia, the YS-derived macrophages in tissues decline from the early postnatal life to the adulthood. On the other hand, the proportions of macrophages derived from the fetal monocytes significantly increase in tissues after definitive hematopoesis[12]. An illustration of the ontogeny of tissue-resident macrophages is shown in figure 2.
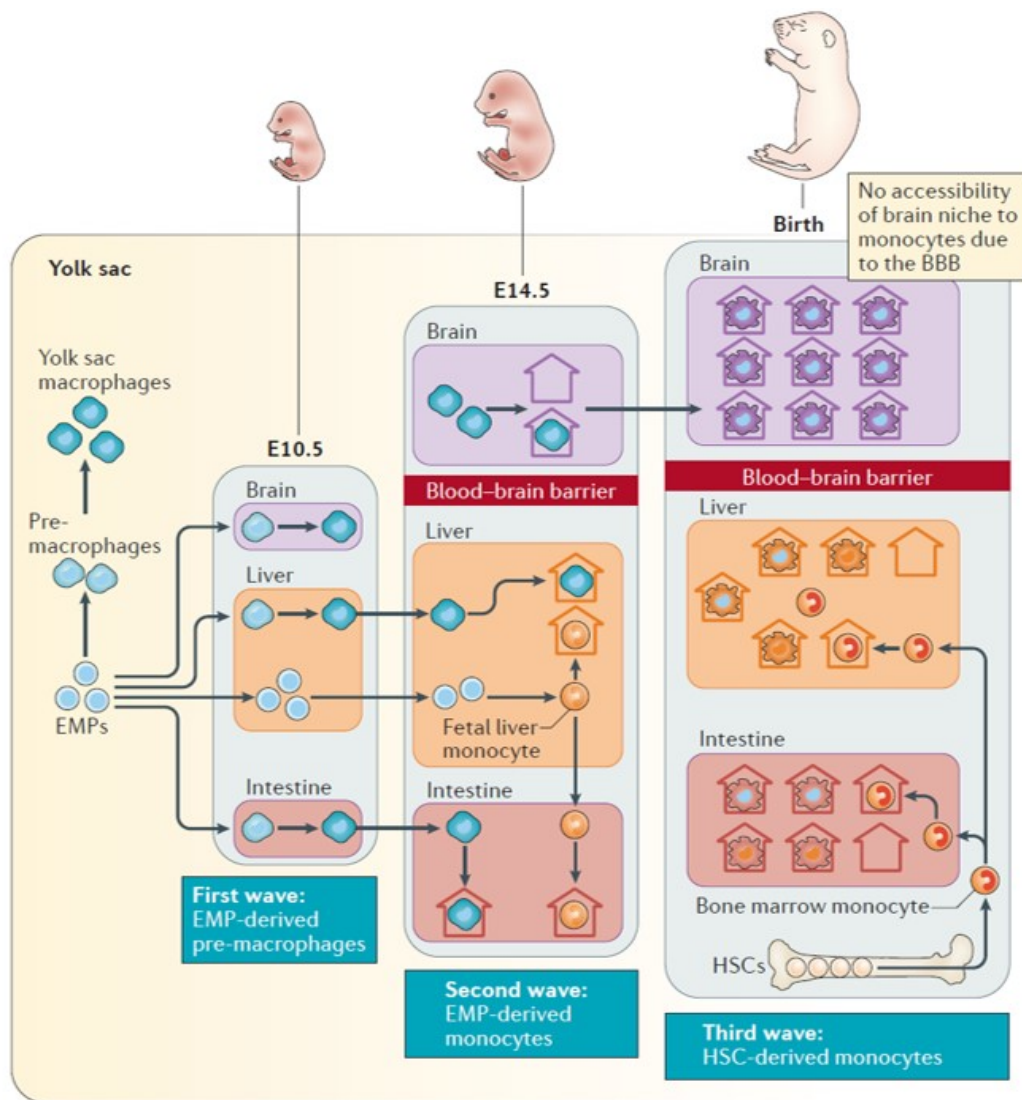
Figure 2. Ontogeny of the tissue-resident macrophages. Tissue-resident macrophages develop from three origins (waves) of precursors that seed tissues at different developmental stages. For the first wave coming between E9.5 and E10.5, the EMPs give rise to EMP-derived pre-macrophages that differentiate to YS-macrophages. The latter colonize and seed tissues from E14.5. The second wave coming from E14.5, coincides with the maturation of fetal liver where EMPs generate the fetal liver monocytes that differentiate to liver macrophages but also migrate to other tissues and form macrophages. At this stage, the blood-brain barrier forms and prevent the entry of the liver monocytes, limiting their contribution to the brain macrophages pool. The third wave of TrMφs results from the differentiation of HSC-derived monocytes after definitive bone marrow formation and the hematopoiesis after birth. Macrophages that seed tissue during the embryogenesis self-maintain locally by proliferation. They have a long turn-over rate and can be renewed by monocytes-derived macrophages that express the same tissue specific macrophages markers. The brain is not accessible to the circulating monocytes due to the blood brain barrier (BBB). Thus, brain macrophages (microglia) self-renewed from local precursors (probably of embryonic origin) at steady state throughout the life. The entry the and

differentiation of monocytes to macrophages may depend on the niche availability in the tissues. Modified after[13].

Macrophages display plasticity depending on the signals they receive from the surrounding environment and following the encounter with pathogens. When activated, they can undergo different states of polarization among which the M1 and M2 phenotypes, corresponding to the classically and the alternatively polarization states respectively. The classical polarization of macrophages is triggered by the toll-like receptor ligands such as the bacterial lipopolysaccharide, the ligand for TLR-4, that induces the expression of pro-inflammatory molecules (IL-1β, IL-6, TNF-α), the inducible nitric oxide synthase (iNOS) and the production of reactive oxygen species (ROS). The generation of nitric oxide by iNOS is known to inhibit M1 macrophage proliferation and to foster pathogen killing. The alternative polarization of macrophages is triggered by IL-4 or IL-13, that induce the expression of type I arginase that metabolizes the L-arginine. The metabolism of this amino acid triggers signaling cascades in M2 macrophages, leading to cell proliferation and collagen production. The M2 polarization state fosters the resolution of inflammation as well as wound healing. In addition to immune stimuli, metabolic products are also known to induce or support macrophage polarization through signaling cascades[14].

2   Heterogeneity of the tissue-resident macrophages

Tissue-resident macrophages display high heterogeneity. This is determined by their anatomical location in the tissues, gene expression profiles as well as functions[15]. Depending on the tissue they occupy, macrophages play different roles in development, immunity as well as homeostasis. For instance, microglia, the macrophages located in the brain are involved in brain development, homeostasis as well as surveillance[59,60] while lung alveolar macrophages are crucial for clearance of respiratory tract infections[61,62]. In addition to functional differences, flow cytometry analysis of plasma membrane proteins as well as single cell RNA sequencing have allowed a breakthrough in the understanding of macrophage heterogeneity. In the sections below, I will describe macrophages residing in the LN and spleen.

2.1   Lymph node CD169^{+} Subcapsular and medullary sinus macrophages

The subcapsular sinus macrophages (SSMs) reside along the subcapsular floor LECs, overlying the B cell follicle areas and the interfollicular zones. They are strategically positioned as the

first filter of innate defense to capture lymph-borne antigens and microorganisms and prevent their dissemination. Their counterparts, the medullary sinus macrophages (MSMs) are positioned in the cavities of the medulla, associated with medullary lymphatics. Both SSM and MSM express the pan-macrophage marker CD11b, the macrophage-colony stimulating factor receptor 1 (M-CSFR), the lymphotoxin β receptor (LTβR) and the Ig superfamily member CD169 (Siglec-1). CD169 is a sialic acid recognition receptor that binds sialylated antigens and is involved in cell-cell or cell-microorganism interactions. It is also the ligand for the mannose receptor (MR) that binds the mannose rich-antigens and activates the complement cascades[16]. In contrast to SSMs, MSMs also express F4/80 and SIGN-R1 that can be used to discriminate them. The differentiation of SSMs requires both M-CSF-1 and lymphotoxin produced by B cells. Mice deficient for these molecules lack SSMs. The differentiation of MSMs also requires M-CSF-1 but is independent of lymphotoxin[17-19].

CD169 belongs to the family of the Siglecs. They are type I transmembrane proteins characterized by an N-terminal V-set immunoglobulin domain ligated to variable numbers of C2-set immunoglobulin domains. The V-set immunoglobulin domain binds to sialic acid on cell and pathogens. Many members of the Siglec-family harbor variable numbers of the immunoreceptor tyrosine-based inhibitory motifs (ITIMs) in their cytosolic portion that give inhibitory signals to the cell. However, CD169 lacks the ITIM motif and has a long cytoplasmic tail, suggesting that it is mainly involved in cell–cell or cell-microorganism interactions rather than cell activation or inhibition. In human and rodent, the Siglec-family proteins may function in the endocytosis of sialylated glycoconjugates from pathogens, in host defense by leukocytes and in antigen presentation[20,21]. Human and rodent Siglec-family proteins and the main cells that express them is shown in figure 3.
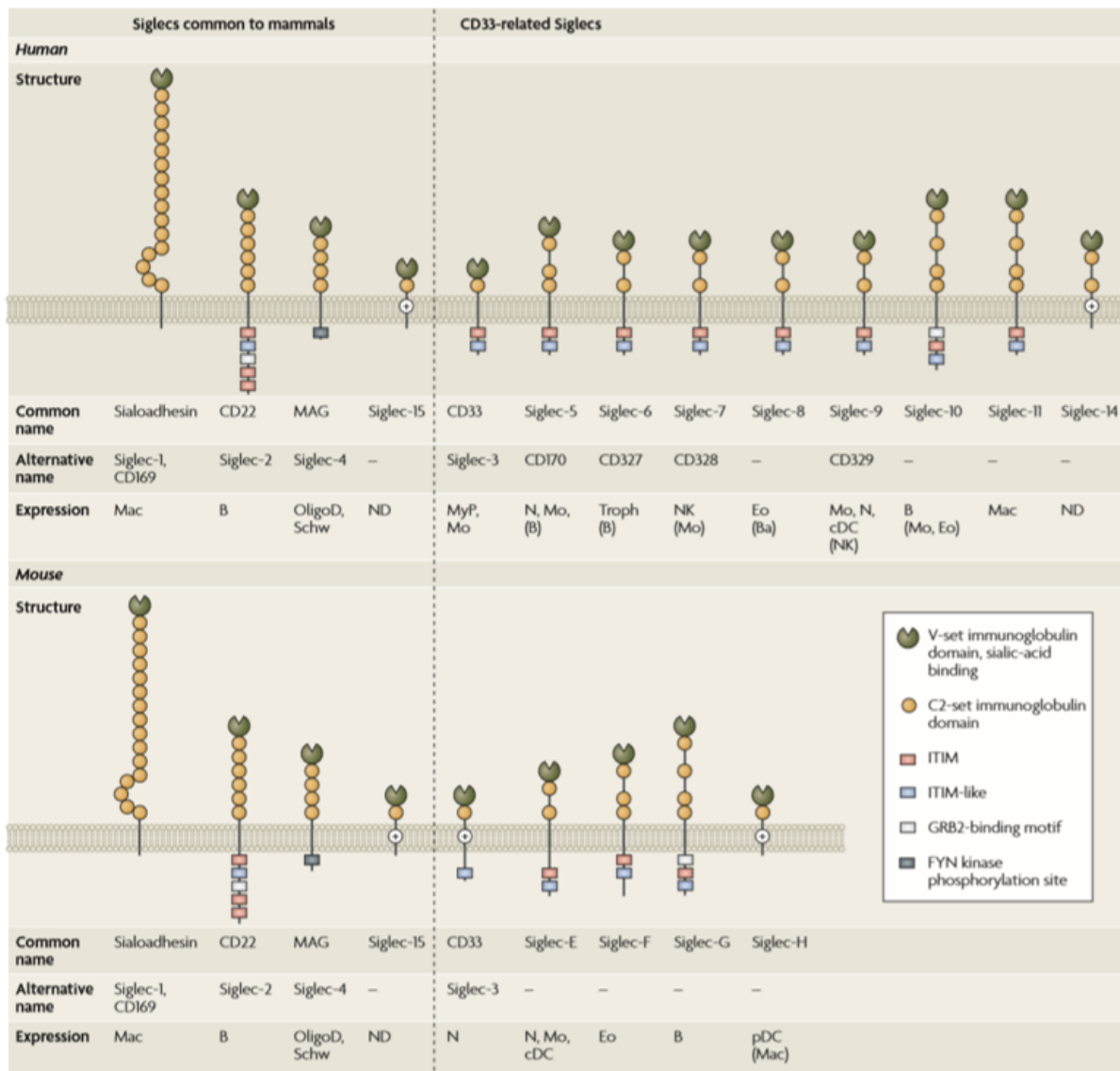
Siglecs common to mammals				CD33-related Siglecs								

Human

Structure

Common name	Sialoadhesin	CD22	MAG	Siglec-15	CD33	Siglec-5	Siglec-6	Siglec-7	Siglec-8	Siglec-9	Siglec-10	Siglec-11	Siglec-14
Alternative name	Siglec-1, CD169	Siglec-2	Siglec-4	–	Siglec-3	CD170	CD327	CD328	–	CD329	–	–	–
Expression	Mac	B	OligoD, Schw	ND	MyP, Mo	N, Mo, (B)	Troph (B)	NK (Mo)	Eo (Ba)	Mo, N, cDC (NK)	B (Mo, Eo)	Mac	ND

Mouse

Structure

Common name	Sialoadhesin	CD22	MAG	Siglec-15	CD33	Siglec-E	Siglec-F	Siglec-G	Siglec-H
Alternative name	Siglec-1, CD169	Siglec-2	Siglec-4	–	Siglec-3	–	–	–	–
Expression	Mac	B	OligoD, Schw	ND	N	N, Mo, cDC	Eo	B	pDC (Mac)

Legend:
- V-set immunoglobulin domain, sialic-acid binding
- C2-set immunoglobulin domain
- ITIM
- ITIM-like
- GRB2-binding motif
- FYN kinase phosphorylation site

Figure 3. **Siglec-family proteins in human and rodent**. Siglec family proteins are classified into two groups that are characterized by an amino terminal V-set immunoglobulin domain ligated to variable numbers of C2-set immunoglobulin domains. The first group of siglecs consists of the orthologues identified in all mammals, comprising CD169 (sailoadhesin), CD22, myelin-associated glycoprotein (MAG) and Siglec-15. These proteins exhibit 25–30% of sequence identity of their extracellular domains and have variable cytosolic tails. The second group consists of CD33-related Siglecs that display high sequence homology of their extracellular domains. Many CD33-related Siglecs and CD22 harbor one or more immunoreceptor tyrosine-based inhibitory motifs (ITIM) in their cytosolic domains. These motifs function in the suppression of activating signals in cell, through the recruitment of tyrosine and inositol phosphatases. Apart from Siglec-4 that is expressed by in the nervous system, the Siglec-proteins are mainly expressed by leukocytes in mammals. B, B cells; Ba, basophils; cDCs, conventional dendritic cells; Eo, eosinophils; GRB2, growth-factor-receptor-bound protein 2; Mac, macrophages; Mo, monocytes; MyP, myeloid progenitors; N, neutrophils; NK, natural killer cells; OligoD, oligodendrocytes;

pDCs, plasmacytoid dendritic cells; Schw, Schwann cells; Troph, trophoblasts; ND, not determined. Modified after[20].

2.1.1 Sinusoidal macrophages in infection

Electron microscopic study of the uptake of horseradish peroxidase in LN has shown that SSMs are less phagocytic than MSMs. Moreover, compared to MSMs, SSMs show slower depletion rate following clodronate liposomes (CLLs) treatment. Indeed, from one day to three days following CCLs administration of animals, MSMs are totally eliminated whereas a small proportion of SSMs still persist before their complete disappearance by 5 days[22,23]. SSM acquires, degrades lymph-borne pathogens and particles and induces B cell response by transferring antigens to these cells[24,25]. In responses to a viral and bacterial infection or to pathogen-derived immune stimuli, SSMs can eliminate the invaders by undergoing pyroptosis and the release of IL-1β, IL-18, type I interferon (IFN-α/β), IFN- γ, as well as other cytokines and pro-inflammatory molecules such as CCL11, CCL22, CXCL2, CXCL10, CCL19, XCL-1, LIF, CCL2, to alert and mobilize other immune cells including DCs, neutrophils, natural killer cells and monocytes[26-28]. In the absence of SSMs, B and T cell responses to viral and bacterial infections are impaired[29,30]. By using two-photon intravital microscopy to track CD8$^+$ T cell (OT-I cells) *in vivo*, Hickman et al., have shown that these cells migrate and accumulate in the LN SSM area upon viral infection and suggested that SSMs may present virus-derived antigens to CD8$^+$ T cells through the major histocompatibility complex (MHC) class I molecule[31]. An illustration of viral elimination by SSMs and the induction of B and T cell responses is shown in figure 5.
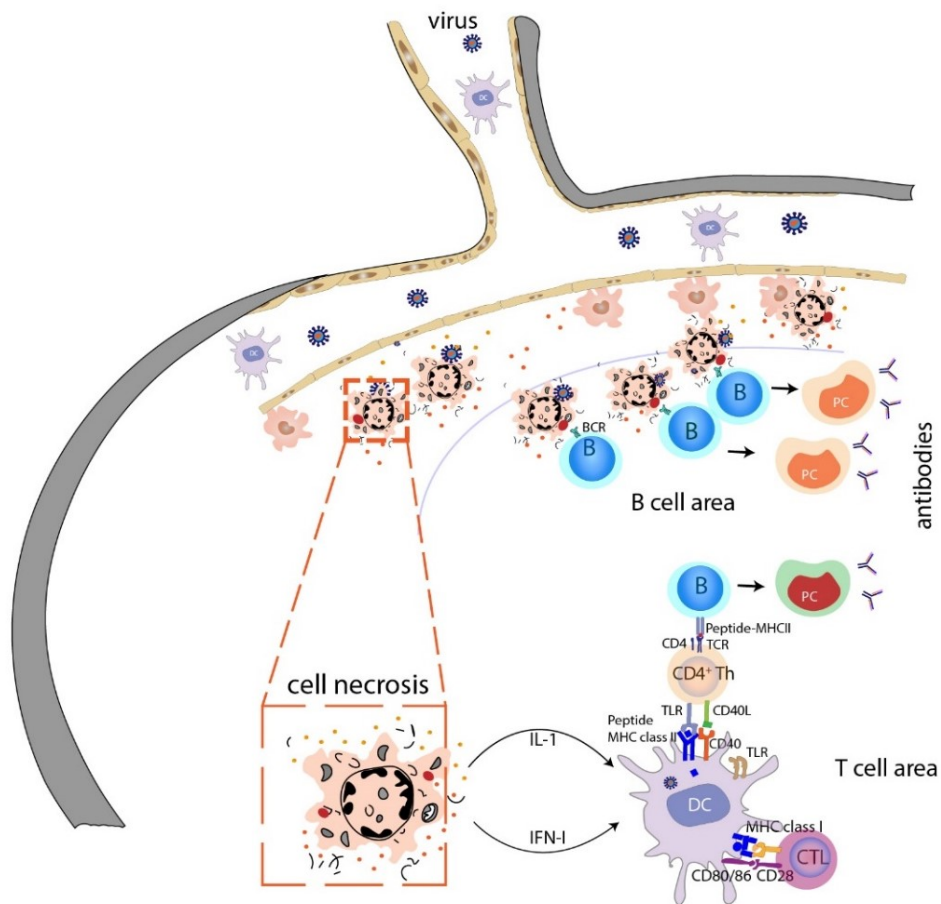
Figure 4. The antiviral response and induction of the adaptive immune responses by subcapsular sinus macrophages. SSMs capture and degrade lymph-borne virus, migrate and transfer viral particles to cognate B cells that may recognize antigen through the B cell receptor (BCR). This leads to the activation of the germinal center B cells and the generation of antibody producing plasma cells. By degrading (eliminating) the virus, SSM can undergo the pyroptosis (or necrosis) few hours after infection. This is concomitant with the recruitment of other innate immune cells such as the DCs in the draining LN. DCs also can capture and degrade the virus and cross-present viral antigens to CD4+ helper T and CD8+ cytotoxic lymphocytes through MHC class II and I respectively. Some pro-inflammatory cytokines such as IL-1 and IFN-I produced by the necrotic SSMs stimulate the DCs for the activation and the induction of T cell responses and T-cell dependent antibody production.

SSMs and MSMs differ in their capture of lymph-borne viruses. Some viruses such as the vesicular stomatitis virus (VSV) are captured only by SSM whereas the modified vaccinia Ankara (MVA) and influenza are captured by both macrophage subsets[24,32,33]. In contrast to SSMs, MSMs are less selective and more rapid and active in the phagocytosis. MSMs exhibit high lysosomal activity and bind any lymph-borne bacteria, particulate antigens, nanoparticles, as well as apoptotic cells[34]. However, in spite of its pronounced capability to phagocyte and destroy the pathogens, MSMs appear to be produce less pro-inflammatory

cytokines than SSM. The differential permissiveness of both macrophage types in response to some lymph-borne pathogens could be explained by different pathogen recognition receptors (PRRs) and by the nature of pathogen-derived components they recognize. For instance, it has been shown that SSMs express the retinoic-acid-inducible protein (RIG-I), a cytoplasmic receptor that may participate in the intracellular recognition of VSV and facilitate its capture of by SSM[35]. This is supported by the fact that in mice deficient for B cell-derived $LT\alpha_1\beta_2$, SSM adopt a MSM-like phenotype and fail to replicate VSV, impairing the antiviral $IFN\alpha/\beta$ production[18].

2.1.2 Sinusoidal macrophages in cancers

In patients of colorectal carcinoma, high density of CD169$^+$ macrophages in the LNs was significantly associated with favorable prognosis[36]. By using imaging and a melanoma tumor-bearing mouse model, Pucci et al., (2006) have shown that SSMs act as tumor suppressive cells by capturing tumor-derived extracellular vesicles, preventing their dissemination and direct interactions with the cortical B cells and the ensuing pro-tumor B cell response. Thus, SSMs appeared to play an important role against cancer by limiting tumor progression and immune activation[37]. Asano et al. (2011) have demonstrated that CD169$^+$ macrophages in the LNs phagocyte dead tumor cells from the lymphatic flow and cross-present cell-associated antigens to tumor antigen-specific CD8$^+$ T cell for the induction of antitumoral immunity. In the absence of these macrophages, as shown in CD169-DTR mice, the antitumor immunity is compromized[38].

2.1.3 Sinusoidal macrophages in inflammation

IBD is a chronic and relapsing inflammatory disorder of the gastrointestinal tract. It is characterized by gastrointestinal bleeding, intestinal tissue damage, abdominal pain and diarrhea. Crohn's disease and ulcerative colitis are two well-known types of IBD. A recent study has shown that CD169$^+$ macrophage numbers strongly increase in the mesenteric LNs (mLNs) during dextran sulfate sodium (DSS)-induced colitis. This is correlated with a significant production of inflammatory factors by these macrophages as well as high proportion of Th17 cells and tissue damage. The high levels of inflammatory cytokines and Th17 cells diminish in CD169$^+$ macrophage-depleted mice. This suggests that sinusoidal macrophage in the mLN promote mucosal inflammation and the pathogenesis of colitis[39]. A similar study has shown that CD169$^+$ macrophages in the intestine promote DSS-induced colitis by recruiting

inflammatory monocytes through CCL8[40]. This raises the question of whether the mesenteric LN or intestine CD169^{+} macrophages are important cell type for IBD.

3   Other lymph node macrophages

3.1   T cell zone macrophages

The para-cortical T cell zone of the LN is populated by a dense network of macrophages called T cell zone macrophages (TZMs). These resident macrophages are long-lived and are slowly replaced by bone marrow-derived monocytes. They can be identified as CD11b^{+} CD11c^{+} CD64^{+} MHC class II^{+} CX3CR1^{hi} MERTK^{+} and do not express CD169. The TZMs are efferocytic, in other words they clean up LN apoptotic cells including dying T cells and DCs in the T cell zone. Efferocytosis is a process by which macrophages engulf and clean up dead or apoptotic cells through specific receptors called efferocytic receptors that are distinct from those that mediate phagocytosis[41] . It is critical for many biological processes such as tissue homeostasis, inflammation resolution as well as immune tolerance. By co-injecting apoptotic T cells irradiated and labeled with different dyes to *Cx3cr1gfp/+*mice[42], Baratin et al., (2017) have shown that TZMs act locally as the professional efferocytes at steady state and throughout the course of an immune response by disposing apoptotic T cells in a CX3CR1-CX3CL1-dependent manner.

3.2   Medullary cord macrophages

A population of macrophages residing in the medullary cords of LNs are named medullary cord macrophages (MCM). They can be identified as CD11b^{+} F4/80^{+} APRIL^{+} and do not express CD169. Like the TZMs, MCMs are known to expand particularly over the course of an immune response. They are less phagocytic than MSMs and strongly stain for non-specific estrase[43]. Electron microscopic analyses have revealed that many MCMs contain plasma cells and may act as cells specialized in the clearing of apoptotic plasma cells. In addition, MCMs may support the development of the plasmablasts and plasma cells by providing trophic factors such as IL-6 and APRIL, the plasma cell survival factor[44].

3.3   Tingible body macrophages

Tingible body macrophages (TBM) represent a predominant subset of phagocytes in the germinal center of LNs and other secondary lymphoid organs. They express macrophage markers CD11b and F4/80 but also the thymocyte marker Thy-1[45]. TBMs are frequently seen

to contain many dead cells that appear as tingible bodies, the stainable debris of nucleus and particles. In addition to their function in "cleaning up" the germinal center, TBMs may be important in the initiation germinal center reaction by retaining antigen on the FDCs and functioning in antigen presentation by B cells to helper T cells. Moreover, as they appear with the germinal center development but are dispensable for this process, studies have suggested that they regulate the magnitude of the GC reaction[46,47]. In human, a defect in the uptake and the removal of apoptotic cells by the TBMs in the GC has been shown in patients suffering from systemic lupus erythematosus[48].

4   Spleen macrophages

4.1   Marginal zone macrophage and marginal metallophilic macrophage

Spleen is the largest SLO populate by heterogenous resident macrophages that sense and eliminate blood-borne pathogens and contribute to its homeostasis. The marginal zone surrounding B and T cell areas is lined by MMMs and MZMs, residing in the inner and the outer sides of the marginal zone, respectively. MMMs are similar to LN-SSMs and are identified as $CD11b^+$ $CD169^+$ $F4/80^{+/-}$ cells. MZMs are similar to LN-MSMs and are identified as $CD11b^+$ $CD169^-$ $SIGN-R1^+$ $F4/80^{+/-}$ $MARCO^+$ cells. Through a wide variety of TLRs and cell receptors, both macrophage types are well known to rapidly phagocyte blood-borne bacteria such as *Staphylococcus aureus, Listeria monocytogenes, Mycobacterium tuberculosis, Streptococcus pneumoniae, Salmonella typhimurium, Escherichia coli* and viruses such as HIV, lymphocytic choriomeningitis virus (LCMV), etc[49]. Studies in mice deficient for MMMs and MZMs by low dose clodronate liposome-mediated depletion showed that they are pivotal in the early control of the bacteremia and viremia[50-52].Their localization around spleen lymphocyte-rich zones makes them suitable to shape several aspects of the adaptive immune response. Mice lacking the macrophage scavenger receptors MARCO and SR-A (single or double knockout) exhibit defective microarchitecture of spleen marginal zone and have fewer numbers of MZMs. They displayed impaired antibody response to T cell-independent pneumococcal polysaccharide vaccine, demonstrating their crucial role in the development of a humoral response to bacteria[53]. In 2010, Backer et al., showed that MMMs can capture antigens, viruses as well as tumor antigen and transfer them to splenic $CD8^+$ DCs that cross-present to induce a $CD8^+$ T-cell cytotoxic response[54]. A schematic illustration of MZMs and MMMs during infection is shown in figure 6.
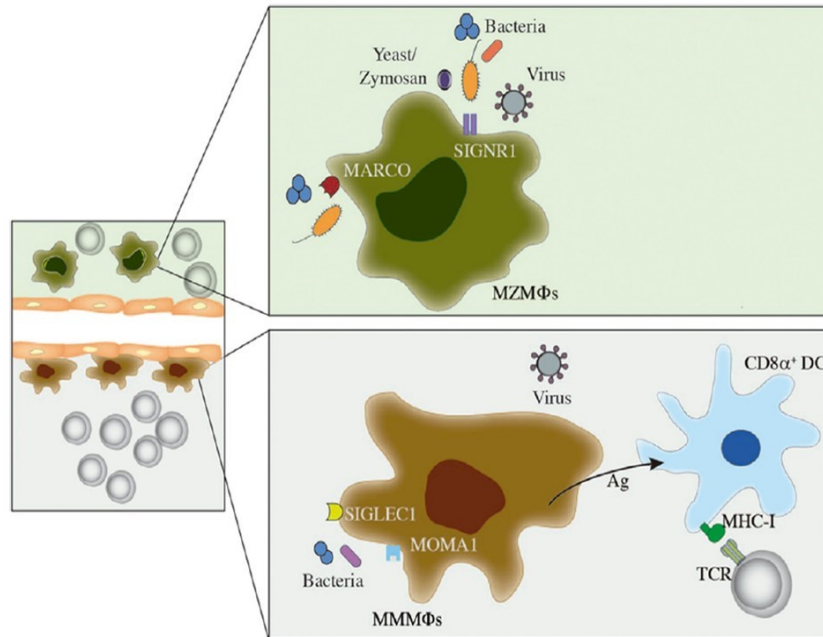
Figure 5. Spleen MZM and MMM in infection. Through their cellular receptors, MZM and MMM capture and phagocyte blood-borne bacteria, viruses and fungi. MZM expresses both MARCO and SIGN-R1 that recognize carbohydrate from bacteria, yeasts and zymosan (a yeast-derived particle) as well as viruses, leading to their internalization and degradation. Similarly, MMM also uptakes and degrades blood-borne microbes through CD169 (Siglec-1). In addition to its innate immune defense, MMM also has the ability to mediate cytotoxic CD8^{+} T cell-response by transferring antigens to DCs. Ag, antigen; TCR, T cell receptor; MHCI, Major histocompatibility Complex Class-I. Modified after[49].

SIGN-R1, also known as the cluster of differentiation 209b (CD209b), is a mouse homolog of human Dendritic Cell-Specific Intercellular adhesion molecule-3-Grabbing Non-integrin (DC-SIGN). They are C-type lectin receptors that belong to a family of PRR mainly expressed by DCs and macrophages in human. However, in mouse, SIGN-R1 is high expressed by LN-MSMs and spleen MZMs. It mediates the engulfment of a wide range of bacteria and viruses by selective recognition of microbial polysaccharides such as dextran, capsular polysaccharides, etc[56] mediated by its large extracellular carbohydrate-recognition domain, which is very conserved in the C-type lectin receptor family (Figure 7)[57]. The carbohydrate-recognition domain of SIGN-R1 is characterized by a primary and a secondary binding site. The primary binding site recognizes dextran, sialic acids and α-2,6-sialylated glycoproteins such as the complement factor 1 (C1q) and Immunoglobulins and functions in a calcium-dependent manner. The secondary binding side recognizes some repeated molecular patterns of microbial organisms

such bacterial capsular polysaccharide and functions independently of the calcium. Simultaneous recognition of glycoproteins and microbial polysaccharide might lead to SIGN-R1-mediated complement activation and pathogen destruction[56,58]. A schematic illustration of the structure of SIGN-R1 and its ligand binding motifs are shown in figure 7.

Figure 6. Structure of SIGN-R1 and its ligands. (A) Organization of the structure of SIGN-R1 with the different domains. NH_2, amino terminal; TM, transmembrane domain; COOH, carboxy terminal. Adapted after[57]. (B-D) Molecular motifs of sialic acid (N-acetylneuraminic acid, NeuAc, red box) of glycoproteins; tetra-saccharide (blue box) or di-saccharide (yellow and green boxes) and repeating unit of the bacterial capsular polysaccharide recognized by the carbohydrate-recognition domain of SIGN-R1. Gal, galactose; GlcNAc, N-acetylglucosamine; Glc, glucose; sulfate (SO_4).

4.2 Red Pulp macrophages

Red pulp macrophages (RPMs) represent the most abundant spleen macrophages. They are identified as F4/80^{hi} CD11b^{low} CD68$^+$ CD163$^+$ cells[49] and are known for the uptake of aging, apoptotic and infected RBCs and for iron homeostasis (recycling), a process that may play a role in their own development. Indeed, RPM development requires the transcription factor Spi-C that is induced through the heme released from the RBC degradation. They self-maintain by local proliferation but are also replaced by circulating monocytes[55]. RPMs are also pivotal in the phagocytosis and the elimination of numerous blood-borne parasites and bacteria[49].

Furthermore, they are recognized for their participation in the early clearance of malaria parasites as well as in the elimination of *plasmodium*-infected RBCs.

5 References

1. Furth, R. van, and Z. A. Cohn. 1968. "The Origin and Kinetics of Mononuclear Phagocytes." *The Journal of Experimental Medicine* 128 (3): 415–35. https://doi.org/10.1084/jem.128.3.415.

2. Guilliams, Martin, Florent Ginhoux, Claudia Jakubzick, Shalin H. Naik, Nobuyuki Onai, Barbara U. Schraml, Elodie Segura, Roxane Tussiwand, and Simon Yona. 2014. "Dendritic Cells, Monocytes and Macrophages: A Unified Nomenclature Based on Ontogeny." *Nature Reviews Immunology* 14 (8): 571–78. https://doi.org/10.1038/nri3712.

3. Gordon, Siamon. 2016. "Phagocytosis: The Legacy of Metchnikoff." *Cell* 166 (5): 1065–68. https://doi.org/10.1016/j.cell.2016.08.017.

4. Gordon, Siamon. 2008. "Elie Metchnikoff: Father of Natural Immunity." *European Journal of Immunology* 38 (12): 3257–64. https://doi.org/10.1002/eji.200838855.

5. Élie Metchnikoff, E. METCHNIKOFF. 1905. *Immunity in Infective Diseases*. University Press. http://archive.org/details/immunityininfec01metcgoog.

6. Freeman, Spencer A., and Sergio Grinstein. 2014. "Phagocytosis: Receptors, Signal Integration, and the Cytoskeleton." *Immunological Reviews* 262 (1): 193–215. https://doi.org/10.1111/imr.12212.

7. Botelho, Roberto J., and Sergio Grinstein. 2011. "Phagocytosis." *Current Biology* 21 (14): R533–38. https://doi.org/10.1016/j.cub.2011.05.053.

8. Melcarne, C., B. Lemaitre, and E. Kurant. 2019. "Phagocytosis in Drosophila: From Molecules and Cellular Machinery to Physiology." *Insect Biochemistry and Molecular Biology* 109 (June): 1–12. https://doi.org/10.1016/j.ibmb.2019.04.002.

9. Lee, Bettina L., and Gregory M. Barton. 2014. "Trafficking of Endosomal Toll-like Receptors." *Trends in Cell Biology* 24 (6): 360–69. https://doi.org/10.1016/j.tcb.2013.12.002.

10. Gordon, Siamon, Annette Plüddemann, and Fernando Martinez Estrada. 2014. "Macrophage Heterogeneity in Tissues: Phenotypic Diversity and Functions." *Immunological Reviews* 262 (1): 36–55. https://doi.org/10.1111/imr.12223.

11. Schulz, Christian, Elisa Gomez Perdiguero, Laurent Chorro, Heather Szabo-Rogers, Nicolas Cagnard, Katrin Kierdorf, Marco Prinz, et al. 2012. "A Lineage of Myeloid Cells Independent of Myb and Hematopoietic Stem Cells." *Science* 336 (6077): 86–90. https://doi.org/10.1126/science.1219179.

12. Hoeffel, Guillaume, Jinmiao Chen, Yonit Lavin, Donovan Low, Francisca F. Almeida, Peter See, Anna E. Beaudin, et al. 2015. "C-Myb+ Erythro-Myeloid Progenitor-Derived Fetal Monocytes Give Rise to Adult Tissue-Resident Macrophages." *Immunity* 42 (4): 665–78. https://doi.org/10.1016/j.immuni.2015.03.011.

13. Guilliams, Martin, and Charlotte L. Scott. 2017. "Does Niche Competition Determine the Origin of Tissue-Resident Macrophages?" *Nature Reviews Immunology* 17 (7): 451–60. https://doi.org/10.1038/nri.2017.42.

14. Puchalska, Patrycja, Xiaojing Huang, Shannon E. Martin, Xianlin Han, Gary J. Patti, and Peter A. Crawford. 2018. "Isotope Tracing Untargeted Metabolomics Reveals Macrophage Polarization-State-Specific Metabolic

Coordination across Intracellular Compartments." *IScience* 9 (November): 298–313. https://doi.org/10.1016/j.isci.2018.10.029.

15. T'Jonck, Wouter, Martin Guilliams, and Johnny Bonnardel. 2018. "Niche Signals and Transcription Factors Involved in Tissue-Resident Macrophage Development." *Cellular Immunology* 330 (August): 43–53. https://doi.org/10.1016/j.cellimm.2018.02.005.

16. Gray, Elizabeth E., and Jason G. Cyster. 2012. "LN Macrophages." *Journal of Innate Immunity* 4 (5–6): 424–36. https://doi.org/10.1159/000337007.

17. Witmer-Pack, M. D., D. A. Hughes, G. Schuler, L. Lawson, A. McWilliam, K. Inaba, R. M. Steinman, and S. Gordon. 1993. "Identification of Macrophages and Dendritic Cells in the Osteopetrotic (Op/Op) Mouse." *Journal of Cell Science* 104 (Pt 4) (April): 1021–29

18. Moseman, E. Ashley, Matteo Iannacone, Lidia Bosurgi, Elena Tonti, Nicolas Chevrier, Alexei Tumanov, Yang-Xin Fu, Nir Hacohen, and Ulrich H. von Andrian. 2012. "B Cell Maintenance of Subcapsular Sinus Macrophages Protects against a Fatal Viral Infection Independent of Adaptive Immunity." *Immunity* 36 (3): 415–26. https://doi.org/10.1016/j.immuni.2012.01.013.

19. Phan, Tri Giang, Jesse A Green, Elizabeth E Gray, Ying Xu, and Jason G Cyster. 2009. "Immune Complex Relay by Subcapsular Sinus Macrophages and Noncognate B Cells Drives Antibody Affinity Maturation." *Nature Immunology* 10 (7): 786–93. https://doi.org/10.1038/ni.1745.

20. Crocker, Paul R., James C. Paulson, and Ajit Varki. 2007. "Siglecs and Their Roles in the Immune System." *Nature Reviews Immunology* 7 (4): 255–66. https://doi.org/10.1038/nri2056.

21. May, A.P., R.C. Robinson, M. Vinson, P.R. Crocker, and E.Y. Jones. 1998. "Crystal Structure of the N-Terminal Domain of Sialoadhesin in Complex with 3' Sialyllactose at 1.85 Å Resolution." *Molecular Cell* 1 (5): 719–28. https://doi.org/10.1016/S1097-2765(00)80071-4.

22. Szakal, A. K., K. L. Holmes, and J. G. Tew. 1983. "Transport of Immune Complexes from the Subcapsular Sinus to LN Follicles on the Surface of Nonphagocytic Cells, Including Cells with Dendritic Morphology." *Journal of Immunology (Baltimore, Md.: 1950)* 131 (4): 1714–27.

23. Delemarre, F.G.A., N. Kors, G. Kraal, and N. van Rooijen. 1990. "Repopulation of Macrophages in Popliteal LNs of Mice After Liposome-Mediated Depletion." *Journal of Leukocyte Biology* 47 (3): 251–57. https://doi.org/10.1002/jlb.47.3.251.

24. Junt, Tobias, E. Ashley Moseman, Matteo Iannacone, Steffen Massberg, Philipp A. Lang, Marianne Boes, Katja Fink, et al. 2007. "Subcapsular Sinus Macrophages in LNs Clear Lymph-Borne Viruses and Present Them to Antiviral B Cells." *Nature* 450 (7166): 110–14. https://doi.org/10.1038/nature06287.

25. Phan, Tri Giang, Irina Grigorova, Takaharu Okada, and Jason G. Cyster. 2007. "Subcapsular Encounter and Complement-Dependent Transport of Immune Complexes by LN B Cells." *Nature Immunology* 8 (9): 992–1000. https://doi.org/10.1038/ni1494.

26. Iannacone, Matteo, E. Ashley Moseman, Elena Tonti, Lidia Bosurgi, Tobias Junt, Sarah E. Henrickson, Sean P. Whelan, Luca G. Guidotti, and Ulrich H. von Andrian. 2010. "Subcapsular Sinus Macrophages Prevent CNS Invasion on Peripheral Infection with a Neurotropic Virus." *Nature* 465 (7301): 1079–83.

https://doi.org/10.1038/nature09118.

27. Sagoo, Pervinder, Zacarias Garcia, Beatrice Breart, Fabrice Lemaître, David Michonneau, Matthew L Albert, Yves Levy, and Philippe Bousso. 2016. "In Vivo Imaging of Inflammasome Activation Reveals a Subcapsular Macrophage Burst Response That Mobilizes Innate and Adaptive Immunity." *Nature Medicine* 22 (1): 64–71. https://doi.org/10.1038/nm.4016.

28. Kastenmüller, Wolfgang, Parizad Torabi-Parizi, Naeha Subramanian, Tim Lämmermann, and Ronald N. Germain. 2012. "A Spatially-Organized Multicellular Innate Immune Response in LNs Limits Systemic Pathogen Spread." *Cell* 150 (6): 1235–48. https://doi.org/10.1016/j.cell.2012.07.021.

29. Gaya, Mauro, Angelo Castello, Beatriz Montaner, Neil Rogers, Caetano Reis e Sousa, Andreas Bruckbauer, and Facundo D. Batista. 2015. "Host Response. Inflammation-Induced Disruption of SCS Macrophages Impairs B Cell Responses to Secondary Infection." *Science (New York, N.Y.)* 347 (6222): 667–72. https://doi.org/10.1126/science.aaa1300.

30. Detienne, Sophie, Iain Welsby, Catherine Collignon, Sandrine Wouters, Margherita Coccia, Sophie Delhaye, Laurye Van Maele, et al. 2016. "Central Role of CD169+ LN Resident Macrophages in the Adjuvanticity of the QS-21 Component of AS01." *Scientific Reports* 6 (1). https://doi.org/10.1038/srep39475.

31. Hickman, Heather D., Kazuyo Takeda, Cara N. Skon, Faith R. Murray, Scott E. Hensley, Joshua Loomis, Glen N. Barber, Jack R. Bennink, and Jonathan W. Yewdell. 2008. "Direct Priming of Antiviral CD8+ T Cells in the Peripheral Interfollicular Region of LNs." *Nature Immunology* 9 (2): 155–65. https://doi.org/10.1038/ni1557.

32. Camara, Abdouramane, Olga G. Cordeiro, Farouk Alloush, Janina Sponsel, Mélanie Chypre, Lucas Onder, Kenichi Asano, et al. 2019. "LN Mesenchymal and Endothelial Stromal Cells Cooperate via the RANK-RANKL Cytokine Axis to Shape the Sinusoidal Macrophage Niche." *Immunity* 50 (6): 1467-1481.e6. https://doi.org/10.1016/j.immuni.2019.05.008.

33. Gonzalez, Santiago F, Veronika Lukacs-Kornek, Michael P Kuligowski, Lisa A Pitcher, Søren E Degn, Young-A Kim, Mary J Cloninger, et al. 2010. "Capture of Influenza by Medullary Dendritic Cells via SIGN-R1 Is Essential for Humoral Immunity in Draining LNs." *Nature Immunology* 11 (5): 427–34. https://doi.org/10.1038/ni.1856.

34. Kuka, Mirela, and Matteo Iannacone. 2014. "The Role of LN Sinus Macrophages in Host Defense: LN Macrophages Orchestrate Antimicrobial Immunity." *Annals of the New York Academy of Sciences* 1319 (1): 38–46. https://doi.org/10.1111/nyas.12387.

35. Kato, Hiroki, Osamu Takeuchi, Shintaro Sato, Mitsutoshi Yoneyama, Masahiro Yamamoto, Kosuke Matsui, Satoshi Uematsu, et al. 2006. "Differential Roles of MDA5 and RIG-I Helicases in the Recognition of RNA Viruses." *Nature* 441 (7089): 101–5. https://doi.org/10.1038/nature04734.

36. Ohnishi, Koji, Yoshihiro Komohara, Yoichi Saito, Yuji Miyamoto, Masayuki Watanabe, Hideo Baba, and Motohiro Takeya. 2013. "CD169-Positive Macrophages in Regional LNs Are Associated with a Favorable Prognosis in Patients with Colorectal Carcinoma." *Cancer Science* 104 (9): 1237–44. https://doi.org/10.1111/cas.12212.

37. Pucci, F., C. Garris, C. P. Lai, A. Newton, C. Pfirschke, C. Engblom, D. Alvarez, et al. 2016. "SCS Macrophages Suppress Melanoma by Restricting tumor-Derived Vesicle-B Cell Interactions." *Science* 352 (6282): 242–46. https://doi.org/10.1126/science.aaf1328.

38. Asano, Kenichi, Ami Nabeyama, Yasunobu Miyake, Chun-Hong Qiu, Ai Kurita, Michio Tomura, Osami Kanagawa, Shin-ichiro Fujii, and Masato Tanaka. 2011. "CD169-Positive Macrophages Dominate Antitumor Immunity by Crosspresenting Dead Cell-Associated Antigens." *Immunity* 34 (1): 85–95. https://doi.org/10.1016/j.immuni.2010.12.011.

39. Li, Qiuting, Dan Wang, Shengyu Hao, Xiaolei Han, Yuan Xia, Xiangzhi Li, Yaoxing Chen, Masato Tanaka, and Chun-Hong Qiu. 2017. "CD169 Expressing Macrophage, a Key Subset in Mesenteric LNs Promotes Mucosal Inflammation in Dextran Sulfate Sodium-Induced Colitis." *Frontiers in Immunology* 8 (June). https://doi.org/10.3389/fimmu.2017.00669.

40. Asano, Kenichi, Naomichi Takahashi, Mikiko Ushiki, Misa Monya, Fumiaki Aihara, Erika Kuboki, Shigetaka Moriyama, et al. 2015. "Intestinal CD169+ Macrophages Initiate Mucosal Inflammation by Secreting CCL8 That Recruits Inflammatory Monocytes." *Nature Communications* 6 (1). https://doi.org/10.1038/ncomms8802.

41. Martin, Constance J, Kristen N Peters, and Samuel M Behar. 2014. "Macrophages Clean up: Efferocytosis and Microbial Control." *Current Opinion in Microbiology* 17 (February): 17–23. https://doi.org/10.1016/j.mib.2013.10.007.

42. Baratin, Myriam, Léa Simon, Audrey Jorquera, Clément Ghigo, Doulaye Dembele, Jonathan Nowak, Rebecca Gentek, et al. 2017. "T Cell Zone Resident Macrophages Silently Dispose of Apoptotic Cells in the LN." *Immunity* 47 (2): 349-362.e5. https://doi.org/10.1016/j.immuni.2017.07.019.

43. Steer, H. W., and R. A. Foot. 1987. "Changes in the Medulla of the Parathymic LNs of the Rat during Acute Gastro-Intestinal Inflammation." *Journal of Anatomy* 152 (June): 23–36.

44. Mohr, Elodie, Karine Serre, Rudolf A. Manz, Adam F. Cunningham, Mahmood Khan, Deborah L. Hardie, Roger Bird, and Ian C. M. MacLennan. 2009. "Dendritic Cells and Monocyte/Macrophages That Create the IL-6/APRIL-Rich LN Microenvironments Where Plasmablasts Mature." *The Journal of Immunology* 182 (4): 2113–23. https://doi.org/10.4049/jimmunol.0802771.

45. Smith, John P., Marie H. Kosco, John G. Tew, and Andras K. Szakal. 1988. "Thy-1 Positive Tingible Body Macrophages (TBM) in Mouse LNs." *The Anatomical Record* 222 (4): 380–90. https://doi.org/10.1002/ar.1092220410.

46. Smith, J. P., A. M. Lister, J. G. Tew, and A. K. Szakal. 1991. "Kinetics of the Tingible Body Macrophage Response in Mouse Germinal Center Development and Its Depression with Age." *The Anatomical Record* 229 (4): 511–20. https://doi.org/10.1002/ar.1092290412.

47. Smith, J. P., G. F. Burton, J. G. Tew, and A. K. Szakal. 1998. "Tingible Body Macrophages in Regulation of Germinal Center Reactions." *Developmental Immunology* 6 (3–4): 285–94.

48. Baumann, Irith, Wasilis Kolowos, Reinhard E. Voll, Bernhard Manger, Udo Gaipl, Winfried L. Neuhuber, Thomas Kirchner, Joachim R. Kalden, and Martin Herrmann. 2002. "Impaired Uptake of Apoptotic Cells into Tingible Body Macrophages in Germinal Centers of Patients with Systemic Lupus Erythematosus." *Arthritis & Rheumatism* 46 (1): 191–201.https://doi.org/10.1002/1529-0131(200201)46:1<191::AID-ART10027>3.0.CO;2-K.

49. Borges da Silva, Henrique, Raíssa Fonseca, Rosana Moreira Pereira, Alexandra dos Anjos Cassado, José Maria Álvarez, and Maria Regina D'Império Lima. 2015. "Splenic Macrophage Subsets and Their Function during Blood-Borne Infections." *Frontiers in Immunology* 6 (September). https://doi.org/10.3389/fimmu.2015.00480.

50. Aichele, Peter, Jana Zinke, Leander Grode, Reto A. Schwendener, Stefan H. E. Kaufmann, and Peter Seiler. 2003. "Macrophages of the Splenic Marginal Zone Are Essential for Trapping of Blood-Borne Particulate Antigen but Dispensable for Induction of Specific T Cell Responses." *The Journal of Immunology* 171 (3): 1148–55. https://doi.org/10.4049/jimmunol.171.3.1148.

51. Chen, Yunying, Fredrik Wermeling, Johanna Sundqvist, Ann-Beth Jonsson, Karl Tryggvason, Timo Pikkarainen, and Mikael C. I. Karlsson. 2010. "A Regulatory Role for Macrophage Class A Scavenger Receptors in TLR4-Mediated LPS Responses." *European Journal of Immunology* 40 (5): 1451–60. https://doi.org/10.1002/eji.200939891.

52. Seiler, Peter, Peter Aichele, Bernhard Odermatt, Hans Hengartner, Rolf M. Zinkernagel, and Reto A. Schwendener. 1997. "Crucial Role of Marginal Zone Macrophages and Marginal Zone Metallophils in the Clearance of Lymphocytic Choriomeningitis Virus Infection." *European Journal of Immunology* 27 (10): 2626–33. https://doi.org/10.1002/eji.1830271023.

53. Chen, Yunying, Timo Pikkarainen, Outi Elomaa, Raija Soininen, Tatsuhiko Kodama, Georg Kraal, and Karl Tryggvason. 2005. "Defective Microarchitecture of the Spleen Marginal Zone and Impaired Response to a Thymus-Independent Type 2 Antigen in Mice Lacking Scavenger Receptors MARCO and SR-A." *The Journal of Immunology* 175 (12): 8173–80. https://doi.org/10.4049/jimmunol.175.12.8173.

54. Backer, R., T. Schwandt, M. Greuter, M. Oosting, F. Jungerkes, T. Tuting, L. Boon, et al. 2010. "Effective Collaboration between Marginal Metallophilic Macrophages and CD8+ Dendritic Cells in the Generation of Cytotoxic T Cells." *Proceedings of the National Academy of Sciences* 107 (1): 216–21. https://doi.org/10.1073/pnas.0909541107.

55. Haldar, Malay, Masako Kohyama, Alex Yick-Lun So, Wumesh Kc, Xiaodi Wu, Carlos G. Briseño, Ansuman T. Satpathy, et al. 2014. "Heme-Mediated SPI-C Induction Promotes Monocyte Differentiation into Iron-Recycling Macrophages." *Cell* 156 (6): 1223–34. https://doi.org/10.1016/j.cell.2014.01.069.

56. Silva-Martín, Noella, Sergio G. Bartual, Erney Ramírez-Aportela, Pablo Chacón, Chae Gyu Park, and Juan A. Hermoso. 2014. "Structural Basis for Selective Recognition of Endogenous and Microbial Polysaccharides by Macrophage Receptor SIGN-R1." *Structure* 22 (11): 1595–1606. https://doi.org/10.1016/j.str.2014.09.001.

57. Parent, Stephen A, Theresa Zhang, Gary Chrebet, Joseph A Clemas, David J Figueroa, BettyKy, Richard A Blevins, Christopher P Austin, and Hugh Rosen. 2002. "Molecular Characterization of the Murine SIGNR1 Gene Encoding a C-Type Lectin Homologous to Human DC-SIGN and DC-SIGNRq," 14.

58. Kang, Young-Sun, Yoonkyung Do, Hae-Kyung Lee, Sung Ho Park, Cheolho Cheong, Rebecca M. Lynch, Jutta M. Loeffler, Ralph M. Steinman, and Chae Gyu Park. 2006. "A Dominant Complement Fixation Pathway for Pneumococcal Polysaccharides Initiated by SIGN-R1 Interacting with C1q." *Cell* 125 (1): 47–58. https://doi.org/10.1016/j.cell.2006.01.046.

59. Paolicelli, Rosa C., Giulia Bolasco, Francesca Pagani, Laura Maggi, Maria Scianni, Patrizia Panzanelli, Maurizio Giustetto, et al. 2011. "Synaptic Pruning by Microglia Is Necessary for Normal Brain Development." Science (New York, N.Y.) 333 (6048): 1456–58. https://doi.org/10.1126/science.1202529.

60. Li, Qingyun, and Ben A. Barres. 2018. "Microglia and Macrophages in Brain Homeostasis and Disease." Nature Reviews Immunology 18 (4): 225–42. https://doi.org/10.1038/nri.2017.125.

61. Byrne, Adam J., Sara A. Mathie, Lisa G. Gregory, and Clare M. Lloyd. 2015. "Pulmonary Macrophages: Key Players in the Innate Defence of the Airways." Thorax 70 (12): 1189–96. https://doi.org/10.1136/thoraxjnl-2015-207020.

62. Gordon, S. B., G. R. Irving, R. A. Lawson, M. E. Lee, and R. C. Read. 2000. "Intracellular Trafficking and Killing of Streptococcus Pneumoniae by Human Alveolar Macrophages Are Influenced by Opsonins." Infection and Immunity 68 (4): 2286–93. https://doi.org/10.1128/iai.68.4.2286-2293.2000.

Chapter 5. Thesis objectives and results

1   Objectives

The RANK-RANKL axis controls the formation of osteoclasts, the bone resorbing macrophages. Mice lacking either RANKL of its receptor are osteopetrotic, characterized by an increased bone density with absence of marrow cavities and display lack of tooth eruption and diminished growth. Genetic mutations in *Rank* are responsible for bone diseases in human. Beyond osteoclastogenesis, whether the RANK-RANKL axis is involved in the differentiation of other macrophage types is unknown. Moreover, other than LN organogenesis, the role of the RANK-RANKL axis in adult LN remains poorly studied, partly because mice deficient for RANKL or RANK lack all LNs.

Marginal reticular cells (MRCs) are LN stromal cells. They are characterized by the absence of the hematopoietic marker CD45 and the endothelial marker PECAM/CD31 but by the presence of podoplanin/Gp38 of FRCs. The current notion is that the precursors for MRCs are the lymphoid tissue organizer cells (LTOs) of embryonic LN anlagen. Both embryonic LTOs and adult MRCs express RANKL. In 2016, our laboratory has shown that stromal RANKL (LTO/MRC) activates the lymphatic endothelial cells to express the integrin alpha 2b (ITGA2b/CD41). In 2017, a study where we have contributed has revealed that RANK mediated signaling in LECs is required for LN formation. These observations demonstrate a functionally relevant crosstalk between mesenchymal stromal cells (LTO/MRC) and LECs that may further influence the immune response in the adult.

The objectives of my thesis consist in the first part to analyze the impact of loss of stromal RANKL on adult LN homeostasis and the immune response. Because the osteoclasts depend on RANKL for their development and functions and since the tissue-resident macrophages require signals from their surrounding environment to complete their differentiation program, we sought to know whether stromal RANKL ablation also affect LN macrophages. Using genetically modified mice, we focused particularly on the CD169$^+$ subcapsular sinus macrophages (SSMs) residing between the MRC network and the subcapsular floor lining LECs (fLECs) and on their counterparts, the CD169$^+$ SIGN-R1$^+$ F4/80$^+$medullary sinus macrophages (MSMs) associated with lymphatic sinuses in the medulla. In the second part, we investigated whether SSMs and MSMs directly require RANKL activation for their differentiation. To do so, we generated a mouse model in which RANK is specifically deleted in CD169$^+$ cells. Finally, in the third part, we investigated the contributions of LN-lymphatic RANK in macrophage

differentiation. For that, we generated a mouse model that allows temporal deletion of RANK from LECs.

2   Results

My thesis work has been published in Immunity as first author and referred as:

Camara et al., 2019. Immunity 50, 1467–1481

June 18, 2019 ª 2019 Elsevier Inc.

https://doi.org/10.1016/j.immuni.2019.05.008

See below

Immunity

Lymph Node Mesenchymal and Endothelial Stromal Cells Cooperate via the RANK-RANKL Cytokine Axis to Shape the Sinusoidal Macrophage Niche

Graphical Abstract
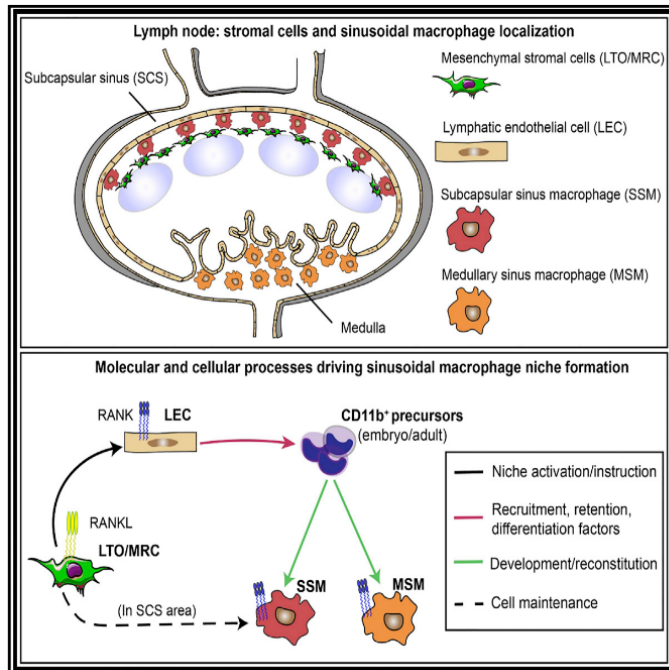
Authors

Abdouramane Camara,
Olga G. Cordeiro, Farouk Alloush, ...,
Burkhard Ludewig, Vincent Flacher,
Christopher G. Mueller

Correspondence

c.mueller@ibmc-cnrs.unistra.fr

In Brief

Tissue-resident macrophages acquire defining genetic programs in response to signals from surrounding cells. Camara et al. reveal that mesenchymal cells and lymphatic endothelial cells within the lymph node interact via RANK-RANKL to generate a niche environment that supports the differentiation of sinusoidal macrophages and their maintenance after an inflammatory challenge.

Highlights

- *Ccl19-cre*-mediated RANKL deletion in LTOs and MRCs inactivates LECs and leads to SM loss

- Development and repair of the SM network fails in mice with RANK-deficient LECs

- *Cd169-cre Rank^{fl/fl}* mice reveal that SSMs but not MSMs require direct RANK signaling

- The stromal RANK-RANKL axis governs the SM-mediated antiviral immune response

CellPress

Article

![CellPress]

Lymph Node Mesenchymal and Endothelial Stromal Cells Cooperate via the RANK-RANKL Cytokine Axis to Shape the Sinusoidal Macrophage Niche

Abdouramane Camara,[1] Olga G. Cordeiro,[1,5] Farouk Alloush,[1,5] Janina Sponsel,[1] Mélanie Chypre,[1] Lucas Onder,[2] Kenichi Asano,[3] Masato Tanaka,[3] Hideo Yagita,[4] Burkhard Ludewig,[2] Vincent Flacher,[1] and Christopher G. Mueller[1,6,*]

[1]CNRS UPR 3572, IBMC, University of Strasbourg, 67000 Strasbourg, France
[2]Institute of Immunobiology, Medical Research Center, Kantonspital St. Gallen, 9007 St. Gallen, Switzerland
[3]Laboratory of Immune Regulation, School of Life Science, Tokyo University of Pharmacy and Life Sciences, Tokyo 192-0392, Japan
[4]Department of Immunology, Juntendo University School of Medicine, Tokyo 113-8421, Japan
[5]These authors contributed equally
[6]Lead Contact
*Correspondence: c.mueller@ibmc-cnrs.unistra.fr
https://doi.org/10.1016/j.immuni.2019.05.008

SUMMARY

Tissue-resident macrophages are receptive to specific signals concentrated in cellular niches that direct their cell differentiation and maintenance genetic programs. Here, we found that deficiency of the cytokine RANKL in lymphoid tissue organizers and marginal reticular stromal cells of lymph nodes resulted in the loss of the CD169+ sinusoidal macrophages (SMs) comprising the subcapsular and the medullary subtypes. Subcapsular SM differentiation was impaired in mice with targeted RANK deficiency in SMs. Temporally controlled RANK removal in lymphatic endothelial cells (LECs) revealed that lymphatic RANK activation during embryogenesis and shortly after birth was required for the differentiation of both SM subtypes. Moreover, RANK expression by LECs was necessary for SM restoration after inflammation-induced cell loss. Thus, cooperation between mesenchymal cells and LECs shapes a niche environment that supports SM differentiation and reconstitution after inflammation.

INTRODUCTION

Lymphoid tissues comprise mesenchymal and endothelial stromal cells. They play a key role in the development of secondary lymphoid organs such as lymph nodes (LNs) (Onder and Ludewig, 2018; van de Pavert and Mebius, 2010) and function in the compartmentalization of B cell and T cell zones, antigen transport, and immune regulation (Buechler and Turley, 2018). Recently, an increasing diversity of mesenchymal stromal cells has emerged (Huang et al., 2018; Rodda et al., 2018; Takeuchi et al., 2018), among which the marginal reticular cells (MRCs). They reside in the LN marginal area between the subcapsular sinus and the B cell follicles and are characterized by the expression of the tumor necrosis factor superfamily (TNFSF) member

receptor activator of nuclear factor kappa-B ligand (RANKL) (TNFSF11) (Katakai et al., 2008; Rodda et al., 2018). RANKL is known for the differentiation of osteoclasts, specialized bone-resorbing macrophages (Dougall et al., 1999; Kong et al., 1999; Walsh and Choi, 2014), but is also required for LN organogenesis given that mice deficient for RANKL or its signaling receptor, receptor activator of NF-κB (RANK) (TNFRSF11a), lack all LNs (Dougall et al., 1999; Kim et al., 2000; Kong et al., 1999). In the embryonic LN anlagen, RANKL is expressed by the stromal lymphoid tissue organizers (LTOs) and lymphoid tissue inducer (LTi) cells (Cupedo et al., 2004; Sugiyama et al., 2012), and it has recently been shown that RANK expression by lymphatic endothelial cells (LECs) is necessary for LN organogenesis (Onder et al., 2017). However, the function of stromal RANKL in LNs remains incompletely understood. We have recently observed that stromal RANKL activates LECs to express integrin alpha 2b (ITGA2b), suggesting that a cross-talk between these two cell types could affect immune function (Cordeiro et al., 2016).

Macrophages that line the lymphatic sinuses of LNs comprise the CD169+ subcapsular sinus macrophages (SSMs), localized between the B cell follicles and the subcapsular sinus, and the CD169+SIGN-R1+F4/80+ medullary sinus macrophages (MSMs) associated with the medullary lymphatics. Both populations play an important role in the initiation and the regulation of innate and adaptive immunity (Gray and Cyster, 2012). In response to viral pathogens, SSMs produce type I interferon (IFN-I) that protects neighboring cells (Iannacone et al., 2010; Moseman et al., 2012) or activate the inflammasome that fuels the immune response (Sagoo et al., 2016). SSMs also transfer lymph-borne antigens to B cells that relay it to the follicular dendritic cells (FDCs) for an efficient secondary immune response (Carrasco and Batista, 2007; Phan et al., 2007). MSMs also contribute to the immune response by the release of inflammatory mediators (Chatziandreou et al., 2017).

Tissue macrophages derive from yolk sac macrophages and fetal liver monocytes or, in the adult, from bone-marrow-derived precursors (Ginhoux and Guilliams, 2016). Lineage-determining transcription factors provide a core macrophage development program, and tissue-derived signals oversee the

final differentiation refinement (Lavin et al., 2015; T'Jonck et al., 2018). Macrophage precursors can receive secondary signals that are unique to each particular cell niche through cell-cell contacts and soluble factors (Guilliams and Scott, 2017). It ensures that the macrophages are well adapted to their local environment. SMs require colony stimulating factor 1 receptor (CSF1R) signals (Witmer-Pack et al., 1993), but in addition, SSM differentiation is dependent on lymphotoxin (LT) $\alpha\beta$ produced by the adjacent B cells (Moseman et al., 2012; Phan et al., 2009).

Here, we examined the role of RANKL expressed by the mesenchymal LTO and MRC stromal cells in the LNs. We found that *Ccl19* promoter-directed RANKL ablation in LTOs and MRCs did not affect LN organogenesis but resulted in the specific loss of SMs. Deficiency in RANK affected SSMs directly given that these cells were absent in *Cd169-cre Rank^{fl/fl}* mice. However, deletion of RANK in LECs during mouse embryogenesis or in the first weeks after birth resulted in the loss of both SM subsets. RANK activation of LECs was also required for SM-network restoration after an inflammatory insult. Inactivation of RANK signaling in LECs correlated with the reduced presence of CD11b$^+$ cells in embryos and adult mice, supporting a role for this axis in cell recruitment or retention. As a result, the absence of mesenchymal RANKL or lymphatic RANK compromised the immune response to a viral pathogen. Altogether, our findings show that this mesenchymal-endothelial cell interaction shapes a niche environment that is mandatory for SM differentiation during development and for reconstitution after inflammation.

RESULTS

RANKL Is Specifically Deleted in LTOs and MRCs without Affecting MRC Differentiation

C-C motif chemokine ligand 19 (CCL19) is expressed in LTOs (Bénézech et al., 2010; Chai et al., 2013) that are presumed to give rise to the MRCs, the main constitutive source of RANKL in the adult LNs (Katakai, 2012; Rodda et al., 2018). Therefore, to address the function of stromal RANKL, we crossed *Rankl^{fl/fl}* mice (Xiong et al., 2011) with mice expressing the cre recombinase under control of the *Ccl19* promoter (Chai et al., 2013). Microscopic inspection of embryonic day (E) 17.5 inguinal LNs of *Ccl19-cre Rankl^{fl/fl}* mice (denoted as *Rankl^{ΔCcl19}*) revealed a markedly diminished expression of RANKL by the LTOs (Figure 1A). At this age, LTi cells express little RANKL (Sugiyama et al., 2012). LECs, identified by murine chloride channel calcium-activated 1 (mCLCA1) (Furuya et al., 2010), and the presence of mature LTi cells expressing CD4 appeared normal. The mice developed all LNs with little alteration in cellularity and cell composition (Figures S1A and S1B), which is in contrast to unconditional RANKL-deficient mice that lack all LNs (Kong et al., 1999). In agreement with a direct lineage relationship between LTOs and MRCs (Takeuchi et al., 2018), the expression of RANKL was no longer observed in MRCs of adult *Rankl^{ΔCcl19}* mice (Figure 1B). To determine whether the disappearance of RANKL altered MRC differentiation, we identified MRCs among the gp38$^+$CD31$^-$ stromal fibroblastic reticular cells (FRCs) on the basis of the expression of mucosal vascular addressin cell adhesion molecule 1 (MAdCAM-1) and vascular cell adhesion protein

(VCAM-1) (Hoorweg et al., 2015; Katakai et al., 2008) (Figure 1C). The proportion of MRCs was not altered in the RANKL mutant mice (Figure 1D). Moreover, when *Rankl^{ΔCcl19}* mice were crossed with tdTomato reporter mice, red fluorescent stromal cells were found between the FDCs and the subcapsular sinus, indicative of correctly positioned MRCs (Figure S1C). TdTomato$^+$ T-cell-zone-residing reticular cells (TRCs) were also observed, suggesting that the lack of RANKL has no effect on other stromal subsets. We determined *Rankl* gene expression by RT-qPCR in sorted MRCs and in the remaining stroma of *Rankl^{ΔCcl19}* and control *Rankl^{fl/fl}* mice. Figure 1E shows that MRCs transcribed *Rankl*, and as expected, there was a clear reduction in the number of transcripts in MRCs from *Rankl^{ΔCcl19}* mice. Altogether, the chosen gene-targeting strategy established a reliable mouse model for *Rankl* deletion from the mesenchymal LN stromal cells.

Stromal RANKL Is Required for SM Differentiation

In light of the expression of RANK by the myeloid lineage in response to CSF-1 (Arai et al., 2012), alongside its role in osteo-clastogenesis (Dougall et al., 1999), we asked whether the loss of stromal RANKL had an effect on macrophage differentiation in the LNs. We first focused on the SSMs because these cells reside in the same zone as the MRCs. SSMs express CD169, and the staining of LN sections for CD169 uncovered that this marker was markedly diminished in *Rankl^{ΔCcl19}* mice (Figure 2A). Given that CD169 expression in wild-type mice is lower in the medullary area, we also stained for specific ICAM-3-grabbing nonintegrin-related 1 (SIGN-R1), expressed by the MSMs but not by the SSMs (Moseman et al., 2012). There was a clear reduction in the extent of SIGN-R1 and CD11b staining, but the formation and the position of B220$^+$ B cell follicles appeared normal (Figure 2A). To quantify a decline in these two macrophage subsets and to assess other myeloid cell populations, we performed analyses by flow cytometry. Among live CD11b$^+$CD11c$^+$ cells, SSMs and MSMs were MHC-II$^+$CD11c^{low} and could be distinguished as CD169$^+$F4/80$^-$ and CD169$^+$F4/80$^+$ cells, respectively (Figure 2B). We found that the numbers of SSMs and MSMs were significantly reduced in the mutant mice (Figure 2B). In contrast, the F4/80 single-positive macrophages were slightly increased, and the remaining double-negative macrophages that likely comprise the T cell zone macrophages (Baratin et al., 2017) were not affected (Figure 2C). We found no alteration in the numbers of the tissue-derived CD11c$^+$CD11b$^+$MHC-II^{hi} DCs or the LN-resident CD11c$^+$CD11b$^+$MHC-II$^+$ DCs (Figure 2D). Thus, stromal RANKL is specifically required for the differentiation of the subcapsular and the medullary SM subsets.

Impaired Immune Response in Stromal RANKL-Deficient Mice

SMs relay lymph-borne antigen to B cells (Phan et al., 2007) and stimulate the immune response to viral pathogens (Chatzian-dreou et al., 2017; Gaya et al., 2015; Sagoo et al., 2016). Therefore, to ascertain that their diminished number in *Rankl^{ΔCcl19}* mice has functional implications, we first tested the relay of immune complexes to B cells. To this end, we passively immunized *Rankl^{ΔCcl19}* or *Rankl^{fl/fl}* mice with anti-phycoerythrin (PE) antibodies and then administered PE into the hind footpad (Phan et al., 2007). Eight hours later, popliteal LNs were processed to harvest B cells. The addition of CD45.1$^+$ lymphocytes from the
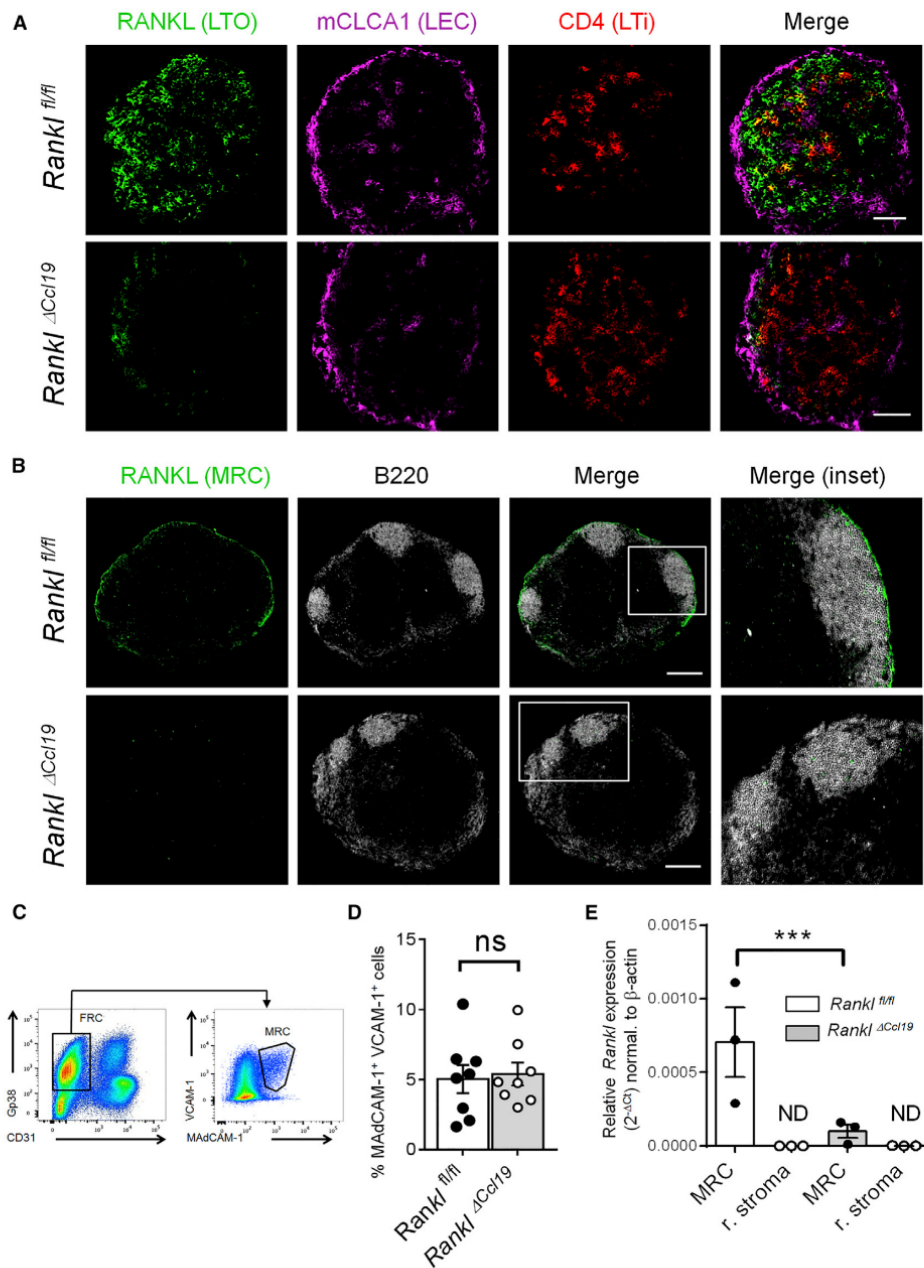
Figure 1. RANKL Specifically Expressed by LTOs and MRCs Is Deleted in *Ccl19-cre Rankl*$^{fl/fl}$ Mice

(A) E17.5 inguinal LNs of *Ccl19-cre Rankl*$^{fl/fl}$ (*Rankl*$^{\Delta Ccl19}$) mice and *Rankl*$^{fl/fl}$ control littermates were stained for LECs (mCLCA1), LTi cells (CD4), and RANKL. Scale bars represent 50 μm.

(B) Popliteal LNs of adult *Rankl*$^{\Delta Ccl19}$ mice and control littermates were stained for B220 and RANKL. Scale bars represent 200 μm.

(C) Flow cytometry gating strategy to identify MRCs among LN stromal cells.

(D) The proportion of MRCs (MAdCAM-1$^+$VCAM-1$^+$ cells) was determined in *Rankl*$^{\Delta Ccl19}$ and *Rankl*$^{fl/fl}$ control mice.

(E) Relative *Rankl* mRNA expression in MRCs and the remaining (r.) stroma of *Rankl*$^{\Delta Ccl19}$ and control mice. ND indicates not detected.

The data are the mean ± SEM with individual data points; each point represents the value of pooled peripheral LNs of one mouse. Statistical significance (Mann-Whitney): ***p < 0.001; ns, not significant. See also Figure S1.

A

CD169 SIGN-R1 CD11b CD11b+B220

Rankl^{fl/fl}

Rankl^{ΔCcl19}

B

CD11b / CD11c

MHC-II / DC

Rankl^{fl/fl} *Rankl*^{ΔCcl19}

F4/80 / CD169 — MSM / SSM

SSM

F4/80⁻ CD169⁺ cell numbers (10³)

****

Rankl^{fl/fl} *Rankl*^{ΔCcl19}

MSM

F4/80⁺ CD169⁺ cell numbers (10³)

****

Rankl^{fl/fl} *Rankl*^{ΔCcl19}

C

CD11b / CD11c

MHC-II

F4/80 / CD169

F4/80⁺ CD169⁻ Ms

F4/80⁺ CD169⁻ cell numbers (10³)

*

Rankl^{fl/fl} *Rankl*^{ΔCcl19}

F4/80⁻ CD169⁻ Ms

F4/80⁻ CD169⁻ cell numbers (10³)

ns

Rankl^{fl/fl} *Rankl*^{ΔCcl19}

D

FSC / CD11c

CD11b / MHC-II

LN-resident DCs

Tissue-derived DC

LN-resident DCs

MHC-II⁺ DC cell numbers (10³)

ns

Rankl^{fl/fl} *Rankl*^{ΔCcl19}

Tissue-derived DCs

MHC-II^{hi} DC cell numbers (10³)

ns

Rankl^{fl/fl} *Rankl*^{ΔCcl19}

Figure 2. Stromal RANKL Deficiency Results in the Loss of Sinusoidal Macrophages

(A) Adult popliteal LN sections from *Ccl19-cre Rankl*^{fl/fl} (*Rankl*^{ΔCcl19}) mice and *Rankl*^{fl/fl} control littermates were stained for CD169, SIGN-R1, CD11b, and B220. Scale bars represent 200 μm.

(legend continued on next page)

Ly5.1 congenic strain to the cell suspension allowed us to distinguish between *in vivo* PE uptake and PE acquisition during cell preparation. B cells from CD45.2 *Rankl^ΔCcl19* or *Rankl^fl/fl* mice were analyzed by flow cytometry. The proportion of PE+ CD45.2 B cells was significantly lower in the conditional RANKL-deficient mice (Figure 3A). Next, we tested the infection with the vesicular stomatitis virus (VSV), known to target SSMs (Iannacone et al., 2010; Junt et al., 2007). RANKL-deficient and control mice received an intra footpad (i.fp.) administration of 10^6 plaque-forming units (PFU) of VSV, and 6 h later, the popliteal LNs were imaged for VSV replication with the anti-VSV-glycoprotein antibody Vi10 (Honke et al., 2011). Although VSV infection of CD169+ SSMs was clearly detected in the control mice, there was a significant drop in infection of *Rankl^ΔCcl19* mice (Figure 3B). Both SM subsets have been implicated in the immune response against modified vaccinia ankara (MVA) virus (Chatziandreou et al., 2017; Gaya et al., 2015; Sagoo et al., 2016). Therefore, the mice received an i.fp. administration of 10^4 PFU of MVA virus, and 7 days later, the formation of germinal center B cells and plasma cells was assessed by flow cytometry. In spite of an increase in general cellularity, indicative of an ongoing immune response (Figure 3C), the capacity of the mutant mice to generate GL-7+Fas+ germinal center and CD138+ plasma B cells was abolished (Figure 3D). Altogether, these results demonstrate that stromal RANKL is a critical component for the response to viral infection by providing the signal required for SM differentiation.

SSMs Are Dependent on Direct RANK Signaling

To address the mechanism underlying RANKL-mediated SM differentiation, we reasoned that the cell differentiation program could be directly instructed by RANKL and sought to genetically delete *Rank* from SMs. Both SM subsets transcribe *Rank*, albeit less then LECs (Figure S2A). However, a gene-targeting strategy in the myeloid lineage via *Cd11c* (*Itgαx*)-*cre* or *LysM* (*Lyz2*)-*cre* mice crossed with *Rank^fl/fl* mice (Rios et al., 2016) had no effect on the SMs (Figure S2B). Because these promoters are poorly active in SMs (Gaya et al., 2015), we next chose the *Cd169-cre* mouse, which faithfully transcribes the cre recombinase from the *Cd169* locus without affecting protein expression (Karasawa et al., 2015). When crossed with the tdTomato reporter mouse, red fluorescence was indeed restricted to the SM compartment (Figure S2C). We therefore generated *Cd169-cre Rank^fl/fl* (*Rank^ΔCd169*) mice. Immunolabeling of LN sections for CD169 uncovered a conspicuous absence in the subcapsular area; however, its expression was maintained in the medulla (Figure 4A). Indeed, the staining for SIGN-R1 revealed a normal presence of MSMs. Moreover, SIGN-R1+ cells were also discernable in the subcapsular area, lining the B cell follicle. This suggests a dysregulation of SSM differentiation, which is reminiscent of the effect of lymphotoxin receptor (LTβR)-inhibition (Moseman et al., 2012). Quantification of the SM cell numbers in *Rank^ΔCd169* and control mice with the previous flow cytometry strategy confirmed a reduc-

tion of the SSM population (Figure 4B). There were no significant alterations in the numbers of the other macrophage subtypes, the LN-resident DCs or the migratory DCs (Figures S2D–S2F). To address the possibility that the normal presence of MSMs was due to inefficient cre-mediated *Rank* gene recombination, we sorted both SM subsets from *Cd169-cre Rank^fl/+* heterozygous mice and verified gene recombination by PCR. However, the expected *Rank* exon deletion occurred in both cell types (Figure S2G). We next treated adult wild-type mice with RANKL-neutralizing antibody (Kamijo et al., 2006) and, as controls, either LTβ receptor (R)-Fc fusion protein or TNFR2-Fc (Etanercept). Three weeks later, the numbers of SMs were determined. RANKL-blocking antibody, LTβR-Fc (Moseman et al., 2012; Phan et al., 2009) but not TNFR2-Fc (Ettinger et al., 1998) significantly diminished SSM numbers, whereas the medullary counterpart was unchanged (Figure 4C). Taken together, the data are in support of a requirement of direct RANK engagement for maintenance of SSMs.

To address the question whether SSMs are dependent on RANK for cell viability, as it has been proposed for DCs (Josien et al., 2000), we irradiated adult *Rank^ΔCd169* and control mice while shielding the brachial LNs. Bone marrow cells from wild-type Ly5.1 mice were then adoptively transferred. Four weeks later, the proportion and the cell numbers of CD45.1+ donor and CD45.2+ recipient SSMs and MSMs in the protected LNs were determined. A more pronounced replacement of the RANK-deficient SSMs by donor cells should be expected in the case of a reduced lifespan, however, the proportion of donor versus recipient SSMs was not different between genetically modified and control mice (Figure S3A). Moreover, the numbers of SSMs remained low in the *Rank^ΔCd169* mice despite the fact that the donor SSMs expressed RANK. This is in accord with the observation that the SSM niche is occupied by CD11b+SIGN-R1+CD169− cells thereby limiting the expansion of RANK-sufficient CD45.1+ cells.

We next determined whether the loss of RANK under *Cd169* gene control affected macrophages of the liver, lung or the splenic red pulp, given the expression of RANK or CD169 by macrophages in these tissues (Chow et al., 2013; Mass et al., 2016). The Kupffer cells, the alveolar macrophages and the splenic red pulp macrophages were identified by using established cell isolation and flow cytometry methods (Scott et al., 2018). Yet, no significant difference in proportion or numbers was observed between *Rank^ΔCd169* and control mice (Figures S3B–S3D). Altogether, RANKL provides mandatory signals for the LN SSM subset, most likely by directly regulating their cell differentiation and maintenance.

The Formation of the SM Niche during Development Is Instructed by RANK-Activated LECs

Because direct activation only partially accounts for the loss of SMs in *Rankl^ΔCcl19* mice, we asked whether the macrophages would be sensitive to a RANKL-stimulated cellular microenvironment. We have previously shown that LECs express

(B) Flow-cytometry gating strategy to identify SSMs and MSMs in the LNs of *Rankl^ΔCcl19* and *Rankl^fl/fl* mice. The graphs depict their absolute cell numbers.
(C) Flow-cytometry gating strategy to identify F4/80+CD169− and F4/80−CD169− macrophages (Ms) in the LNs of *Rankl^ΔCcl19* and *Rankl^fl/fl* mice. The graphs depict their absolute cell numbers.
(D) Gating strategy to identify LN-resident and tissue-derived DCs in the LNs of *Rankl^ΔCcl19* and *Rankl^fl/fl* mice. Their absolute numbers are shown.
The data are the mean ± SEM with individual data points from inguinal, brachial, and auricular LNs. Statistical significance (Mann-Whitney): ****p < 0.0001, *p < 0.05; ns, not significant.
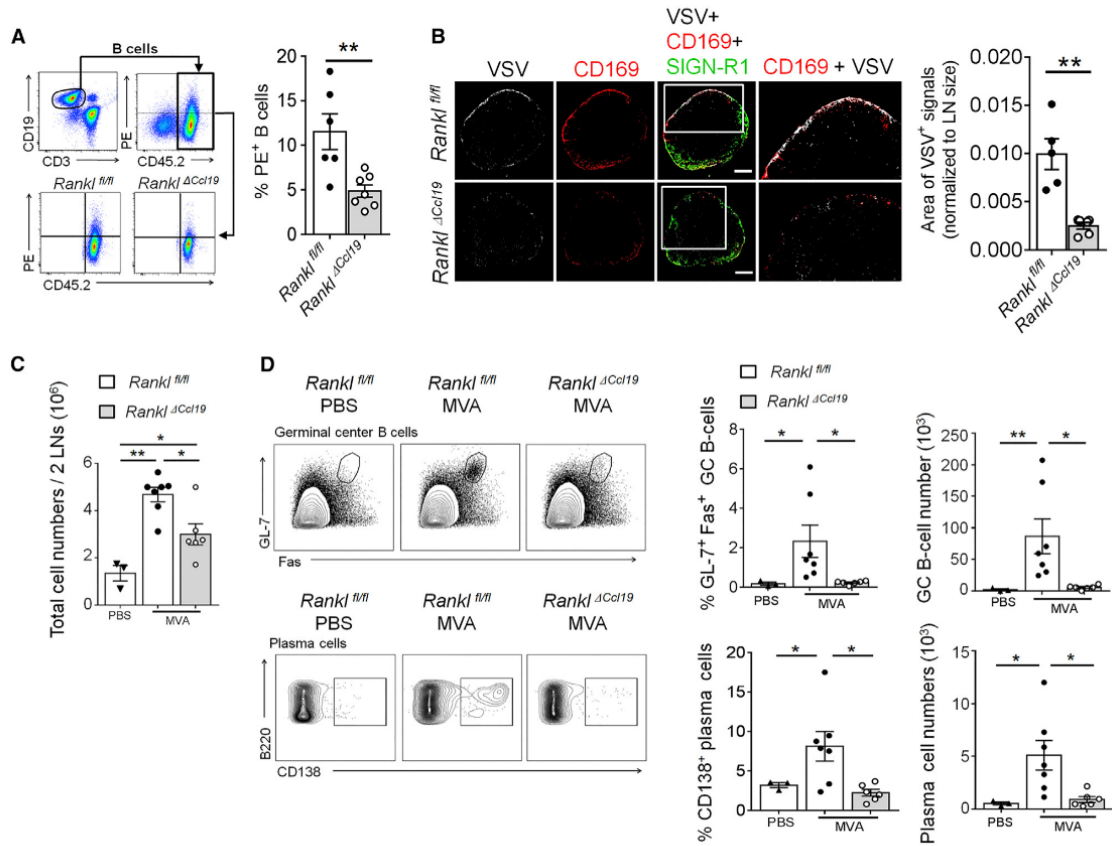
Figure 3. Stromal RANKL Deficiency Leads to Defects in Immunity

(A) Gating strategy to identify the B cells of popliteal LNs that had captured PE-immune complexes delivered by i.fp. injection of PE after passive immunisation with anti-PE antibody. To assure that B cells were not labeled during the cell manipulation, we added lymphocytes from CD45.1 (Ly5.1) mice to the cell suspension. The graph shows the proportion of B cells having captured PE in $Rankl^{\Delta Ccl19}$ and $Rankl^{fl/fl}$ mice.

(B) RANKL mutant or control mice received an i.fp. injection of 10^6 PFU of VSV, and 6 h later popliteal LN sections were stained for CD169 and SIGN-R1 and with the anti-VSV-glycoprotein antibody Vi10. Scale bars represent 200 μm. The graph depicts the quantification of the VSV$^+$ area normalized to LN size. The data are the mean ± SEM with individual data points.

(C) Popliteal LN cellularity was determined in PBS-treated control mice and in $Rankl^{\Delta Ccl19}$ and $Rankl^{fl/fl}$ mice 7 days after i.fp. injection of 10^4 PFU of MVA virus.

(D) Flow-cytometry profiles of B220$^+$GL-7$^+$Fas$^+$ germinal center B cells and B220$^+$CD138$^+$ plasma cells in popliteal LNs from PBS-mock- or MVA-infected mice. The proportion and the number of germinal center B cells and plasma cells are shown in the graphs. The data are the mean ± SEM with individual data points and are representative of three independent experiments.

Statistical significance (Mann-Whitney): *p < 0.05, **p < 0.005; ns, not significant.

MAdCAM-1 and ITGA2b in response to RANKL (Cordeiro et al., 2016) and that RANK expression by LECs is required for LN formation (Onder et al., 2017). Therefore, we crossed the $Rank^{fl/fl}$ mice with $Prox1$-cre^{ERT2} mice, which express a tamoxifen-inducible cre recombinase specifically in LECs (Bazigou et al., 2011). Tamoxifen delivery to $Prox1$-$cre^{ERT2}Rank^{fl/fl}$ ($Rank^{\Delta Prox1}$) mice resulted in the expected gene segment excision in LECs, but not in blood endothelial cells (BECs) nor in FRCs (Figure S4A). We administered tamoxifen to 4-week-old $Rank^{\Delta Prox1}$ mice or to their $Rank^{fl/fl}$ littermates and then every 2 weeks for 8 weeks. Immunofluorescence staining showed that MAdCAM-1 expression by LECs was abolished (Figure 5A), which was validated by flow cytometry (Figure S4B), yet the MRCs were still present

(Figure S4C). Immunolabelling and flow cytometry analysis of the SSMs and MSMs revealed that both subsets were normal in position and numbers (Figure 5A). Because low cell turnover rate and/or already differentiated SMs might render the cells insensitive to the absence of LEC-delivered signals, we hypothesized that $Rank$ excision might have more effect when triggered earlier. Therefore, we delivered tamoxifen to 2-week-old mice and then every 2 weeks. Indeed, this resulted in a marked reduction in CD169 and SIGN-R1 expression and a significant loss of SSM and MSM cell numbers (Figures 5B). In contrast, the other macrophage populations, DCs and B and T cells were unaffected (Figures S5A–S5C). Finally, we administered tamoxifen to pregnant dams to target E18.5 embryos. This procedure resulted
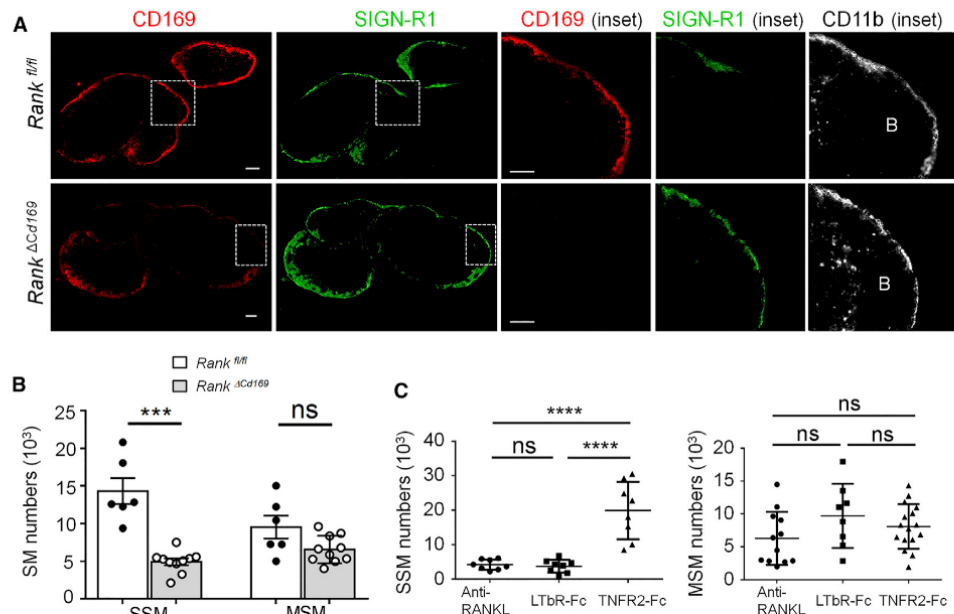
Figure 4. RANKL Directly Activates the Subcapsular Sinus Macrophages

(A) Adult brachial LN sections from *Rank^{fl/fl}* control and *Cd169-cre Rank^{fl/fl}* (*Rank^{ΔCd169}*) mice were stained for CD169, SIGN-R1, and CD11b. Scale bars represent 200 μm. The insets show higher magnification of the area around a B cell follicle "B." Scale bar represents 100 μm.

(B) The number of subcapsular sinus macrophages (SSMs) and medullary sinus macrophages (MSMs) were determined in *Rank^{ΔCd169}* and *Rank^{fl/fl}* mice. The data are shown as the mean ± SEM with individual data points of inguinal and brachial LNs. Statistical significance (Mann-Whitney): ***p < 0.001; ns, not significant.

(C) Adult C57BL/6 mice received 20 μg of anti-RANKL antibody IK22-5, LTbR-Fc, or TNFR2-Fc 3 times a week for 3 weeks, and the number of SMs was assessed in inguinal and brachial LNs. Statistical significance (one-way ANOVA with Bonferroni correction): ****p < 0.0001; ns, not significant.

See also Figures S2 and S3.

in the absence of CD169 and an almost complete loss of SIGN-R1 (Figure 5C). As expected (Onder et al., 2017), embryonic RANK deletion in LECs also negatively affected organ size. However, intra-gastric tamoxifen delivery to post-natal day 1 (P1)–P4 newborns had a reduced effect on organ size and allowed a more accurate assessment of SM numbers; it confirmed the reduction of both sinusoidal subsets (Figure 5D). To verify that SMs are already present in the embryonic LNs, we stained E17.5 LN anlagen for CD169, together with CD4 and lymphatic vessel endothelial receptor 1 (LYVE-1) for LTi cells and LECs, respectively. CD169+ cells were detected at this age and were found closely associated with the LECs (Figure S5D). Although some macrophages might express LYVE-1, these embryonic CD169+ macrophages appeared to lack this marker. Indeed, LYVE-1 was evenly distributed throughout the LECs at this age (Bovay et al., 2018). At post-natal day 6, SSMs and MSMs had taken residence in their distinctive anatomical sites and their numbers increased with age (Figure S5E). These data demonstrate that RANK-activated LECs function in the formation of the SM compartment during late embryogenesis and early post-natal life.

Reconstitution of the SM Network Relies on RANK-Activated LECs

The findings agree with the model of a cooperation of LECs with the RANKL-expressing mesenchymal cells to constitute a microenvironmental niche tailored for SMs when their precursors take up residence in the embryonic LN anlagen. We next asked whether the niche activation would again be required to reconstitute the macrophage population after its integrity has been disrupted. It has been shown that SMs vanish in response to innate immune stimuli, which provided a means to test this possibility (Chatziandreou et al., 2017; Gaya et al., 2015; Sagoo et al., 2016). In response to an i.fp. injection of Toll-like receptor 9 (TLR9) agonist CpG, but not PBS, the CD169+ SSMs and the CD169+SIGN-R1+ MSMs were undetectable after 4 days, in spite of a massive recruitment of CD11b+ cells (Figure 6A). Yet, 4 weeks later, when inflammation had receded, the SM compartment had normalized. This procedure was repeated in *Rank^{ΔProx1}* and *Rank^{fl/fl}* mice with tamoxifen delivered 5 days after CpG and renewed every 2 weeks. We observed by immunofluorescence and flow cytometry that, although in *Rank^{fl/fl}* controls both subsets had reconstituted within 5 weeks, SM restoration was incomplete in *Rank^{ΔProx1}* mice (Figures 6B and 6C). To confirm these findings in the context of a relevant immune response, we repeated the procedure, and MVA was i.fp. administered at 5 weeks. Seven days later, the cell proportions and the numbers of germinal center B cells and plasma cells were measured. The silencing of RANK expression after CpG-induced SM loss perturbed the normal formation of germinal center B cells and plasma cells (Figure 6D). Therefore,
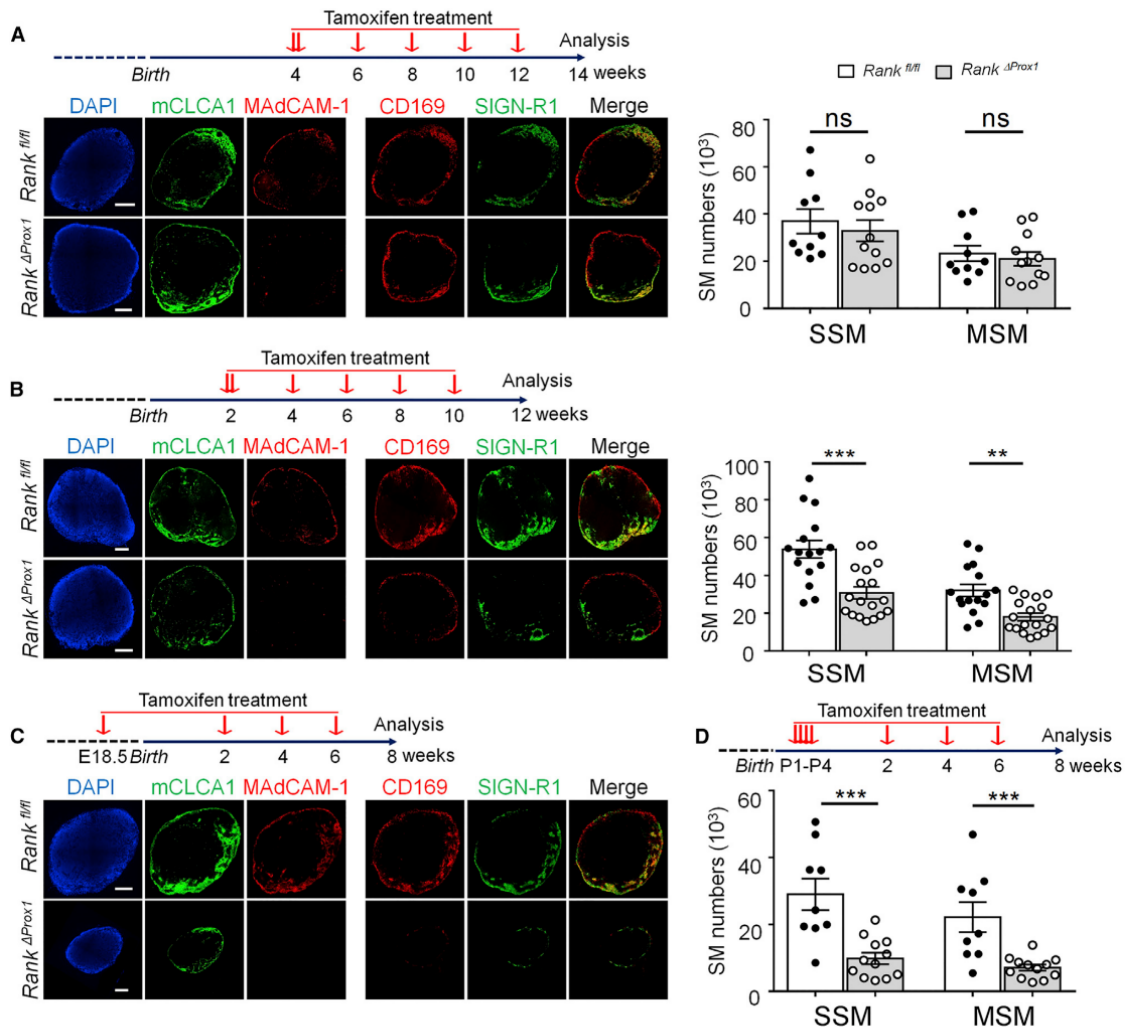
Figure 5. RANK Signaling in Lymphatic Endothelial Cells Is Required for Both Sinusoidal Macrophage Subsets

RANK deficiency in lymphatic endothelial cells (LECs) was induced by tamoxifen delivery to *Prox1-cre*[ERT2]*Rank*^{fl/fl} mice (*Rank*[ΔProx1]) at different ages. As control, *Rank*^{fl/fl} mice were treated identically. Tamoxifen administration was started at 4 weeks (A), 2 weeks (B), E18.5 (C), postnatal days 1–4 (D), and then every 2 weeks until analysis. In (A)–(C), popliteal LN sections were stained for mCLCA1 (LECs), MAdCAM-1, SIGN-R1, and CD169 and counterstained with DAPI. Scale bars represent 200 μm. In (A), (B), and (D), the numbers of subcapsular sinus macrophages (SSMs) and medullary sinus macrophages (MSMs) were determined in the LNs. The data are the mean ± SEM with individual data points of inguinal and brachial LNs. Statistical significance (Mann-Whitney): **p < 0.01, ***p < 0.001; ns, not significant. See also Figures S4 and S5.

LEC activation by RANKL is required to reconstitute the niche environment for SM restoration after network disruption by innate immune stimuli.

Impaired SM Niche Constitution Correlates with Fewer CD11b+ Cells

To obtain an insight into the downstream pathways induced by RANK signaling in LECs, we performed RNA-sequencing of LECs purified from *Rankl*[ΔCcl19] and control mice. In addition to the diminished gene expression of *Madcam-1* and *Itga2b*, we

observed reduced *Ccl20* and increased *Ackr4* (*Ccrl1*) transcription (Figure 7A). These variations in gene expression were validated by RT-qPCR in LECs purified from *Rank*[ΔProx1] and control mice (Figure 7B). A downstream pathway analysis uncovered, among others, those involved in chemotaxis and myeloid cell differentiation (Figure S6). We next determined whether RANK activation of LECs translated into an increased recruitment or retention of potential myeloid precursor cells. The immunofluorescence analysis of LN sections of *Rank*[ΔProx1] mice 5 weeks after CpG stimulation and tamoxifen treatment showed a
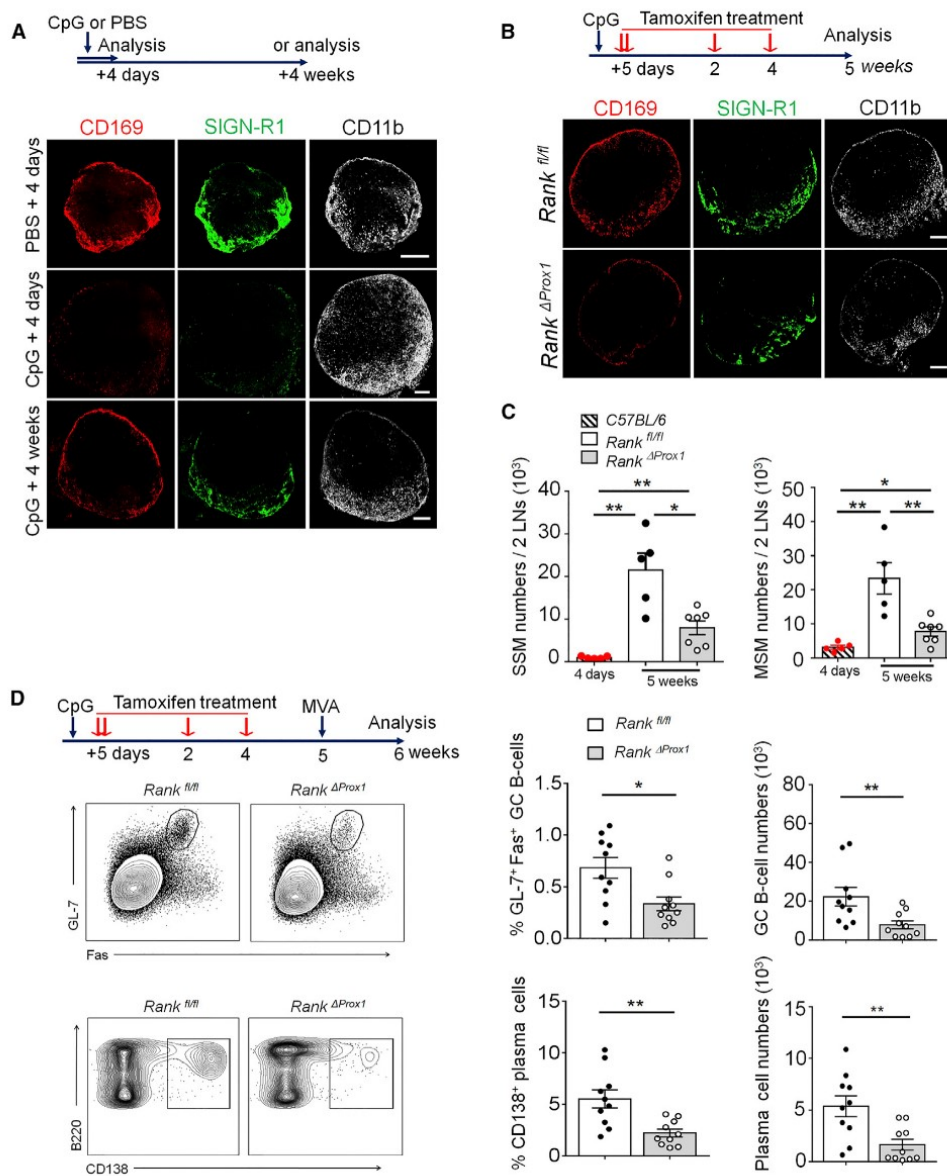
Figure 6. RANKL-Activated Lymphatic Endothelial Cells Restore the Sinusoidal Macrophage Compartment

(A) C57BL/6 mice received an i.fp. injection of either PBS or CpG, and 4 days or 4 weeks afterward, popliteal LNs were stained for CD169, SIGN-R1, and CD11b. Scale bars represent 200 μm.

(B and C) CpG was i.fp. administered to *Prox1-cre*[ERT2]*Rank*^{fl/fl} mice (*Rank*[ΔProx1]) and control *Rank*^{fl/fl} mice, which then received tamoxifen, as schematized. Five weeks afterward, the popliteal LNs were stained for CD169, SIGN-R1, and CD11b (B) or processed to assess the number of subcapsular sinus macrophages (SSMs) and medullary sinus macrophages (MSMs) (C). Scale bars represent 200 μm. The graphs also show the number of SSMs and MSMs 4 days after i.fp. injection of CpG in C57BL/6 mice. The data are the mean ± SEM with individual data points.

(D) CpG was i.fp. administered to *Rank*[ΔProx1] and *Rank*^{fl/fl} mice, which then received tamoxifen, as depicted, and after 5 weeks, the mice were immunized by an i.fp. injection of 10^4 PFU of MVA virus. Seven days later, the proportions and numbers of B220^{+}GL-7^{+}Fas^{+} germinal center B cells or B220^{+}CD138^{+} plasma cells in the popliteal LNs were determined. The data are the mean ± SEM with individual data points and are representative of three independent experiments. Statistical significance (Mann-Whitney): *p < 0.05, **p < 0.01.
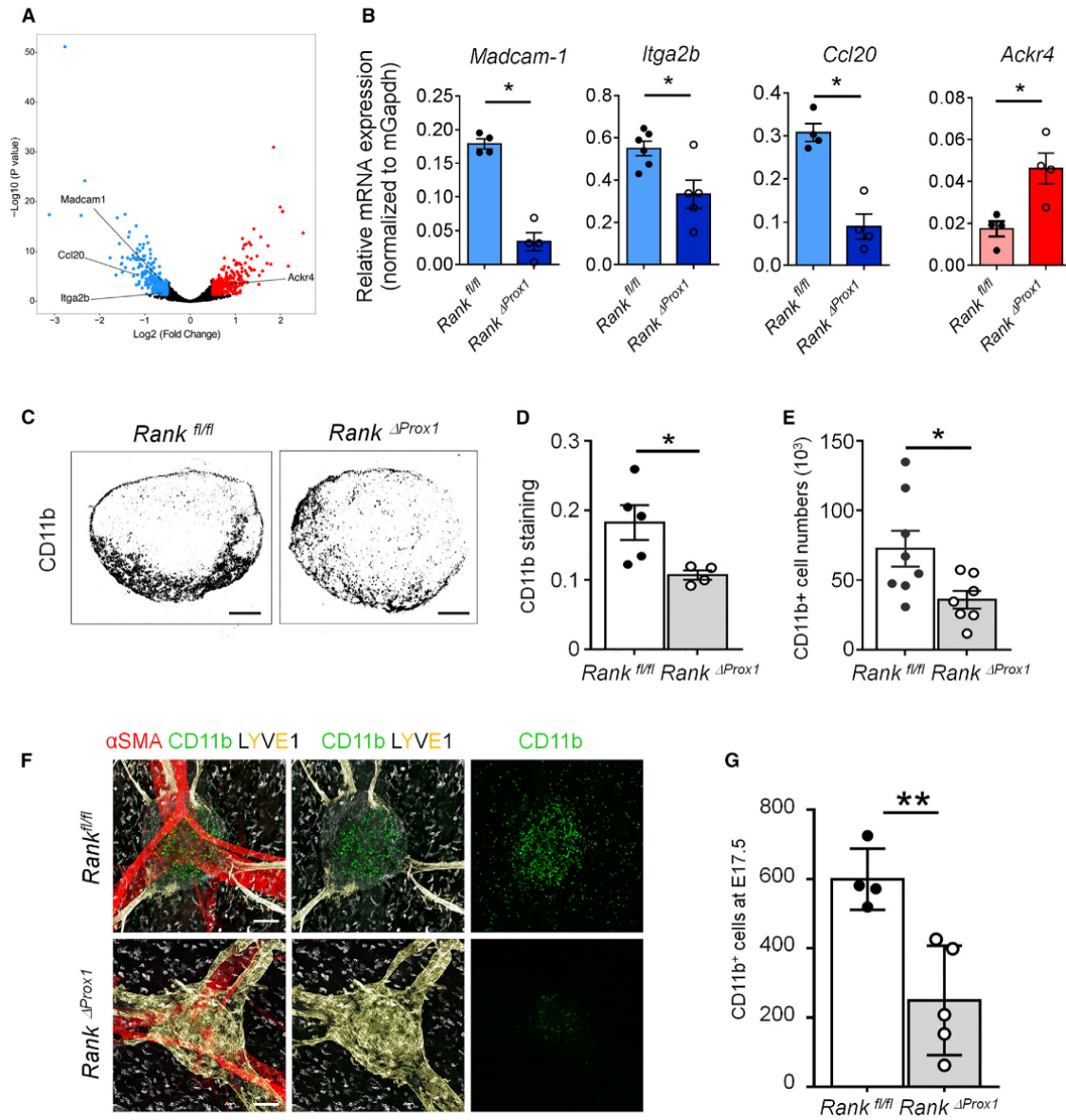
Figure 7. RANK-Activated LECs Positively Regulate the Presence of CD11b⁺ Myeloid Cells

(A) Volcano plot showing the genes whose expression is significantly reduced (blue) or increased (red) in LECs sorted from *Ccl19-cre Rankl*$^{fl/fl}$ and *Rankl*$^{fl/fl}$ control mice. Selected differentially expressed genes were indicated on the plot.

(B) Selected genes that displayed changes in expression were validated by RT-qPCR on LECs sorted from *Prox1-cre Rank*$^{fl/fl}$ mice versus control *Rank*$^{fl/fl}$ mice. Target-gene expression was normalized to mGapdh. The data, identified by dots, are the mean of replicates from individual mice. Statistical significance (Mann-Whitney): *p < 0.5.

(C and D) *Prox1-cre*^{ERT2}*Rank*$^{fl/fl}$ mice (*Rank*$^{\Delta Prox1}$) and control *Rank*$^{fl/fl}$ mice received first an i.fp. administration of CpG, followed 5 days later by tamoxifen gavage. After 5 weeks, popliteal LNs were imaged for CD11b expression (C) that was quantified (D) as CD11b⁺ area normalized to LN area. The data are the mean ± SEM with individual data points of popliteal LN sections. Statistical significance (Mann-Whitney): *p < 0.05.

(E) The number of CD11b^{Hi} cells were determined in the popliteal LNs by flow cytometry using the gating strategy described in Figure 2. The data are the mean ± SEM with individual data points of popliteal LNs. Statistical significance (Mann-Whitney): *p < 0.05.

(legend continued on next page)

discernable deficiency in CD11b⁺ cells in the subcapsular and medullary sinusoidal areas (Figures 7C and 7D). A reduction in CD11b⁺ cells was confirmed by flow cytometry (Figure 7E). This supports a role of RANK-activated LECs in the recruitment and/or the retention of myeloid cells that would subsequently give rise to SSMs and MSMs. To explore this notion further, we asked whether RANK deficiency in LECs would likewise result in diminished numbers of CD11b⁺ cells in the embryonic LNs. Tamoxifen was delivered to pregnant dams at the embryonic ages of E11.5 and E12.5 when LTi cells populate the developing LN (Bovay et al., 2018; Onder et al., 2017). Whole mounts of E17.5 inguinal LN anlagen were stained for CD11b alongside smooth muscle actin (SMA) to mark vascular smooth muscle cells around major blood vessels and LYVE-1 for lymphatics. CD11b⁺ embryonic cells were present in control LN anlagen; however, they were significantly reduced in embryos with LEC-specific RANK deletion (Figures 7F and 7G). These findings show that RANK-activated LECs increase the numbers of LN CD11b⁺ cells that might function as SM precursors during embryonic development and in inflammatory situations in the adult.

DISCUSSION

Secondary lymphoid organs comprise different stromal cells that map to distinct anatomical locations. They interact directly with immune cells to compartmentalize and regulate the immune response. Here, we demonstrated that mesenchymal stromal cells, through RANK-RANKL signaling, created a niche environment with LECs for specialized macrophages to take up residence, complete their differentiation program, and fulfill their immune function. Mice deficient in stromal RANKL showed reduced numbers of SSMs and MSMs and, as a consequence, were compromised in antigen-transport to B cells, viral infection, and the anti-viral immune response. The absence of SSMs in mice with RANK deficiency in CD169⁺ cells and after RANKL neutralization demonstrated that SSMs were dependent on direct and continuous RANKL stimulation. Moreover, RANK activation of LECs was mandatory during development and after inflammation for the formation of both SM subtypes. Finally, the data suggest that activated LECs contribute to the SM compartment by regulating the presence of myeloid cell precursors.

RANKL is expressed by the mesenchymal LTOs in the embryonic LN anlagen and the MRCs in the adult LNs (Katakai, 2012; Sugiyama et al., 2012). To address the function of stromal RANKL in lymphoid tissue, we made use of the *Ccl19-cre* mice that allow genetic ablation in LTOs and in mesenchymal cells of most adult secondary lymphoid organs (Chai et al., 2013). Using this strategy, the removal of RANKL from LTOs and MRCs did not markedly affect LN organogenesis except for a slightly reduced inguinal LN size. This is in contrast to the effect of RANK silencing in LECs that resulted in a smaller organ even when deleted late in embryogenesis at E18.5. Because at this stage in development LTi cells express little RANKL (Sugiyama et al., 2012), it might be supplemented from other cellular sources. For instance, we and others have shown that soluble RANKL is produced by embryonic and newborn skin and can reach the draining LNs (Duheron et al., 2011; Kartsogiannis et al., 1999). Alternatively, it is not excluded that stromal RANKL deletion is insufficient or belated, given that residual stromal RANKL was indeed observed at E17.5 before a complete shutdown in the adult. The low RANKL expression sufficed to support the ongoing organogenesis but could not complete the installation of the SM populations. We found a marked reduction in the SM compartment, SSMs and MSMs being both profoundly impacted in the *Rankl^ΔCcl19* mice. This finding was based on the expression of the key markers for these cells (CD169 is expressed exclusively by both subsets, and SIGN-R1 is restricted to the MSMs), as well as impaired function. Mice lacking stromal RANKL showed diminished immune complex transfer to B cells, normally ensured by SSMs (Phan et al., 2007), impaired infection with the SSM-targeting VSV (Iannacone et al., 2010; Junt et al., 2007), and a failure to mount an SM-dependent immune response to MVA (Chatziandreou et al., 2017; Gaya et al., 2015; Sagoo et al., 2016).

We uncovered two underlying mechanism for stromal RANKL dependence of SMs. First, SSMs required direct RANK signaling; second, both subsets relied on RANK-activated LECs. By silencing RANK expression in the SM compartment using *Cd169-cre* mice, we observed a reduction in CD169 expression and aberrant expression of SIGN-R1 by CD11b⁺ cells of the subcapsular zone. This indicates that RANK-deficient macrophages can take residence in this zone but are unable to complete their differentiation program. The absence of restoration of the SSM population by donor-derived RANK-sufficient precursors after a partial irradiation supports the occupation of the niche by other cells. The unchanged renewal rate makes the possibility that RANK conveys cell survival or proliferative signals unlikely. A similar phenotypic change is observed when LTbR signaling is blocked by LTbR-Fc resulting in the presence of SIGN-R1⁺ cells in place of SSMs (Moseman et al., 2012). All things considered, the data support the idea that RANK directly activates a differentiation program that also requires LTbR signaling. Because RANK and LTbR activate unique and overlapping cell signaling pathways, (Remouchamps et al., 2011; Walsh and Choi, 2014) it is conceivable that both receptor transduction pathways cooperate to direct SSM differentiation. Yet, conclusive confirmation for this model awaits *in vitro* differentiation experiments.

The nature of a secondary differentiation signal used by MSMs remains open to conjecture. Given that F4/80 is frequently found on different types of tissue macrophages, it is possible that a co-stimulus might not play an important role for MSMs and that this cell type reflects a default program arising in the absence of continuous RANK-engagement. Indeed, because MSMs transcribed *Rank* and gene recombination occurred in MSMs of *Cd169-cre* mice, the simplest explanation would be that RANK is not engaged in these cells because of insufficient RANKL.

(F) Pregnant dams received tamoxifen at ages E11.5 and E12.5 to trigger genetic *Rank* removal in LECs of embryos. Inguinal LN anlagen of *Rank^ΔProx1* and control *Rank^fl/fl* E17.5 embryos were stained for SMA, LYVE-1, and CD11b in whole mounts. Scale bar represents 80 μm.
(G) The number of CD11b⁺ cells was determined by isosurface cell quantification in whole-mount LN anlagen. The data show the mean ± SD with individual data points. Statistical significance (Student's t test): *p < 0.05, **p < 0.01.
See also Figure S6.

Admittedly, confirmation that RANK protein is expressed by MSMs is lacking because of difficulties in detecting cellular RANK on murine primary cells. It would therefore be of interest to scrutinize the medullary zone during an ongoing immune reaction to find out whether MSMs can acquire features of SSMs in an environment rich in other RANKL-producing cells such as activated T cells and type 3 innate lymphoid cells (Bando et al., 2018; Josien et al., 1999).

We have previously shown that LECs respond to RANKL by the expression of ITGA2b (Cordeiro et al., 2016), and here, we confirmed this sensitivity to RANKL by using MAdCAM-1 (Cohen et al., 2014; Cordeiro et al., 2016). The absence of MAdCAM-1 expression by LECs lacking RANK had no impact on the presence of MAdCAM-1 on MRCs. This indicates that its presence on MRCs is not secondary to cell membrane sharing with LECs and invokes post-transcriptional mechanisms to explain the increased MAdCAM-1 expression by MRCs compared with TRCs (Rodda et al., 2018). Deleting RANK from LECs had a clear effect on both SM subtypes when gene excision occurred during late embryogenesis and the first post-natal weeks. This is compatible with a critical role of RANK activation of LECs when SMs start occupying the embryonic LN anlagen and throughout the LN growth phase of the first few weeks. Once the SM population was established and maximal LN organ size had been attained, the importance of RANK for the LECs was minimal. Although RANK activation of LECs was required for the accumulation of embryonic macrophages in the LN anlagen, evidence is so far lacking to propose a direct relationship between the control over macrophage arrival and the future presence of SMs in the adult. Further studies are necessary to understand the molecular and cellular processes that oversee the formation of the complete macrophage compartment in the developing LNs. Of further complication is the presence of the basement membrane of subcapsular and medullary sinuses (Pfeiffer et al., 2008), an extracellular matrix that not only serves as cell-anchoring substrate but might also affect cell differentiation. We cannot formally rule out a function of RANK-activated LECs in the maintenance of the SM compartment, but because of the slow SM replacement rate, at least in the adult, it is likely that the consequences of *Rank* deletion in LECs will only be noticeable months later. Of note, reconstitution of the SM population takes months after clodronated-lipososome-mediated ablation (Delemarre et al., 1990). Yet, when the SM compartment was "emptied" by inflammation, RANK activation of LECs was clearly mandatory to fully reconstitute the SM pool. The finding that SSMs and MSMs were slowly replaced from CD45.1$^+$ bone marrow precursors in the shielded irradiation experiments supports the idea of an input from an external (circulating) source under situations of inflammation. As a consequence of incomplete macrophage replenishment, subsequent immune reactions against the MVA virus were significantly diminished. Under these inflammatory conditions, it would be again of interest to determine whether activated T cells and type 3 innate lymphoid cells provide RANKL in addition to MRCs.

The analysis of the gene profiles provided information on the downstream pathways and the effector molecules produced by LECs. Loss of *Ccl20* expression and upregulation of *Ackr4* in RANK-deficient LECs suggest a role in chemotaxis. Increased CCL20 production has also been observed in astrocytes in response to RANKL (Guerrini et al., 2015). In the LN, this chemokine plays a role in the recruitment of CCR6$^+$ innate-like lymphocytes to the subcapsular area (Zhang et al., 2016). ACKR4 is produced by the subscapular ceiling layer of LECs but not by the floor layer (Ulvmar et al., 2014). Mice lacking the CCL20 receptor CCR6 comprise a normal SM compartment (Zhang et al., 2016), but whether ACKR4 affects the SMs has not been reported. Expression of MAdCAM-1 and ITGA2b was validated on the mRNA and the protein level. Intriguingly, the neutralization of MAdCAM-1 in developing LNs leads to more LN macrophages whereas lymphocyte numbers are reduced (Mebius et al., 1996). However, the interpretation of this result is complicated by the fact that MAdCAM-1 is also expressed by BECs and plays an important role in the recruitment of lymphocytes. ITGA2b is not expressed by LN BECs, and, although this integrin is already expressed by LECs of the LN anlagen (Bovay et al., 2018; Cordeiro et al., 2016), a defect in the SM compartment is not observed in *Itga2b*$^{-/-}$ mice (Cordeiro et al., 2016). Altogether, the data suggest that LECs affect the recruitment and/or retention of SMs or their progenitors, but a direct impact on cell differentiation is not excluded.

Clinical use of RANKL-antagonists is approved to treat osteoporosis and bone-metastasizing cancers such as mammary and prostate carcinoma (Ahern et al., 2018). In the light of our findings, the effect of RANKL-neutralization on immune responses should be carefully evaluated. Notably, it has been shown that SSMs can function as tumor suppressor cells (Pucci et al., 2016). In accordance with the concept that peripheral tissues, including lymphoid organs, shape resident immune cell composition, we demonstrated here that mesenchymal cells and LECs are essential elements to shape the niche for LN sinusoidal macrophages. Our findings are likely of importance to further advance current immunotherapies.

STAR★METHODS

Detailed methods are provided in the online version of this paper and include the following:

- KEY RESOURCES TABLE
- CONTACT FOR REQUESTS AND RESOURCE SHARING
- EXPERIMENTAL MODEL AND SUBJECT DETAILS
  - Mice
- METHOD DETAILS
  - Immunizations and reagent administration
  - Partial irradiation and adoptive transfer
  - Immunofluorescence of adult LN
  - Immunofluorescence of embryonic LN anlagen
  - Isolation and analysis of LN cells
  - Flow cytometry and immunofluorescence
  - PCR
  - RNA sequencing and data processing
- QUANTIFICATION AND STATISTICAL ANALYSIS
- DATA AND SOFTWARE AVAILABILITY

SUPPLEMENTAL INFORMATION

Supplemental Information can be found online at https://doi.org/10.1016/j.immuni.2019.05.008.

REFERENCES

Ahern, E., Smyth, M.J., Dougall, W.C., and Teng, M.W.L. (2018). Roles of the RANKL-RANK axis in antitumour immunity - implications for therapy. Nat. Rev. Clin. Oncol. *15*, 676–693.

Anders, S., Pyl, P.T., and Huber, W. (2015). HTSeq–a Python framework to work with high-throughput sequencing data. Bioinformatics *31*, 166–169.

Arai, A., Mizoguchi, T., Harada, S., Kobayashi, Y., Nakamichi, Y., Yasuda, H., Penninger, J.M., Yamada, K., Udagawa, N., and Takahashi, N. (2012). Fos plays an essential role in the upregulation of RANK expression in osteoclast precursors within the bone microenvironment. J. Cell Sci. *125*, 2910–2917.

Bando, J.K., Gilfillan, S., Song, C., McDonald, K.G., Huang, S.C., Newberry, R.D., Kobayashi, Y., Allan, D.S.J., Carlyle, J.R., Cella, M., and Colonna, M. (2018). The tumor necrosis factor superfamily member RANKL suppresses effector cytokine production in group 3 innate lymphoid cells. Immunity *48*, 1208–1219.e4.

Baratin, M., Simon, L., Jorquera, A., Ghigo, C., Dembele, D., Nowak, J., Gentek, R., Wienert, S., Klauschen, F., Malissen, B., et al. (2017). T cell zone resident macrophages silently dispose of apoptotic cells in the lymph node. Immunity *47*, 349–362.e5.

Bazigou, E., Lyons, O.T., Smith, A., Venn, G.E., Cope, C., Brown, N.A., and Makinen, T. (2011). Genes regulating lymphangiogenesis control venous valve formation and maintenance in mice. J. Clin. Invest. *121*, 2984–2992.

Bénézech, C., White, A., Mader, E., Serre, K., Parnell, S., Pfeffer, K., Ware, C.F., Anderson, G., and Caamaño, J.H. (2010). Ontogeny of stromal organizer cells during lymph node development. J. Immunol. *184*, 4521–4530.

Benjamini, Y., and Hochberg, Y. (1995). Controlling the false discovery rate: a practical and powerful approach to multiple testing. J.R. Stat. Soc. *57*, 289–300.

Bovay, E., Sabine, A., Prat-Luri, B., Kim, S., Son, K., Willrodt, A.H., Olsson, C., Halin, C., Kiefer, F., Betsholtz, C., et al. (2018). Multiple roles of lymphatic vessels in peripheral lymph node development. J. Exp. Med. *215*, 2760–2777.

Buechler, M.B., and Turley, S.J. (2018). A short field guide to fibroblast function in immunity. Semin. Immunol. *35*, 48–58.

Carrasco, Y.R., and Batista, F.D. (2007). B cells acquire particulate antigen in a macrophage-rich area at the boundary between the follicle and the subcapsular sinus of the lymph node. Immunity *27*, 160–171.

Chai, Q., Onder, L., Scandella, E., Gil-Cruz, C., Perez-Shibayama, C., Cupovic, J., Danuser, R., Sparwasser, T., Luther, S.A., Thiel, V., et al. (2013). Maturation of lymph node fibroblastic reticular cells from myofibroblastic precursors is critical for antiviral immunity. Immunity *38*, 1013–1024.

Chatziandreou, N., Farsakoglu, Y., Palomino-Segura, M., D'Antuono, R., Pizzagalli, D.U., Sallusto, F., Lukacs-Kornek, V., Uguccioni, M., Corti, D., Turley, S.J., et al. (2017). Macrophage death following influenza vaccination initiates the inflammatory response that promotes dendritic cell function in the draining lymph node. Cell Rep. *18*, 2427–2440.

Chow, A., Huggins, M., Ahmed, J., Hashimoto, D., Lucas, D., Kunisaki, Y., Pinho, S., Leboeuf, M., Noizat, C., van Rooijen, N., et al. (2013). CD169⁺ macrophages provide a niche promoting erythropoiesis under homeostasis and stress. Nat. Med. *19*, 429–436.

Cohen, J.N., Tewalt, E.F., Rouhani, S.J., Buonomo, E.L., Bruce, A.N., Xu, X., Bekiranov, S., Fu, Y.X., and Engelhard, V.H. (2014). Tolerogenic properties of lymphatic endothelial cells are controlled by the lymph node microenvironment. PLoS ONE *9*, e87740.

Cordeiro, O.G., Chypre, M., Brouard, N., Rauber, S., Alloush, F., Romera-Hernandez, M., Bénézech, C., Li, Z., Eckly, A., Coles, M.C., et al. (2016). Integrin-Alpha IIb identifies murine lymph node lymphatic endothelial cells responsive to RANKL. PLoS ONE *11*, e0151848.

Cupedo, T., Vondenhoff, M.F., Heeregrave, E.J., De Weerd, A.E., Jansen, W., Jackson, D.G., Kraal, G., and Mebius, R.E. (2004). Presumptive lymph node organizers are differentially represented in developing mesenteric and peripheral nodes. J. Immunol. *173*, 2968–2975.

Delemarre, F.G., Kors, N., Kraal, G., and van Rooijen, N. (1990). Repopulation of macrophages in popliteal lymph nodes of mice after liposome-mediated depletion. J. Leukoc. Biol. *47*, 251–257.

Dougall, W.C., Glaccum, M., Charrier, K., Rohrbach, K., Brasel, K., De Smedt, T., Daro, E., Smith, J., Tometsko, M.E., Maliszewski, C.R., et al. (1999). RANK is essential for osteoclast and lymph node development. Genes Dev. *13*, 2412–2424.

Duheron, V., Hess, E., Duval, M., Decossas, M., Castaneda, B., Klöpper, J.E., Amoasii, L., Barbaroux, J.B., Williams, I.R., Yagita, H., et al. (2011). Receptor activator of NF-kappaB (RANK) stimulates the proliferation of epithelial cells of the epidermo-pilosebaceous unit. Proc. Natl. Acad. Sci. USA *108*, 5342–5347.

Ettinger, R., Mebius, R., Browning, J.L., Michie, S.A., van Tuijl, S., Kraal, G., van Ewijk, W., and McDevitt, H.O. (1998). Effects of tumor necrosis factor and lymphotoxin on peripheral lymphoid tissue development. Int. Immunol. *10*, 727–741.

Furuya, M., Kirschbaum, S.B., Paulovich, A., Pauli, B.U., Zhang, H., Alexander, J.S., Farr, A.G., and Ruddell, A. (2010). Lymphatic endothelial murine chloride channel calcium-activated 1 is a ligand for leukocyte LFA-1 and Mac-1. J. Immunol. *185*, 5769–5777.

Gaya, M., Castello, A., Montaner, B., Rogers, N., Reis e Sousa, C., Bruckbauer, A., and Batista, F.D. (2015). Host response. Inflammation-induced disruption of SCS macrophages impairs B cell responses to secondary infection. Science *347*, 667–672.

Ginhoux, F., and Guilliams, M. (2016). Tissue-resident macrophage ontogeny and homeostasis. Immunity *44*, 439–449.

Gray, E.E., and Cyster, J.G. (2012). Lymph node macrophages. J. Innate Immun. *4*, 424–436.

Guerrini, M.M., Okamoto, K., Komatsu, N., Sawa, S., Danks, L., Penninger, J.M., Nakashima, T., and Takayanagi, H. (2015). Inhibition of the TNF family

1

98

cytokine RANKL prevents autoimmune inflammation in the central nervous system. Immunity *43*, 1174–1185.

Guilliams, M., and Scott, C.L. (2017). Does niche competition determine the origin of tissue-resident macrophages? Nat. Rev. Immunol. *17*, 451–460.

Honke, N., Shaabani, N., Cadeddu, G., Sorg, U.R., Zhang, D.E., Trilling, M., Klingel, K., Sauter, M., Kandolf, R., Gailus, N., et al. (2011). Enforced viral replication activates adaptive immunity and is essential for the control of a cytopathic virus. Nat. Immunol. *13*, 51–57.

Hoorweg, K., Narang, P., Li, Z., Thuery, A., Papazian, N., Withers, D.R., Coles, M.C., and Cupedo, T. (2015). A stromal cell niche for human and mouse type 3 innate lymphoid cells. J. Immunol. *195*, 4257–4263.

Huang, H.Y., Rivas-Caicedo, A., Renevey, F., Cannelle, H., Peranzoni, E., Scarpellino, L., Hardie, D.L., Pommier, A., Schaeuble, K., Favre, S., et al. (2018). Identification of a new subset of lymph node stromal cells involved in regulating plasma cell homeostasis. Proc. Natl. Acad. Sci. USA *115*, E6826–E6835.

Iannacone, M., Moseman, E.A., Tonti, E., Bosurgi, L., Junt, T., Henrickson, S.E., Whelan, S.P., Guidotti, L.G., and von Andrian, U.H. (2010). Subcapsular sinus macrophages prevent CNS invasion on peripheral infection with a neurotropic virus. Nature *465*, 1079–1083.

Josien, R., Wong, B.R., Li, H.L., Steinman, R.M., and Choi, Y. (1999). TRANCE, a TNF family member, is differentially expressed on T cell subsets and induces cytokine production in dendritic cells. J. Immunol. *162*, 2562–2568.

Josien, R., Li, H.L., Ingulli, E., Sarma, S., Wong, B.R., Vologodskaia, M., Steinman, R.M., and Choi, Y. (2000). TRANCE, a tumor necrosis factor family member, enhances the longevity and adjuvant properties of dendritic cells in vivo. J. Exp. Med. *191*, 495–502.

Junt, T., Moseman, E.A., Iannacone, M., Massberg, S., Lang, P.A., Boes, M., Fink, K., Henrickson, S.E., Shayakhmetov, D.M., Di Paolo, N.C., et al. (2007). Subcapsular sinus macrophages in lymph nodes clear lymph-borne viruses and present them to antiviral B cells. Nature *450*, 110–114.

Kamijo, S., Nakajima, A., Ikeda, K., Aoki, K., Ohya, K., Akiba, H., Yagita, H., and Okumura, K. (2006). Amelioration of bone loss in collagen-induced arthritis by neutralizing anti-RANKL monoclonal antibody. Biochem. Biophys. Res. Commun. *347*, 124–132.

Karasawa, K., Asano, K., Moriyama, S., Ushiki, M., Monya, M., Iida, M., Kuboki, E., Yagita, H., Uchida, K., Nitta, K., and Tanaka, M. (2015). Vascular-resident CD169-positive monocytes and macrophages control neutrophil accumulation in the kidney with ischemia-reperfusion injury. J. Am. Soc. Nephrol. *26*, 896–906.

Kartsogiannis, V., Zhou, H., Horwood, N.J., Thomas, R.J., Hards, D.K., Quinn, J.M., Niforas, P., Ng, K.W., Martin, T.J., and Gillespie, M.T. (1999). Localization of RANKL (receptor activator of NF kappa B ligand) mRNA and protein in skeletal and extraskeletal tissues. Bone *25*, 525–534.

Katakai, T. (2012). Marginal reticular cells: a stromal subset directly descended from the lymphoid tissue organizer. Front. Immunol. *3*, 200–206.

Katakai, T., Suto, H., Sugai, M., Gonda, H., Togawa, A., Suematsu, S., Ebisuno, Y., Katagiri, K., Kinashi, T., and Shimizu, A. (2008). Organizer-like reticular stromal cell layer common to adult secondary lymphoid organs. J. Immunol. *181*, 6189–6200.

Kim, D., Mebius, R.E., MacMicking, J.D., Jung, S., Cupedo, T., Castellanos, Y., Rho, J., Wong, B.R., Josien, R., Kim, N., et al. (2000). Regulation of peripheral lymph node genesis by the tumor necrosis factor family member TRANCE. J. Exp. Med. *192*, 1467–1478.

Kong, Y.Y., Yoshida, H., Sarosi, I., Tan, H.L., Timms, E., Capparelli, C., Morony, S., Oliveira-dos-Santos, A.J., Van, G., Itie, A., et al. (1999). OPGL is a key regulator of osteoclastogenesis, lymphocyte development and lymph-node organogenesis. Nature *397*, 315–323.

Lavin, Y., Mortha, A., Rahman, A., and Merad, M. (2015). Regulation of macrophage development and function in peripheral tissues. Nat. Rev. Immunol. *15*, 731–744.

Love, M.I., Huber, W., and Anders, S. (2014). Moderated estimation of fold change and dispersion for RNA-seq data with DESeq2. Genome Biol. *15*, 550.

Mass, E., Ballesteros, I., Farlik, M., Halbritter, F., Günther, P., Crozet, L., Jacome-Galarza, C.E., Händler, K., Klughammer, J., Kobayashi, Y., et al. (2016). Specification of tissue-resident macrophages during organogenesis. Science *353*, aaf4238.

Mebius, R.E., Streeter, P.R., Michie, S., Butcher, E.C., and Weissman, I.L. (1996). A developmental switch in lymphocyte homing receptor and endothelial vascular addressin expression regulates lymphocyte homing and permits CD4$^+$ CD3$^-$ cells to colonize lymph nodes. Proc. Natl. Acad. Sci. USA *93*, 11019–11024.

Moseman, E.A., Iannacone, M., Bosurgi, L., Tonti, E., Chevrier, N., Tumanov, A., Fu, Y.X., Hacohen, N., and von Andrian, U.H. (2012). B cell maintenance of subcapsular sinus macrophages protects against a fatal viral infection independent of adaptive immunity. Immunity *36*, 415–426.

Onder, L., and Ludewig, B. (2018). A fresh view on lymph node organogenesis. Trends Immunol. *39*, 775–787.

Onder, L., Mörbe, U., Pikor, N., Novkovic, M., Cheng, H.W., Hehlgans, T., Pfeffer, K., Becher, B., Waisman, A., Rülicke, T., et al. (2017). Lymphatic endothelial cells control initiation of lymph node organogenesis. Immunity *47*, 80–92.e4.

Pfeiffer, F., Kumar, V., Butz, S., Vestweber, D., Imhof, B.A., Stein, J.V., and Engelhardt, B. (2008). Distinct molecular composition of blood and lymphatic vascular endothelial cell junctions establishes specific functional barriers within the peripheral lymph node. Eur. J. Immunol. *38*, 2142–2155.

Phan, T.G., Grigorova, I., Okada, T., and Cyster, J.G. (2007). Subcapsular encounter and complement-dependent transport of immune complexes by lymph node B cells. Nat. Immunol. *8*, 992–1000.

Phan, T.G., Green, J.A., Gray, E.E., Xu, Y., and Cyster, J.G. (2009). Immune complex relay by subcapsular sinus macrophages and noncognate B cells drives antibody affinity maturation. Nat. Immunol. *10*, 786–793.

Pitulescu, M.E., Schmidt, I., Benedito, R., and Adams, R.H. (2010). Inducible gene targeting in the neonatal vasculature and analysis of retinal angiogenesis in mice. Nat. Protoc. *5*, 1518–1534.

Pucci, F., Garris, C., Lai, C.P., Newton, A., Pfirschke, C., Engblom, C., Alvarez, D., Sprachman, M., Evavold, C., Magnuson, A., et al. (2016). SCS macrophages suppress melanoma by restricting tumor-derived vesicle-B cell interactions. Science *352*, 242–246.

Remouchamps, C., Boutaffala, L., Ganeff, C., and Dejardin, E. (2011). Biology and signal transduction pathways of the Lymphotoxin-αβ/LTβR system. Cytokine Growth Factor Rev. *22*, 301–310.

Rios, D., Wood, M.B., Li, J., Chassaing, B., Gewirtz, A.T., and Williams, I.R. (2016). Antigen sampling by intestinal M cells is the principal pathway initiating mucosal IgA production to commensal enteric bacteria. Mucosal Immunol. *9*, 907–916.

Rodda, L.B., Lu, E., Bennett, M.L., Sokol, C.L., Wang, X., Luther, S.A., Barres, B.A., Luster, A.D., Ye, C.J., and Cyster, J.G. (2018). Single-Cell RNA sequencing of lymph node stromal cells reveals niche-associated heterogeneity. Immunity *48*, 1014–1028.e6.

Sagoo, P., Garcia, Z., Breart, B., Lemaître, F., Michonneau, D., Albert, M.L., Levy, Y., and Bousso, P. (2016). In vivo imaging of inflammasome activation reveals a subcapsular macrophage burst response that mobilizes innate and adaptive immunity. Nat. Med. *22*, 64–71.

Scott, C.L., T'Jonck, W., Martens, L., Todorov, H., Sichien, D., Soen, B., Bonnardel, J., De Prijck, S., Vandamme, N., Cannoodt, R., et al. (2018). The transcription factor ZEB2 is required to maintain the tissue-specific identities of macrophages. Immunity *49*, 312–325.e5.

Sugiyama, M., Nakato, G., Jinnohara, T., Akiba, H., Okumura, K., Ohno, H., and Yoshida, H. (2012). Expression pattern changes and function of RANKL during mouse lymph node microarchitecture development. Int. Immunol. *24*, 369–378.

T'Jonck, W., Guilliams, M., and Bonnardel, J. (2018). Niche signals and transcription factors involved in tissue-resident macrophage development. Cell. Immunol. *330*, 43–53.

Takeuchi, A., Ozawa, M., Kanda, Y., Kozai, M., Ohigashi, I., Kurosawa, Y., Rahman, M.A., Kawamura, T., Shichida, Y., Umemoto, E., et al. (2018). A

distinct subset of fibroblastic stromal cells constitutes the cortex-medulla boundary subcompartment of the lymph node. Front. Immunol. *9*, 2196.

Ulvmar, M.H., Werth, K., Braun, A., Kelay, P., Hub, E., Eller, K., Chan, L., Lucas, B., Novitzky-Basso, I., Nakamura, K., et al. (2014). The atypical chemokine receptor CCRL1 shapes functional CCL21 gradients in lymph nodes. Nat. Immunol. *15*, 623–630.

van de Pavert, S.A., and Mebius, R.E. (2010). New insights into the development of lymphoid tissues. Nat. Rev. Immunol. *10*, 664–674.

Walsh, M.C., and Choi, Y. (2014). Biology of the RANKL-RANK-OPG System in immunity, bone, and beyond. Front. Immunol. *5*, 511.

Witmer-Pack, M.D., Hughes, D.A., Schuler, G., Lawson, L., McWilliam, A., Inaba, K., Steinman, R.M., and Gordon, S. (1993). Identification of macrophages and dendritic cells in the osteopetrotic (op/op) mouse. J. Cell Sci. *104*, 1021–1029.

Xiong, J., Onal, M., Jilka, R.L., Weinstein, R.S., Manolagas, S.C., and O'Brien, C.A. (2011). Matrix-embedded cells control osteoclast formation. Nat. Med. *17*, 1235–1241.

Zhang, Y., Roth, T.L., Gray, E.E., Chen, H., Rodda, L.B., Liang, Y., Ventura, P., Villeda, S., Crocker, P.R., and Cyster, J.G. (2016). Migratory and adhesive cues controlling innate-like lymphocyte surveillance of the pathogen-exposed surface of the lymph node. eLife *5*, e18156.

100

STAR★METHODS

KEY RESOURCES TABLE

REAGENT or RESOURCE	SOURCE	IDENTIFIER
Antibodies		
Syrian hamster anti-Mouse CLCA1 (10.1.1)	Andy Farr, University of Washington, Seattle, US	Furuya et al., 2010
Rat anti-Mouse MAdCAM-1 (MECA-367)	Santa Cruz Biotech eBioscience	Cat#sc-19604
Rat anti-Mouse RANKL (IK22-5)	Hideo Yagita, Juntendo University, Tokyo, Japan	Kamijo et al., 2006
Rat anti-Mouse CD45R / B220 (RA3-6B2)	BD	Cat#53092 Cat#553086
Rat anti-Mouse CD169 (3D6-112)	Biolegend	Cat#BLE142416 Cat#142406
Rat anti-Mouse SIGN-R1 (22D1)	BioXcell	Cat#BE0220
Rat anti-Mouse CD11b (M1/70)	BD Biolegend	Cat#13-0112-82 Cat#BLE101228
Armenian hamster anti-Mouse CD11c (HL3)	BD	Cat#558079
Rat anti-Mouse I-A/I-E (M5/114.15.2)	Biolegend	Cat#107622
Rat anti-Mouse F4/80 (BM8)	Biolegend	Cat#BLE123116
Armenian hamster anti-Mouse CD3e (145-2C11)	eBioscience	Cat#45-0031-82
Rat ant-Mouse GL7 (GL7)	BD	Cat#553666
Armenian hamster anti-Mouse CD95 (JO2)	BD	Cat#557653
Rat anti-Mouse CD138 (281.2)	BD	Cat#553714
Rat anti-Mouse CD45 (30F11)	Biolegend	Cat#103115
Rat anti-Mouse TER119 (TER-119)	eBioscience	Cat#47-5921-8
Rat anti-Mouse CD31 (390)	eBioscience	Cat#46-0311-82
Syrian hamster anti-Mouse gp38 Podoplanin (8.1.1)	eBioscience	Cat#53-5381-82
Rat anti-Mouse CD106 (429)	Biolegend	Cat#105718
Rat anti-Mouse CD19 (1D3)	BD	Cat#553786
Rat anti-Mouse CD45.1 (A20)	eBioscience	Cat#47-0453
Rat anti-Mouse CD45.2 (104)	BD	Cat#558702
Rat anti-Mouse CD4 (RM4-5)	ThermoFisher	Cat#48-0042-82
Rat anti-Mouse LYVE-1 (ALY7)	ThermoFisher	Cat#53-0443-82
Mouse anti- αSMA (1A4)	Sigma-Aldrich	C6168
Rat anti-Mouse Gr-1 (RB6-8C5)	BD	Cat#553128
Rat anti-Mouse Ly6G (1A8)	BD	Cat#551461
Rat anti-Mouse CD64 (X54-5/7.1)	Biolegend	Cat#139305
Rat anti-Mouse SiglecF (E50-2440)	BD	Cat#562068
Anti-Mouse CLEC4F	R&D	Cat#AF2784
Rat anti-Mouse TIM-4 (RMT4-54)	eBioscience	Cat#46-5866-80
Mouse anti VSV-glycoprotein, AF488 (Vi10)	Philippe Lang, Univ of Düsseldorf, Germany	Honke et al., 2011
Goat anti-Syrian Hamster (Polyclonal)	Thermo Fisher	Cat#A21110 RRID: AB_2535759
Donkey anti-Rat (Polyclonal)	Jackson	Cat#712-166-153; RRID: AB_2340669
Donkey anti-Goat (Polyclonal)	Jackson	Cat#705.116.147
Rabbit anti-Phycoerythrin (PE)	Rockland	Cat#100-4199

REAGENT or RESOURCE	SOURCE	IDENTIFIER
Bacterial and Virus Strains		
Modified Vaccinia Ankara (MVA)	Transgene, Inc.	MVATGN33.1
Vesicular stomatitis virus (VSV, Indiana serotype)	S. Pfeffer, University of Strasbourg, France	N/A
Biological Samples		
Normal Goat Serum (NGS)	Invitrogen	10000C
Normal Rat Serum (NRS)	Own production	N/A
Fetal Bovine Serum (FBS)	BioWhittaker™	DE14-801F
Chemicals, Peptides, and Recombinant Proteins		
Streptavidin conjugates	Molecular probes	532357
Streptavidin PE-CF594	BD Horizon	Cat#562318
Depleting anti-CD45 microbeads	Miltenyi Biotech	Cat#130-052-301
Depleting anti-Ter119 microbeads	Miltenyi Biotech	Cat#130-049-901
FcR Blocking Reagent mouse	Miltenyi Biotec	Cat#130-104-443
mLTbR-Fc	Biogen, Inc	N/A
mTNFR2-Fc	Amgen, Inc	Etanercept
Phycoerythrin (PE)	ThermoFisher	Cat#P801
OCT Embedding Matrix	Cell Path™	Cat#KMA-0100-00A
Collagenase D	ROCHE, Sigma-Aldrich	Cat#11088866001
Dispase II	ROCHE, Sigma-Aldrich	Cat#04942078001
Dnase I	ROCHE, Sigma-Aldrich	Cat#10104159001
(Ethylenedinitrilo)tetraacetic acid (EDTA)	Sigma-Aldrich	Cat#E5134-500G
Liberase	ROCHE, Sigma-Aldrich	Cat#05401119001
Tamoxifen	Sigma Aldrich	Cat#T5648-1G
Corn oil	Sigma Aldrich	Car#C8267-500
4',6-Diamidine-2'-phenylindole dihydrochloride (DAPI)	ROCHE, Sigma-Aldrich	Cat#10236276001
7-Aminoactinomycine D (7-AAD)	BD PharMingen	Cat#559925
Fluoromount-G™	Invitrogen™	Cat#00-4958-02
Class C CpG oligonucleotide (ODN 2395)	InvivoGen	Cat#tlrl-2395
Paraformaldehyde	Sigma-Aldrich	Cat#0571709
Acetone	vwr Chemicals	Cat#20066.296
Agarose	Sigma-Aldrich	Cat#A6877
GelRed	BIOTUM	Cat#41003
Critical Commercial Assays		
DNA isolation kit	Machery-Nagel	Cat#740984
DNA-genotyping kit	Sigma Aldrich	Cat#R4775
RNA isolation kit	QIAGEN	Cat#74034
RNA isolation kit	Machery-Nagel	Cat#740990
cDNA synthesis Kit	Takara	Cat#634894
cDNA synthesis Kit	Promega	Cat#A3800
cDNA synthesis Kit	Thermo Fisher	Cat#10282650
qPCR kit	Thermo Fisher	Cat#13233189
Deposited Data		
Raw and analyzed data	Gene Expression Omnibus	GEO: GSE129315
Experimental Models: Organisms/Strains		
Mouse: C57BL/6N	Charles River (France)	N/A
Mouse: C57BL/6N-Tg(Ccl19-Cre)489Biat (*Ccl19-Cre*)	Burkhard Ludwig, St Gallen	N/A
Mouse: B6;129-Tnfsf11tm1.1Caob/J (*Rank*flox)	Jackson Laboratories	Stock No. 018978

102

Continued

REAGENT or RESOURCE	SOURCE	IDENTIFIER
Mouse: C57BL/6N-Tg(*Prox1-Cre*^ERT2)	Taija Makinen, Univ. Uppsala	N/A
Mouse: C57BL/6N.Cg-Tnfrsf11a^tm1.1Irw/J (*Rank*^flox)	Jackson Laboratories	Stock No. 027495
Mouse: C57BL/6-Siglec1tm1(cre)Mtaka (*Cd169-Cre*)	RIKEN BioResource Center	Stock No. 06239
Mouse: B6.129P2-Lyz2tm1(cre)Ifo/J	Jackson Laboratories	Stock No. 004781
Mouse: B6.Cg-Tg(Itgax-cre)1-1Reiz/J	Jackson Laboratories	Stock No. 008068
Mouse: CD45.1 (B6-Ly5.1)	European Mouse Mutant Archive	Stock No. 00039
Mouse: B6;129S6-Gt(ROSA)26Sor^tm9(CAG-tdTomato)Hze/J	Jackson Laboratories	Stock No. 007905
Oligonucleotides		
Primer for RT-qPCR (*Rankl*), Forward: CAGCCATTTGCACACCTCAC	This paper	N/A
Primer for RT-qPCR (*Rankl*), Reverse: GTCTGTAGGTACGCTTCCCG	This paper	N/A
Primer for RT-qPCR (*Actin-β*), Forward: CACTGTCGAGTCGCGTCCA	This paper	N/A
Primer for RT-qPCR (*Actin-β*), Reverse: CATCCATGGCGAACTGGTGG	This paper	N/A
Primer for RT-qPCR (*Gapdh*), Forward: GGTGTGAACGGATTTGGCCGTATTG	This paper	N/A
Primer for RT-qPCR (*Gapdh*), Reverse: CCGTTGAATTTGCCGTGAGTGGAGT	This paper	N/A
Primer for RT-qPCR (*Rank*), Forward: TGCGTGCTGCTCGTTCCA	This paper	N/A
Primer for RT-qPCR (*Rank*), Reverse: ACCGTCCGAGATGCTCATAAT	This paper	N/A
Primer for RT-qPCR (*Madcam-1*), Forward: GACCCATAGAAAGGAGATTCCAGTA	This paper	N/A
Primer for RT-qPCR (*Madcam-1*), Reverse: TGAGCCCAGTGGAGACTGC	This paper	N/A
Primer for RT-qPCR (*Itga2b*), Forward: ATTCCTGTTTAGGACGTTTGGG	This paper	N/A
Primer for RT-qPCR (*Itga2b*), Reverse: TCTTGACTTGCGTTTAGGGC	This paper	N/A
Primer for RT-qPCR (*Ccl20*), Forward: AATCTGTGTGCGCTGATCCA	This paper	N/A
Primer for RT-qPCR (*Ccl20*), Reverse: CCTTGGGCTGTGTCCAATTC	This paper	N/A
Primer for RT-qPCR (*Ackr4*), Forward: TGG ATC CAA GAT AAA GGC GGG GTG T	This paper	N/A
Primer for RT-qPCR (*Ackr4*), Reverse: TGA CTG GTT CAG CTC CAG AGC CAT G	This paper	N/A
Primer for genotyping (*Ccl19-cre*), Forward: TCTCTGCCCAGAGTCATCCT	This paper	N/A
Primer for genotyping (*Ccl19-cre*), Reverse: ATGCTCCTGTCTGTGTGCAG	This paper	N/A
Primer for genotyping (*Prox1-cre*), Forward: TTCCCGCAGAACCTGAAGATGTTCG	This paper	N/A
Primer for genotyping (*Prox1-cre*), Reverse: GCAAGATTACGTATATCCTGGCAGC	This paper	N/A
Primer for genotyping (*Cd169-cre*), Forward: GCTTACGGTGCTTGCTGGAT	This paper	N/A
Primer for genotyping (*Cd169-cre*), Reverse1: CATAGTCTAGGCTTCTGTGC	This paper	N/A

Continued

REAGENT or RESOURCE	SOURCE	IDENTIFIER
Primer for genotyping (*Cd169-cre*), Reverse2: AGGGACACAGCATTGGAGTC	This paper	N/A
Primer for genotyping (*Rankl flox*), Forward: CTGGGAGCGCAGGTTAAATA	This paper	N/A
Primer for genotyping (*Rankl flox*), Reverse: GCCAATAATTAAAATACTGCAGGAAA	This paper	N/A
Primer for genotyping (*Rank flox*), Forward: TGTCCCACTGACACAGGAGA	This paper	N/A
Primer for genotyping (*Rank flox*), Reverse: AGCTCACAACGCACAAAACA	This paper	N/A
Software and Algorithms		
Gallios Acquisition Software, FACS Gallios	Beckman Coulter	https://www.beckman.fr/flowcytometry/cytometrie-enflux/gallios/b43618
BD FACS Diva Software	BD Biosciences	BD FACSDiva Version 8.0
FlowJo versions 7 and 10	TreeStar, Ashland, Oregon	https://www.flowjo.com
U:Genius 3	Syngene	https://syngene.com
GraphPad Prism 5	Graphpad Software, Inc.	https://www.graphpad.com/demos/
Metamorph	Molecular Devices LLC	http://www.moleculardevices.com/
Zeiss ZEN 2010	Carl Zeiss	http://www.zeiss.com
imageJ	NIH, Bethesda, Maryland	https://imagej.net/Welcome
Imaris (versions 7 and 8)	Bitplane	https://www.Bitplane.com
RStudio (ggplot2 package)		https://www.Rstudio.com
Metascape tool		https://www.metascape.org
Illustrator CS5.1	Adobe	https://www.adobe.com

CONTACT FOR REQUESTS AND RESOURCE SHARING

Further information and requests for resources and reagents should be directed to and will be fulfilled by the Lead Contact, Christopher Mueller (c.mueller@ibmc-cnrs.unistra.fr).

EXPERIMENTAL MODEL AND SUBJECT DETAILS

Mice

C57BL/6J (Charles River Laboratories, France), *Ccl19*-cre (Chai et al., 2013), *Cd169-cre* (Karasawa et al., 2015), *Prox1-cre*[ERT2] (Bazigou et al., 2011), *Rankl*^{fl/fl} (Xiong et al., 2011), *Rank*^{fl/fl} (Rios et al., 2016), *CAG-tdTomato* and CD45.1 (Jackson Laboratories) mice were kept in specific pathogen-free conditions. Virus infections were carried out in A3 confined conditions with individual, filtered cages. Female and male mice were analyzed at adult age (7–14 weeks), unless specified, and age-matched littermates were used as controls. All transgenic or knock-in Cre mice as well as the dtTomato reporter mouse were used in heterozygous state. Tamoxifen (1 mg) was delivered to pregnant females by oral gavage at E11.5, E12.5, and at E18.5. Newborns were treated by intra-gastric injection of 50 μg at P1 and 100 μg from P2 to P4 (Pitulescu et al., 2010). Two-week old mice were gavaged with 0.5 mg tamoxifen/day on the first 2 days, and then a single 1 mg tamoxifen dose was delivered by gavage every 2 weeks. Adults (4 weeks onward) were gavaged with 1 mg/day on the first 2 days and then a single 1 mg tamoxifen dose every 2 weeks. All experiments were carried out in conformity to the animal bioethics legislation approved by and according to national guidelines of the CREMEAS (Comité Régional d'Ethique en Matière d'Expérimentation Animale de Strasbourg) and the RCAI and Tokyo University of Pharmacy and Life Sciences animal use committee.

104

METHOD DETAILS

Immunizations and reagent administration

Passive immunization with PE-immune complexes and PE uptake were performed as described (Phan et al., 2009). In brief, mice were injected i.p. with 2 mg of rabbit IgG anti-PE (Rockland) 12-16 h before i.fp. administration of 10 μg PE (Thermo Fisher). Mice were sacrificed 8 h later. For VSV infection, mice received an i.fp. injection of 10^6 pfu of VSV (serotype Indiana), and 6h later the popliteal LNs were taken and imaged for VSV replication using the anti-VSV-glycoprotein antibody Vi10 (Honke et al., 2011). Mice received an i.fp. administration of 10^4 pfu of MVA virus, and 7 days later the popliteal LNs were taken. Mice were injected i.fp. with 10 μg of CpG (ODN 2395, InvivoGen). To inhibit RANK, LTbR and TNFR signaling, adult C57BL/6 mice received i.p. injections of 20 μg of IK22-5, LTbR fused to murine IgG1 Fc or TNFR2-Fc (Etanercept) 3 times a week for 3 weeks.

Partial irradiation and adoptive transfer

Mice were anesthetized with a solution of ketamine and medetomidine and a 7 mm lead bridge placed over the upper back and head to shield the brachial LNs. The mice were then irradiated at a dose of 9.5 Gy from an X-ray source and reconstituted with 10^7 bone marrow cells of Ly5.1/CD45.1 mice. After 4 weeks the blood chimerism and brachial LNs were analyzed.

Immunofluorescence of adult LN

LNs were freshly harvested from mice and embedded in OCT embedding matrix (Cell Path), or for tdTomato analysis pre-fixed in 4% PFA/PBS, and frozen in liquid nitrogen. Organs were cut into sections using the cryostat (Leica CM3050 S) and fixed in cold acetone for 20 min before freezing at $-80°C$. Sections were blocked with PBS containing 2% normal goat serum or 2% fetal bovine serum. For cell staining, antibodies and reagents were used (see key resource table) and DAPI (Sigma-Aldrich) was used to stain nuclei. Sections were mounted with Fluoromount-G (Invitrogen, Thermo Fisher Scientific). Images were acquired on a Microscope Zeiss Axio Observer Z1 Confocal LSM780 and LSM710 (Carl Zeiss) with the Carl Zeiss proprietary software Zen and on a spinning disk inverted microscope (Carl Zeiss) with a confocal head Yokogawa CSU and a Metamorph software (Metamorph). For *Cd169*-directed tdTomato expression analysis, sections were imaged using a Keyence BZ-X700 microscope. Analysis of all microscopic images was done using the open source imageJ-based Fiji distribution.

Immunofluorescence of embryonic LN anlagen

For histological analysis, embryos were fixed in 4% paraformaldehyde, dorsal and abdominal skin was removed together with the fat pad and directly used for immunofluorescence staining or for cryo-sectioning. Inguinal LN anlagen were identified by the bifurcation of major blood vessels in the inguinal fat pad. Whole mount or sections of LN anlagen were stained with mouse anti-mouse alpha smooth muscle actin-Cy3 (Sigma Aldrich), rat anti-mouse CD11b-A488 (Invitrogen, Thermo Fisher Scientific), rat anti-mouse CD169-A488, rat anti-mouse CD4-Pacific Blue and rat anti-mouse LYVE-1-A660 (Invitrogen, Thermo Fisher Scientific). Histomorphometric analysis, such as isosurface rendering and quantification of microscopic images was done using the open source imageJ-based Fiji software and Imaris, version 9 (Bitplane).

Isolation and analysis of LN cells

For stromal cells and macrophages, the LNs, cut into small pieces, were digested with an enzyme mix prepared in RPMI 1640 GIBCO®, 2% fetal bovine serum, and 1 mg/mL collagenase D (Roche), 0.1 mg/mL DNase I (Roche), and 1 mg/mL Dispase II (Roche) at 37°C for 1 hour under agitation. Cells were gently homogenized by pipetting and the digestion stopped with EDTA. The cell suspension was filtered through a 100 μm cell strainer. For stromal cell analysis and sorting, skin-draining LNs (inguinal, axillary, brachial, cervical, auricular, and popliteal) were pooled. Red blood cells were lysed in ammonium-chloride-potassium buffer (NH_4CL 0.15 M, $KHCO_3$ 1 mM, and EDTA 0.1 mM) for 1 min and the cells were washed. $CD45^+$ and $Ter119^+$ cells were depleted using microbeads (MACS Miltenyi Biotec) and also out-gated into a dump channel. Lymphocytes were isolated by crushing the LNs in PBS with a glass pestle and mortar followed by filtering the cells through a 40 μm cell strainer (Becton Dickinson Biosciences).

Flow cytometry and immunofluorescence

Flow cytometry was performed on a Gallios (Beckman-Coulter) and analyzed with FlowJo software (Treestar). Cell sorting was performed on an ARIA (Becton Dickinson Biosciences). Binding to Fc receptor was blocked with FcR Blocking Reagent (Miltenyi Biotec) and 5% rat serum. DAPI or 7-AAD was used for exclusion of dead cells. Stromal cells were identified as live $CD45^-Ter119^-gp38^+$ cells and MRCs as VCAM-1^+ MAdCAM-1^+ among them. For macrophages, following antibodies were used: CD11b (M1/70), CD11c (HL3), I-A/I-E (M5/114.15.2), CD169 (3D6-112), F4/80 (BM8) and CD45.1 (A20). Lymphocytes were stained for CD45R/B220 (RA3-6B2), CD3e (145-2C11), GL7 (GL7), CD95 (JO2), CD138 (281.2).

PCR

RNA was extracted using the RNeasy Mini or Micro kit (QIAGEN) or NuceloSpin RNA Plus XS kit (Macherey-Nagel), and cDNA was synthesized with Maxima First Strand cDNA Synthesis Kit (Thermo Scientific) or Improm-II (Promega) using oligo(dT)15 primers. RT-PCR was performed using Luminaris color HiGreen qPCR Master Mix (Thermo Scientific). Quantitative RT-PCR was run on a Bio-Rad CFX96 thermal cycler, and threshold values (Ct) of the target genes "X" were normalized to housekeeping gene *β-actin*

or *Gapdh* using the formula $\Delta Ct = Ct_X - Ct_{HKG}$. The relative quantification was expressed as $2^{-\Delta Ct}$. Genomic DNA was recovered from gDNA Removal Column XS of NuceloSpin RNA Plus XS kit (Macherey-Nagel) by washing with ethanol (70%) and elution with a small volume of DNAase-free water. PCR with the specific primers (see key resource table) was run on a Bio-Rad Thermal cycler C1000^{TM}. PCR products were separated in agarose containing fluorescent nucleic acid dye (GelRed, Biotum). Photographic images were taken using U:Genius 3 (Syngene, Ozyme).

RNA sequencing and data processing

LEC mRNA profiles of 8 week old littermate (*Rankl^fl/fl*) and conditional RANKL-deficient (*Ccl19-cre Rankl^fl/fl*) mice were generated by deep sequencing. LECs were sorted from LNs by flow cytometry on the basis of CD45$^-$TER119$^-$CD31$^+$ podoplanin/gp38$^+$ cells and RNA was harvested using QIAGEN RNA isolation kit. cDNA was generated using the Takara SMART-Seqv4 Ultra Low Input RNA Kit and the library sequenced on Illumina Hiseq 4000 sequencer following Illumina's instructions. Quantification of gene expression was performed HTSeq v0.6.1 (Anders et al., 2015) using gene annotations from Ensembl release 81. Read counts were normalized across libraries (Anders et al., 2015), and low-abundance genes on the basis of the mean reads $\leq$ 1000- and highly variable genes SD $\geq$ 1 were removed. Comparisons were performed using the method previously described (Love et al., 2014). Resulting p values were adjusted for multiple testing using the Benjamini and Hochberg method (Benjamini and Hochberg, 1995). Analysis was restricted to genes showing a p value < 0.05 and a 1.5-fold change difference between LECs sorted from *Ccl19-cre Rankl^fl/fl* and control mice. Plots have been generated using RStudio interface (ggplot2 package). Pathway analysis was performed using Metascape tool (http://metascape.org) on genes with reduced expression in *Ccl19-cre Rankl^fl/fl* mice compared to control. For each selected pathway, the top 30 genes were displayed with their associated Log2 fold change value.

QUANTIFICATION AND STATISTICAL ANALYSIS

Statistical analyses, as described in figure legends, were performed with Prism 5.0 (Graphpad Software Inc.). Data were analyzed with the Mann Whitney test, the non-paired Student's t test or one-way ANOVA (with Bonferroni correction). A p value of < 0.05 was considered as significant, *p < 0.05, **p < 0.01, ***p < 0.001, ****p < 0.0001.

DATA AND SOFTWARE AVAILABILITY

The RNA-sequencing data have been deposited in the Gene Expression Omnibus public database under accession number GEO: GSE129315.

106

Supplemental Information

Lymph Node Mesenchymal and Endothelial Stromal

Cells Cooperate via the RANK-RANKL Cytokine Axis

to Shape the Sinusoidal Macrophage Niche

Abdouramane Camara, Olga G. Cordeiro, Farouk Alloush, Janina Sponsel, Mélanie Chypre, Lucas Onder, Kenichi Asano, Masato Tanaka, Hideo Yagita, Burkhard Ludewig, Vincent Flacher, and Christopher G. Mueller

Supplemental Figure 1
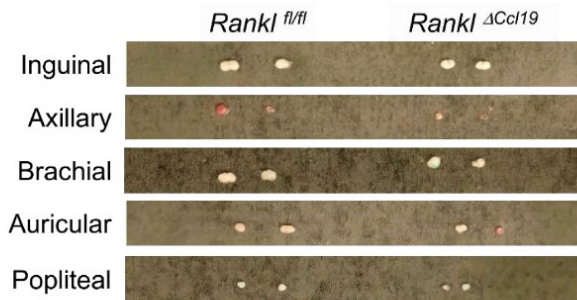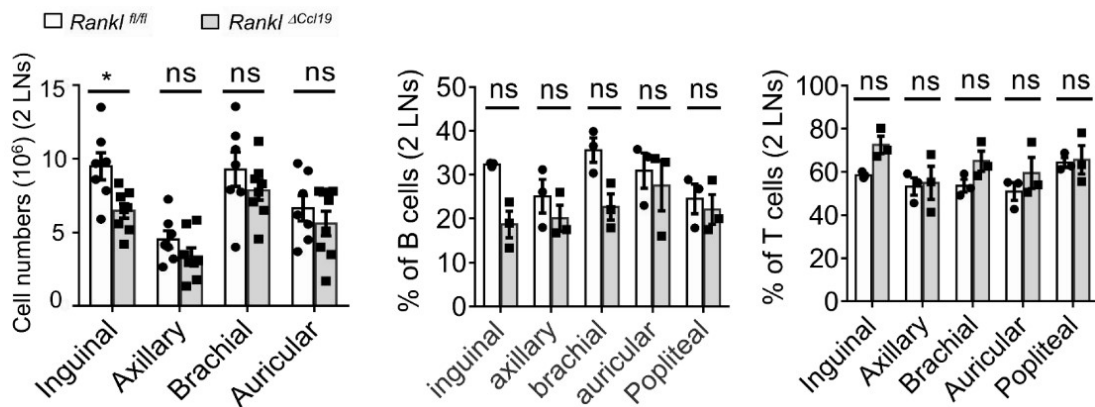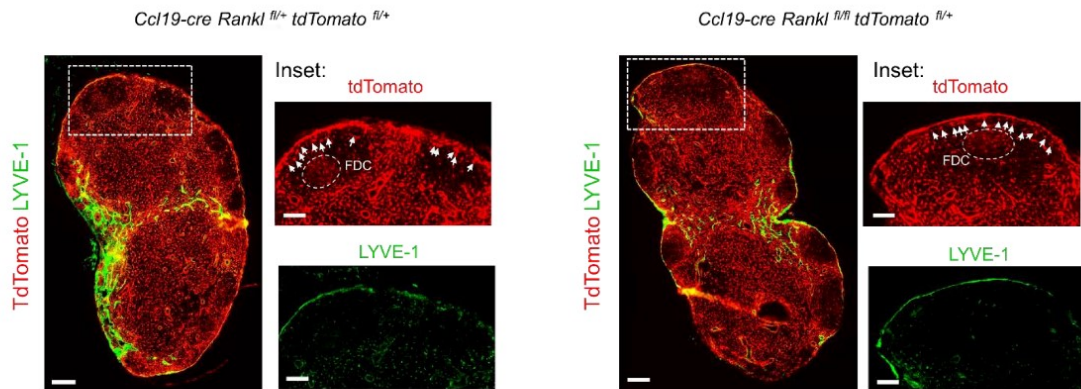
Supplemental Figure S1, relates to Figure 1. Cellular characterization of the *Ccl19-cre Rankl^{fl/fl}* mice.
(**A**) Photographic images of the different LNs from the *Ccl19-cre Rankl^{fl/fl}* (*Rankl^{ΔCcl19}*) and the *Rankl^{fl/fl}* control mice. (**B**) The cell numbers of the different LNs were determined for *Rankl^{ΔCcl19}* and *Rankl^{fl/fl}* mice. The data are shown as the mean ± SEM with individual data points. The proportions of CD3^+ T cells and B220^+ B cells were assessed by flow cytometry in the different LNs of *Rankl^{ΔCcl19}* and *Rankl^{fl/fl}* mice. The data are shown as the mean ± SEM obtained from three different mice. Statistical significance (Mann-Whitney): *=p<0.05, ns=not significant. (**C**) Immunofluorescence visualization for tdTomato and LYVE-1 in LNs of mice with the indicated genotype. The insets show B cell follicles with the different fluorochrome filters individually. Arrows point to MRCs, and the follicular dendritic cell (FDC) network is indicated. Scale bars are 200 µm and for the insets 100 µm.

Supplemental Figure 2

A Sinusoidal macrophages / LECs

B Rank fl/fl, Itgax-cre Rank fl/fl

C *Cd169-cre tdTomato fl/+*

D Rank fl/fl / Rank ΔCd169 — Other macrophages (cell number 10³); F4/80+ CD169- Ms, F4/80- CD169- Ms; ns

E DC subsets (cell number 10³); Tissue-derived DCs, LN resident DCs; ns

F Lymphocyte populations (cell number 10⁶); B cells, T cells; ns

G Rank fl/+, Cd169-cre Rank fl/+, C57BL/6
Floxed allele (1+2: 469bp)
Deleted allele (1+3: 392bp)
WT allele (1+2: 290bp)
WT (+), Floxed, Deleted

Supplemental Figure S2, relates to Figure 4. Assessment of LN cell populations in *Cd169-cre Rank^fl/fl* mice and *Rank^fl/fl* mice, as well as *Rank*-gene expression and recombination in the SM subsets.

(**A**) Quantitative RT-PCR for *Rank* normalized to *Gapdh* in SSMs and MSMs sorted from C57BL/6 mice (left) and in LECs isolated from *Prox1-cre^ERT2 Rank^fl/fl* or control mice (right). Each data point is the mean of triplicates from 2-3 different experiments and the bars correspond to the mean ± SEM of the three data points. (**B**) Flow cytometry profiles of CD169$^+$ F4/80$^-$ SSMs and CD169$^+$ F4/80$^+$ MSMs among live CD11b$^+$ CD11c^{low} cells of LN from *Rank^fl/fl* control or *Itgax-cre Rank^fl/fl* mice. The gating and the relative cell numbers are shown. The graphs depict the mean (± SEM) relative cell numbers of SSMs and MSMs in *Rank^fl/fl* control, *Lys2-cre Rank^fl/fl* and *Itgax-cre Rank^fl/fl* mice with individual data points. Immunofluorescence show CD169 expression in inguinal LNs of the mice with the indicated genotype. Scale bars are 300 μm and for insets 50 μm. (**C**) An inguinal LN of *Cd169-cre tdTomato* mice was imaged for expression of the red fluorescence reporter protein. Insets show the subcapsular sinus (a) and the medullary regions (b,c). Scale bars represent 200 μm and for insets 50 μm. (**D-F**) Different macrophage and dendritic cell populations were identified using the flow cytometry strategy shown in Figure 2. The numbers of (**D**) F4/80$^+$ CD169$^-$ and F4/80$^-$ CD169$^-$ macrophages (Ms), as well as (**E**) tissue-derived and LN-resident DCs were determined. (**F**) The numbers of CD3$^+$ T cells and B220$^+$ B cells were also obtained. The data are the mean ± SEM with individual data points of inguinal and brachial LNs. Statistical significance (Mann-Whitney): ns=not significant. (**G**) Verification of cre-mediated recombination of the *Rank* gene in MSMs and SSMs. The two cell types were flow cytometry-sorted from the mice with the indicated genotype and processed for genomic DNA PCR with primers 1+2 and 1+3 (Rios et al., 2016). Shown is a schematic illustration of primer position relative to the LoxP sites and exons (E) 2 and 3 in the WT, floxed and deleted alleles.

Supplemental Figure 3

A

Donor
Ly5A mouse
BM (CD45.1)

Lead shield

Recipient (CD45.2)
Rank fl/fl or *Rank* ΔCd169

4 weeks
BM chimera reconstitution

CD45.1/CD45.2
Chimerism (blood)

Brachial LNs

Rank fl/fl   *Rank* ΔCd169

B   Liver

C   Lungs

D   Spleen

ns
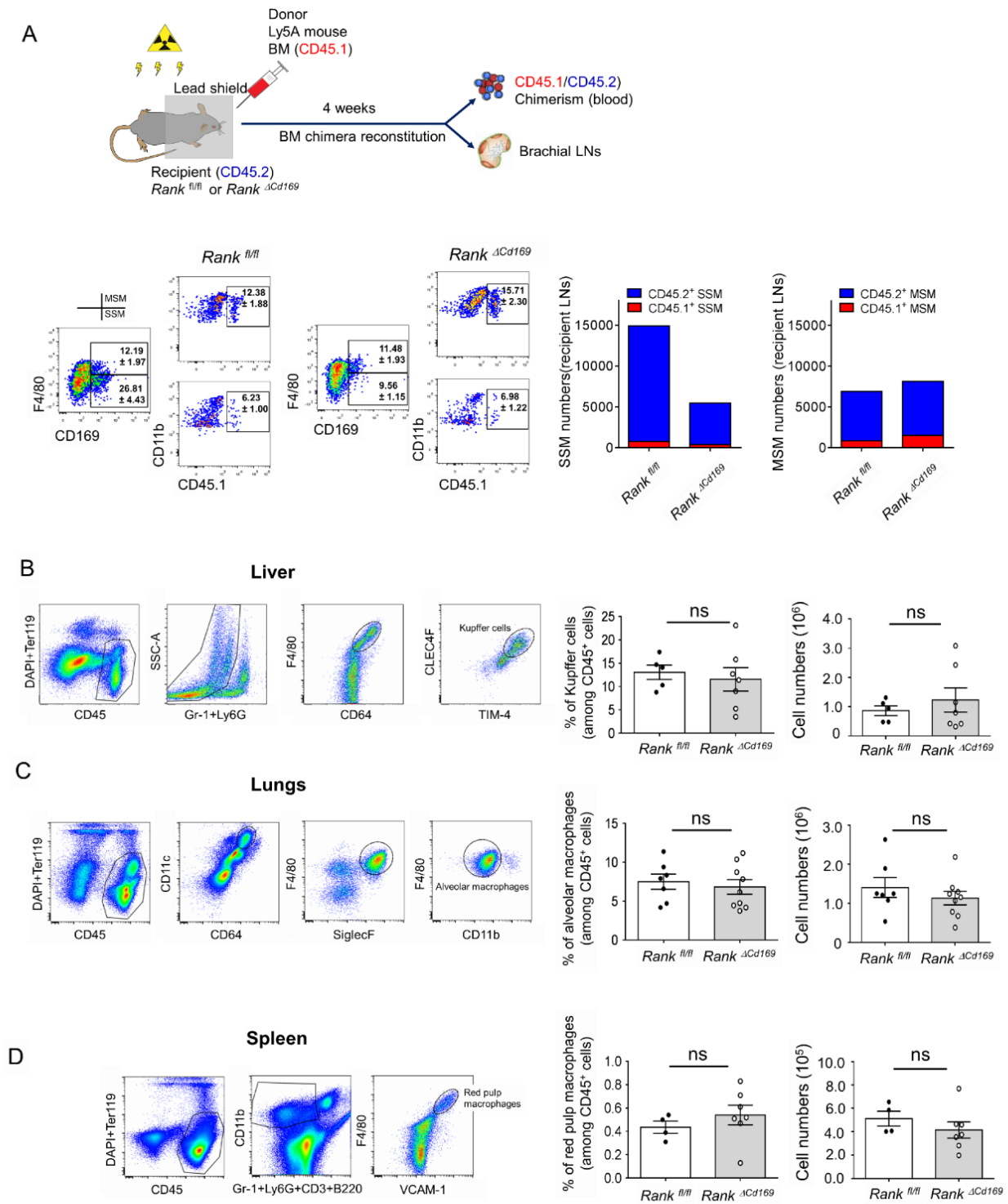
Supplemental Figure S3, relates to Figure 4. Measure of the SM turn-over rate and consequences of loss of RANK expression for macrophages of other tissues.

(**A**) Schematic illustration of the experimental set up. *Rank^{fl/fl}* control or *Cd169-cre Rank^{fl/fl}* (*Rank^{ΔCd169}*) CD45.2 mice were irradiated with the shoulder/head shielded. CD45.1 bone marrow cells were then adoptively transferred and 4 weeks later blood chimerism as well as proportion and number of CD45.1 (donor) /CD45.2 (recipient) SSMs and MSMs were determined in the brachial LNs of the irradiation-protected area. Below is shown the flow cytometry profile and the proportion $\pm$ SEM (n=4 control and n=6 mutant) of CD45.1$^+$ versus CD45.2$^+$ SSMs and MSMs. The graphs depict the mean numbers of CD45.1$^+$ versus CD45.2$^+$ SSMs and MSMs. (**B-D**) Flow cytometry strategy to identify (**B**) liver Kupffer cells, (**C**) alveolar and (**D**) splenic red pulp macrophages. Graphs (mean $\pm$ SEM with individual data points) show their relative and absolute numbers in *Rank^{fl/fl}* and *Rank^{ΔCd169}* mice. ns: statistical comparisons by Mann-Whitney tests did not demonstrate significant differences (p<0.05).

Supplemental Figure 4
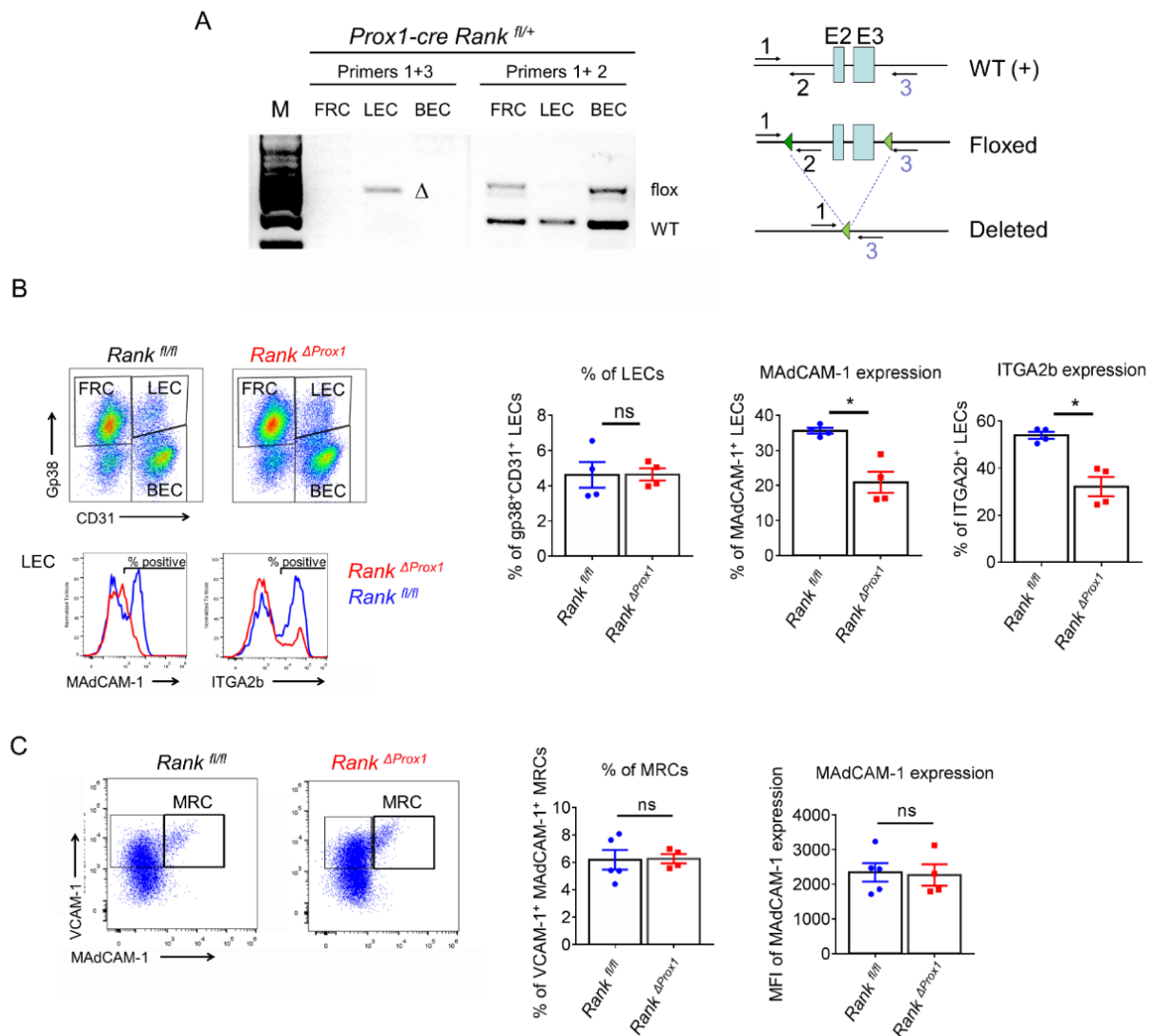
Supplemental Figure S4, relates to Figure 5. Characterization of LECs and MRCs in *Prox1-cre^ERT2^Rank^fl/fl^* and *Rank^fl/fl^* mice.

(**A**) Genomic PCR to verify the cre-recombinase-mediated deletion of *Rank* in LECs. Schematic illustration of primer position relative to the LoxP sites and exons (E) 2 and 3 in the WT, floxed and deleted alleles. (**B**) Expression of MAdCAM-1 and ITGA2b in LECs. Mice had received tamoxifen at 4 weeks of age and then every 2 weeks until the age of 12 weeks. Flow cytometry-based identification of gp38⁺ CD31⁺ LECs among the CD45⁻ TER119⁻ stromal cells and representative flow cytometry profiles of MAdCAM-1 and ITGA2b expression by LECs in *Prox1-cre^ERT2^;Rank^fl/fl^* (*Rank^ΔProx1^*) and *Rank^fl/fl^* control mice. The graphs show the proportion of gp38⁺ CD31⁺ LECs, of MAdCAM-1⁺ and of ITGA2b⁺ LECs in the control and the mutant mice. The data are the mean ± SEM of 4 mice with individual data points. (**C**) Representative flow cytometry profiles of MAdCAM-1⁺ VCAM-1⁺ MRCs gated from CD45⁻ TER119⁻ gp38⁺ CD31⁻ mesenchymal stromal cells. Graphs depict the proportion of MRCs among the gp38⁺ CD31⁻ cells and the mean fluorescence intensity of MAdCAM-1 expression by MRCs (data is the mean ± SEM (4-5 mice with individual data points)). Statistical significance (Mann-Whitney): *=p<0.05, ns=not significant.
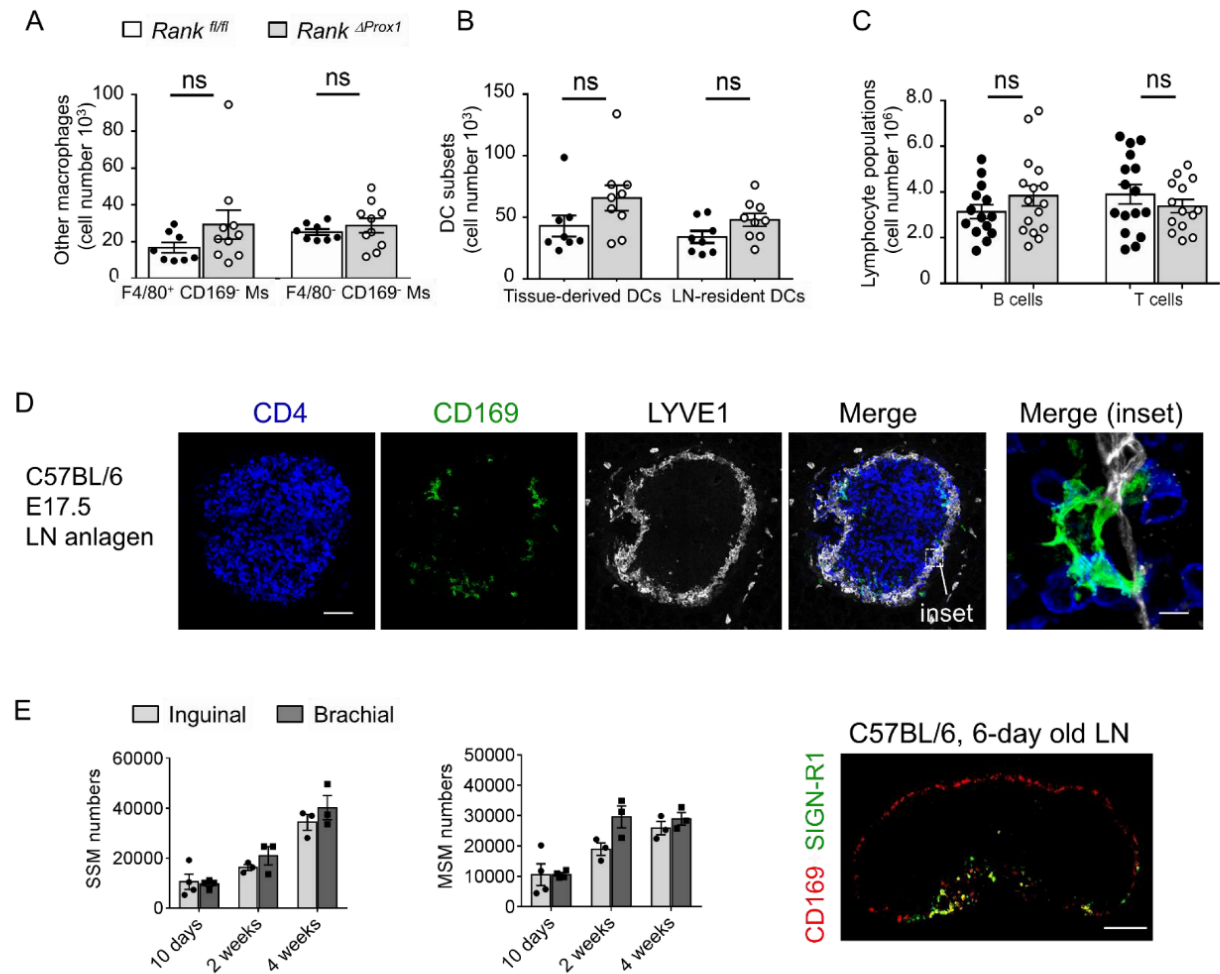
Supplemental Figure S5, relates to Figure 5. **Assessment of LN cell populations *Prox1-cre^{ERT2} Rank^{fl/fl}* (*Rank^{ΔProx1}*) and *Rank^{fl/fl}* mice.**

Rank^{fl/fl} control and *Prox1-cre^{ERT2} Rank^{fl/fl}* (*Rank^{ΔProx1}*) mice were treated with tamoxifen at the age of 2 weeks and the number of (**A**) F4/80^+ CD169^- and F4/80^- CD169^- macrophages (Ms), (**B**) tissue-derived and LN-resident DCs, as well as (**C**) B cells and T cells were determined. The data are shown as the mean ± SEM with individual data points of inguinal and brachial LNs. Statistical significance (Mann-Whitney): ns=not significant. (**D**) E17.5 inguinal LN anlagen of C57BL/6 mice were immunolabelled for CD4 (LTi cells), CD169 and LYVE-1 (LECs). The insert focuses on a CD169^+ macrophage closely associated with a LYVE-1^+ LEC. (**E**) The numbers of SSMs and MSMs were determined in inguinal and brachial LNs of C57BL/6 mice at different ages. The data are shown as the mean ± SEM with individual data points of 2 pooled LNs of each type. Immunofluorescence imaging of a brachial LNs from a 6-day old C57BL/6 mouse for CD169 and SIGN-R1 expression. The scale bar represents 200 μm.

Supplemental Figure 6
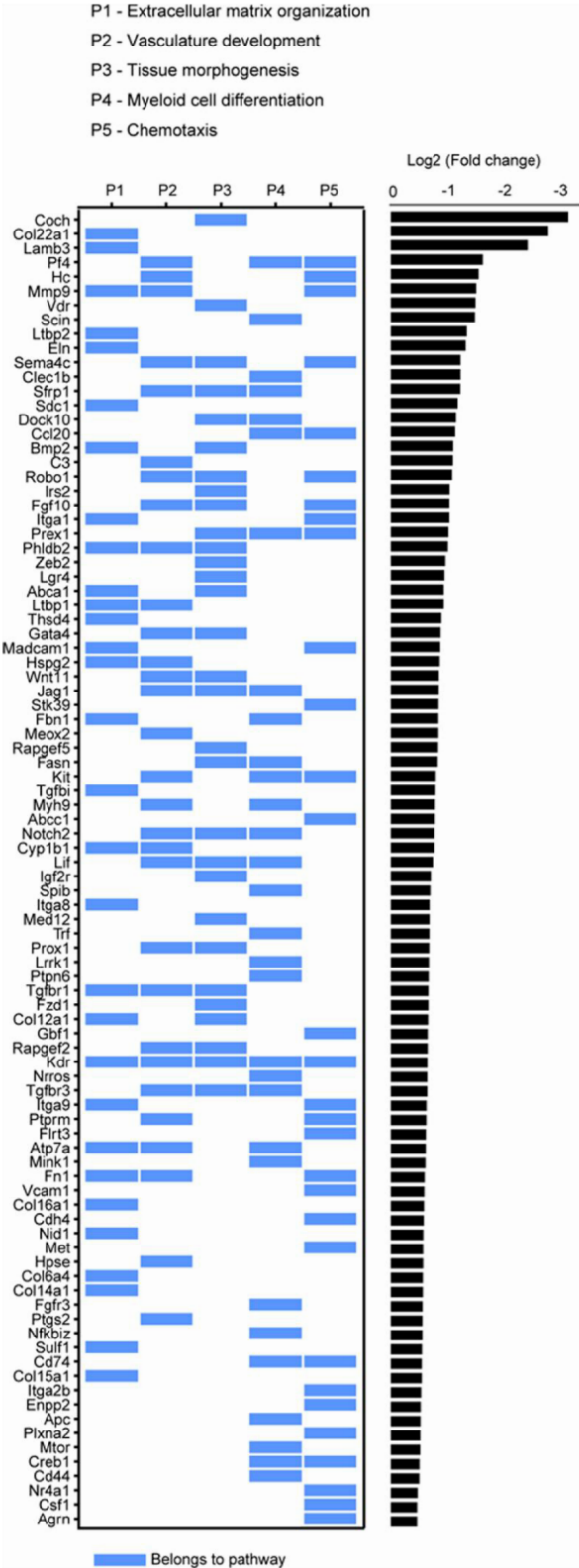
Supplemental Figure S6, relates to Figure 7. Assessment of RANK signaling pathways in LECs.

The plot depicts significant RANK signaling pathways, uncovered by pathway analysis of the RANK-regulated genes. The blue bars indicates the association of a gene to one of the five (P1-5) pathways. The fold change in the selected gene expression in LECs from LNs of *Ccl19-cre Rankl*^{fl/fl} relative to control mice is shown.

Chapter 6. General discussion and perspectives

1   General discussion and perspectives

The RANK-RANKL axis is involved in LN organogenesis, osteoclastogenesis, mammary gland and hair follicle formation as well as DC activation and function[1,2]. Osteoclasts are the bone resorbing macrophages that depend on both RANKL and the macrophage-colony stimulating factor 1 for their differentiation and function[3,4]. Stromal cells are the non-hematopoietic cells that support tissue parenchyma and contribute to its homeostasis and funtions[5]. In 2012, Mueller CG et al., have summarized the emerging role of the stromal cells in immune functions as introduction to a series of articles on immune stroma[6].

Tissue-resident macrophage differentiation depends on several factors such as the myeloid transcription factor (PU.1), the macrophage-inducing transcription factors (c-Maf and MafB), etc[7], that determine the macrophage lineage. They also depend on the tissue specific signals that shape their transcriptional programs[8]. However, the tissue-derived signals that specifically induce either one or another macrophage subtype are still subject to explorations.

We have shown that LN stromal RANKL is required for the differentiation of both the subcapsular and the medullary sinus macrophages (SSM and MSM). In mice lacking RANKL from LTOs/MRCs, the numbers of both macrophage subtypes are strongly decreased. Flow cytometry quantification of the proportion of MRCs in the adult knockout mice compared to their littermate controls revealed no alteration. By crossing *Ccl19-cre;Rankl* $^{fl/+}$ mice with *tdTomato* $^{fl/+}$ mice that enables tdTomato expression in CCL19$^+$ cells following deletion of one allele of *Rankl,* immunofluorescence visualization of LN sections revealed a normal positioning of MRCs (see paper supplementary figure S1). However, whether RANKL deletion induces an intrinsic change in the phenotype of these cells still requires proper analyses.

Unlike MSM, SSM needs constitutive and direct RANK activation to maintain its phenotype. These observations raised the hypothesis of an unknown mechanism through which, the stromal RANKL controls the fate of both macrophage subtypes. For instance, another RANKL sensitive cell that may participate in the process of SSM and MSM differentiation. In 2016, our laboratory has shown that LECs are sensitive to stromal RANKL stimulation. Indeed, in addition to the loss of SSMs and MSMs, stromal RANKL deletion leads to reduced expression of the integrin alpha 2b (ITGA2b/CD41) and the mucosal vascular addressin cell adhesion molecule 1 (MAdCAM-1), reported as the LEC activation markers[30].

We generated a tamoxifen-inducible cre recombinase mouse model that enables the temporal deletion of RANK from the LECs under the control of Prox1, the master regulator of the LEC lineage. When induced from four weeks after birth, LEC RANK deletion did not affect the phenotype nor the numbers of SSM and MSM. Thus, we reasoned that at four weeks, both macrophages have already completed their differentiation programs and occupied their niches of residence. In contribution is a low cell turn-over rate to explain why LEC RANK conditional deletion at that time does not notably affect the macrophages. This led us to investigate whether LEC RANK deletion earlier during the development affect the macrophages. In 2017, Onder et al., have shown that RANK-mediated signaling in LECs is required for LN organogenesis. Indeed, they observed that when *Prox1-cre^ERT2 Rank^{fl/fl}* mice were treated with tamoxifen at the embryonic days E11 and E12, they lack LNs after birth. On the other hand, when induced at E17, LEC RANK deletion did not significantly affect LN formation, suggesting that RANK-activated LECs are essential for LN initiation that occurs before E17. This study gave to us the knowledge to delete RANK from LEC as early as possible during the development without preventing LN formation in order to analyze the impact on macrophage differentiation. When induced from two weeks of age, LEC RANK deletion led to significant decrease of both SSM and MSM numbers. Finally, when induced at embryonic day E18.5, LEC RANK deletion results to an almost complete loss of both macrophages.

Some inflammatory stimuli and infections induce the disappearance of SSM and MSM probably by pyroptosis[9]. However, four weeks after disappearance, their respective niches are repopulated by macrophages displaying the same markers[10]. Thus, we sought to know whether LECs are required for the reconstitution of SSM and MSM populations after inflammation-induced cells loss. By injecting the bacterial DNA (CpG oligonucleotide) in the hind foot pad of mice, both macrophages in the draining LNs disappear by four days. When we induced LEC RANK deletion from 5 days after macrophage depletion, the numbers of SSM and MSM remain significantly lower in the knockout mice compared to the control littermates after four weeks, indicating a delay in the reconstitution of their populations. Thus, these results showed that the stromal RANKL-activated LECs control the differentiation of both SSM and MSM from the embryonic development to around four weeks after birth. Moreover, RANK-activated LECs are also required for the reconstitution of SSM and MSM populations after inflammation-induced cell loss. However, in inflammatory situation, we could not exclude the contributions other RANKL sources since this cytokine is expressed also by

activated T cells[11] as well as by type 3 innate lymphoid cells[12].

Although immunolabeling for specific markers (mCLCA1 and LYVE1) of LN-LECs revealed normal staining in tamoxifen-treated knockout mice, our study lacks deeper analysis of the impact on LEC network, that seems to be altered as noticeable in two weeks and embryonic day LEC RANK deletion experiments (see paper figure 5). A 3D pattern organization of LN-LEC network could be performed.

The fact that only SSM needs continuous stromal RANKL stimulation to maintain its phenotype although both macrophage subtypes depend on stromal RANKL for the early differentiation could be explained by the model that, before LN compartmentalization in early life, the cooperation between LTOs/MRCs and LECs shape the niches for SSM and MSM precursors to differentiate. As LN compartmentalization occurs and progresses, each cell completes its differentiation program while colonizing its residing niche. Thus, in adult LNs, SSMs reside in the microenvironment of MRCs and depend on the continuous RANKL stimulation whereas MSMs residing in the medulla do not or may require another mechanism for maintenance. The fact that both macrophages express RANK, could suggest that MSMs is sensitive to another RANKL source for other cellular purposes. In bone marrow transfer after irradiation experiments, we and others have shown that both macrophages have a low turn-over rate at steady state and bone marrow-derived monocytes contribute to their networks more importantly in inflammatory situations[13,14]. It has also been shown that SSMs self-renew by local proliferation at steady state and after transient depletion by inflammation of infection[14].

Now, the factor(s) through which RANKL-activated LECs control the differentiation as well as the reconstitution of SSMs and MSMs is open to conjecture. Because ablation of either stromal RANKL or LEC RANK results in the loss of ITGA2b/CD41 and MAdCAM-1, we reasoned that these cell adhesion molecules may be important for the attraction and or the retention of macrophage precursors to ensure their differentiation to SSM and MSM. In *Itga2b* $^{-/-}$ mice, both macrophages appear normal (data not shown). *In vivo* blockade of the integrin $\alpha_4\beta_7$ (the ligand for MAdCAM-1) from the first to the forth week after birth surprisingly results in an increase of the proportion of SSMs[Appendix1]. However, integrin $\alpha4\beta7$ neutralization also significantly increased the proportion of B cells whereas LN-derived DCs and T cells decreased as shown in another study[15]. This simultaneous increase of SSMs and B cells is consistent with

the findings that B cell-derived lymphotoxin is required for SSMs[16]. Moreover, it is conceivable that SSMs influence B cell development or recruitment by activating the stromal cells (LTO/MRCs) since MRCs are known as producers of B cell chemoattractant chemokine CXCL13. However, this strategy of *in vivo* blockade of MAdCAM-1 results in a broad effect on LN cellularity. To overcome this issue, a mouse model in which *Madcam1* is specifically deleted in LECs would be needed to properly check its contribution for sinusoidal macrophage differentiation. Otherwise, our RNA sequencing of LN-LECs sorted from stromal RANKL-deficient mice compared to their littermate controls confirms the loss of *Igta2b* and *MAdcam1* as well as other genes including *Ccl20*, the platelet factor 4 (*Pf4*), etc, in the knockout. A study has reported that the gut resident, RANKL-expressing mesenchymal cells activate the enterocytes to produce CCL20, the epithelium specific chemokine associated with follicles, important for B cell migration and IgA production. To check a possible role of CCL20, we stained LN sections of mice lacking CCR6, the ligand for CCL20. However, both macrophages appear unaffected in these mice[Appendix 2]. In the future works, the contributions of PF4 as well as other LEC-derived factors should be investigated in genetically modified mouse models. Of note, our study misses the information of how RANK signaling, triggered by the stromal RANKL, activates LECs to induce sinusoidal macrophage differentiation. This could be investigated by western bot analysis of activation of either NIK (non-canonical pathway) or IkB Kinases (canonical pathway) in LN-LECs sorted from wild type and stimulated with RANKL recombinant or in LN-LECs from stromal RANKL deficient and LEC RANK deficient mice.

In mice lacking RANK signaling in CD169^{+} cells, SSM acquire a MSM-like phenotype, replaced by a CD11b^{+} SIGN-R1^{+} CD169^{-} population whereas MSMs remain unaffected. This observation was surprising but not unfamiliar. Indeed, a similar phenotype was observed in mice treated with LTβR-Ig, the decoy receptor that blocks LTβR signaling[17]. Two years before, it had been shown that lymphotoxin ($LT\alpha_1\beta_2$) produced by B cells maintains the number and the phenotype of SSMs[16]. Both SSM and MSM subsets express not only RANK but also LTβR[13,16]. In agreement with these observations, we hypothesize that the direct activation of RANK signaling in SSM may support the cell differentiation program by maintaining continuous surface LTβR expression. We generated a mouse model in which LTβR is ablated from CD169^{+} cells and observed that SSM are replaced by the CD11b^{+} SIGN-R1^{+} CD169^{-} cells[Appendix 3]. Thus, our data revealed that RANK and LTβR signaling pathways cooperate for the homeostatic

maintenance SSM and its number. However, the relation between RANK and LTβR still needs to be determined. In future experiments, *in vitro* stimulation of precursors with RANKL and/or with the lymphotoxin should be performed to confirm the requirement of direct co-activation for differentiation into SSMs. Furthermore, which NF-kB signaling pathway(s) is (are) induced in SSM following RANK and or LTβR activation should be investigated by western bot analysis of activation of either the non-canonical pathway and or the canonical pathway.

Since the MSMs reside in an area where RANKL and $LT\alpha_1\beta_2$ stimuli are absent or insufficient after LN compartmentalization, it is conceivable that these cells do not require RANK and LTβR for maintenance after acquisition of a full differentiation program. However, the functions of these receptors and the nature of the factor(s) that support MSM survival in adult remain enigmatic. Single cell-RNA sequencing and comparative analysis of genes differentially expressed between SSM and MSM sorted from adult and young mice LNs would be of much of interest.

Beyond the LNs, RANK or LTβR conditional deletion from CD169^{+} cells also affect bone marrow CD169^{+} macrophages and spleen CD169^{+} marginal zone metallophilic macrophages (MMMs)[Appendixes 4,5], although the nature of the source of RANKL in these organs remain obscure. In 2011, Chow et al., have shown that bone marrow-CD169^{+} macrophages promote the retention of hematopoietic stem cells (HSCs) and progenitor cells through the bone marrow-mesenchymal stem cells by regulating the HSC retention chemokine (CXCL12) expression in these stromal cells. By depleting macrophages in CD169-DTR (*CD169[DTR/+]*) animals, they observed an increased egress of HSCs and progenitor cells to the bloodstream and suggested that the targeting of bone marrow-CD169^{+} macrophages could represent a clinical interest, for example to augment the HSC yields in some patients[18]. In contrast to the CD169-DTR model which requires the treatment of animals with the diphtheria toxin, our mouse models of RANK or LTβR ablation from CD169^{+} could be of much interest for the understanding of the role of these macrophages in bone marrow homeostasis as well as in diseases. For instance, although they express VCAM-1[23] which is an important cell adhesion molecule in the bone marrow plasma cell niche[24], their role in the control of residence and long-term survival of plasma cells is presently unknown. Thus, our models provide us with the conditions to explore their role for entry, residence and longevity of plasma cells.

In both models of RANK and LTβR conditional deletion from CD169^{+} cells, spleen CD169^{+}

MMMs are affected as shown by the loss of CD169 whereas the SIGN-R1^{+} MZMs remain intact[Appendix 5]. Because the MZMs do not express CD169, one cannot exclude a possible contamination of SIGN-R1^{+} cells by a pool of CD169^{-} SIGN-R1^{+} cells arising as consequence of inactivation of RANK or LTβR signaling. However, the use of more macrophage markers is required to check whether MMMs are replaced by a subset of CD11b^{+} SIGN-R1^{+} CD169^{-} cells as was seen for SSMs in the LN. Quantitative RT-PCR performed from spleen cells isolated by enzymatic digestion showed the loss of *Cd169* expression in both RANK and LTβR conditional deletion mice and revealed a tendency of the loss of *Ltbr* expression in RANK conditional knockout[Appendix 6], suggesting that RANK could be required for LTβR expression, also needed for MMM differentiation as suggested for SSMs in LNs.

A summary of the outcomes of stromal RANKL deficiency, lymphatic endothelial cell RANK deficiency and RANK or LTβR ablation from CD169^{+} cells is shown in **Appendix 7**.

The loss of both SSM and MSM, owing to the lack of stromal RANKL or LEC RANK, impaired the germinal center formation and the plasma cell differentiation. This validates published data from others studies[10,13]. However, the observation that only the SSM subset is missing in our models of RANK or LTβR conditional deletion from CD169^{+}, provides us with the conditions to unambiguously determine the function of this subset in the control of the immune responses to a soluble antigen in LNs. To do so, mice will be immunized subcutaneously with hapten carrier, the high molecular mass hemocyanin (KLH), widely known to activate both humoral and cellular immune responses[31]. In that way, KLH should be captured by SSM layer in the draining LNs of wild type mice and not in knockout mice, and B and T cell responses will be analyzed. Of note, small molecules alone often fail to raise efficient immune responses because they pass through conduits and may escape antigen capturing immune cells.

MZMs and MMMs are known for their important roles in the innate immunity through the elimination of blood-borne pathogens (antigens, bacteria, virus, parasites, etc) and for their role in the development of an adaptive immune responses[19]. Most of the studies concerning their roles in the immune responses use different genetic or ablation approaches that generally target both macrophage subtypes[20-22]. However, in our models of RANK or LTβR conditional deletion from CD169^{+}, only the MMM subset is lost. This allows us to investigate their role in splenic immune responses. In the future experiments, we will assess the control

of the humoral immune response by MMMs. To do so, animals will be intraperitoneally immunized with a T cell-dependent antigen, that requires the activity of helper T cells to induce antibody production by B cells. T cells do not recognize native antigen and because the latter should be firstly processed by APCs, we reason that antigen capturing and processing by MMMs and the ensuing B cell response should be impaired in our knockout mice. A T cell-independent antigen, that can trigger B cell responses without the participation helper T cells will be used for control.

Denosumab is a fully human monoclonal antibody raised against RANKL and blocks its binding to RANK. It is clinically used in the treatment of the osteoporosis[25,29]. Beyond this pathology, denosumab is also in clinical use against myeloma bone disease, plasma cell malignancy[26] as well as against the osteolytic lesions arising in autoimmune diseases such as systemic lupus erythematosus, rheumatoid arthritis and Sjögren's syndrome[27]. Furthermore, RANK and RANKL are expressed by distinct immune cells infiltrating human cancers and clinical treatment of bone-metastasizing cancers such as mammary and prostate carcinoma with denosumab are underway[28]. In light of our findings of the RANK-RANKL axis requirement for the development of CD169+ macrophages in LN, spleen and bone marrow, and by keeping in mind the crucial functions of these cells in several aspects of innate and adaptive immunity as well as in tissue homeostasis, the outcomes of RANKL-neutralization with denosumab should be carefully evaluated in human and mouse.

2 References

1. Kong, Y. Y., H. Yoshida, I. Sarosi, H. L. Tan, E. Timms, C. Capparelli, S. Morony, et al. 1999. "OPGL Is a Key Regulator of Osteoclastogenesis, Lymphocyte Development and Lymph-Node Organogenesis." Nature 397 (6717): 315–23. https://doi.org/10.1038/16852.

2. Dougall, W. C., M. Glaccum, K. Charrier, K. Rohrbach, K. Brasel, T. De Smedt, E. Daro, et al. 1999. "RANK Is Essential for Osteoclast and Lymph Node Development." Genes & Development 13 (18): 2412–24. https://doi.org/10.1101/gad.13.18.2412.

3. Marks, S. C., and P. W. Lane. 1976. "Osteopetrosis, a New Recessive Skeletal Mutation on Chromosome 12 of the Mouse." The Journal of Heredity 67 (1): 11–18. https://doi.org/10.1093/oxfordjournals.jhered.a108657.

4. Simonet, W.S, D.L Lacey, C.R Dunstan, M Kelley, M.-S Chang, R Lüthy, H.Q Nguyen, et al. 1997. "Osteoprotegerin: A Novel Secreted Protein Involved in the Regulation of Bone Density." Cell 89 (2): 309–19. https://doi.org/10.1016/S0092-8674(00)80209-3.

5. Mueller, Scott N., and Ronald N. Germain. 2009. "Stromal Cell Contributions to the Homeostasis and Functionality of the Immune System." *Nature Reviews*. *Immunology* 9 (9): 618–29. https://doi.org/10.1038/nri2588.

6. Mueller, Christopher G., and Mark Christopher Coles. 2014. "Emerging Immune Functions of Non-Hematopoietic Stromal Cells." *Frontiers in Immunology* 5 (September). https://doi.org/10.3389/fimmu.2014.00437.

7. Geissmann, Frederic, Markus G. Manz, Steffen Jung, Michael H. Sieweke, Miriam Merad, and Klaus Ley. 2010. "Development of Monocytes, Macrophages, and Dendritic Cells." *Science (New York, N.Y.)* 327 (5966): 656–61. https://doi.org/10.1126/science.1178331.

8. T'Jonck, Wouter, Martin Guilliams, and Johnny Bonnardel. 2018. "Niche Signals and Transcription Factors Involved in Tissue-Resident Macrophage Development." *Cellular Immunology* 330 (August): 43–53. https://doi.org/10.1016/j.cellimm.2018.02.005.

9. Gaya, Mauro, Angelo Castello, Beatriz Montaner, Neil Rogers, Caetano Reis e Sousa, Andreas Bruckbauer, and Facundo D. Batista. 2015. "Host Response. Inflammation-Induced Disruption of SCS Macrophages Impairs B Cell Responses to Secondary Infection." *Science (New York, N.Y.)* 347 (6222): 667–72. https://doi.org/10.1126/science.aaa1300.

10. Gaya, Mauro, Angelo Castello, Beatriz Montaner, Neil Rogers, Caetano Reis e Sousa, Andreas Bruckbauer, and Facundo D. Batista. 2015. "Host Response. Inflammation-Induced Disruption of SCS Macrophages Impairs B Cell Responses to Secondary Infection." *Science (New York, N.Y.)* 347 (6222): 667–72. https://doi.org/10.1126/science.aaa1300.

11. Josien, R., B. R. Wong, H. L. Li, R. M. Steinman, and Y. Choi. 1999. "TRANCE, a TNF Family Member, Is Differentially Expressed on T Cell Subsets and Induces Cytokine Production in Dendritic Cells." Journal of Immunology (Baltimore, Md.: 1950) 162 (5): 2562–68.

12. Bando, Jennifer K., Susan Gilfillan, Christina Song, Keely G. McDonald, Stanley C.-C. Huang, Rodney D. Newberry, Yasuhiro Kobayashi, et al. 2018. "The tumor Necrosis Factor Superfamily Member RANKL Suppresses

Effector Cytokine Production in Group 3 Innate Lymphoid Cells." Immunity 48 (6): 1208-1219.e4. https://doi.org/10.1016/j.immuni.2018.04.012.

13. Camara, Abdouramane, Olga G. Cordeiro, Farouk Alloush, Janina Sponsel, Mélanie Chypre, Lucas Onder, Kenichi Asano, et al. 2019. "Lymph Node Mesenchymal and Endothelial Stromal Cells Cooperate via the RANK-RANKL Cytokine Axis to Shape the Sinusoidal Macrophage Niche." *Immunity* 50 (6): 1467-1481.e6. https://doi.org/10.1016/j.immuni.2019.05.008.

14. Mondor, Isabelle, Myriam Baratin, Marine Lagueyrie, Lisa Saro, Sandrine Henri, Rebecca Gentek, Delphine Suerinck, Wolfgang Kastenmuller, Jean X. Jiang, and Marc Bajénoff. 2019. "Lymphatic Endothelial Cells Are Essential Components of the Subcapsular Sinus Macrophage Niche." Immunity 50 (6): 1453-1466.e4. https://doi.org/10.1016/j.immuni.2019.04.002.

15. Mebius, R. E., P. R. Streeter, S. Michie, E. C. Butcher, and I. L. Weissman. 1996. "A Developmental Switch in Lymphocyte Homing Receptor and Endothelial Vascular Addressin Expression Regulates Lymphocyte Homing and Permits CD4+ CD3- Cells to Colonize Lymph Nodes." *Proceedings of the National Academy of Sciences* 93 (20): 11019–24. https://doi.org/10.1073/pnas.93.20.11019.

16. Phan, Tri Giang, Jesse A Green, Elizabeth E Gray, Ying Xu, and Jason G Cyster. 2009. "Immune Complex Relay by Subcapsular Sinus Macrophages and Noncognate B Cells Drives Antibody Affinity Maturation." *Nature Immunology* 10 (7): 786–93. https://doi.org/10.1038/ni.1745.

17. Moseman, E. Ashley, Matteo Iannacone, Lidia Bosurgi, Elena Tonti, Nicolas Chevrier, Alexei Tumanov, Yang-Xin Fu, Nir Hacohen, and Ulrich H. von Andrian. 2012. "B Cell Maintenance of Subcapsular Sinus Macrophages Protects against a Fatal Viral Infection Independent of Adaptive Immunity." *Immunity* 36 (3): 415–26. https://doi.org/10.1016/j.immuni.2012.01.013.

18. Chow, Andrew, Daniel Lucas, Andrés Hidalgo, Simón Méndez-Ferrer, Daigo Hashimoto, Christoph Scheiermann, Michela Battista, et al. 2011. "Bone Marrow CD169+ Macrophages Promote the Retention of Hematopoietic Stem and Progenitor Cells in the Mesenchymal Stem Cell Niche." *Journal of Experimental Medicine* 208 (2): 261–71. https://doi.org/10.1084/jem.20101688.

19. Borges da Silva, Henrique, Raíssa Fonseca, Rosana Moreira Pereira, Alexandra dos Anjos Cassado, José Maria Álvarez, and Maria Regina D'Império Lima. 2015. "Splenic Macrophage Subsets and Their Function during Blood-Borne Infections." *Frontiers in Immunology* 6 (September). https://doi.org/10.3389/fimmu.2015.00480.

20. Claassen, E., N. Kors, and N. Van Rooijen. 1986. "Influence of Carriers on the Development and Localization of Anti-2,4,6-Trinitrophenyl (TNP) Antibody-Forming Cells in the Murine Spleen. II. Suppressed Antibody Response to TNP-Ficoll after Elimination of Marginal Zone Cells." *European Journal of Immunology* 16 (5): 492–**97.** https://doi.org/10.1002/eji.1830160505.

21. Miyake, Yasunobu, Kenichi Asano, Hitomi Kaise, Miho Uemura, Manabu Nakayama, and Masato Tanaka. 2007. "Critical Role of Macrophages in the Marginal Zone in the Suppression of Immune Responses to Apoptotic Cell-Associated Antigens." *The Journal of Clinical Investigation* 117 (8): 2268–78. https://doi.org/10.1172/JCI31990.

22. A-Gonzalez, Noelia, Jose A. Guillen, Germán Gallardo, Mercedes Diaz, Juan V. de la Rosa, Irene H. Hernandez, Maria Casanova-Acebes, et al. 2013. "The Nuclear Receptor LXRα Controls the Functional Specialization of Splenic Macrophages." Nature Immunology 14 (8): 831–39. https://doi.org/10.1038/ni.2622

23. Chow, Andrew, Matthew Huggins, Jalal Ahmed, Daigo Hashimoto, Daniel Lucas, Yuya Kunisaki, Sandra Pinho, et al. 2013. "CD169⁺ Macrophages Provide a Niche Promoting Erythropoiesis under Homeostasis and Stress." *Nature Medicine* 19 (4): 429–36.

24. Hiepe, Falk, Thomas Dörner, Anja E. Hauser, Bimba F. Hoyer, Henrik Mei, and Andreas Radbruch. 2011. "Long-Lived Autoreactive Plasma Cells Drive Persistent Autoimmune Inflammation." *Nature Reviews. Rheumatology* 7 (3): 170–78. https://doi.org/10.1038/nrrheum.2011.1.

25. Nagy, Vanja, and Josef M. Penninger. 2015. "The RANKL-RANK Story." *Gerontology* 61 (6): 534–42. https://doi.org/10.1159/000371845.

26. Vallet, Sonia, Julia-Marie Filzmoser, Martin Pecherstorfer, and Klaus Podar. 2018. "Myeloma Bone Disease: Update on Pathogenesis and Novel Treatment Strategies." Pharmaceutics 10 (4): 202. https://doi.org/10.3390/pharmaceutics10040202.

27. Sawamura, Masato, Atsushi Komatsuda, Masaru Togashi, Hideki Wakui, and Naoto Takahashi. 2017. "Effects of Denosumab on Bone Metabolic Markers and Bone Mineral Density in Patients Treated with Glucocorticoids." Internal Medicine (Tokyo, Japan) 56 (6): 631–36. https://doi.org/10.2169/internalmedicine.56.7797.

28. Ahern, Elizabeth, Mark J. Smyth, William C. Dougall, and Michele W. L. Teng. 2018. "Roles of the RANKL-RANK Axis in Antitumor Immunity - Implications for Therapy." *Nature Reviews. Clinical Oncology* 15 (11): 676–93. https://doi.org/10.1038/s41571-018-0095-y.

29. Cummings, Steven R., Javier San Martin, Michael R. McClung, Ethel S. Siris, Richard Eastell, Ian R. Reid, Pierre Delmas, et al. 2009. "Denosumab for Prevention of Fractures in Postmenopausal Women with Osteoporosis." *New England Journal of Medicine* 361 (8): 756–65. https://doi.org/10.1056/NEJMoa0809493.

30. Cordeiro, Olga G., Mélanie Chypre, Nathalie Brouard, Simon Rauber, Farouk Alloush, Monica Romera-Hernandez, Cécile Bénézech, et al. 2016. "Integrin-Alpha IIb Identifies Murine Lymph Node Lymphatic Endothelial Cells Responsive to RANKL." Edited by Jörg Hermann Fritz. PLOS ONE 11 (3): e0151848. https://doi.org/10.1371/journal.pone.0151848.

31. Harris, J. R, and J Markl. 1999. "Keyhole Limpet Hemocyanin (KLH): A Biomedical Review." Micron 30 (6): 597–623. https://doi.org/10.1016/S0968-4328(99)00036-0.

3 Appendixes

Appendix 1
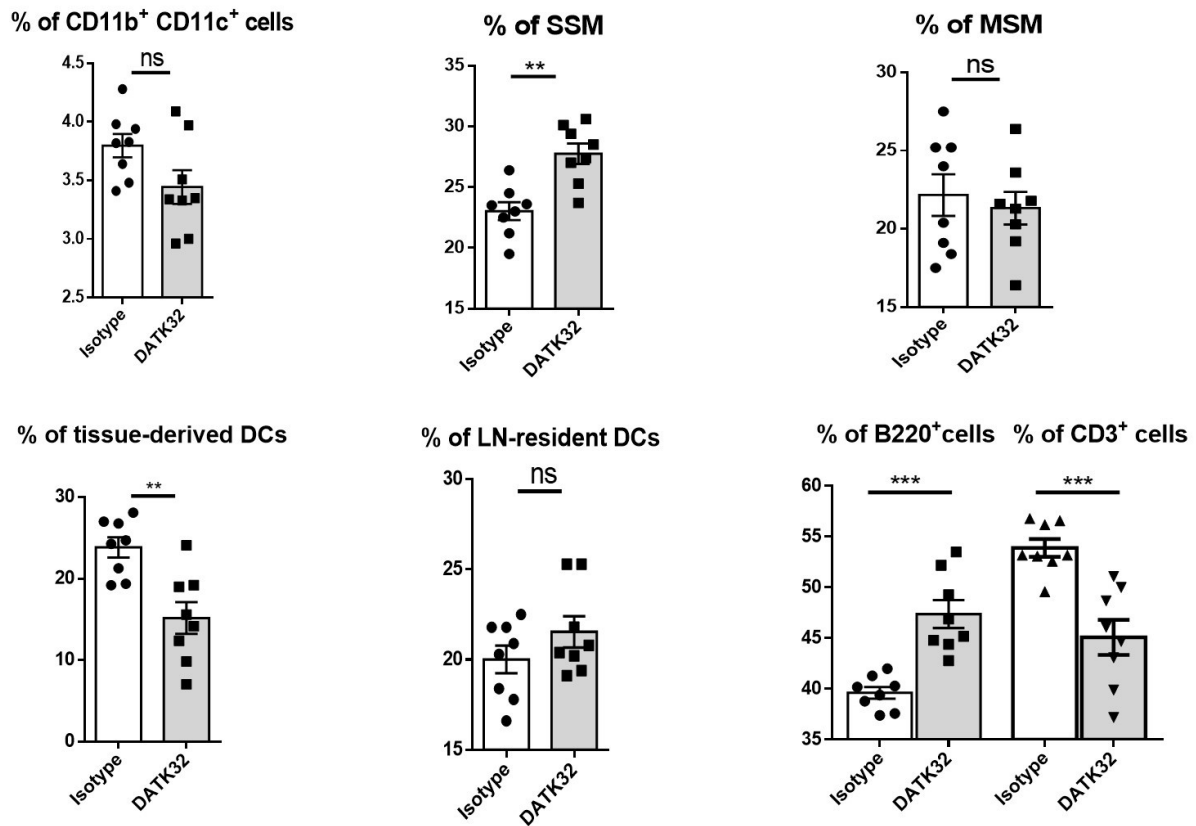
Figure A1. In vivo blockade of MAdCAM-1 binding with anti-$\alpha_4\beta_7$ heterodimer, DATK-32.

One-week-old C57BL/6 mice received subcutaneous injection of anti-mouse integrin $\alpha_4\beta_7$ (LPAM-1, clone DATK-32, BioXcell) or Rat IgG2a (isotype control, BioXcell) at a dose of 3.75 µg/g three days/week for four weeks. At the end of treatment, animals were sacrificed and the percentage of macrophages, DCs and lymphocytes were quantified by flow cytometry from single cells isolated from inguinal and brachial LNs by enzymatic digestion (see paper). The data are the mean ± SEM with individual data points; each point represents the value of one peripheral LN of one mouse. Statistical significance (Mann-Whitney): ***p < 0.001; **p< 0.01; ns, not significant.

Appendix 2
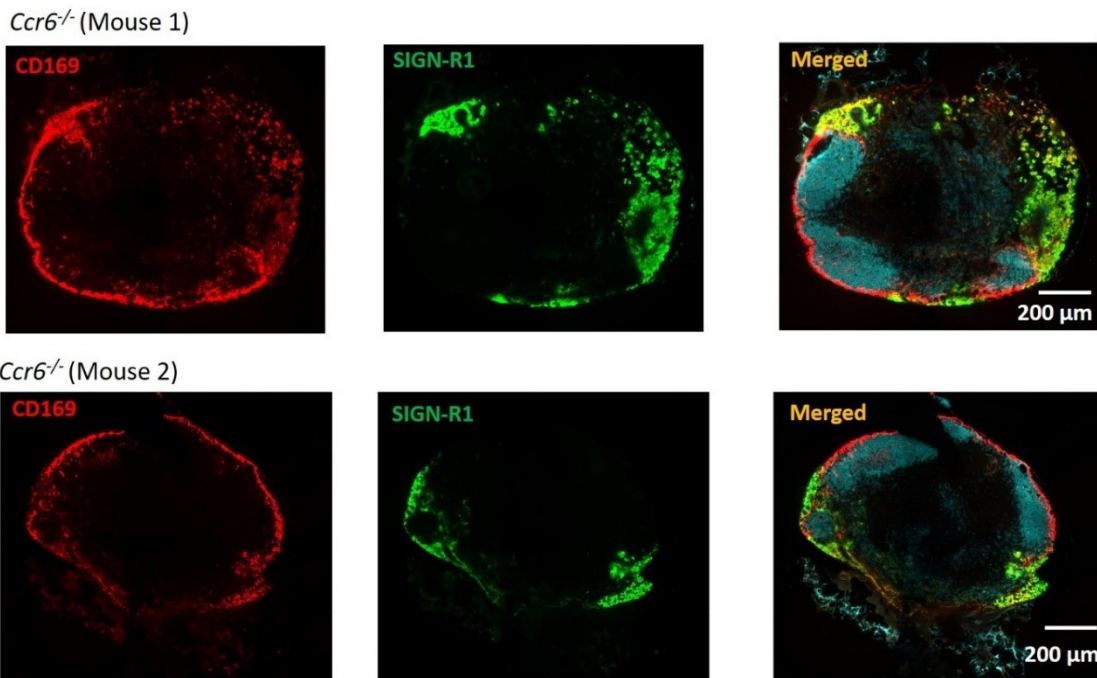
Figure A2. CCR6 deletion does not affect LN sinusoidal macrophages. Adult popliteal LN sections from *two Ccr6 null* mutant mice were stained for CD169, SIGN-R1, and B220. Scale bars represent 200 μm.

Appendix 3
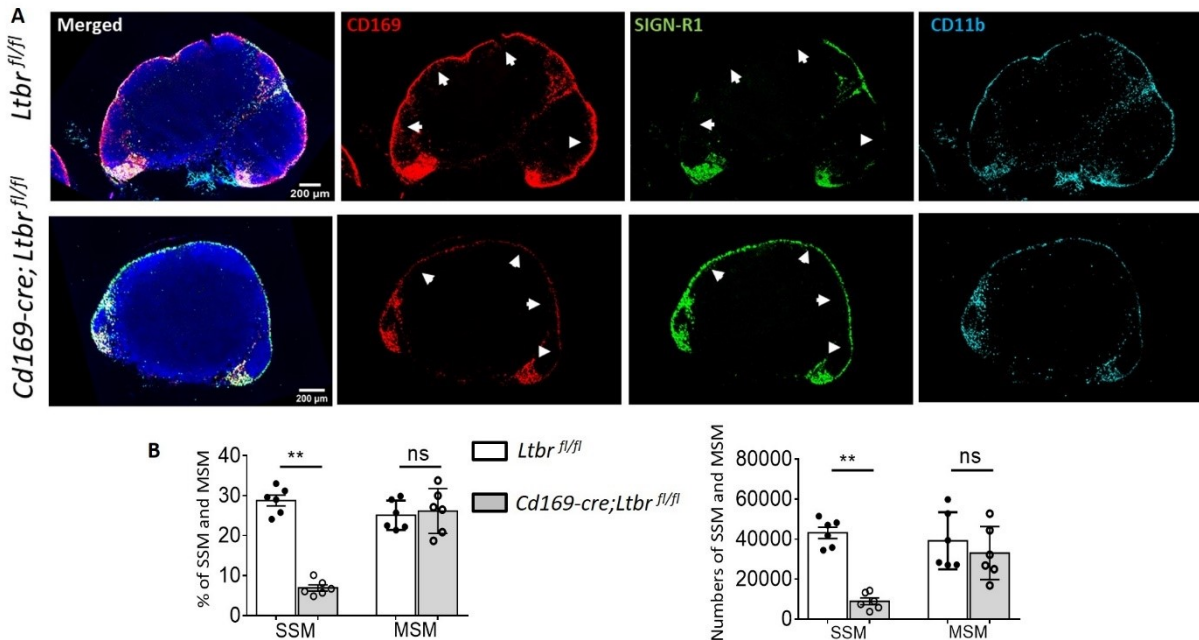
Figure A3. Phenotypic change of subcapsular sinus macrophages (SSM) in mice lacking LTβR signaling from CD169⁺ cells. (A) Adult brachial LN sections from *Ltbr^{fl/fl}* control and *Cd169-cre;Ltbr^{fl/fl} (Ltbr ^{ΔCd169})* mice were stained for CD169, SIGN-R1, CD11b and counterstained with DAPI. Scale bars represent 200 μm. The arrows show the subcapsular sinus/B cell follicle area. (B) The percentages and numbers of SSMs and MSMs) were

determined in *Ltbr*^{fl/fl} control and *Cd169-cre;Ltbr*^{fl/fl} mice. The data are shown as the mean ± SEM with individual data points of brachial LNs. Statistical significance (Mann-Whitney): **p < 0.01; ns, not significant.

Appendix 4

The femur and tibia were freshly collected from mice and bone marrow was isolated by flushing with 1 ml syringe containing PBS and dissociated by pipetting and filtering through 40 µm cell strainer. After a centrifugation at 450xg (5 minutes, 4°C), supernatant was discarded, and red blood cells were lysed with the ammonium-chloride-potassium (ACK) buffer during 8 minutes on ice. Lysis were stopped by diluting with a maximum volume of PBS and samples were centrifuged to eliminate the supernatant. Cell pellet was resuspended in PBS and enumerated. For the flow cytometry, 10^6 cells were incubated with FcR blocking reagent containing 5% of normal rat serum and stained with following antibodies: CD11b (M1/70), F4/80 (BM8), CD115 (AFS98), Ly6G and C (Gr-1, RB6-8C5) and CD169 (3D6-112). The acquisition was performed on a Gallios (Beckman-Coulter) and data were analyzed with FlowJo software (Treestar). DAPI was used for the discrimination of dead cells.
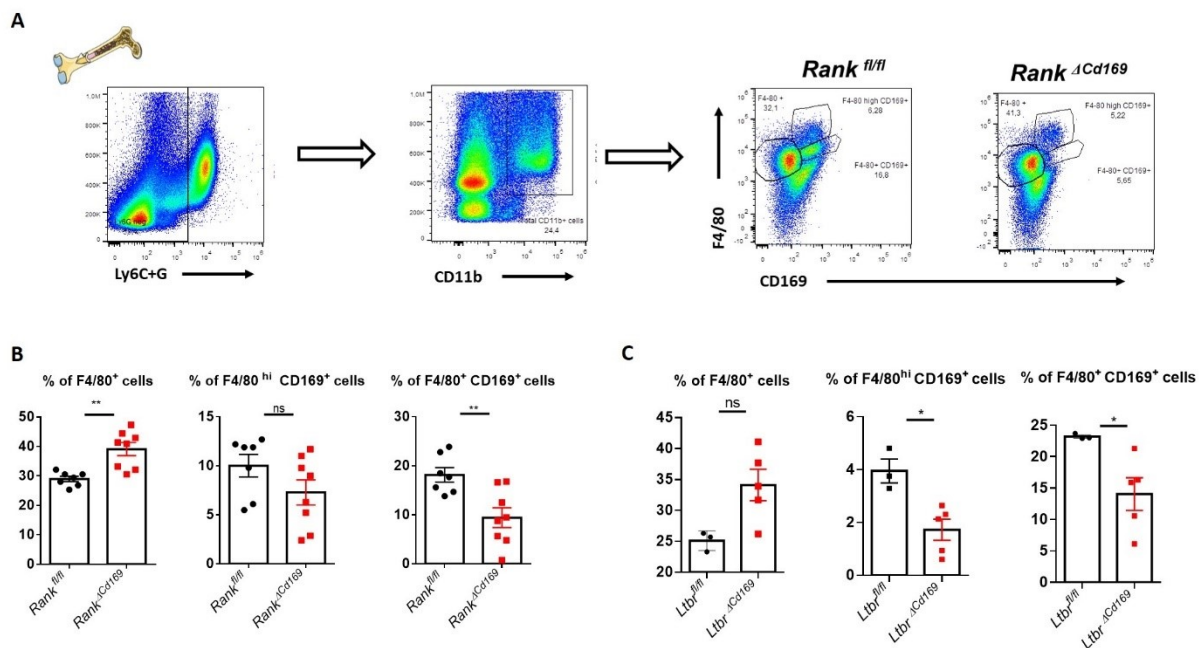
Figure A4. Quantification of bone marrow CD169+ macrophages. (A) Gating strategy of identification of live BM CD169+ and or F4/80+ macrophages from total CD11b+ cells of Ly6C+ G- population. (B) The percentages of single F4/80+, double F4/80[hi] CD169+ and double F4/80+ CD169+ macrophages were determined from the BM of *Rank*^{fl/fl} control and *Cd169-cre;Rank*^{fl/fl} (*Rank* [ΔCd169]) mice. (C) The percentages of single F4/80+, double F4/80[hi] CD169+ and double F4/80+ CD169+ macrophages were determined from the bone marrow of *Ltbr*^{fl/fl} control and *Cd169-*

cre;Ltbr^{fl/fl} (Ltbr ^{ΔCd169}) mice. The data are shown as the mean ± SEM with individual data points of pooled femur and tibia of one mouse. Statistical significance (Mann-Whitney): **p < 0.01; *p < 0.05; ns, not significant.

Appendix 5
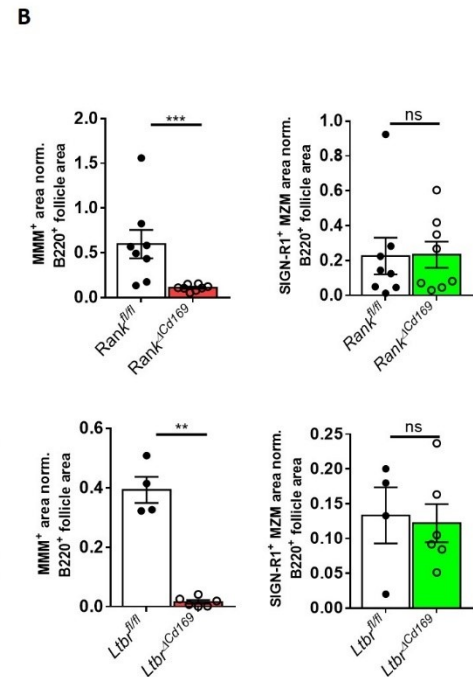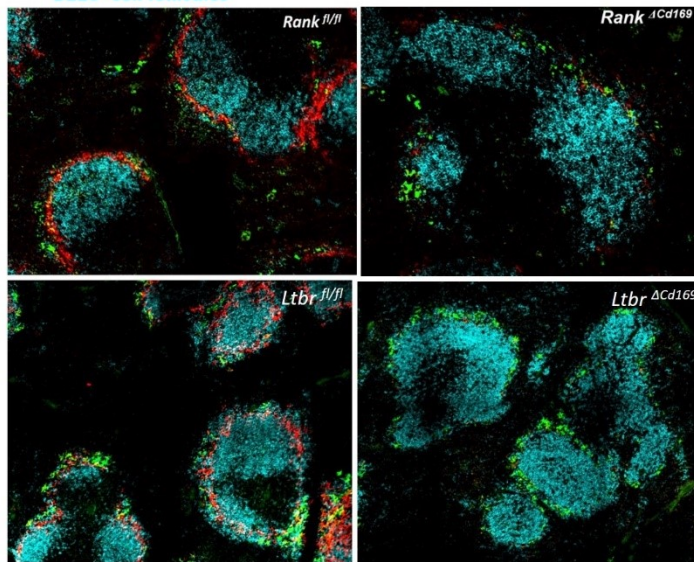
Figure A5. Image J quantification of spleen MMM and MZM. (A) Adult spleen LN sections from *Cd169-cre;Rank^{fl/fl} (Rank ^{ΔCd169})* and *Cd169-cre;Ltbr^{fl/fl} (Ltbr ^{ΔCd169})* mice ^{with} control littermates were stained for CD169, SIGN-R1, B220. (B) The areas of CD169^{+} MMM and SIGN-R1^{+} MZM were quantified and normalized to the areas of B220^{+} cells. The data are shown as the mean ± SEM with individual data points; each point represents the value for a spleen section of one mouse. Statistical significance (Mann-Whitney): ***p < 0.001; ns, not significant.

Spleen was enzymatically digested with liberase (20 µg/ml) and DNase I (50 µg/ml) in RPMI medium supplemented with 2% of FCS, at 37°C under agitation (1000 rpm) during 45 min. Cells were filtered using 70 µm filter and centrifuged at 1500 rpm for 5 min. Red blood cells were lysed with ACK buffer on ice during 8-10 min and samples were centrifuged at 1500 rpm for 5 min. Pellet were resuspended in a flow cytometry buffer and cells were enumerated in trypan blue using the kova slide. One to two million of cells were used for RNA extraction using the kit NucleoSpin RNA Plus Macherey Nagel (740984.50) and cDNA was synthesized with Maxima First Strand cDNA Synthesis Kit (Thermo Scientific). Quantitative PCR was performed using Luminaris color HiGreen qPCR Master Mix (Thermo Scientific) and was runned on a Bio-Rad CFX96 thermal cycler. Following primers were used: *Cd169* (Forward): CTTGGGTCAGCCAACAGTTC, *Cd169* (Reverse): GGTGATGGTGAAACCTGGAC; *Ltbr* (Forward): AAATCCCCCAGAGCCAGGA, *Ltbr* (Reverse): GGTGCCGCTTGAGCAGAGT. Threshold values (Ct) of the target genes were normalized to housekeeping gene mGapdh.
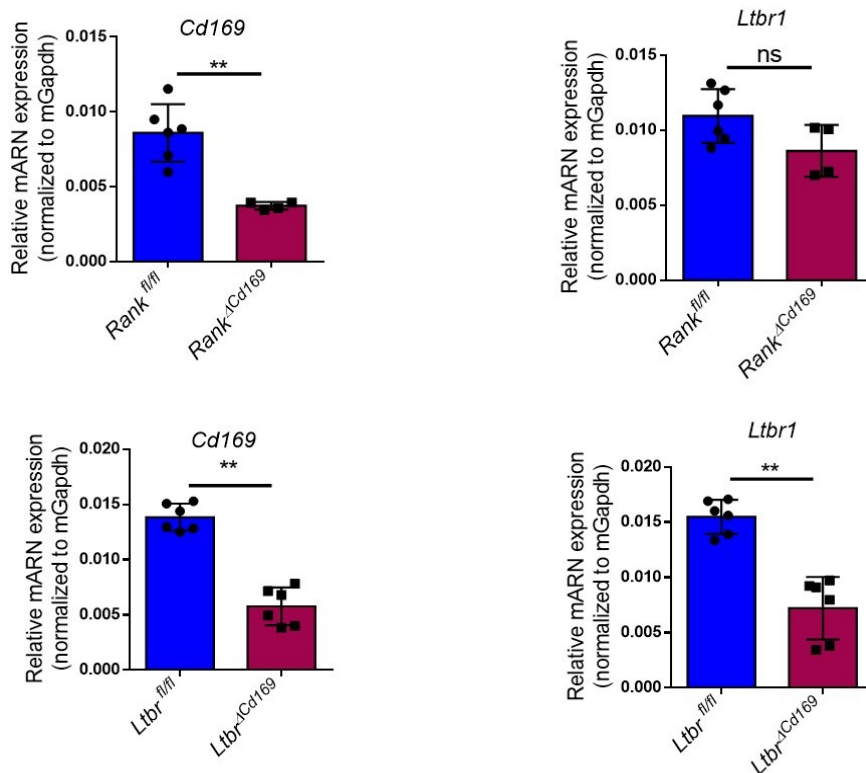
Figure A6. Assessment of CD169 and LTβR expression from spleen cells. Changes in the expression of *Cd169* and *Ltbr* were analyzed by quantitative RT-PCR using primers (see above). Gene expression was normalized to mGapdh. The data, identified by dots, are the mean of replicates from individual mice. Statistical significance (Mann-Whitney): **p < 0.01; ns, not significant.

Appendix 7

Summary of CD169⁺ macrophage subsets and their RANK, RANKL and LTβR-dependency.

Tissue	Sinusoidal macrophage type	Markers	Macrophage-targeted genetic ablation: *Cd169-cre; Rank^{fl/fl}*	Macrophage-targeted genetic ablation: *Cd169-cre; Ltbr^{fl/fl}*	Fibroblast stroma-targeted genetic ablation: *Ccl19-cre;Rankl^{fl/fl}*	Lymphatic endothelial-targeted: *Prox-1-cre^{ERT2};Rank^{fl/fl}* (tamoxifen at E18.5)
Lymph node	Subcapsular (SSM)	CD169	Absent	Absent	↓↓	↓↓
	Medullary (MSM)	CD169, SIGNR1, F4/80	Present	Present	↓↓	↓↓
Spleen	Marginal metallophilic (MMM)	CD169	Absent	Absent	Unknown	Unknown
	Marginal zone (MZM)	SIGN-R1, MARCO	Present	Present	Unknown	Unknown
Bone	CD169⁺ osteomacs	CD169, F4/80, VCAM-1	↓↓	↓↓	Unknown	Unknown

E, embryonic day 18.5; CD169⁺ osteomacs, bone marrow CD169⁺ macrophages;

VCAM-1, vascular cell adhesion molecule 1; ↓: the type macrophage is reduced in number.

Talks

Abdouramane Camara, and Christopher G. Mueller. Lymph Node Mesenchymal and Endothelial Stromal Cells Cooperate via the RANK-RANKL Cytokine Axis to Shape the Sinusoidal Macrophage Niche (2019). **Oral presentation delivered at the annual meeting of the Société Française d'Immunologie, Nantes, France**. *November 2019*.

Abdouramane Camara, and Christopher G. Mueller. Lymph Node Mesenchymal and Endothelial Stromal Cells Cooperate via the RANK-RANKL Cytokine Axis to Shape the Sinusoidal Macrophage Niche (2019). **Oral presentation delivered at the 17th International Congress of Immunology (IUIS 2019), Beijing, China**. *October 2019*.

Bourse de voyage de la Société Française de l'Immunologie

Abdouramane Camara, and Christopher G. Mueller. Lymph Node Mesenchymal and Endothelial Stromal Cells Cooperate via the RANK-RANKL Cytokine Axis to Shape the Sinusoidal Macrophage Niche (2019). **Oral presentation delivered at the 3rd Upper Rhine Immunology Group meeting, Basel, Switzerland**. *October 2019*.

Efficient anti-viral immune response requires a CD169+ sinusoidal macrophage niche constituted by lymphatic endothelial cells

Abdouramane Camara, Olga G. Cordeiro, Janina Sponsel, Christopher G. Mueller

CNRS UPR 3572, University of Strasbourg, IBMC, Strasbourg, France

Poster panels: Introduction, Methodology and Results, Conclusions, References

Poster presentation delivered to the 2nd regional North African Immunology Course on Cancer, Inflammation and Immunotherapy. FES, Morocco. *April 2018.*

First poster price

UNIVERSITE DE STRASBOURG

RESUME DE LA THESE DE DOCTORAT

Discipline : Biologie

Spécialité (facultative) : Immunologie

Présentée par : CAMARA Abdouramane

Titre :   **Régulation de la différentiation des macrophages CD169+ des organes lymphoïdes par les cellules stromales**.

Unité de Recherche : Immunologie, Immunopathologie et Chimie Thérapeutique - CNRS UPR 3572

Directeur de Thèse : Mueller Christopher, Directeur de Recherche (CNRS)

Localisation : Institut de Biologie Moléculaire et Cellulaire (IBMC), Strasbourg

ECOLES DOCTORALES :

☐ ED - Sciences de l'Homme et des sociétés	☐ ED 269 - Mathématiques, sciences de l'information et de l'ingénieur
☐ ED 99 – Humanités	☐ ED 270 – Théologie et sciences religieuses
☐ ED 101 – Droit, sciences politique et histoire	☐ ED 413 – Sciences de la terre, de l'univers et de l'environnement
☐ ED 182 – Physique et chimie physique	☒ ED 414 – Sciences de la vie et de la santé
☐ ED 221 – Augustin Cournot	
☐ ED 222 - Sciences chimiques	

Introduction

La cytokine RANKL (Receptor activator of NF-kB ligand) et son récepteur RANK contrôlent la formation des ostéoclastes, les macrophages spécialisés dans la résorption osseuse. Les souris dépourvues de RANKL ou de RANK sont atteintes d'ostéopétrose, une pathologie caractérisée par une densité osseuse accrue (Dougall et al., 1999; Kong et al., 1999; Walsh et Choi, 2014). Chez l'Homme, les mutations génétiques de RANK sont responsables des anomalies osseuses telle que la maladie de Paget (Whyte et al., 2002). RANKL est aussi requise pour l'organogenèse du ganglion lymphatique (GL) car les souris déficientes en RANKL ou en RANK sont dépourvues de ces organes (Dougall et al., 1999; Kim et al., 2000; Kong et al., 1999). Cependant, en dehors des ostéoclastes, il n'est pas connu si la signalisation RANKL-RANK est aussi requise pour le développement d'autres types de macrophages.

Le GL est un organe lymphoïde secondaire où se rencontrent les antigènes et cellules immunitaires pour une réponse immunitaire adaptative. Les cellules marginales réticulaires (MRCs en anglais) font partie des cellules stromales ganglionnaires. Elles sont caractérisées par l'absence du marqueur hématopoïétique CD45 et du marqueur endothélial PECAM/CD31 mais par la présence de la podoplanine/Gp38 des cellules fibroblastiques réticulaires (FRCs). Il semble que les cellules précurseurs pour les MRCs sont les cellules organisatrices des tissus lymphoïdes (LTOs) retrouvées dans les GLs embryonnaires. Les deux types de cellules, MRC et LTO, expriment la cytokine RANKL (Katakai et al., 2008; Rodda et al., 2018). En 2016, une étude de notre laboratoire a montré que la RANKL stromale active les cellules endothéliales lymphatiques (LECs) pour induire l'expression de l'intégrine alpha 2b (Cordeiro et al., 2016). En 2017, une étude chez la souris a révélé que la formation du GL nécessite l'activation du récepteur RANK des LECs pendant l'embryogenèse (Onder et al., 2017). Cela montre un dialogue croisé entre les cellules stromales mésenchymateuses (LTO / MRC) et les LECs via RANKL-RANK, qui pourrait influencer la réponse immunitaire chez l'adulte.

Les macrophages qui tapissent les sinus (cavités) du GL comprennent les macrophages du sinus sous-capsulaires (SSMs) exprimant le marqueur CD169 et localisés entre les follicules de lymphocytes B et le sinus sous-capsulaire, et les macrophages du sinus médullaire (MSMs) exprimant les marqueurs CD169, SIGN-R1 et F4/80, associés aux vaisseaux lymphatiques médullaires (**Figure 1**). Ces macrophages jouent un rôle prépondérant dans l'initiation et la régulation de l'immunité innée et adaptative (Gray et Cyster, 2012; Iannacone et al., 2010; Moseman et al., 2012; Sagoo et al., 2016; Carrasco et Batista, 2007; Phan et al., 2007; Chatziandreou et al., 2017). Cependant, les facteurs qui gouvernent leur différenciation ne sont pas connus.

Les objectifs de ma thèse consistent :

1. D'inactiver la RANKL stromale et d'analyser son impact sur l'homéostasie du GL et la réponse immunitaire chez l'adulte. Comme les ostéoclastes nécessitent la RANKL pour se développer et en tenant compte du fait que les macrophages résidents reçoivent des signaux de leurs microenvironnements pour compléter leur différenciation, nous avons examiné si cette inactivation affecte les macrophages ganglionnaires. Pour cela, nous avons généré un modèle de souris permettant d'inactiver RANKL dans les LTOs/MRCs. Nous nous sommes intéressés particulièrement aux SSMs, qui résident dans l'environnement du réseau des MRCs, ainsi qu'à leurs homologues MSMs associés aux sinus médullaires (**Figure 1**).

2. Dans la seconde partie, nous avons examiné si les SSMs et les MSMs requièrent l'activation directe de RANK à la surface cellulaire pour se différencier. Pour cela, nous avons généré un modèle de souris dans lequel RANK est inactivé spécifiquement dans les cellules CD169^{+}.

3. Enfin, dans la troisième partie, nous avons étudié la contribution des LECs activées par RANKL dans la différenciation de ces macrophages. Pour cela, nous avons généré un modèle de souris qui permet d'inactiver RANK spécifiquement et temporellement dans les LECs.
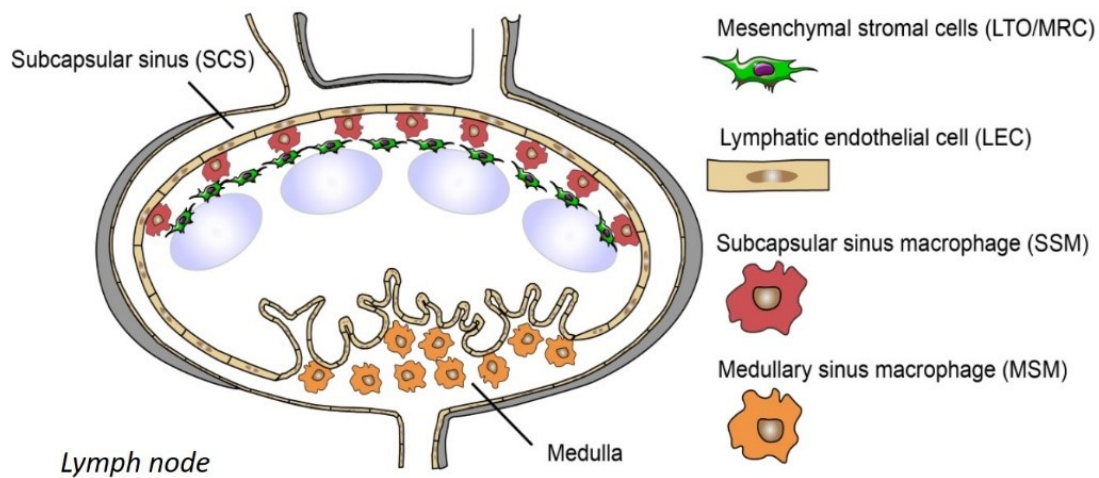

Figure 1. Organisation des cellules stromales mésenchymateuses (LTOs/MRCs), lymphatiques endothéliales (LECs) et les macrophages sinusoïdaux (SSMs, MSMs) dans le ganglion lymphatique adulte.

Résultats

Pour inactiver RANKL dans les LTOs/MRCs, nous avons croisé la souris exprimant la Cre recombinase sous le contrôle du promoteur Ccl19 (Chai et al., 2013) avec la souris *Rankl* [fl/fl] chez laquelle *Rankl* est flanqué de part et d'autre par deux sites *LoxP* (Xiong et al., 2011). Les résultats présentés dans la figure 2 montrent que RANKL stromale est requise pour la différenciation des macrophages SSMs et MSMs.
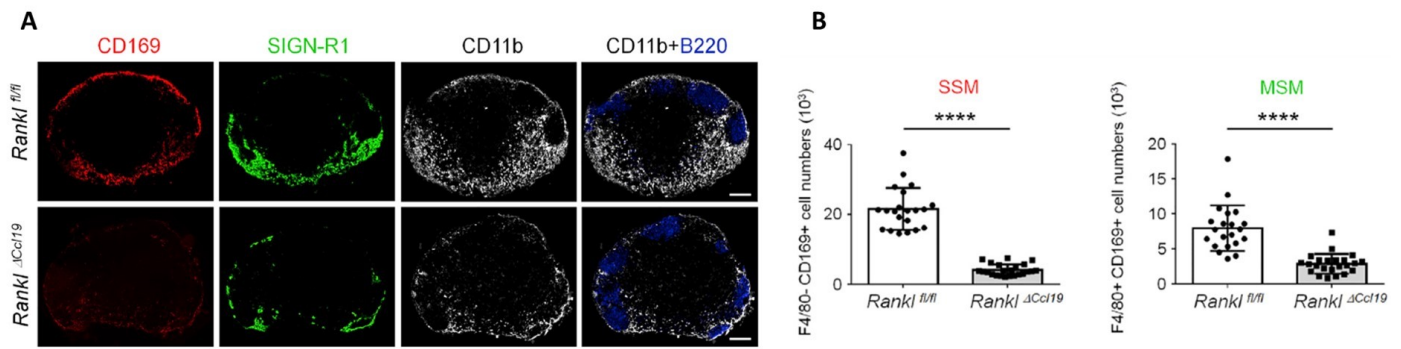
Figure 2. L'inactivation de RANKL stromale entraîne la perte des deux types de macrophages sinusoïdaux ganglionnaires. (A). Immunofluorescence (IF) sur sections de GLs de souris knockout (*Rankl[ΔCcl19]*) et contrôle (*Rankl [fl/fl]*) marquées pour CD169, SIGN-R1, CD11b et B220. Barre d'échelle (200 µm). (B) Quantification par cytométrie en flux des nombres absolus de SSMs et MSMs dans les GLs.

Pour inactiver RANK spécifiquement dans les macrophages CD169+, nous avons croisé la souris exprimant la Cre recombinase introduite dans le locus du gène *Cd169* (Karasawa et al., 2015) avec la souris *Rank [fl/fl]* chez laquelle *Rank* est flanqué de part et d'autre par deux sites *LoxP* (Rios et al., 2016). Les résultats présentés dans la figure 3 montrent que RANK est requis pour la différenciation des macrophages SSMs mais dispensable pour les MSMs.
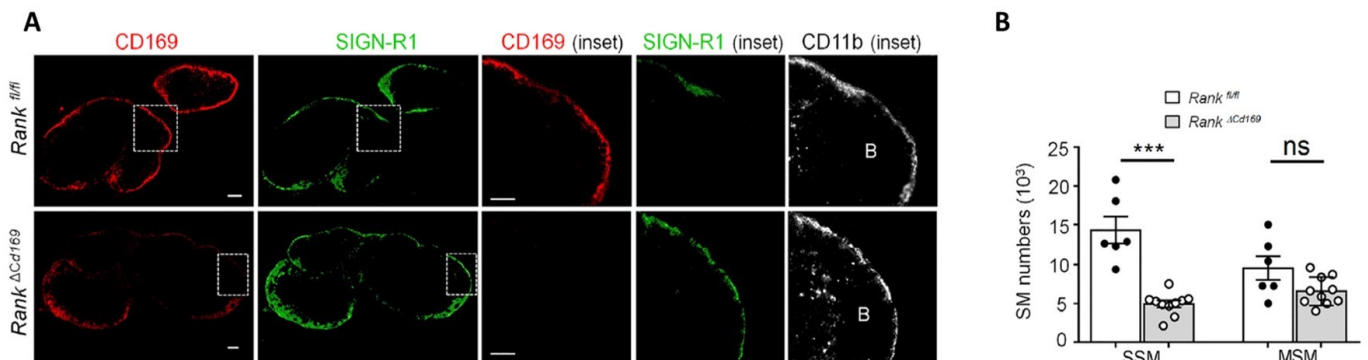

Figure 3. L'inactivation de RANK dans les cellules CD169+ bloque la différenciation des SSMs (A) Immunofluorescence sur sections de GLs de souris knockout (*Rank[ΔCd169]*) et contrôle (*Rank [fl/fl]*) marquées pour CD169, SIGN-R1 et CD11b. Barres d'échelle (100/200 µm). (B) Quantification par cytométrie en flux des nombres absolus de SSMs et MSMs dans les GLs.

Pour inactiver RANK spécifiquement dans les LECs, nous avons croisé la souris exprimant la Cre recombinase inductible au tamoxifène sous le contrôle du promoteur Prox1 (Bazigou et al., 2011) avec la souris *Rank [fl/fl]*. Les résultats présentés dans la figure 4 montrent que l'activation de RANK des LECs est requise pour la différenciation des SSMs et des MSMs pendant l'embryogenèse et les premières semaines après la naissance.
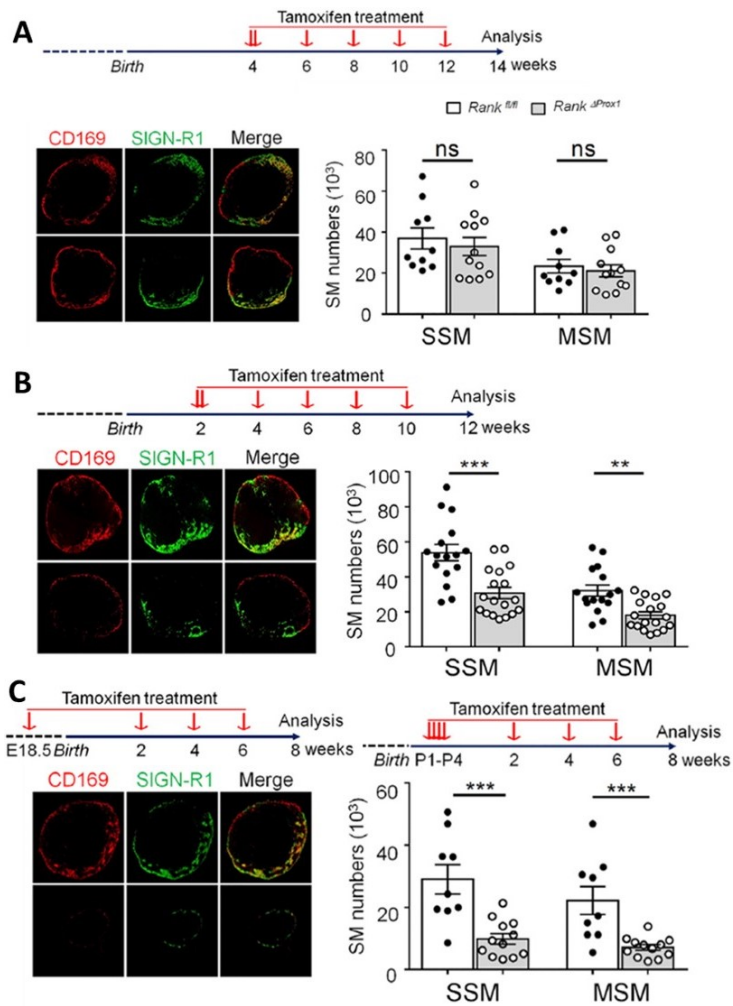
Figure 4. L'activation de RANK dans les LECs est nécessaire pour la différenciation les deux types de macrophages sinusoïdaux ganglionnaires. Pour inactiver RANK, les souris ont été traitées au tamoxifène à 4 semaines (A), à deux semaines (B), ou pendant les stades embryonnaires et postnatals (C). Les macrophages ont été marqués par IF pour CD169, SIGN-R1 et CD11b sur sections de GLs et leurs nombres absolus ont été quantifiés par la cytométrie en flux.

Par ailleurs, en provoquant la disparition de ces macrophages par mort cellulaire induite par le stimulus inflammatoire bactérien, l'oligonucléotide CpG (Gaya et al., 2015; Sagoo et al., 2016), nous avons observé que l'activation de RANK dans les LECs est requise pour la reconstitution de leurs populations (**Figure 5**).
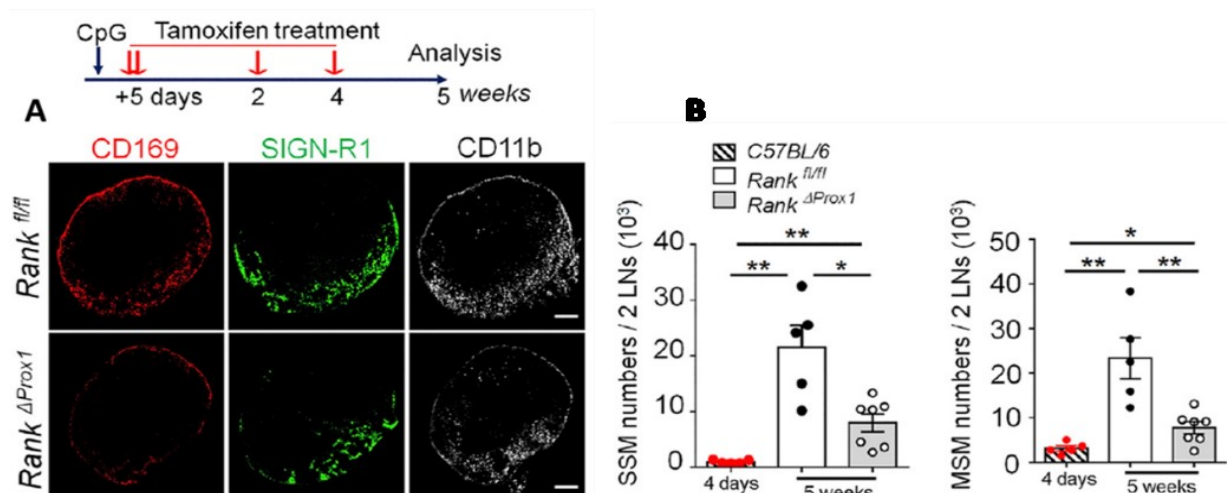
Figure 5. L'activation de RANK dans les LECs est nécessaire pour la reconstitution de la niche des macrophages sinusoïdaux ganglionnaires. La déplétion de SSMs et MSMs a été induite par l'injection de CpG dans les pattes des souris KO (*Rank^ΔProx1*) et les contrôles (*Rank ^fl/fl^*). Quatre jours plus tard, le traitement au tamoxifène a commencé. Les GLs drainants ont été prélevés au bout de 5 semaines). (A) Les macrophages ont été marqués par IF pour CD169, SIGN-R1 et CD11b et (B) leurs nombres absolus ont été quantifiés et comparés aux nombres des macrophages équivalents restants 4 jours après l'administration de CpG aux souris C57BL/6.

Pour consolider que la signalisation RANK-RANKL est cruciale pour la différenciation des macrophages sinusoïdaux ganglionnaires, nous avons réalisé des tests fonctionnels en infectant nos modèles de souris avec des pathogènes viraux. Les souris déficientes en RANKL stromale (*Rankl^ΔCcl19*) ont reçu une injection du virus MVA (Modified Ankara Vaccinia), connu pour cibler à la fois les SSMs et les MSMs (Chatziandreou et al., 2017; Gaya et al., 2015; Sagoo et al., 2016). Sept jours plus tard, la réponse antivirale a été mesurée. Les résultats, présentés dans la figure 6 montrent que la réponse immunitaire antivirale est altérée dans les souris déficientes en RANKL stromale. Les phénotypes similaires ont été confirmés dans les souris déficientes en activité de RANK des LECs (Camara et al., 2019).
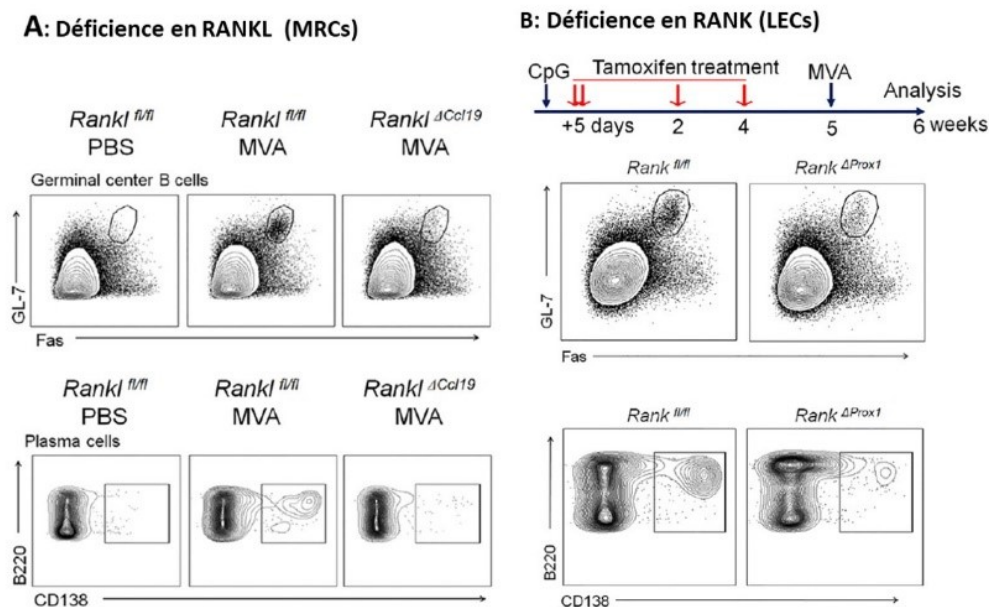

Figure 6. RANKL stromale est importante pour la réponse antivirale médiée par les macrophages sinusoïdaux ganglionnaires. (A) Les souris déficientes en RANKL stromale (*Rankl^ΔCcl19*) et les contrôles (*Rankl ^fl/fl^*) ont été infectées par injection de 10^4 plaques formant unité (PFU) de virus MVA ou du PBS dans les pattes postérieurs. Après 7 jours, la formation du centre germinal par le marqueur GL-7 et la génération des plasmocytes par B220 et CD138 ont été quantifiées dans les GLs drainants par la cytométrie en flux. (B) Du CpG a été injecté dans les pattes postérieures des souris déficientes en activité de RANK des LECs (*Rank^ΔProx1*) et contrôles (*Rank ^fl/fl^*) pour dépléter les macrophages, puis traitées au tamoxifène avant l'infection virale à 5 semaines après CpG. Sept jours plus tard, la réponse virale a été mesurée dans les GLs drainants comme ci-dessus.

Conclusions et perspectives

Au cours ma thèse, nous avons démontré pour la première fois que les cellules stromales mésenchymateuses et les cellules endothéliales lymphatiques interagissent via la signalisation RANK-RANKL pour créer un environnement permettant aux macrophages sinusoïdaux ganglionnaires de compléter leur programme de différenciation et de remplir leurs fonctions immunitaires. Les souris déficientes en RANKL stromale ont montré une forte réduction de SSMs et de MSMs, compromettant le transport d'antigène aux lymphocytes B et la réponse antivirale. La perte de SSMs dans les souris déficientes en RANK fonctionnel dans les cellules CD169^{+} a montré que ces macrophages dépendent de la stimulation continue par RANKL stromale pour se maintenir. Cependant, de l'embryogenèse aux premières semaines après la naissance, l'activation de RANK des cellules endothéliales lymphatiques est indispensable à la différenciation simultanée de SSMs et de MSMs (**Figure 7**). En plus, nos données ont montré que les LECs activées par RANKL stromale sont essentielles à la reconstitution de la niche de SSMs et MSMs, suite à leur disparition (Gaya et al., 2015; Sagoo et al., 2016) provoquée l'inflammation, afin de préparer leurs compartiments pour une agression ultérieure.

Cependant, le(s) factor(s) dérivé(s) des LECs qui contrôlent à la fois la différenciation des deux types de macrophages aussi bien que le(s) second(s) facteur(s) requis(s) pour le maintien des MSMs restent à être élucidés. En comparant le profil transcriptomique des LECs triées des GLs de souris déficientes en RANKL stromale à celui des souris contrôles, nous avons observé une diminution significative de l'expression de certains gènes tels que *Madcam1, Itga2b, Ccl20, Pf4, Ackr4, etc.* Les contributions de certains de gènes candidats seront investiguées par l'inactivation spécifique dans les LECs chez des modèles animaux.

Par ailleurs, au-delà du GL, l'inactivation de RANK des cellules CD169^{+} diminue significativement les nombres des macrophages CD169^{+} dans la rate et dans la moelle osseuse (données non publiées). Les impacts de ces observations seront évalués sur différents aspects de la réponse immunitaire au cours des futures expérimentations de notre laboratoire.
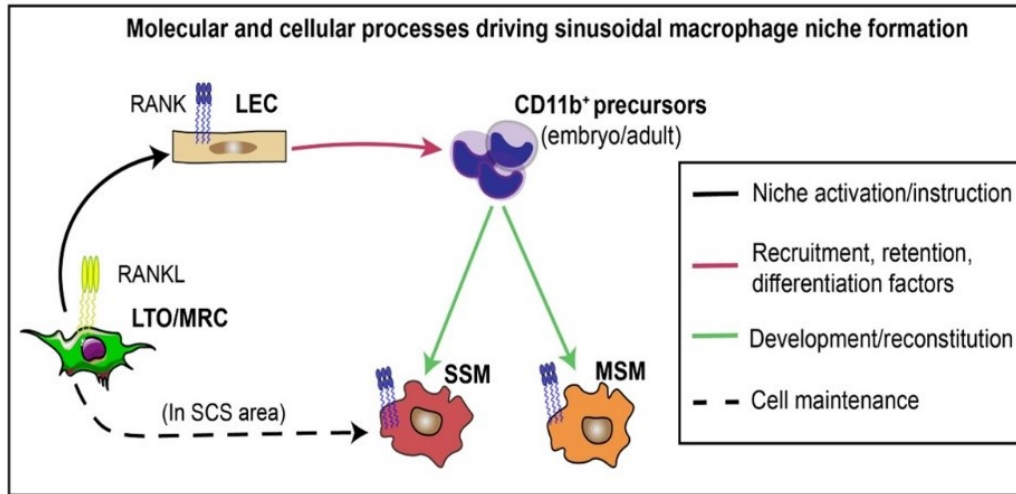
Figure 7. Illustration schématique du mécanisme cellulaire et moléculaire de la régulation la différenciation des macrophages sinusoïdaux ganglionnaires par les cellules stromales. 1) Au cours du développement embryonnaire jusqu'aux quatre premières semaines après la naissance, les LTOs/MRCs engagent RANK et activent les LECs. 2) Celles-ci construisent la niche favorable au recrutement et la rétention des précurseurs pour la différentiation en SSMs et/ou en MSMs. 3) Chez l'adulte, les MRCs maintiennent la population des SSMs en engageant RANK directement sur ces derniers.

Article publié

Ces travaux ont été publiés en juin 2019, dans le journal **Immunity** (Camara et al., 2019), où figurent les articles cités ci-dessus.

Abdouramane Camara, Olga G. Cordeiro, Farouk Alloush, Janina Sponsel, Mélanie Chypre, Lucas Onder, Kenichi Asano, Masato Tanaka, Hideo Yagita, Burkhard Ludewig, Vincent Flacher, and Christopher G. Mueller (2019). *Lymph Node Mesenchymal and Endothelial Stromal Cells Cooperate via the RANK-RANKL Cytokine Axis to Shape the Sinusoidal Macrophage Niche*. **Immunity** 50, 1467–1481 June 18, 2019.

Communications orales

Titre : Lymph Node Mesenchymal and Endothelial Stromal Cells Cooperate via the RANK-RANKL Cytokine Axis to Shape the Sinusoidal Macrophage Niche (2019).

Présentation orale faite au (à la) :

- 52ème congrès annuel de la Société Française d'Immunologie (SFI), à Nantes-France, Novembre 2019
- 17ème congrès de l'Union Internationale des Sociétés d'Immunologie (IUIS), à Beijing-Chine, Octobre 2019. Bourse de voyage de la société française d'immunologie.
- 3ème rencontre annuelle de Upper Rhine Immunology Group (URI), à Bâle-Suisse, Octobre 2019

Communications par affiches

Titre : Efficient antiviral immune response requires a CD169+ sinusoidal macrophage niche constituted by lymphatic endothelial cells

Poster présenté au :

- 8ème symposium de Infectious Diseases in Africa (IDA), à Cape Town-Afrique du Sud, Novembre 2018

Titre : Stromal RANKL-activated Lymphatic Endothelial Cells control Sinusoidal Macrophage niche constitution in lymph nodes

Posters présentés à la :

- 2ème édition des cours d'immunologie en Afrique du Nord, à Fès-Maroc, Avril 2018. Bourse de voyage de la société française d'immunologie. *Meilleur prix de poster*
- 2ème rencontre annuelle de Upper Rhine Immunology Group (URI), à Freiburg-Allemagne, Octobre 2018

Titre : RANKL-activated lymphatic endothelial cells control sinusoidal macrophage differentiation

Poster présenté à la :

- 1ère rencontre annuelle de Upper Rhine Immunology (URI) Group, à Strasbourg-France, Decembre 2017.

Abdouramane CAMARA

Control of lymphoid organ CD169$^+$ macrophage differentiation by stromal cells through RANK-RANKL signaling axis

Résumé

Au-delà de leurs rôles de sentinelles, de reconnaissance du danger et d'initiation des réponses protectrices, les signaux et le mécanisme qui gouvernent la formation des macrophages CD169$^+$ sinusoïdaux ganglionnaires sont mal connus. Au cours de ma thèse, j'ai montré que la cytokine Receptor Activator of NF-kB Ligand (RANKL) est requise pour la formation de ces macrophages dès l'embryogenèse jusqu'aux quatre semaines après la naissance. Celle-ci est contrôlée par les cellules endothéliales lymphatiques (LECs) activées par RANKL produite par les cellules mésenchymateuses. Chez l'adulte, les LECs activées par RANKL sont encore nécessaires pour la reconstitution des populations de ces macrophages en cas de déplétion transitoire induite par un stimulus inflammatoire. En complément à cela, j'ai aussi démontré l'importance générale du double signal RANKL & lymphotoxine LT$\alpha_1\beta_2$ dans la formation des macrophages non-ostéoclastiques de la rate et de la moelle osseuse.

Mots clés : macrophages, RANKL, cellules endothéliales lymphatiques, cellules mésenchymateuses, différenciation, reconstitution.

Résumé en anglais

Lymph node CD169$^+$ sinusoidal macrophages are sentinel cells that recognize the danger signals and initiate the protective immune responses. However, the signals and the mechanism underlying their formation are not well known. During my thesis, I have shown that the cytokine Receptor Activator of NF-kB Ligand (RANKL) is required for their differentiation, starting from the embryogenesis up to four weeks after birth. The lymphatic endothelial cells (LECs) activated by RANKL expressed by mesenchymal cells form the niches for the primary differentiation of these macrophages. Yet, in adults, RANKL-activated LECs are required for their niche replenishment after transient depletion induced by an inflammatory stimulus. Beyond lymph node, my research has revealed a general requirement of the double signal RANKL & lymphotoxin LT$\alpha_1\beta_2$ for the differentiation of non-osteoclastic CD169$^+$ macrophages of spleen and bone marrow.

Keywords : macrophages, RANKL, lymphatic endothelial cells, mesenchymal cells, differentiation, replenishment.